The effects of TAR DNA binding protein mutations on RNA processing associated with Amyotrophic Lateral Sclerosis

By

Afnan Ali Al Sultan

Submitted for the degree of Doctor of Philosophy (PhD)

Sheffield Institute for Translational Neuroscience

University of Sheffield

November, 2016

This PhD thesis is dedicated to my dear loving husband,

Ahmed Alamer,

Without your tremendous support, encouragement and love

my dream would not have been possible

Abstract

Introduction: Amyotrophic Lateral Sclerosis (ALS) is a devastating, chronic progressive neurodegenerative disorder, characterized by the loss of the upper motor neurons in the motor cortex and the lower motor neurons of the brainstem and spinal cord. This leads to muscle weakness, atrophy and paralysis. Death usually occurs 3-5 years from onset. In familial ALS, mutations in *TARDBP*, encoding the RNA binding protein TDP-43, cause 5% of cases. TDP-43 is mainly localized in the nucleus and has multiple functions, of which the best characterised is regulation of splicing/alternative splicing of hnRNA. In ALS TDP-43 mislocates to the cytoplasm causing the characteristic protein aggregations. The current work investigates the possible effects of both *TARDBP* missense mutations and a truncation mutation on RNA processing. This was approached by examining the changes in gene expression in both the cytoplasm and nucleus in fibroblasts derived from familial ALS-*TARDBP* patients. **Hypothesis:** The cytoplasmic and nuclear transcriptomic profile from mutant *TARDBP* fibroblasts will generate different transcriptomic profiles than control fibroblasts and will establish transcripts and pathways dysregulated in the presence of mutations in *TARDBP.* The objectives were 1) to optimize the separation of nuclear and cytoplasmic RNA from patient and control fibroblasts, 2) to compare the expression profiles of the cytoplasmic and nuclear compartments from control and mutant fibroblasts and 3) to determine the effect of both mutation types on gene expression in fALS. **Methodology:** Fibroblast cell culture from fALS-*TARDBP* missense mutation, truncation mutation and controls was performed. In addition, cell fractionation and RNA extraction were performed by two methods, osmotic pressure and Trizol and commercially available kit. Gene expression profiling was achieved using the Human Exon Array 1.0 ST, Human Transcriptome Array 2.0 (HTA) and RNA Sequencing. **Findings:** The presence of a *TARDBP* mutation causes change in gene expression in fALS. Cytoplasmic fALS-*TARDBP* missense mutations were significantly enriched with dysregulated RNA processing genes using both the Human Exon Arrays 1.0 ST and the HTAs while cytoplasmic fALS-*TARDBP* truncated mutation were enriched with dysregulated angiogenesis using the HTA and dysregulated vesicle mediated transport genes using RNA sequencing. The nuclear fALS-*TARDBP* missense

mutations demonstrated dysregulated RNA splicing using both the Human Exon Arrays 1.0 ST and the HTA while nuclear fALS-*TARDBP* truncated mutation was mainly enriched with G-protein coupled receptors using the HTAs. Therefore, fALS-*TARDBP* subtype mutations revealed distinct affected biological processes. **Conclusion:** The different types of *TARDBP* mutations assayed here have different effects on gene expression and subsequently on cellular pathways involved in *TARDBP*-related ALS.

Acknowledgement and dedication

I would like to thank my supervisors, Dr Paul Heath and Dr Janine Kirby for encouragement, support and guidance throughout my PhD. I would like extend my sincerest thanks to Mrs Catherine Gelsthorpe and Mr Matthew Wyles for providing me with technical assistance in the lab. I would also like to thank my friends in Sheffield for support. My deepest gratitude goes to ALS patients who donated samples for my project. I would also like to thank the University of Dammam for funding my project.

I would like to dedicate this PhD thesis to my adorable three years old daughter, Huda. Also to my loving parents Ali and Bahia, my brother Adam and my sister Eman.

Table of contents

List of tables

Chapter 1: Introduction

Chapter 2: Materials and methods

Human Exon Array 1.0 ST (HEA) and Human Transcriptome Array (HTA)

Q-RCR

RNA sequencing

Fluorescence In situ hybridization

Chapter 3: Human Exon 1.0 ST Arrays Genechip®

Chapter 4: Human Transcriptome Array Genechip®

Chapter 5: Next generation sequencing (RNA sequencing)

List of figures

Chapter 1: Introduction

Chapter 2: Materials and methods

Chapter 3: Human Exon 1.0 ST Arrays Genechip®

Chapter 4: Human Transcriptome Array 2.0 GeneChip®

Chapter 5: Next generation sequencing (RNA sequencing)

List of abbreviations

AD	Alzheimer's disease
ALS	Amyotrophic lateral sclerosis
AR	Autosomal recessive
B. subtilis	Bacillus subtilis
bp	Base pair
C9ORF72	Chromosome 9 open reading frame 72
cDNA	Complementary DNA
CNS	Central nervous system
CON	Control
DAVID	Database for Annotation, Visualization and Integrated Discovery
DMSO	Dimethyl sulfoxide
EJC	Exon junction complex
ES	Enrichment score
fALS	Familial amyotrophic lateral sclerosis
FC	Fold change
FTD	Frontotemporal dementia
FU	Fluorescence
FUS	Fused in sarcoma
hnRNP	Heterogeneous nuclear ribonucleoprotein
HEA	Human Exon Array 1.0 ST
HTA	Human transcriptome array
Inher	Inheritance
FISH	Fluorescence in situ hybridization
IVT	In vitro transcription
KCl	Potassium chloride
KEGG	Kyoto Encyclopedia of Genes and Genome
MgCl2	Magnesium chloride
MT	Missense mutation
Nt	Nucleotide
PCA	Principal component analysis
PD	Parkinson's disease
qRT-PCR	Quantitative Reverse transcription polymerase chain reaction
RIN	RNA integrity number
sALS	Sporadic amyotrophic lateral sclerosis
SMN1	Survival motor neuron 1
SOD1	Copper-zinc (Cu-Zn) superoxide dismutase1
ss	Single stranded
TAC	Transcriptome analysis console
TARDBP	Trans active response DNA binding protein
TDP-43	Trans active response DNA binding protein-43
TT	Truncation mutation
UV	Ultraviolet

Chapter 1: Introduction

1.1 Amyotrophic Lateral Sclerosis

Jean Marie Charcot was the first to report the characteristics of Amyotrophic Lateral Sclerosis (ALS) in the early 18th century. ALS is known as Charcot disease in many countries as an appreciation of his work. It is also known as Lou Gehrig's disease after the death of a famous New Yorker baseball player Lou Gehrig who suffered from ALS in 1939 (Kumar et al., 2011). ALS is a devastating chronic progressive neurodegenerative disorder characterized by the loss of the upper motor neurons in the motor cortex and the lower motor neurons of the brainstem and spinal cord. The average disease onset is 55 – 60 years. However, there is a juvenile form of ALS where patients are diagnosed in their twenties or earlier. Patients generally present with voluntary muscle weakness beginning in the limbs or bulbar musculature with progressive atrophy and paralysis. The fatality of the disease usually results from respiratory failure (Chen et al., 2013).

The average survival rate is approximately 2-5 years from the appearance of symptoms. The prevalence of ALS is nearly 2:100,000 with a higher incidence in men than in women (Ferraiuolo et al., 2011). ALS is multifactorial and in the majority of cases the actual cause is unknown. Moreover, ALS is categorized into two major types: familial ALS (fALS); which accounts for 5-10% of the cases; and sporadic ALS (sALS); which accounts for 90-95% of the cases. Both types present similarly, which may suggest common pathological causes. It was estimated that around 3-10% of ALS patients develop frontotemporal dementia (FTD) which is a condition characterized by the degeneration of the anterior part of the brain and also involves memory loss (Cooper-Knock et al., 2015c).

1.1.1 Clinical features

Most ALS cases present with limb onset ALS which accounts for ~80% of the cases. Limb onset ALS is further subdivided into lower limb onset ALS and upper limb onset ALS according to the location of motorneuron cell loss. Lower limb onset ALS patients usually complain about tripping or stumbling when walking.

However, the upper limb onset ALS patients usually complain from finger stiffness and weakness of the hand muscles. In ~20% of cases, ALS patients present with bulbar complications and are referred to as bulbar onset ALS. The bulbar onset ALS patients mainly suffer from slurred speech, dysphagia and excessive salivation (Kiernan et al., 2011). Also, rare cases of respiratory onset ALS have been reported accounting for <3% of cases (Shoesmith et al., 2007).

1.1.2 Diagnosis

ALS diagnosis is mainly dependent on the patient's symptoms across time. As motor neuron diseases (MND) have overlapping symptoms a definitive diagnosis may require a period of time to observe disease progression. Diagnosis is mainly accomplished by physical examination, investigative family history and electrodiagnostic testing, excluding other disorders. Electromyography and nerve conduction studies are both mostly used to assess and to evaluate muscle and nerve function. fALS patients may be offered genetic testing to confirm the diagnosis. Therefore, recent research has been focusing on the identification of biomarkers that help in the early detection of ALS and monitor the disease progression (Turner et al., 2009).

1.1.3 Treatment and management

To date there is no cure for ALS. However, there are a limited number of treatments available in the market which manage the disease progress. In most ALS cases, rapid deterioration as a result of disease is observed. Riluzole is the treatment given to all ALS patients in an attempt to slow the disease progression. It requires careful monitoring as it may induce liver damage and may suppress immunity by reducing leucocytes (Miller et al., 2007). Dramatic changes in ALS patient life style occur within the short course of the disease. Percutaneous endoscopic gastrostomy is offered to ALS patients to minimize the amount of body mass loss during disease progression and is especially given to those with bulbar disease onset who experience dysphagia (Spataro et al., 2011). Also, non-

invasive ventilation is offered to overcome respiratory insufficiency. In some countries, when disease worsens ALS patients undergo invasive ventilation due to respiratory failure (Swash, 2013).

1.1.4 Pathogenesis

To date, the exact defective molecular pathways in ALS are not fully understood, however, several studies have revealed evidence of pathogenic mechanisms involved in the disease. These include: genetic factors, dysregulated RNA processing, oxidative stress, mitochondrial dysfunction, glutamate excitotoxicity, defective axonal transport, protein aggregation, neuroinflammation, dysregulated endosomal trafficking and endoplasmic reticulum stress (Ferraiuolo et al., 2011) (Figure 1.1). An expanded elucidation of the role of the genetic risk factors and the dysregulated RNA processing proteins in ALS will be discussed.

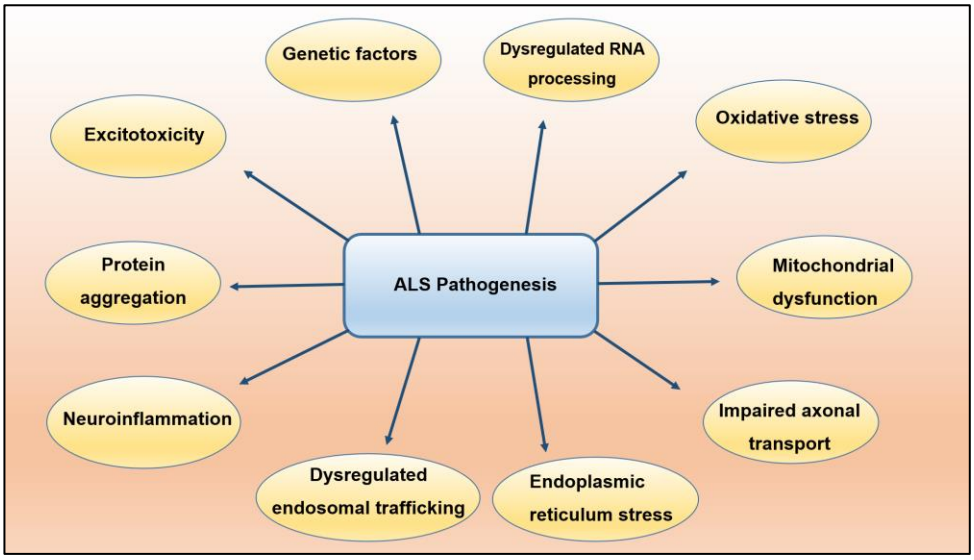

Figure 1.1: *Pathogenic mechanisms involved in amyotrophic lateral sclerosis*

1.1.4.1 The role of genetic risk factors in ALS

Genetic studies of fALS are growing rapidly in the field. To date there are 22 identified genes associated with disease (Table 1.1). The most common mutated genes related to ALS are: copper zinc (Cu-Zn) superoxide dismutase1 (*SOD1*) which is responsible of 12-20% of fALS and 1-2% of sALS (Banci et al., 2008, Marangi and Traynor, 2015), the trans active response DNA binding protein (*TARDBP*) which accounts for 4% of fALS and nearly 1% of sALS (Kirby et al., 2010, Millecamps et al., 2010, Ticozzi et al., 2011), fused in sarcoma (*FUS*) which was shown to be responsible for ~5% of fALS and ~1% of sALS (Rademakers et al., 2010, Ticozzi et al., 2011) and the newly discovered gene chromosome 9 open reading frame 72 (*C9ORF72)* which is responsible for 43% of fALS and 7% in sALS (Cooper-Knock et al., 2015c). A further discussion of these genes occurs below.

Table1.1: ALS types. AD= Autosomal dominant, AR= Autosomal recessive, Inher.= inheritance

ALS types	Locus	Gene symbol	Gene name	Inher	Onset	Reference
ALS1	21q22.11	*SOD1*	Cu/Zn superoxide dismutase	AD	Adult	(Rosen, 1993)
ALS2	2q33.1	*ALS2*	Alsin	AR	Juvenile	(Yang et al., 2001)
ALS3	18q21	*Unknown*	Unknown	AD	Adult	(Hand et al., 2002)
ALS4	9q34.13	*SETX*	Senataxin	AD	Juvenile	(Chen et al., 2004)
ALS5	15q21.1	*SPG11*	Spatacsin	AR	Juvenile	(Orlacchio et al., 2010)
ALS6	16p11.2	*FUS*	Fused in sarcoma	AD/ AR	Adult	(Kwiatkowski et al., 2009),(Vance et al., 2009)
ALS7	20p13	*Unknown*	Unknown	AD	Adult	(Sapp et al., 2003)
ALS8	20q13.23	*VAPB*	VAMP-associated protein B	AD	Adult	(Nishimura et al., 2004)
ALS9	14q11.2	*ANG*	Angiogenion	AD	Adult	(Greenway et al., 2006)
ALS10	1p36.22	*TARDBP*	TAR DNA-binding protein	AD	Adult	(Sreedharan et al., 2008)
ALS11	6q21	*FIG4*	Polyphosphoinositide phosphatase	AD	Adult	(Chow et al., 2009)
ALS12	10p13	*OPTN*	Optineurin	AD/AR	Adult	(Maruyama et al., 2010)
ALS13	12q24.12	*ATAXN2*	Ataxin-2	AD	Adult	(Figueroa et al., 2009), (Van Damme et al., 2011)
ALS14	9p13.3	*VCP*	Valosin-containing protein	AD	Adult	(Johnson et al., 2010)
ALS15	Xp11.21	*UBQLN2*	Ubiquilin 2	X-linked	Adult	(Deng et al., 2011)
ALS16	9p13.3	*SIGMAR1*	σ Non opioid receptor 1	AD	Adult/ Juvenile	(Luty et al., 2010) (Al-Saif et al., 2011)
ALS17	3p11.2	*CHMP2B*	Charged Multivesicular Body Protein 2B	AD	Adult	(Parkinson et al., 2006)
ALS18	17p13.2	*PFN1*	Proflin1	AD	Adult	(Wu et al., 2012)
ALS19	2q34	*ERBB4*	Erythroblastic Leukemia Viral Oncogene	AD	Adult	(Takahashi et al., 2013)
ALS20	12q13.13	*hnRNPA1*	Heterogeneous nuclear ribonucleoprotein A1	AD	Adult	(Kim et al., 2013)
ALS21	5q31.2	*MATR3*	Matrin 3	AD	Adult	(Johnson et al., 2014)
ALS22	2q35	*TUBA4A*	Tubulin alpha-4A	AD	Adult	(Smith et al., 2014)
FTD-ALS1	9q21	*C9ORF72*	Unknown	AD	Adult	(Hosler et al., 2000), (Renton et al., 2011), (DeJesus-Hernandez et al., 2011)
FTD-ALS2	5q35.3	*CHCHD10*	Coiled-coil-helix-coiled-coil-helix domain-containing protein 10	AD	Adult	(Bannwarth et al., 2014)
FTD-ALS3	12q14.2	*SQSTM1*	Sequestosome1	AD	Adult	(Fecto et al., 2011)
FTD-ALS4	12q14.2	*TBK1*	TANK-binding kinase1	AD	Adult	(Freischmidt et al., 2015)

1.1.4.1.1 Cu-Zn superoxide dismutase1 (*SOD1*)

A mutation in the *SOD1* gene was the first described genetic cause of ALS. In 1993, Rosen and his colleagues discovered mutations in the *SOD1* gene on chromosome 21q22.11 to be associated with the disease (Rosen, 1993). The pattern of inheritance of *SOD1* mutation(s) is primarily autosomal dominant. *SOD1* mutations are mainly missense however insertions and deletions have also been reported (Lill et al., 2011). The mutations are not restricted to the familial ALS; they were also reported in apparent sALS (Mackenzie et al., 2007).

The *SOD1* gene encodes for the enzyme Cu-Zn superoxide dismutase 1; a 153 amino acids long protein which is localized in the cytoplasm and the mitochondria. Normally it converts harmful superoxide radicals into oxygen and hydrogen peroxide (Yamanaka and Cleveland, 2005). Mutated SOD1 protein results in a toxic gain of function though the nature of this is unclear. It was shown that over expression of SOD1 mutation, mutant $SOD1^{G93A}$ and $SOD1^{A4V}$, in transgenic mice causes the mice to develop an ALS-like phenotype (Gurney et al., 1994). Overexpression of wild type *SOD1* gene in mouse has also shown a neuropathological outcome resembling ALS (Jaarsma et al., 2000). A complete depletion of the *SOD1* gene in mouse model did not show any ALS-like phenotype (Bruijn et al., 1998). Therefore, it hypothesized that dysfunctional SOD1 enzyme causes ALS through a toxic gain of function, rather than a loss of function (Ince et al., 2011).

1.1.4.1.2 Trans-active response DNA-binding protein (*TARDBP*)

The *TARDBP* encoded TDP-43 was first recognized by Neumann et al. as a major protein signature for ALS and FTD. Using immunohistochemical methods, TDP-43 was found to be present in the ubiquitinated cytoplasmic inclusions in ALS (Neumann et al., 2006). *TARDBP* is located on chromosome 1p36.22 and *TARDBP* mutations are inherited in an autosomal dominant pattern (Sreedharan et al., 2008). 53 *TARDBP* mutations have been identified so far with the majority being missense mutations located in the glycine rich domain of the encoded protein and only one truncation mutation has been identified

(http://alsod.iop.kcl.ac.uk/Overview/gene.aspx?gene_id=TARDBP) (Figure 1.2, adapted from (Lagier-Tourenne et al., 2010)). There are several protein isoforms encoded by the *TARDBP* gene which are mainly localized in the nucleus. TDP-43 is recognized to be the most significant isoform that plays a major role in ALS. Structurally, TDP-43 consists of 414 amino acids with a molecular weight of 43 kDa. It has three major domains; two RNA recognition motifs (RRM1 and RRM2) and a glycine rich domain. These structures facilitate nuclear localization and protein-protein interaction (Van Deerlin et al., 2008, Kuo et al., 2009a). TDP-43 binds directly to RNA preferably at the UG-rich sequences and also binds to double strand DNA at the TG-rich sequences. Therefor it is involved in transcription and RNA processing (Kuo et al., 2009c, Kirby et al., 2010) (see section 1.1.4.2.1 for more details).

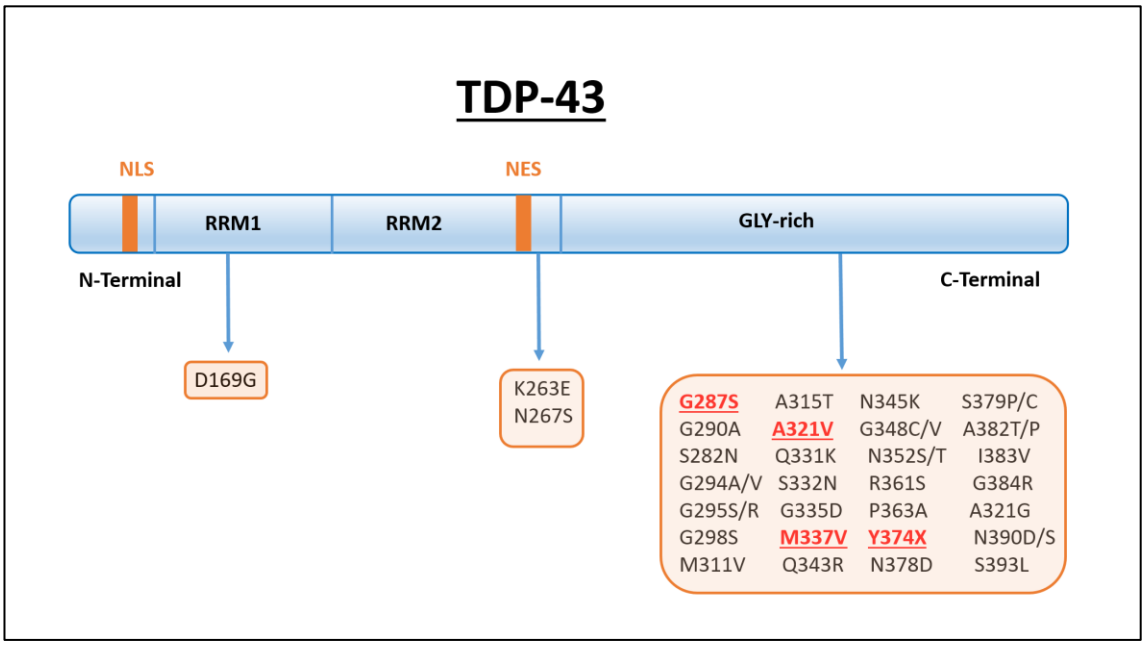

Figure 1.2: *Illustrates the location of 38 of the 53 mutations identified to date in TDP-43. RRM1= RNA recognition motifs1, RRM2= RNA recognition motifs2, GLY-rich= Glycine rich, NLS= nuclear localization signal, NES= nuclear export signal, variants labelled in red were studied in the current work. Figure adapted from (Lagier-Tourenne et al., 2010), http://alsod.iop.kcl.ac.uk/Overview/gene.aspx?gene_id=TARDBP.*

1.1.4.1.3 Fused in sarcoma/ translocated in liposarcoma (FUS/TLS)

The *FUS* gene was identified as playing a role in ALS by Kwiatkowski and colleagues in a Cape Verde family. The *FUS* gene is linked to chromosome 16p11.2 and the related defect is inherited both in autosomal dominant and autosomal recessive patterns. 25% of *FUS* mutations are located in exon 5-6 and 75% in exon 13-14 (Kwiatkowski et al., 2009, Vance et al., 2009, Hewitt et al., 2010). Mutations mostly occur in the glycine rich domain or at the nuclear signal domain, as a result the protein molecule loses its nuclear compartmentalization and there is an increase in cellular toxicity (Ince et al., 2011). FUS belongs to the heterogeneous ribonucleoprotein (hnRNP) family. It was shown that FUS binds directly to RNA and also to single strand DNA. Therefore it is involved in transcription and splicing (Wang et al., 2015).

1.1.4.1.4 Chromosome 9 open reading frame 72 (*C9ORF72)*

The large expansion hexanucleotide *GGGGCC* repeats of *C9ORF72* was recently discovered to be the most common cause of ALS and FTD. The mutation is located in intron 1 of the *C9ORF72* gene which is located at chromosome 9q21 (DeJesus-Hernandez et al., 2011, Renton et al., 2011). It was reported that the frequency of *C9ORF72* in ALS patients is ~43% in fALS and 7% in sALS (Cooper-Knock et al., 2012a). In addition, up to ~50% of ALS-*C9ORF72* had a history of FTD. Furthermore, it has been shown that both ALS-*C9ORF72* positive and ALS-*C9ORF72* negative patients share similar clinical presentation however the ALS-*C9ORF72* positive patients demonstrated a shorter survival rate (mean<32 months) (Cooper-Knock et al., 2012a). Also, a study has shown that in ALS-*C9ORF72*, neurons and glial cells from post mortem tissue showed TDP-43 positive inclusions (Stewart et al., 2012).

1.1.4.2 The role of RNA processing in ALS

RNA processing is a group of different molecular events that take place in the nucleus (Figure 1.3). These events include: 5'capping (7-methylguanosine), splicing and 3' polyadenylation (Garneau et al., 2007). Transcription is the first

step in which a DNA template is copied, both exons and introns, with the thymine replaced by uracil. 5'capping-7-methylguanosine is added simultaneously during transcription processes. Splicing occurs co-transcriptionally, this is a modification step in which intronic regions (noncoding) are removed and the exonic regions (coding) are joined. Also 3' polyadenylation takes place. (Garneau et al., 2007).

Mutations in RNA processing genes have been identified in ALS. Mutations in the *TARDBP* gene which encodes for the RNA binding protein TDP-43 were identified in both fALS and sALS (Neumann et al., 2006, Van Deerlin et al., 2008). Furthermore, changes in FUS were then discovered and it was found to be an hnRNP that is involved in several aspects of RNA processing. Mutations in *FUS* were associated with ALS (Kwiatkowski et al., 2009). The newly identified mutation in the *C9ORF72* gene, which is responsible for the majority of the genetic related cases of ALS, has also been demonstrated to disrupt RNA processing (Cooper-Knock et al., 2015a)

Additional RNA processing proteins that are involved in the pathogenesis of ALS have been described. Some variants of the angiogenin gene (*ANG*) were suggested as a risk factor for fALS and sALS in individuals of Scottish or Irish ancestry (Greenway et al., 2006). ANG is considered a member of the pancreatic RNase A superfamily. It is also capable of stimulating rRNA transcription under hypoxic conditions, thereby promoting neovascularisation (Gao and Xu, 2008). Furthermore, mutations in senataxin (*SETX)* were associated with a juvenile form of ALS (Chen et al., 2004). SETX has a DNA/RNA helicase activity which is involved in RNA processing by unwinding the DNA or RNA molecule (Zhao et al., 2009). Mutations in some variants of the elongator protein 3 (*ELP3*) were suggested be a risk factor for ALS. ELP3 is a component of the RNA polymerase II which is involved in RNA processing (Simpson et al., 2009a). In addition, abnormal copy number of the survival motor neuron 1 (*SMN1*) gene is a risk factor for sALS (Corcia et al., 2002). SMN1 is also involved in transcription and RNA splicing (Eggert et al., 2006).

As TDP-43, FUS and C9ORF72 are three most commonly dysregulated RNA processing proteins associated with ALS, further discussion of their pathogenic mechanisms in relation to RNA processing will follow.

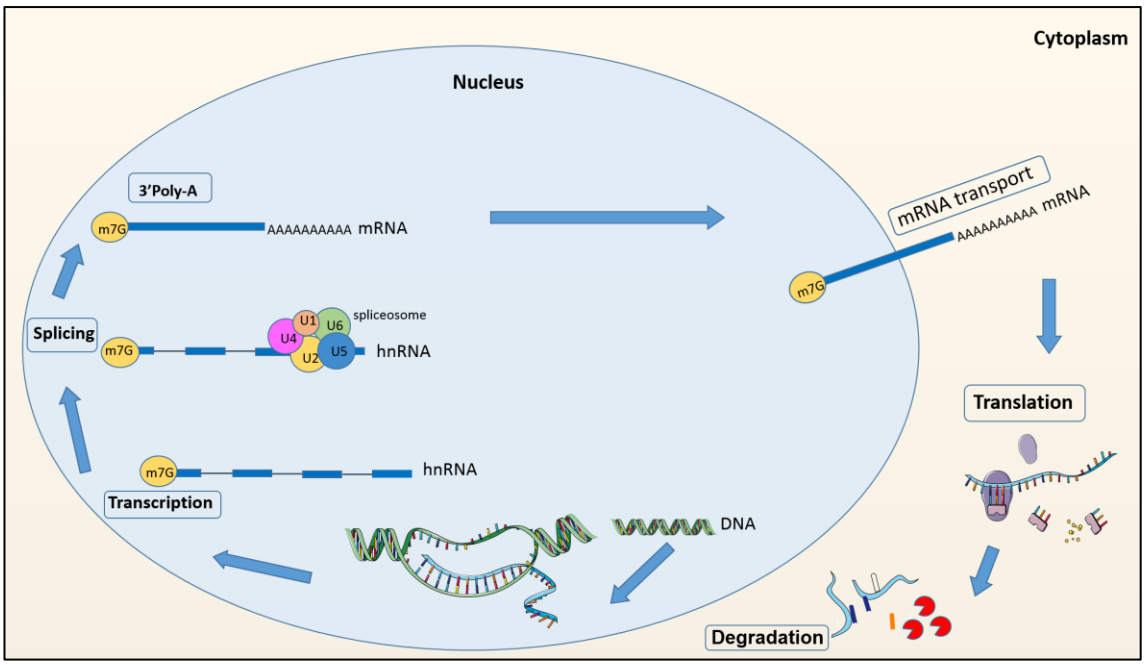

Figure 1.3: *Schematic diagram representing the transcription, co-transcriptional processing event, mRNA transport, translation and degradation.*

1.1.4.2.1 TAR DNA binding protein 34 (TDP-43)

TDP-43 is a heterogeneous ribonucleoprotein (hnRNP) with a 43kDa molecular weight. As explained previously (section 1.1.4.1.2), TDP-43 consists of 414 amino acids. It has N terminus homodimerization domain with an ubiquitin-like fold, RNA recognition motifs (RRM1 and RRM2) and a glycine rich domain (Kuo et al., 2009a). TDP-43 was first recognized as a transcription repressor which binds to TAR DNA in Human immunodeficiency virus-1(HIV-1) (Ou et al., 1995). In addition, Abhyankar et al. demonstrated that TDP-43 is capable of binding to the *SP-10* promoter region in mouse which is essential for spermatogenesis (Abhyankar et al., 2007).

The majority of TDP-43 functions were observed in regulation of other RNA processing mechanisms. TDP-43 has been shown to regulate alternative splicing of the genes for several proteins such as: apolipoprotein A-II and cystic fibrosis trans-membrane regulator (*CFTR*). In the case of *CFTR*, TDP-43 binds to a UG rich area of a *CFTR* intronic region, specifically the intron 8 – exon 9 junction. This action promotes exon 9 skipping of *CFTR* mRNA (Buratti et al., 2001). Depletion of TDP-43 leads to ineffective exon 9 skipping (D'Ambrogio et al., 2009). TDP-43 also regulates alternative splicing of the apolipoprotein A-II gene by binding to the intron 2 – exon 3 region (Mercado et al., 2005).

In sALS mutant forms of TDP-43 has been strongly implicated in dysregulated RNA splicing and affected spliceosome components (Highley et al., 2014). Furthermore, genes involved in RNA splicing were also shown to be dysregulated in sALS cases with *TARDBP* mutations (Raman et al., 2015). A recently identified function of TDP-43 was its ability to suppress cryptic exonic splicing. Cryptic exons are non-conserved sequences expression of which might result in faulty mRNA transcripts that deteriorate and therefore be cleared by the nonsense-mediated decay machinery. De Conti et al. has recently shown that the loss of TDP-43 function directly affects the splicing profile of six genes which were: *BIM, SKAR/POLDIP3, STAG2, MADD, FNIP1* and *BRD8* (De Conti et al., 2015). Studies have also shown that TDP-43 binds to multiple mRNA transcripts and is hence thought to regulate their splicing (Polymenidou et al., 2011, Sephton et al.,

2011, Xiao et al., 2011). Ayala et al., have recently shown the role of TDP-43 in autoregulation. It was demonstrated the ability of TDP-43 to bind to the 3' end untranslated region (3'UTR) of *TARDBP* mRNA leading to instability and decay (Ayala et al., 2011). Moreover, Tollervey et al., showed that TDP-43 binds to transcripts at the UG-rich sequences of long pre-mRNAs (Tollervey et al., 2011).

TDP-43 has also been demonstrated to play a role in microRNA processing. It was shown that TDP-43 is capable of binding to the RNA III endonuclease Drosha in the nucleus during microRNA synthesis. It was also shown to participate in microRNA cleavage in the cytoplasm by interacting with the protein argonaute 2 during microRNA maturation (Freibaum et al., 2010). Finally, TDP-43 may be involved in mRNA transport to the cytoplasm (Wang et al., 2008).

1.1.4.2.2 Fused in sarcoma/ translocated in liposarcoma (FUS/TLS)

The FUS protein consists of 526 amino acids and is characterized by; an N-terminal domain rich in tyrosine, serine, glycine and glutamine, a C-terminal domain which contain a nuclear localization signal (NLS), an RNA recognition motif (RRM) and a zinc finger motif (Kwiatkowski et al., 2009, Vance et al., 2009). Similarly to TDP-43, FUS belongs to the heterogeneous ribonucleoprotein (hnRNP) family and is mainly involved in RNA processing such as: transcription, transport, and splicing (Lagier-Tourenne et al., 2010). FUS is an ubiquitinated protein which is normally located in the nucleus, however in ALS it is mutated and was shown to form characteristic cytoplasmic inclusion bodies (Kwiatkowski et al., 2009, Vance et al., 2009).

1.1.4.2.3 Chromosome 9 open reading frame 72 (*C9ORF72)*

C9ORF72 was shown to encode for three mRNA isoforms which encode for two protein isoforms of 481 amino acids ~50kDa and 222 amino acids ~25 kDa (DeJesus-Hernandez et al., 2011). The normal function of *C9ORF72* is still not fully understood. However, a recent study by Webster et al., showed that normal C9ORF72 mediates the initiation of the autophagy pathway by forming complexes with two other proteins, Rab1a and ULK1, to facilitate the

autophagosome formation (Webster et al., 2016). Furthermore, it was also suggested that C9ORF72 is a nucleocytoplasmic shuttling protein (Xiao et al., 2015). Other studies showed the possible pathological role of the C9ORF72 in the disease pathogenesis. Researchers have suggested two main pathologic mechanisms of the *C9ORF72,* either loss of function or toxic gain of function. These proposed mechanisms were based on current observations, first was the low expression levels of the *C9ORF72* variant 1 in patients compared to controls which may support loss of function (Fratta et al., 2012). In contrast, the toxic gain of function was proposed based on two suggestions, *GGGGCC* hexanucleotide repeats were suggested to undergo a non-ATG translation which results in the formation of pathogenic toxic dipeptide proteins (Cleary and Ranum, 2013). In addition, the formation of nuclear RNA foci which sequestered RNA and RNA binding proteins which might be toxic to the cell and their presence may indicate a defective RNA processing mechanism however this is still under study (Mizielinska and Isaacs, 2014). A study by Cooper-Knock et al., showed that RNA splicing was defective which may lead to neuron injury. In ALS-*C9ORF72* cases, defective RNA splicing correlated positively with the disease progression (Cooper-Knock et al., 2015a). This supports the hypothesis that the C9ORF72 hexanucleotide expansion disrupts RNA processing. Whether the normal protein is involved in RNA processing remain to be established.

1.1.5 Gene expression profiling in ALS using human tissues and cells

An adequate amount of RNA is required for gene expression profiling studies and for qRT-PCR validations. Current studies showed that different tissue sources from ALS patients can be used to extract RNA material and study gene expression changes that occur in the disease process. The three main tissue types previously used to study ALS are: motor neurons extracted from post-mortem tissue, venous whole blood and fibroblasts. Each of the advantages and limitation of these tissue sources will be discussed below.

1.1.5.1 Use of human CNS tissue

There is no doubt that motor neurons from the central nervous system (CNS) are the best source to study ALS as they demonstrate the actual changes that occur in the disease. However major limitations have been identified. Motor neurons are not accessible during the course of the disease and only available from post-mortem tissue where most of the motor neurons are lost. This may result in an examination of a sub-population of motor neurons that have survived the worst of the disease process and hence are not fully representative. RNA extracted from post-mortem tissue is often markedly degraded. This may be due to delay in processing the CNS tissue, the pre-mortem state of the sample and also as an effect of any chemical preservation (Sidova et al., 2015). As stated another essential point is that studying gene expression changes from post-mortem tissue will only reflect the end stage of the disease giving limited therapeutic approaches (Cooper-Knock et al., 2012d). With these kind of limitations a shift towards utilizing peripheral tissue derived from ALS patients has been applied.

1.1.5.2 Use of human peripheral tissue

1.1.5.2.1 Venous whole blood

Venous whole blood has been shown to overcome some of the limitations of post-mortem tissues. Fresh blood samples are easy to collect from ALS patients at any stage of the disease. Also, adequate quantities of RNA can be obtained from blood collected via a simple venipuncture procedure. Studies on ALS using peripheral blood were shown to be a great source that may mimic some changes in the motor neurons (Bayatti et al., 2014, Bury et al., 2016). The limitation of using of whole blood is the mixed cell population and the increased amount of globin RNA which may mask some changes in gene expression (Wright et al., 2008), though this can be limited by using commercially available globin RNA removal kits. However, this remains a favourable source of material for diagnostic biomarker identification.

1.1.5.2.2 Fibroblasts

Fibroblasts are easy to collect from patients via skin biopsies and also are easy to grow in the laboratory. They have shown to be a good model to study gene expression profiling in neurodegenerative disorders. Fibroblasts from Parkinson's disease patients with a mutated *parkin* gene showed mitochondrial abnormalities which mimic the changes in the neurons (Mortiboys et al., 2008). Fibroblasts from siblings to familial Alzheimer's disease patients with mutations in one of the genes, amyloid precursor protein (*APP*), presenilin 1 (*PSEN1*) and presenilin 2 (*PSEN2*), were utilized to detect diagnostic biomarkers before the onset of cognitive decline (Nagasaka et al., 2005). Furthermore, fibroblasts from ALS patients were used to study gene expression changes during the disease (Raman et al., 2015). Fibroblasts have been used to investigate the role of oxidative stress, mitochondrial dysfunction and dysregulated RNA processing in ALS (Allen et al., 2014, Highley et al., 2014, Raman et al., 2015). In these studies, fibroblasts have been shown to be a good source of cells that can be used in the laboratory and showed changes that mimics those observed in the disease process.

1.1.6 Gene expression profiling

The discovery of microarray technology has helped considerably in understanding the gene activity in biological samples (Heller, 2002). In research, GeneChip® microarrays have been used for a wide range of purposes, such as: identification of biomarkers and discovery of novel genes. Whilst several GeneChip® arrays have been designed throughout the years they share common method of design and production. GeneChip® platforms consist of short sequences of probes attached to a plastic wafer via both chemical reactions and photolithography (http://www.affymetrix.com).

The three main human microarray GeneChips® designed by Affymetrix® used to study global gene expression were, the In Vitro Transcription (IVT) Array, Human Exon 1.0 ST Array and Human Transcriptome Arrays 2.0. More recently next generation sequencing (RNA sequencing) has been developed to study global

gene expression profiling. A further description of these microarrays and the next generation sequencing is shown below.

1.1.6.1 In Vitro Transcription (IVT) Array GeneChip®

The IVT Array GeneChip® were first made commercially available in April 2001, to enable global gene expression profiling. The arrays were designed targeting the 3' end region of mRNA. It consists of 1.3 million features with a total of ~ 54,000 probe sets. Each transcript is represented with 11 perfect match probes and 11 mismatched probes at the 13th position of the 25 base pair long probe. The probe sequences were designed against the available known sequences in the data bases NCBI, dbEST, GenBank® and RefSeq database (http://www.affymetrix.com).

Gene expression profiling using the IVT arrays has been used extensively. However, these arrays had limitations. They were dependent on the detection of polyadenylated mRNA which may result in the loss of several transcripts that lack a poly A tail. A challenging issue was also the detection of mRNA transcripts which undergo alternative polyadenylation. The 3' IVT arrays probe sets were designed based on available known 3' end sequences. Therefore, they were unable to detect alternatively polyadenylated transcripts (D'Mello et al., 2006). With these limitations in mind Affymetrix® designed the Human Exon 1.0 ST Array GeneChip® with better features (see 1.1.6.2).

1.1.6.2 Human Exon 1.0 ST Array GeneChip®

The Human Exon 1.0 ST Array GeneChip® has shown several advantages over the conventional 3' IVT array GeneChip®. They provide the maximum information needed to understand total gene expression as their target is to detect transcripts along the entire length of mRNA rather than the 3' end region. This unique feature also suggested that novel spliced transcripts could be discovered. Each exon is presented on the GeneChip® by four perfect match probes scattered throughout the chip. The array consists of 1.4 million probe sets and over a million exon clusters. The feature size is 5µm X 5µm and each probe is 25 base pair long.

These exons were identified against known sequences from databases, Genbank, Ensembl and dbEST (*in July, 2003*) (www.Affymetrix.com).

1.1.6.3 Human Transcriptome Arrays 2.0 GeneChip®

In 2011, Affymetrix® designed the Human Transcriptome Arrays 2.0 (HTA) which showed improved features compared to the Human Exon 1.0 ST Array GeneChip®. This was achieved by increasing the probe density from 4 probes per exon to 10 probes per exon and including 4 probes for each predicted exon-exon splice junction. Furthermore, these probe sequences have been compared to an available mRNA database. ~94% of mRNA sequences in the data mapped to the probes designed on the arrays. 85% of the mapped mRNA sequences from the database were exons and 7% were exon-exon junctions (Xu et al., 2011). The HTA contain > 6.0 million feature oligonucleotides and they utilize low RNA concentrations of total RNA (50ng – 500ng) for input. These highly efficient arrays were designed to identify instances of alternative splicing, coding SNP and noncoding transcripts. Furthermore, they are designed to be analysed with their own software known as Transcriptome Analysis Console (TAC). The software has a unique feature which is the assembling of multiple data sources in one compact software package. Thus, all transcript isoforms of a known gene can be analysed in a single analysis tool (Xu et al., 2011).

1.1.6.4 Next generation sequencing (NGS) (RNA sequencing)

The first widely used DNA sequencing method was developed by Frederick Sanger who described the chain-termination method that led to the initial identification of the human genome sequence (Sanger et al., 1977). In the past decade there has been a rapid development of new sequencing technologies. Now, NGS is widely available in the market and serves numerous areas such as: clinical diagnostics, genetic disease studies and molecular biology studies (Morozova and Marra, 2008). The most commonly used type of DNA sequencing nowadays is the sequencing by synthesis which was first introduced by Balasubramanian and Klenerman in 1989 and commercialised under the banner Solexa (http://www.illumina.com/technology/next-generation-sequencing/solexa-

technology.html). In 2004, the Solexa technology was purchased and enhanced by introducing the DNA cluster amplification method which increased the accuracy of base calling which was then known as Illumina sequencing. (http://www.illumina.com/technology/next-generation-sequencing/solexa-technology.html)

The principle of this method is that mRNA is converted into double stranded cDNA molecule which is then fragmented and tagged by an index sequence and a flow cell adaptor sequence. Each fragmented single stranded molecule is clustered via an isothermal amplification method. This is performed within a flow cell glass slide that is composed of different lanes. Each lane is internally coated with short sequence oligonucleotides complementary to the adaptor region on the fragmented single stranded cDNA. Once the reaction starts the fragmented double stranded molecules are made single stranded and bound to the short sequence oligonucleotides complementary to the adapter region. These processes initiate the DNA polymerase to synthesise the reverse stand. The original stand is denatured and cleaved. The reverse strand is then cloned by a bridge amplification method forming millions of clusters. This process is followed by the sequencing step, also known as sequencing by synthesis, reversible fluorescent terminator nucleotides are incorporated into the newly synthesised DNA sequence. The four chemically modified nucleotides (2,3 dideoxynucleotide) are added to the DNA molecule by DNA polymerase allowing one of the four nucleotides to bind to the DNA sequence in each synthesis cycle as a result of complementary hybridisation. This is followed by a washing step to remove all the remaining nucleotides. The nucleotides are then excited by a light source and a snapshot image of the incorporated terminated nucleotides is taken by a camera. The synthesis cycle is repeated until the cDNA fragment is sequenced. These images are then combined and interpreted as a cDNA sequence (http://www.illumina.com/technology/next-generation-sequencing/sequencing-technology.html) (Figure 1.4).

This method has major advantages. It is the only one that can perform a single read as well as paired-end reads which increases the efficiency and resolution of the genome sequence. Paired-end read generation overcomes many issues that

are faced in sequencing, for example: the alignment of DNA sequence that contains repetitive sequences. It can, to some degree, identify rearrangements such as deletions, insertions and inversions in addition to novel spliced isoforms (Figure 1.5), depending on the size of the expansion, insertion, deletion or inversion.
(http://www.illumina.com/technology/next-generation-sequencing/sequencing-technology.html)

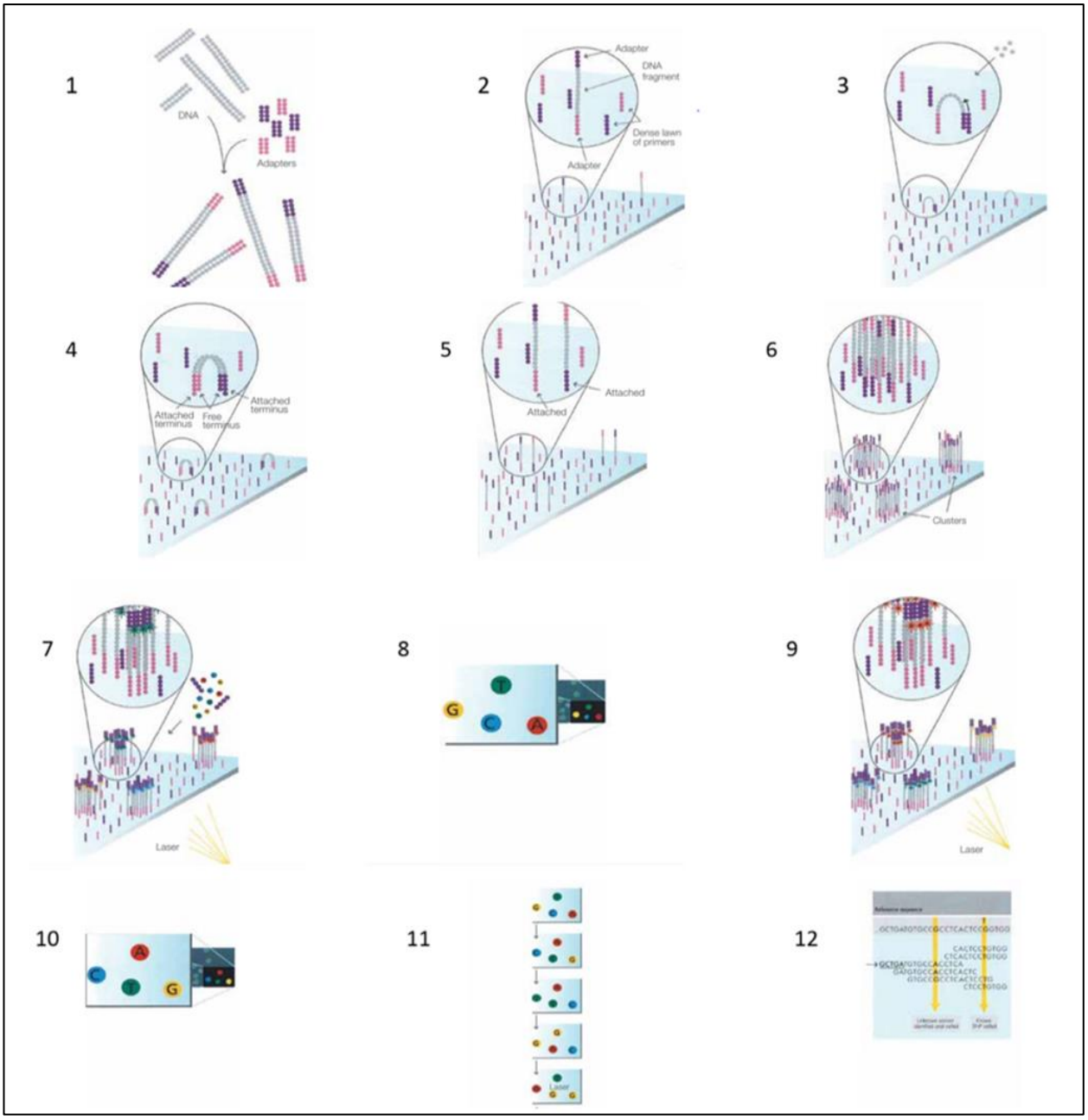

Figure 1.4: *Illumina Sequencing workflow. (1) the DNA is fragmented and ligated to the adaptors (2)The fragmented single stranded DNA is attached to the surface of the flow cell in the channels (3) unlabelled nucleotides are added along with enzymes to initiate the bridge amplification (4) A double strand bridge is synthesis on the flow cell (5) the original stand is denatured and cleaved leaving the reverse strand (6) bridge amplification continues to form millions of clusters (7) the sequencing cycle starts by the addition of the four labelled reverse terminator nucleotides along with DNA polymerase and primers (8) the laser excite the fluorescent labelled incorporated nucleotide and an image is captured to detect the first base (9&10) is a repeated process of the synthesis cycle steps 7&8 (11) all the images are combined to identify the DNA sequence (12) data alignment to the reference sequence. (Image from Illumina sequencing webpage:* http://www.illumina.com/documents/products/techspotlights/techspotlight_sequencing.pdf *)*

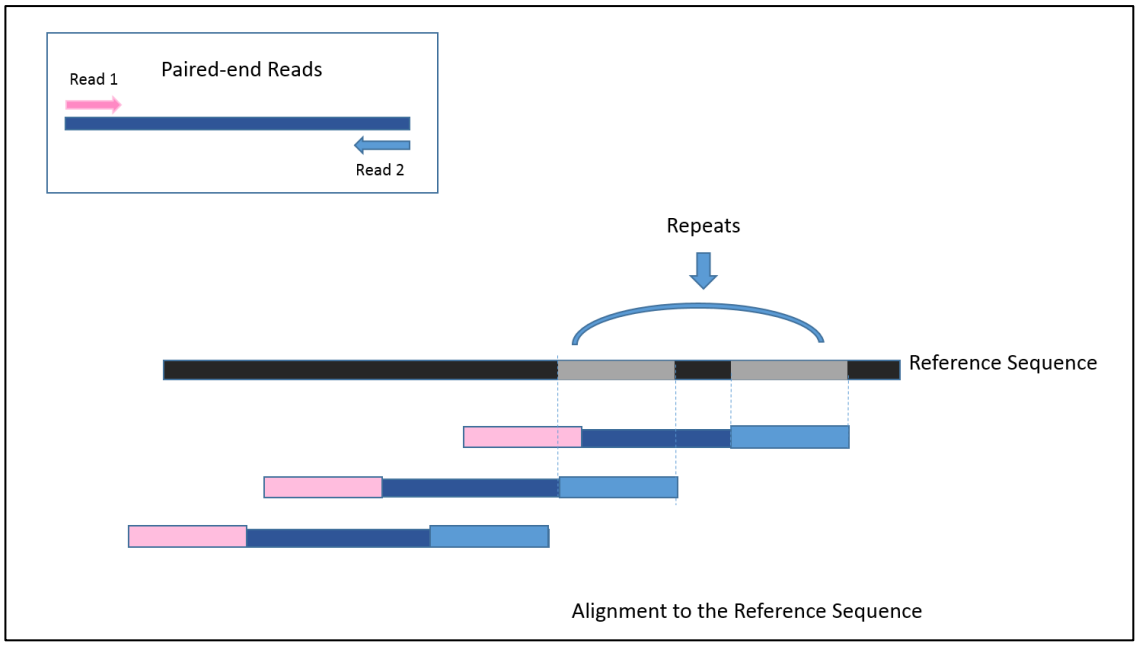

Figure 1.5: *Paired-end Sequencing and alignment detecting sequence repeats.*
(Adapted from: http://www.illumina.com/technology/next-generation-sequencing/paired-end-sequencing_assay.html)

1.1.7 Studying alternative splicing

Alternative splicing is defined as the mechanism that allows the production of different transcript isoforms from a single gene. It is one of the most complex functions that the human genome undergoes. Over 92% of the human genome is alternatively spliced which indicates its importance in many cellular mechanisms and pathways (Blencowe et al., 2009). A defective alternative splicing process has been implicated in several neurodegenerative disorders. Mutations in RNA processing genes lead to disorders other than ALS, for example: Alzheimer's disease (AD) (Amyloid-β), Parkinson's disease (PD) (α-synuclein), FTD (TDP-43) and spinal muscular atrophy (SMA) (SMN1) (Tang, 2016). Each of these neurological disorders has distinct complex defective cellular mechanisms and pathways. Thus, studying the role of RNA processing

genes is potentially important to underline how these diseases develop as well to establish therapy.

1.1.8 The rationale behind the project 'cytoplasmic and nuclear gene expression profiling'

This study was developed based on two major observations. The first was that TDP-43 is an RNA binding protein that is normally located in the nucleus and has a role in RNA processing and particularly in splicing. In ALS TDP-43 is mutated and mislocalized resulting in the characteristic cytoplasmic inclusion bodies (Neumann et al., 2006). Studies have shown that TDP-43 binds to multiple mRNA transcripts, thereby thought to regulate their splicing (Polymenidou et al., 2011, Sephton et al., 2011, Xiao et al., 2011). However the actual effect of how mutant TDP-43 dysregulates the splicing machinery in ALS has not been studied before. Thus, the current work aimed to uncover possible dysregulated mRNA spliced transcripts in fALS-*TARDBP*.

The second observation which initiated this current work was an interesting study conducted by Trask et al., in 2009, which studied gene expression profiling on separate cellular components i.e. cytoplasmic RNA and nuclear RNA extracted from the same cell line. They showed strong supporting evidence that mRNA extracted from the whole cell does not accurately represent cytoplasmic mRNA and that polyadenylated nuclear mRNA should not be neglected as their contribution is significant (Trask et al., 2009).

Therefore, it was interesting to explore the possible effects of mutant TDP-43 on mRNA splicing on both cellular compartments in fALS-*TARDBP* mutations as this was not been studied before. As TDP-43 is an ubiquitinated protein which is expressed in fibroblasts of ALS patients (Sabatelli et al., 2015), the present study aimed to utilize fibroblasts derived from fALS patients to understand the cellular defective mechanisms and pathways related to TDP-43 mutation using the

following technologies: the Human Exon 1.0 ST Arrays, the Human Transcriptome Arrays and RNA sequencing.

1.1.9 Hypothesis

Cytoplasmic and nuclear transcriptomic profile from mutant *TARDBP* will generate different transcriptomic profiles than control fibroblasts.

This will establish the dysregulated pathways in the presence of mutations in *TARDBP*.

1.1.10 Objectives

1. To produce a good quality and quantity of separated cytoplasmic and nuclear RNA from mutant *TARDBP* fibroblasts and control fibroblasts.

2. To compare the expression profiles of the cytoplasmic and nuclear compartments of the cell from control and mutant *TARDBP* fibroblasts.

3. To determine the effect of the *TARDBP* mutation in the cytoplasmic and nuclear RNA expression profile.

Chapter 2: Materials and methods

Table 2.1: Reagents and suppliers

Reagents	Supplier
Agencourt AMPure XP beads	Beckman Coulter
Ammonium acetate	Sigma
Chloroform	Fisher Scientific
Cytoplasmic and nuclear RNA purification kit	Norgen biotek
DMSO	Sigma
DNase treatment	New England Biolabs
Dithiothreitol	Sigma
Ethanol	Fisher scientific
Ethidium bromide	Fluka
Essential Media (MEM) with Earle's Salts and L-Glutamine	Lonza
Fetal bovine serum (FBS)	Biosera
GeneChip® arrays and reagents	Affymetrix
Glycoblue	Ambion
HEPES	Sigma
Hyper ladder lV	Bioline
Hyper ladder V	Bioline
Isopropanol	Fisher Scientific
KCl	Fisher
MgCl2	Sigma
MycoAlert ® *Mycoplasma* Detection Kit	Lonza
Na pyruvate	Sigma
Non-essential amino acids	Lonza
Penicillin / streptomycin solution	Lonza
pH meter	ORION
Protease Inhibitor Cocktail	Sigma
Quantitect Reverse Transcriptase kit	Qiagen
RNAse inhibitor	Bioline
RNase-free water	Ambion
Stratagene Brilliant II SYBR® Green PCR Master Mix	Agilent Technologies
Trizol	Ambion
Trypan blue	Sigma
Trypsin	Lonza
Uridine	Alfa Aesar
Vitamins	Lonza

Table 2.2: Equipment and suppliers

Equipment	Supplier
BioAnalyser 2100	Agilent
Centrifuge	Sigma
Filtered pipette tips	Fisher Scientific
G25 needles	BD microlance TM
Hoods	Envair
Incubator	SANYO
M3000P qPCR	Agilent Technologies
Nanochips	Agilent Technologies
Nanodrop 1000 Spectrophotometer	Labtech International, UK
Next generation sequencing (Hi scan SQ system)	Illumina
PCR plates and sealing caps	BIOplastics
Serological pipette	Fisherbrand
TBE gel (4-20%)	Invitrogen
Thermo Cycler	MJ Research
T75 flasks	Thermo scientific
Water bath	Grant

2.1 Fibroblast cell culture

All samples were collected according to the ethical approval granted by NRES Committee for Yorkshire and Humber (REC ref 12/YH/0330; Protocol number STH16573).Frozen control and *TARDBP* patient fibroblasts were closely matched for age and sex (Table 2.3).

Control and *TARDBP* patient fibroblasts were defrosted from liquid nitrogen at room temperature and were cultured using the minimum essential media (MEM) with Earle's Salts and L-Glutamine supplemented with the following: 10%fetal bovine serum (FBS), 1%Sodium pyruvate, 1%non-essential amino acids, 1%vitamins, 0.25mg/ml uridine and 1%penicillin streptomycin solution. To each cultured fibroblasts 10ml of pre-warmed media was added to the cells in a T75 flask and allowed to grow at 37°C, 5%CO_2 in a humid incubator. Cells were examined regularly under a light microscope and estimated confluency was recorded.

Table 2.3: Control and patient fibroblasts characteristics. Fibcon= Fibroblast control, Fibpat=Fibroblast patient

Condition	Fibroblast ID	Gender	Mutation	Age at time of skin biopsy
Controls	Fibcon 2303	Male	None	62
	Fibcon 155	Male		40
	Fibcon 170	Male		63
	Fibcon 159	Female		62
	Fibcon 8	Female		41
	Fibcon 11	Male		58
Missense mutation	Fibpat 48	Female	p.A321V	40
	Fibpat 51	Male	p.M337V	62
	Fibpat 55	Male	p.G287S	56
Truncated mutation	Fibpat 192	Male	p.Y374X	41
	Fibpat 193	Male	p.Y374X	53
	Fibpat 194	Male	p.Y374X	68

2.1.1 Splitting fibroblasts

Fibroblasts were passaged regularly when they reached ~90% confluency. Cells were washed with 5ml of 1x phosphate buffered saline (PBS), harvested with 1ml of trypsin (0.5µg/l-EDTA 0.2µg/L) and neutralized with MEM at a ratio of 1:3. Then cells were equally distributed into a number of flasks with 10ml of pre-warmed MEM, incubated at 37°C, 5% CO_2.

2.1.2 *Mycoplasma* testing

In SITraN all cell samples were tested by a member of the technical team staff. The kit used was *MycoAlert ® Mycoplasma Detection Kit by Lonza.*

2.2 Cell fractionation and RNA extraction

2.2.1 Cell fractionation and RNA extraction using Norgen kit for Cytoplasmic and Nuclear RNA Purification

When fibroblasts reached ~90% confluency they were harvested for cell fractionation and RNA extraction (Figure 2.1). The procedure was performed using *Norgen kit for cytoplasmic and nuclear RNA purification,* (*product number 2100*).

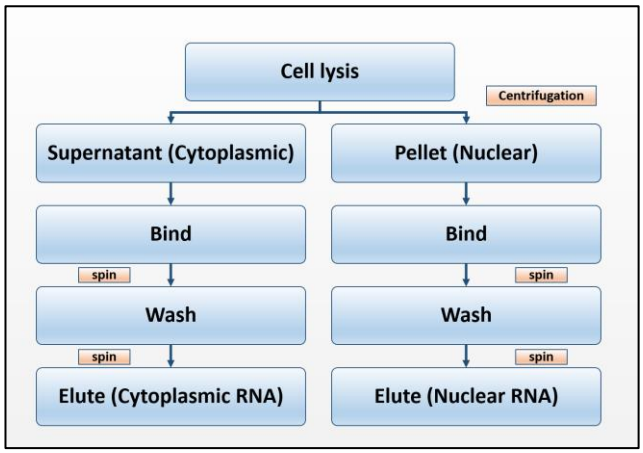

Figure 2.1: *A flow chart illustrating cell fractionation and RNA extraction. Adapted from: https://norgenbiotek.com/sites/default/files/resources/Cytoplasmic-Nuclear-RNA-Kit-Insert-PI21000-19-M14.pdf*

2.2.2 Cell fractionation by osmotic pressure

Fibroblast cell membranes were lysed using freshly prepared lysis buffer (1ml of hypotonic lysis buffer (10mM HEPES pH 7.9, 1.5mM $MgCl_2$,10mM KCl, 0.5mM DTT), 1x of protease inhibitors complete (PIC), 2µl of (40 u=U/µl) RNAse inhibitor. To the contents of three combined confluent T75 flasks 200µl of lysis buffer was added. Cells were slowly re-suspended then passed through a G25 needle 10 times every 10min. The lysate was examined under light microscope to evaluate the lysed cells and to monitor the nucleus integrity. Trypan blue was used to stain the nuclei by mixing 1:10 ratio of lysate to trypan blue. 10µl of the stained lysate was applied on a plain slide and covered with coverslip then examined under a light microscope. After 20min, the cytoplasm was separated from nuclei by centrifugation at 13,000rpm for 3min at 4°C. At that point the supernatant was the cytosol and the pellet was the nuclei. The supernatant was transferred to a fresh tube and placed on ice. 100µl of lysis buffer was then added to the nuclei to lyse the nuclear membrane. It was carefully mixed and passed through a G25 needle several times. The nuclear lysate was examined under light microscope to evaluate nuclei lysis. After complete nuclear lysis, RNA extraction was performed on both the cytoplasmic and the nuclear fractions.

2.2.2.1 RNA extraction by Trizol method

A ratio of 3:1 of Trizol was mixed with the lysate and incubated for 10min at room temperature. Afterwards, 1:5 ratio of chloroform was added and mixed for 20sec then incubated for 5min at room temperature followed by centrifugation at 11,000rpm for 10min at room temperature. The aqueous phase was transferred to a new tube. Then RNA was washed with equal volume of absolute isopropanol. The precipitated using the glycoblue precipitation method (see below section 2.3)

2.3 Glycoblue precipitation method

1µl of 15mg/ml glycoblue reagent was applied to the RNA samples. Next, a ratio of 1:15 of 7.5M ammonium acetate was added. Then, an equal amount of

absolute isopropanol was added to the total volume, mixed and incubated at -20°C overnight. After incubation, RNA samples were spun down at 12000g for 20 min at 4°C. The supernatant was removed and the blue pellet was resuspended in 100µl of 75% ethanol. Samples were spun down at 12000g for 20 min at 4°C. The ethanol was discarded and the tubes were left to air dry. The concentrated RNA was then resuspended in the 50µl of nuclease free water.

2.4 Nanodrop 1000 spectrophotometer

The principle of the Nanodrop 1000 spectrophotometer was to measure the quantity of RNA by measuring the absorbance of UV light at a wavelength 260nm and 280nm. The measurement at 260nm indicates the amount of RNA in the sample and the amount of protein was estimated at 280nm. In addition, the purity was measured by the calculating the ratio of both absorbance which ranges between1.8 - 2.0.

2.5 Agilent Bioanalyser 2100

The Agilent Bioanalyser analyzer was used to analyse the RNA quality. The technique is based on using chips designed with a set of microchannels that separates nucleic acid species based on size by electrophoresis. The procedure was performed using the manufacture instructions. (http://www.genomics.bham.ac.uk/Nano_Kit.pdf).

2.6 DNase treatment

DNase treatment was performed on the nuclear samples. 1µg of RNA was mixed with 1x DNase I reaction buffer. 2 units of DNase I was added and the mixture was incubated at 37°C for 10min. Finally, to stop the reaction 1µl 0.5M EDTA was added. The mixture was then incubated at 75°C for 10min.

2.7 GeneChip® Arrays

Two GeneChip® array types were used in the current work, therefore, two manuals were followed to prepare the samples for hybridization. The Human Exon Arrays 1.0 ST (*The Ambion® WT Expression Kit For Affymetrix® GeneChip® Whole Transcript (WT) Expression Arrays and GeneChip® Whole Transcript (WT) Sense Target Labeling Assay Manual part number 701880*) and for the Human Transcriptome Arrays (*GeneChip® WT PLUS Reagent Kit Manual Target Preparation for GeneChip® Whole Transcript (WT) Expression Arrays part number 703174*). Most of the steps were similar therefore were described together. However some steps were different thus were described separately.

2.7.1 Sample preparation for both Human Exon Arrays 1.0 ST (HEA) and Human Transcriptome Arrays (HTA) RNA samples

The ultimate RNA concentration prior RNA labelling was ~200ng diluted in 3µl of RNase free water. Thus, the amount of RNA required in the experiment was calculated then precipitated using the glycoblue method and resuspended in 3µl of RNase free water (Table 2.4 & 2.5).

The poly-A RNA spike in controls, synthesis of first strand cDNA, synthesis of second strand cDNA, synthesis of cRNA by In Vitro Transcription (IVT), purifying cRNA, synthesis of 2nd cycle cDNA, Hydrolysis using RNase H and purifying 2nd cycle cDNA steps were performed as shown below.

Table 2.4: RNA precipitation by glycoblue method for the HEA. ng/µl =nanograms/ microliter, µl =microliter, GB= glycoblue, conc=concentration, pat=patients, con=control

Cell fraction	Mutation type	Fibroblasts ID	RNA conc. (ng/µl)	200ng of RNA	GB (µl)	Ammonium acetate	100% Isopropanol
Cytoplasm	-	Con 8	60.5	5	1	0.3	7
		Con 11	27	10	1	0.6	12
		Con 170	70	5	1	0.3	7
	Missense mutation	Pat 48	16	15	1	1	17
		Pat 51	20	12	1	0.8	14
		Pat 55	82	5	1	0.3	7
Nuclear	-	Con 8	13	20	1	1.3	23
		Con 11	21	20	1	1.3	23
		Con 170	25	20	1	1.3	23
	Missense mutation	Pat 48	11	20	1	1.3	23
		Pat 51	15	20	1	1.3	23
		Pat 55	12	20	1	1.3	23

Table 2.5: RNA precipitation by glycoblue method for HTA. ng/µl =nanograms/ microliter, µl =microliter, GB= glycoblue.

Cell fraction	Mutation type	Fibroblasts ID	RNA conc. (ng/µl)	Amount required 200ng	GB (µl)	Ammonium acetate	100% Isopropanol
Cytoplasm	-	Con 155	284	1	-	-	-
		Con 2303	198	1	-	-	-
		Con 170	148	1.5	-	-	-
		Con 159	216	1	-	-	-
	Missense mutation	Pat 48	81	2.5	-	-	-
		Pat 55	68	3	-	-	-
		Pat 51	100	2	-	-	-
	Truncated mutation	Pat 192	81	2.5	-	-	-
		Pat 193	128	2.5	-	-	-
		Pat 194	50	4	1	0.5	5.5
Nuclear	-	Con 155	128	2	-	-	-
		Con 2303	192	1.5	-	-	-
		Con 170	136	1.5	-	-	-
		Con 159	218	1	-	-	-
	Missense mutation	Pat 48	27	8	1	0.5	9.5
		Pat 55	72	3	-	-	-
		Pat 51	147	1.5	-	-	-
	Truncated mutation	Pat 192	36	6	1	0.5	7.5
		Pat 193	144	1.5	-	-	-
		Pat 194	16	13	-	0.8	13.8

2.7.2 Poly-A RNA controls preparation for both HEA and HTA RNA samples

To each RNA sample a series of exogenous positive controls were added to the reaction in order to monitor the labelling process. These controls were artificially polyadenylated RNA designed against *B. subtilis* genes which are absent in human cells. The genes were: *lys, phe, thr,* and *dap*. The *dap* gene was expected to show the highest intensity followed by *thr*, *phe* and *lys*. The poly-A RNA controls were spiked in at a certain concentration prior to the first strand synthesis reaction step (Table 2.6).

Stepwise, first 2µl of poly-A control stock was mixed with 38µL of poly-A control dilution buffer to achieve (1:20) dilution. Secondly, 2µL of the first dilution was added to 98µL of poly-A control dilution buffer to prepare the second dilution (1:50). Afterwards, 2µL of the second dilution was mixed with 98µL of poly-A control dilution buffer to make the third dilution (1:50). Finally, the fourth dilution was prepared by diluting the third dilution (1:4) using poly-A control dilution buffer according to the number to samples in the experiment. 2µL of this fourth dilution was added to the prepared 200ng of total RNA samples (Table 2.7).

Table 2.6: Final concentrations of the spiked in poly-A RNA controls for both HEA and HTA

Poly-A RNA Spike	Final concentration
lys	1:100,000
phe	1:50,000
thr	1:25,000
dap	1:6,667

Table 2.7: Total RNA/Poly-A RNA control mixture for both HEA and HTA

Component	Volume for one reaction (µl)
Total RNA sample (200ng)	3
Diluted 4th Poly-A RNA Controls	2
Total volume	5

2.7.3 Synthesis of first strand cDNA, second strand cDNA and cRNA by In Vitro Transcription (IVT) for both HEA and HTA

To synthesize the first strand cDNA a reverse transcription reaction was performed (Tables 2.8 and 2.9). The RNA samples were primed with a mixed random and oligo dT primer each supplemented with T7 promoter sequence. This reaction produced ss cDNA. The ss cDNA was then converted to double stranded cDNA and the T7 polymerase promoter was completed (Tables 2.10, 2.11 & 2.12). Afterwards, using T7 RNA polymerase enzyme, an antisense cRNA was synthesized and amplified from the second strand cDNA template (Tables 2.13, 2.14).

Table 2.8: First strand master mix components for both HEA and HTA

First strand master mix component	Volume for one reaction (µl)
First strand buffer mix	4
First strand enzyme mix	1
Total volume added to each sample	5

Table 2.9: First strand amplification protocol using thermocycler for both HEA and HTA

	Temperature (°C)	Time
Annealing	25	1 hour
Reverse transcription	42	1 hour
Hold	4	2 min
Single cycle		

Table 2.10: Second strand cDNA master mix components of the HEA

Second-Strand Master Mix component	Volume for one reaction (µL)
Nuclease-free Water	32.5
Second-Strand Buffer Mix	12.5
Second-Strand Enzyme Mix	5
Total Volume	50

Table 2.11: Second strand cDNA master mix components for the HTA

Second strand master mix component	Volume for one reaction (µL)
Second strand buffer	18
Second strand enzyme	2
Total volume	20

Table 2.12: Second strand amplification protocol using thermocycler for both HEA and HTA

	Temperature (°C)	Time
Second strand synthesis	16	1 hour
Enzyme denaturation	65	10 min
Hold	4	2 min
Single cycle		

Table 2.13: IVT Master Mix components for both HEA and HTA

IVT master mix component	Volume for one reaction (µL)
IVT buffer mix	24
IVT enzyme mix	6
Total volume	30

Table 2.14: IVT amplification protocol using thermocycler for both HEA and HTA

	Temperature (°C)	Time
Incubation	40	16 hour
Hold	4	Indefinitely

2.7.4 cRNA purification for both HEA and HTA

In this step all interfering substances are removed leaving a clean stable cRNA. These substances include: salts, enzymes, unincorporated nucleotides and inorganic phosphates. The purification step is based on using nucleic acid binding beads. cRNA binds to the magnetic beads which allows the removal of all the unbound interfering material. The procedure was performed using the manufacturer's instructions.

2.7.5 Synthesize 2nd cycle cDNA

2.7.5.1 Synthesize 2nd cycle cDNA for HEA

A sense strand cDNA was synthesized by using random primers and the purified cRNA. In this step 10µg of cRNA was required diluted in a total volume of 22ul of nuclease free water (Table 2.15). 2µl of random primers were added to the 10µg cRNA, mixed thoroughly and incubated in the thermal cycler (Table 2.16). Afterwards, the 2nd-cycle master mix was prepared as shown in (Table 2.17) and 16µL of the master mix was added to each sample, mixed and incubated in the thermal cycler (Table 2.20).

Table 2.15: 2nd cycle cDNA synthesis (10µg /22µl) of cRNA for the HEA. ng/ µl= nanograms/microliter, µl=microliter, con=control, pat=patient

Cellular fraction	Mutation type	Sample ID	cRNA (ng/µl)	cRNA (µl)	Nuclease free water (µl)
Cytoplasm	-	Con 8	1688.73	6ul	16ul
		Con 11	481.41	20ul	2ul
		Con170	1093.68	9ul	13ul
	Missense mutation	Pat 48	718.27	14ul	8ul
		Pat 51	2406.26	4ul	18ul
		Pat 55	1412.87	7ul	15ul
Nuclear	-	Con 8	1494.49	7ul	15ul
		Con 11	2658.18	4ul	18ul
		Con 170	3010.44	3ul	19ul
	Truncated mutation	Pat 48	1312.43	8ul	14ul
		Pat 51	2223.56	5ul	17ul
		Pat 55	616.55	16ul	6ul

Table 2.16: Thermocycler protocol for 2nd cycle cDNA synthesis using random primers for the HEA

	Temperature (°C)	Time
Denature	70	5 min
Annealing	25	5 min
Hold	4	2 min
Single cycle		

Table 2.17: 2nd cycle master mix components for the HEA

2nd cycle master mix component	Volume for one reaction (µL)
2nd cycle buffer mix	8
2nd cycle enzyme mix	8
Total volume	16

2.7.5.2 Synthesize 2nd cycle ss cDNA for HTA

In this step, 15µg cRNA in a total volume of 24µL was required (Table 2.18).To each 15µg sample 4µl of 2nd cycle primers was added, mixed thoroughly by vortexing and incubated for 5 min at 70°C, 5min at 25°C, then 2min at 4°C. Immediately after the incubation, 2nd cycle sense strand cDNA master mix was prepared and 12µl of the master mix was added to each sample (Table 2.19). Samples were incubated in the thermal cycler (Table 2.20).

Table 2.18: 2nd-cycle ss cDNA (15µg /24µl cRNA) for the HTA. ng/ µl= nanograms/microliter, µl=microliter, con=control, pat=patient

Cellular fraction	Mutation type	Sample ID	cRNA (µl)	Nuclease-free water (µl)
Cytoplasmic	-	Con 2303	12.3	11.7
		Con 155	7	17
		Con 170	13.6	10.4
		Con159	20.3	3.7
	Missense mutation	Pat 51	16.9	7.1
		Pat 48	13	11
		Pat 55	4.5	19.5
	Truncated mutation	Pat 192	8	16
		Pat 193	10	14
		Pat 194	8	16
Nuclear	-	Con 2303	12.5	11.5
		Con 155	4.5	19.5
		Con 170	7.3	16.7
		Con 159	10	14
	Missense mutation	Pat 48	8.7	15.3
		Pat 55	10	14
		Pat 51	23	1
	Truncated mutation	Pat 192	6.5	17.5
		Pat 193	5	19
		Pat 194	8	16

Table 2.19: 2nd cycle sense strand cDNA master mix for HTA

Master mix component	Volume for one reaction (µL)
2nd cycle sense strand cDNA buffer	8
2nd cycle sense strand cDNA enzyme	4
Total volume	12

Table 2.20: 2nd cycle cDNA thermocycler protocol for both HEA and HTA

	Temperature (°C)	Time
Annealing	25	10min
extension	42	90min
stop reaction	70	10min
Hold	4	2min
Single step		

2.7.6 Hydrolyze cRNA using RNase H

cRNA template was degraded using RNase H enzyme leaving ss cDNA.

2.7.6.1 Hydrolyze cRNA using RNase H for HEA

2µl of RNase H was added to the sense strand cDNA samples. The samples were mixed thoroughly and incubated using the thermocycler (Table 2.21).

2.7.6.2 Hydrolyze cRNA using RNase H for the HTA

4µl of the RNase H was added to sense strand cDNA samples. The samples were mixed thoroughly and incubated using the thermocycler (Table 2.21). After incubation, 11µL of the nuclease-free water was added to each sample to achieve a final volume of 55ul.

Table 2.21 The thermocycler protocol for the hydrolysis of cRNA using RNase H for both HEA and HTA

	Temperature (°C)	Time
Incubation	37	45min
Enzyme denaturation	95	5min
Hold	4	2min
Single cycle		

2.7.7 Purify 2nd cycle cDNA for both the HEA and HTA

This step is similar to the previous purification procedure. All interfering substances were removed. These include: salts, enzymes and unincorporated dNTPs. The purification step was based on using nucleic acid binding beads which allows the removal of all the unbound interfering material leaving purified sense strand cDNA. The procedure was performed using the manufacturers' instructions (refer to section 2.7)

2.7.8 Fragmentation for both HEA and HTA

The ss cDNA was fragmented by uracil-DNA glycosylase (UDG) and apurinic/apyrimidinic endonuclease 1 (APE 1) at the unnatural dUTP residues which resulted in DNA breakage. Sense strand cDNA samples were prepared to achieve 5.5µg in a total volume of 31.2µl (Tables 2.22 and 2.23). Fragmentation master mix was prepared (Table 2.24) and 16.8µL of mixture was added to each sample, mixed and incubated in the thermocycler (Table 2.25). The quality of the samples was examined using the Agilent Bioanalyser.

Table 2.22: HEA sample preparation for fragmentation

Cellular component	Mutation type	Sample ID	ss-cDNA =5.5µg	RNase free water
Cytoplasmic	-	Con 8	15	16.2
		Con 11	22	9.2
		Con 170	20	11.2
	Missense mutation	Pat 48	18	13.2
		Pat 51	18	13.2
		Pat 55	21	10.2
Nuclear	-	Con 8	18	13.2
		Con 11	17	14.2
		Con 170	18	13.2
	Missense mutation	Pat 48	20	11.2
		Pat 51	20	11.2
		Pat 55	21	10.2

Table 2.23: HTA sample preparation for fragmentation. ss cDNA = sense strand complementary DNA , Con=control, Pat=patient, µl= microliter, µg= micrograms

Cellular fraction	Mutation type	Sample ID	5.5µg ss cDNA	Nuclease free water 31.2µl
Cytoplasmic	-	Con 2303	10.8	20.4
		Con 155	8	23.2
		Con 170	11.4	19.8
		Con 159	12.6	18.6
	Missense mutation	Pat 48	12.7	18.5
		Pat 51	11.5	19.7
		Pat 55	7.5	23.7
	Truncated mutation	Pat 192	9	22.2
		Pat 193	9	22.2
		Pat 194	10	21.2
Nuclear	-	Con 2303	11.3	19.9
		Con 155	7	24.2
		Con 170	9.5	21.7
		Con 159	10.4	20.8
	Missense mutation	Pat 48	10	21.2
		Pat 51	13.5	17.7
		Pat 55	8.5	22.7
	Truncated mutation	Pat 192	8.5	22.7
		Pat 193	7	24.2
		Pat 194	11.5	19.7

Table 2.24: Fragmentation master mix for both HEA and HTA

Component	Volume for one reaction (µl)
RNase-free Water	10
10X cDNA Fragmentation Buffer	4.8
UDG, 10 U/µL	1
APE 1, 1,000 U/µL	1
Total Volume	16.8

Table 2.25: Thermocycler protocol for fragmentation step for both HEA and HTA

	Temperature (°C)	Time
Incubation	37	60min
Stop reaction	93	2min
Hold	4	2min
Single cycle		

2.7.9 Labelling for both HEA and HTA

The fragmented ss cDNA were labelled with biotin by adding 60µl of labelling reaction master mix to each sample (Table 2.26). The samples were incubated using the thermocycler (Tables 2.27)

Table 2.26: The labelling reaction master mix for both HEA and HTA

Component	Volume for one reaction (µl)
Fragmented sense strand DNA	45
5X TdT Buffer	12
TdT	2
DNA Labeling Reagent, 5mM	1
Total Volume	60

Table 2.27: The thermocycler protocol for labelling for both HEA and HTA

	Temperature (°C)	Time
Incubation	37	60min
Enzyme denaturation	70	10min
Keep	4	2min
Single cycle		

2.7.10 Gel-Shift Assay for both HEA and HTA

The gel shift assay is a procedure that assesses the efficiency of the labelling step. This will prevent poor hybridization of fragmented ss cDNA to the targeted probe on the array. First, 2mg/mL of NeutrAvidin solution was prepared in of in 1XPBS. Meanwhile, 4-20% gradient TBE gel was placed into the gel holder and loaded with 1XTBE buffer. Random samples were selected to be tested as positive and negative controls. 1µL of the fragmented ss cDNA was heated at 70°C for 2min. For the positive samples, 5µL of 2mg/mL NeutrAvidin was added to each sample. Samples were mixed and incubated for 5min at room temperature. Negative samples were treated with 1µL of 1XPBS instead of NeutrAvidin. 5µl of loading dye was added to all samples and 10µl of the samples were loaded to the wells and 5µl of Hyper ladder lV or Hyper ladder V was added to the first well. The samples were then run at 150 volts for 1h. After the run was

completed the gel was stained with 1X ethidium bromide for 10min. Finally, the gel was visualized under UV light.

2.7.11 Hybridization

BioB, BioC, BioD and Cre are pre-labeled hybridization controls that monitor the hybridization, washing and staining process of the each array. These controls are a mixture of fragmented and biotinylated cRNA extracted from Escherichia.*coli* except for Cre which is extracted from P1 bacteriophage. They were designed to bind to the arrays in different intensities. It is expected that the Cre generates the highest signal intensity followed by BioD, BioC, BioB.

Hybridization Cocktail was prepared in a 1.5mL RNase-free microfuge tube as shown below (Table 2.28 and 2.29). The 20X Eukaryotic Hybridization Controls was heated at 65°C for 5min to ensure a complete dissolution before use. The complete Hybridization Cocktail was heated at 99°C for 5min then cool to 45°C for 5min. The GeneChip® Arrays were labelled and allowed to equilibrate to 21°C prior use. 200µl of the mixture was injected to each array then were placed in 45°C hybridization oven, rotating at 60rpm, and incubated for 16h.

Table 2.28: Hybridization cocktail for HEA

Component	Volume in each sample (µl)
Fragmented and labeled DNA target	59
Control oligonucleotide B2 (3 nM)	3.7
20X Eukaryotic hybridization controls (bioB, bioC, bioD, cre)	1
2X Hybridization mix	110
DMSO	15.4
Nuclease-free water	20.9
Total volume	220

Table 2.29: Hybridization cocktail for the HTA

Component	Volume in each sample (µl)
Control oligonucleotide B2 (3 nM)	3.7
20X Eukaryotic Hybridization Controls (bioB, bioC, bioD, cre)	11
2X Hybridization mix	110
DMSO	15.4
Nuclease-free Water	19.9
Total Volume	160

2.7.12 Wash, Stain and Scan for both HEA and HTA

The Genechips® were serially washed to remove any unspecific materials followed by staining with Streptavidin Phycoerythrin (SAPE). Afterwards, the Genechips® were scanned (Table 2.30). The scanner emits laser that detects the bound labelled sense strand fragmented cDNA which corresponds to the level of expression.

Table 2.30: Fluidics protocols for the GeneChip® ST Arrays

	Fluidics Station
Post Hyb Wash #1	10 cycles of 2 mixes/cycle with Wash Buffer A at 30°C
Post Hyb Wash #2	6 cycles of 15 mixes/cycle with Wash Buffer B at 50°C
Stain	Stain the probe array for 5 minutes in SAPE solution at 35°C
Post stain wash	10 cycles of 4 mixes/cycle with Wash Buffer A at 30°C
2nd Stain	Stain the probe array for 5 minutes in antibody solution at 35°C
3rd Stain	Stain the probe array for 5 minutes in SAPE solution at 35°C
Final wash	15 cycles of 4 mixes/cycle with Wash Buffer A at 35°C.
Holding buffer	Fill the probe array with Array Holding Buffer.

2.7.13 Quality control for both HEA and HTA

The raw data was generated as CEL files using the Affymetrix GeneChip Command Console (AGCC) software. Quality control checks of the arrays was performed through Affymetrix Expression Console v1.0 software. This was used to check the hybridization quality control of the arrays as it produces informative quality control charts and graphs.

2.8 Gene expression analysis

2.8.1 Gene expression analysis using Partek® Genomics Suite ™ software

Partek® Genomics Suite ™ 6.6 software was used to explore the differentially expressed genes of the Human Exon Array 1.0 ST. An ANOVA test was performed and the genes with a significant P-value ≤ 0.05 and FC $\geq$ $\pm$1.2 were identified. The analysis was performed as the following: cytoplasmic missense mutation MT vs. cytoplasmic controls CON and nuclear missense mutation MT vs. nuclear controls CON. This allows the identification of differentially expressed genes in the cellular compartments. DAVID v6.7 was used to identify the biological processes dysregulated in fALS-*TARDBP* fibroblasts. Biological pathways containing differentially expressed genes that had an enrichment score (ES) $\geq$ 1.3 were highlighted as significant which is equivalent to p-value of 0.05.

2.8.2 Gene expression profiling using Qlucore Omics Explorer software

Qlucore Omics Explorer software was used to explore the differentially expressed genes of the HTA. CEL files were uploaded into the Qlucore Omics Explorer software and samples were normalized according to their cellular fraction type prior to the analysis. The p-value was set to $\leq$ 0.05 and fold change to $\geq$ $\pm$ 1.2. Two comparison studies were carried out on each type of mutation. For the missense mutation; cytoplasmic missense mutation MT vs. cytoplasmic controls

CON and nuclear missense mutation MT vs. nuclear controls CON. For the truncated mutation, cytoplasmic missense mutation TT vs. cytoplasmic controls CON and nuclear missense mutation TT vs. nuclear controls CON. Similarly to the Human Exon Arrays 1.0 ST, DAVID v6.7 was used to identify the dysregulated biological processes in fALS-*TARDBP* fibroblasts in both mutation types. Biological pathways with enrichment score $\geq$ 1.3 were highlighted as significant which is equivalent to p-value of 0.05 (Huang da et al., 2009).

2.9 Quantitative reverse transcription polymerase chain reaction (qRT-PCR)

2.9.1 cDNA synthesis

1µg of RNA was converted into cDNA using the (*QuantiTect® reverse transcription kit*). First, a genomic DNA elimination reaction was prepared for each sample as shown in (Table 2.31). Samples were incubated at 42°C for 2min then were placed immediately on ice. Next, the reverse transcription reaction was prepared as shown (Table 2.32). Samples were incubated at 42°C for 15 min. The reaction was completed by an enzyme inactivation step, 95°C for 3 min. cDNA samples were stored at -20°C.

Table 2.31: Genomic DNA elimination reaction component

Component	Volume (µl)
gDNA wipeout buffer	2
Template RNA (1µg)	variable
RNase free water	variable
Total reaction volume	14

Table 2.32: Reverse transcription reaction component

Component	Volume (µl)
Reverse transcription master mix	1
Quantiscript RT buffer	4
RT primer mix	1
The template RNA after genomic DNA elimination	14
Total volume	20

2.9.2 SYBR green qRT-PCR method

SYBR green is a dye has the ability to bind to double stranded DNA and is widely used in experimental studies. In the current work primers were optimized prior to use.

The optimal forward and reverse primers were determined by testing a combination of primer concentrations, 150nmol, 300nmol and 600nmol. This was achieved by testing the multiple primer concentrations against a universal total cDNA. 1µg of universal total RNA was converted to cDNA using *(QuantiTect® reverse transcription kit*) and the staring concentration for the optimization utilized 12.5ng/µl of cDNA as a starting concentration. The test was performed in triplicates using the Brilliant II SYBR green master mix from with a total volume 20µl for each reaction (Table 2.33). The samples were run on the MX3000P Real-Time PCR machine (Table 2.34). For primer sequences see (Table 2.35).

The optimal primers where those with the lowest cycle thresholds (Ct) value showing a single amplified product in the dissociation curve. The efficiency of the optimal primers to detect variable cDNA concentrations tested by generating a standard curve of two fold serial dilution of the universal cDNA, 12.5ng/µl-0.0ng/µl against the optimized primers. The statistical analysis was carried out using *Graph Pad Prism Software*.

Table 2.33: Primer optimization using SYBR green method

Forward primer concentration	Reverse primer concentration	SYBR green x2 master mix (µl)	Universal cDNA (12.5ng/µl)	RNase free water (µl)
150nmol (0.6µl)	150nmol (0.6µl)	10	1	7.8
150nmol (0.6µl)	300nmol (1.2µl)	10	1	7.2
300nmol (1.2µl)	150nmol (0.6µl)	10	1	7.2
300nmol (1.2µl)	300nmol (1.2µl)	10	1	6.6
300nmol (1.2µl)	600nmol (2.4µl)	10	1	5.4
600nmol (2.4µl)	600nmol (2.4µl)	10	1	4.2
NTC 300nmol (1.2µl)	300nmol (1.2µl)	10	-	7.6

Table 2.34: qRT-PCR thermocycler program using SYBR green method

	Temperature (°C)	Time (min)
Initial denaturation	95	10min
Denaturation	95	30sec
Annealing and extension	60	1min
Number of cycles	40	

Table 2.35: Primer sequences generated by prime blast (SYBR green method)

Gene symbol	Gene name	Sequence 5' -> 3' Forward	CG%	Tm ºC	Sequence 5' -> 3' Reverse	CG %	Conc. (pmol/µl)	Tm ºC	Primer location
ACTB	Actin beta	TCCCCCAACT TGAGATGTAT GAAG	46	58	AACTGGTCT CAAGTCAG TGTACAGG	48	100	58	Exon 6-6
TARDBP	TAR DNA binding protein	ACAACCGAA CAGGACCTG AA	50	57.3	ACGAACAA AGCCAAAC CCCT	50	100	57.3	Exon 3-4
SRSF10	FUS interacting protein (serine/argi nine-rich) 1	TCTGTTCGTC AGGAACGTG G	55	59.4	AAATCCTCT TGGACGGC GAG	55	100	59.4	Exon 1-2
NRNP200	Small nuclear ribonucleop rotein 200kDa (U5)	GGATGTAAC CGCCCGTAG TC	60	61.4	CAAACAAG GGACAGCA CCTCT	55	100	59.4	Exon 1-2
SF3A1	Splicing factor 3a, subunit 1, 120kDa	CAAGACTGC CAGCTTTGTG G	55	59.4	GACCTTGT GGCGGTAG TAGG	60	100	59.4	Exon 2-3

2.9.3 Prime time qRT-PCR method

The prime time qRT-PCR application guide fourth edition (IDT) was followed in this reaction.

This method was developed to increase primer specificity by utilizing a third oligonucleotide labelled probe that binds to the targeted sequence of interest along with the forward and the reverse primers but which is tagged with a fluorescent label and a quencher. The principle of the reaction is that after primers and probes anneal to the targeted DNA sequence, the Taq polymerase enzyme extends the forward and reverse primer sequences. Thus, as Taq polymerase encounters the bound labelled probe, it cleaves the labelled molecule on the probe by 5'->3' nuclease activity which releases the quencher and causes an excitation that is detected by the instrument. This method has better measures than the classical SYBR green methods as it has higher sensitivity, primers were optimized by the manufacturer (IDT) and are heat stable.

Samples were run in triplicates. Table 2.36 and 2.37 shows the qRT-PCR component for a single reaction and the thermocycler program followed respectively. For primer specification see (Table 2.38).

Table 2.36: Prime time qRT-PCR reaction component using prime time qRT-PCR method

Component	Amount for 1 reaction (µl)
20X prime time assay	0.5
2X master mix	5
50ng cDNA	1
RNase free water	3.3
Total volume	10

Table 2.37: qRT-PCR thermocycler program using prime time qRT-PCR method

	Temperature (°C)	Time (min)
Initial denaturation	95	10min
Denaturation	95	30sec
Annealing and extension	60	1min
Number of cycles	40	

Table 2.38: Primer sequences using prime time qRT-PCR method

Gene symbol	Gene name	Sequence 5' -> 3' Forward	GC%	Sequence 5' -> 3' Reverse	GC%	Conc. (nM)	Probe 5' -> 3'	Primer location	Probe location
GAPDH	Glyceraldehyde-3-phosphate dehydrogenase	TGTAGTTGAGGTCAATGAAGGG	45.5	ACATCGCTCAGACACCATG	52.6	500	56-FAM/AAGGTCGGA/ZEN/GTCAACGGATTTGGTC/31ABkFQ	Exon 2-3	Exon 3
ADARB1	Adenosine deaminase, RNA-specific, B1 (RED1 homolog rat)	TGGGATCAGAGCAAGACATAAAG	47.6	GCGGTTTTCCTTCACATTCAG	45.5	500	56-FAM/TCCGCCAGT/ZEN/CAAGAAACCCTCAAA/31ABkFQ	Exon 2-4	Exon 3
METTL1	Methyltransferase like 1	AGCCACGATGACCCAAAG	55.6	CTTGTGCTTTGTCCGCTTG	52.6	500	56-FAM/TCTTCCTCT/ZEN/TCCCCGACCCACAT /31ABkFQ	Exon 2-3	Exon 3
SEMA5A	Sema domain, seven thrombospondin repeats (type 1 and type 1-like), transmembrane domain (TM) and short cytoplasmic domain, (semaphorin) 5A	CAGATCCTGCACAGCCAG	61.1	TCTTCATTACCACATCCCAGC	47.6	500	56-FAM/CAGTTCTAC/ZEN/CGCACACACGCAGC/31ABkFQ	Exon 12-14	Exon 13
ENAH	Enabled homolog (Drosophila)	ACTCACAACTACCTGCTCAAG	45.5	CTCTCCAACCTTTCTCTTTCCA	50	500	56-FAM/TCTTTCTCG/ZEN/CTCCAGCCTTTCCC/31ABkFQ	Exon 4-6	Exon 5

2.10 RNA Sequencing

The mRNA isolation, fragmentation and priming, first strand cDNA synthesis, second strand cDNA synthesis, end prep of cDNA library, adaptor ligation and PCR library enrichment were performed using *NEBNext® Ultra™ Directional RNA library prep kit for Illumina, part number NEB #E7420S/L*.

2.10.1 The mRNA Isolation, fragmentation and priming

The sample concentrations were calculated to achieve 500ng of RNA in a total volume of 50µl of nuclease-free water. First, 20µl of the NEBNext Oligo $d(T)_{25}$ beads were aliquoted in a clean-up plate and washed by adding 100µl of RNA binding buffer (2X) to the beads and mixed by pipetting the entire volume up and down 6 times. The plate was then placed on the magnetic rack for 2min at room temperature. After incubation, all the supernatant was removed and discarded without disturbing the beads. The plate was then removed from the magnetic rack and a second washing step was performed. 50µl of RNA binding buffer (2X) and 50µl of total RNA sample was added to the beads. The whole mixture was carefully resuspended. The plate was then placed on the thermal cycler and incubated at 65°C for 5min then kept at 4°C to denature the RNA and facilitate binding of the polyadenylated mRNA to the beads. After incubation, the plate was removed from the thermocycler. The beads were resuspended by slow mixing followed by 5min incubation at room temperature this allowed mRNA to bind to the beads. The beads were mixed for a second time and incubated for 5min at room temperature. After incubation the plate was placed on the magnetic rack for 2min at room temperature in order to separate the polyadenylated mRNA that was bound to the beads from the solution. Carefully, the supernatant was aspirated and discarded. Then the plate was removed from the magnetic rack and the beads were washed. The unbound RNA was washed-out by adding 200µl of wash buffer to each sample. This was then mixed thoroughly by pipetting the entire volume up and down 6 times. The plate was placed on the magnetic rack for 2min. The supernatant was carefully removed and discarded without

disturbing the beads. The plate was then removed from the magnetic rack and the washing step was repeated for a total of two washes. Afterwards, 50µl of Tris buffer was added to each well and gently mixed by pipetted up and down 6 time. The plate was then placed on the thermal cycler, incubated at 80°C for 2min, then hold at 25°C in order to elute the polyadenylated mRNA from the beads. After incubation was completed 50µl of RNA binding buffer (2X) was added to each sample allowing the mRNA to rebind to the beads. The entire volume was mixed thoroughly and incubated at room temperature for 5min. After incubation the mixture was resuspended by pipetting up and down 6 times and left at room temperature for 5min in order for mRNA to bind to the beads. Next, the plate was placed on the magnetic rack for 2min at room temperature. The supernatant was aspirated and discarded without disturbing the beads. The plate was then removed from the magnetic rack and the beads were washed. 200µl of wash buffer was added to each sample and was mixed thoroughly by pipette the entire volume up and down 6 times. The plate was then placed on the magnetic rack at room temperature for 2min. The entire supernatant was removed and discarded. The mRNA was eluted from the beads by adding 15.5µl of the first strand synthesis reaction buffer and random primer mix (2X) (Table 2.39), the samples were then incubated at 94°C for 15min and immediately placed on the magnetic rack. 13.5µl of the supernatant was transferred to a clean nuclease-free PCR tube which contains the purified mRNA. The purified mRNA were paced on ice to be taken forward for the next step first strand cDNA synthesis.

The first strand cDNA synthesis reaction was prepared as shown in (Table 2.40) and incubated in the thermocycler (Table 2.41). Then, the second strand cDNA synthesis reaction was immediately prepared as described in (Table 2.42) and was incubated in the thermocycler for 1 hour at 16°C, with heated lid set at ≤ 40°C.

Table 2.39: First strand synthesis reaction buffer and random primer mix (2X)

Component	Amounts per reaction (µl)
NEBNext first strand synthesis reaction buffer (5X)	8
NEBNext random primers	2
Nuclease-free water	10
Total volume	20

Table 2.40: First strand cDNA synthesis

Component	Amounts per reaction (µl)
Murin RNase inhibitor	0.5
Actinomycin D (0.1 µg/µl)	5
ProtoScript Reverse transcriptase	1
Total volume	20

Table 2.41: Thermocycler incubation, heated lid set 105°C

Temperature	Time
25°C	10 min
42°C	15 min
70°C	15 min
4°C	Hold

Table 2.42: Second strand cDNA synthesis

Component	Amount per reaction (µl)
Second Strand Synthesis Reaction Buffer (10X)	8
Second Strand Synthesis Enzyme Mix	4
RNase free water	48
Total volume	80

2.10.2 Purify the double stranded cDNA using 1.8X Agencourt AMPure XP Beads

144µl of (1.8x) resuspended AMPure XP Beads was added to each second strand synthesis reaction. The mixture was thoroughly mixed by pipetting up and down 10 times followed by 5min incubation at room temperature. Next the plate was placed on the magnetic rack to separate the beads from the supernatant. After 5min the clear supernatant was removed and discarded. A washing step

was performed by adding 200µl of freshly prepared 80% ethanol to each sample while the plate on magnetic rack. The samples were incubated for 30sec then the ethanol was aspirated and discarded. This washing step was repeated for a total of two washes. Afterwards, the beads were incubated for 5min to air dry while on magnetic rack. The plate was then removed in order to elute the ds cDNA target from the beads. 60µl of 10mM Tris-HCl was added to each sample, mixed well and incubated at room temperature for 2min. The plate was placed on the magnetic rack and left until the solution was clear. 55.5µl of the supernatant was removed and transferred to a clean nuclease free PCR tube. The ds cDNA samples were then taken forward to perform the end preparation and adaptor ligation.

2.10.3 End preparation and adaptor ligation

The end preparation was prepared as shown in (Table 2.43) and was incubated in the thermocycler (Table 2.44). In addition, 15µM NEBNext Adaptor for Illumina was diluted 10 fold to achieve a concentration of 1.5µM using 10mM Tris-HCl. The adaptor ligation components were directly added to each sample and were not pre-mixed (Table 2.45), as this would prevent adaptor-dimer formation. The samples were mixed by pipetting and incubated at 20°C for 15min in thermocycler with the heated lid turned off.

Table 2.43: End preparation of cDNA Library

Component	Amount per reaction (µl)
Purified ds cDNA	55.5
NEBNext End Repair Reaction Buffer (10X)	6.5
NEBNext End Prep Enzyme Mix	3
Total	65

Table 2.44: The thermocycler incubation

Temperature	Time
20°C	30 min
65 °C	30 min
4°C	Hold

Table 2.45: Adaptor ligation

Components	Amounts per reaction (µl)
End Prep Reaction	65
Blunt/TA Ligase Master Mix	15
Diluted NEBNext Adaptor	1
Nuclease-free Water	2.5
Total	83.5

2.10.4 Purify the Ligation Reaction Using AMPure XP Beads

16.5µl of nuclease-free water was added to each ligation reaction to bring the final volume to 100µl prior to adding AMPure XP Beads. 100µl of (1.0X) resuspended AMPure XP Beads was added to each sample, mixed well by pipetting the entire volume up and down 10 times followed by 5min incubation at room temperature. After incubation the plate was placed on the magnetic rack to separate the beads from the supernatant. Once the supernatant was clear (~ 5min), it was discarded. A washing step was performed by adding 200µl of freshly prepared 80% ethanol to each sample on the magnetic rack, incubated for 30sec at room temperature then was carefully removed and discarded. This step was repeated for a total of two washes. The beads were left to air dry for 5min while the plate on the magnetic rack. Next, the DNA target was eluted from the beads with 52µl of 10mM Tris-HCl. The beads were mixed thoroughly and incubated for 2min at room temperature. Then, the plate was placed on the magnetic rack until the solution was clear (~2min). 50µl of the supernatant was transferred to a clean well-plate and the beads were discarded. 50µl of (1.0X) resuspended AMPure XP Beads were added to each sample and mixed well by pipetting up and down 10 times, incubated for 5min at room temperature. After incubation, the plate was placed on the magnetic rack and incubated for about 5min, until the supernatant was clear then was discarded.

A washing step was then performed by adding 200µl of freshly prepared 80% ethanol to each sample on the magnetic rack, incubated for 30sec at room temperature then was carefully removed and discarded. This step was repeated

for a total of two washes. The beads were left to air dry for 5min while the plate on the magnetic rack. Next, the DNA target was eluted from the beads with 19µl of 10mM Tris-HCl, mixed well and incubated for 2min. Then, the plate was placed on the magnetic rack until the solution was clear (~2min). 17µl of the supernatant was transferred to a clean PCR tube and proceed to PCR enrichment.

2.10.5 PCR library enrichment

To each 17µl a PCR library enrichment was performed as shown in (Table 2.46). The samples were mixed and a PCR reaction was performed (Table 2.47).

Table 2.46: PCR library enrichment component

Components	Amounts per reaction (µl)
NEBNext USER enzyme	3
NEBNext Q5 Hot Start HiFi PCR Master	25
Index (X) primer	1
Universal PCR primer	1
Sterile H2O	3
Total	50

(X) Index number

Table 2.47: PCR cycling conditions

Cycle step	Temperature	Time	Cycles
USER Digestion	37 °C	15 min	1
Initial denaturation	98 °C	30 sec	1
Denaturation	98 °C	10 sec	12
Annealing/Extension	65 °C	75 sec	
Final Extension	65 °C	5 min	1
Hold	4°C	∞	

2.10.6 Purify the PCR reaction using Agencourt AMPure XP Beads

The samples were transferred from the PCR tubes to a PCR plate. 45µl (0.9X) of resuspended Agencourt AMPure XP Beads were added to each 50µl PCR reaction, mixed well and incubated for 5min at room temperature. After incubation the plate was placed on the magnetic rack. After 5min carefully the supernatant was aspirated and discarded without disturbing the beads. A washing step was performed by adding 200µl of freshly prepared 80% ethanol to each sample while on the magnetic rack, incubated for 30sec at room temperature then was carefully removed and discarded. This step was repeated for a total of two washes. The beads were left to air dry for 5min with the plate on the magnetic rack. Next, the plate was removed and the DNA target was eluted from the beads with 23µl 0.1XTE. The beads were mixed thoroughly and incubated for 2min at room temperature. The plate was then placed on the magnetic rack until the solution was clear (~ 2min). Next, 20µl of the supernatant was transferred to a clean PCR tube and stored at –20°C.

The quality of the fragmented ds cDNA libraries were assessed using Bioanlayser High Sensitivity DNA Chip, product number G2938-90321. The libraries were quantified using the Qubit Fluorometer. 2ul from each DNA library was measured and the concentration of each library was obtained, this was then converted into nmol/µl. The total nM for each sample was calculated and diluted to achieve 2nM. 10 libraries were pooled together in a lane i.e. lane 6 and 7. The libraries were loaded into the Illumina HiScan SQ and the standard protocol was followed for 2x93bp paired end sequencing. The bioinformatics analysis was performed in collaboration with Dr Wenbin Wei/ Professor Winston Hide group.

The Illumina sequencer generated the bcl files which then were converted to fastq files by bcl2fastq program. The fastq files were then aligned to the GRCh37 human genome using bcbio's star aligner. The reads were counted using the feature Counts. Furthermore, the differentially expressed genes were identified using the edgeR program with the criteria of a fold change $\geq \pm 1.5$ and p-value ≤ 0.05 (Figure 2.2).
(http://bcbionextgen.readthedocs.io/en/latest/contents/introduction.html)

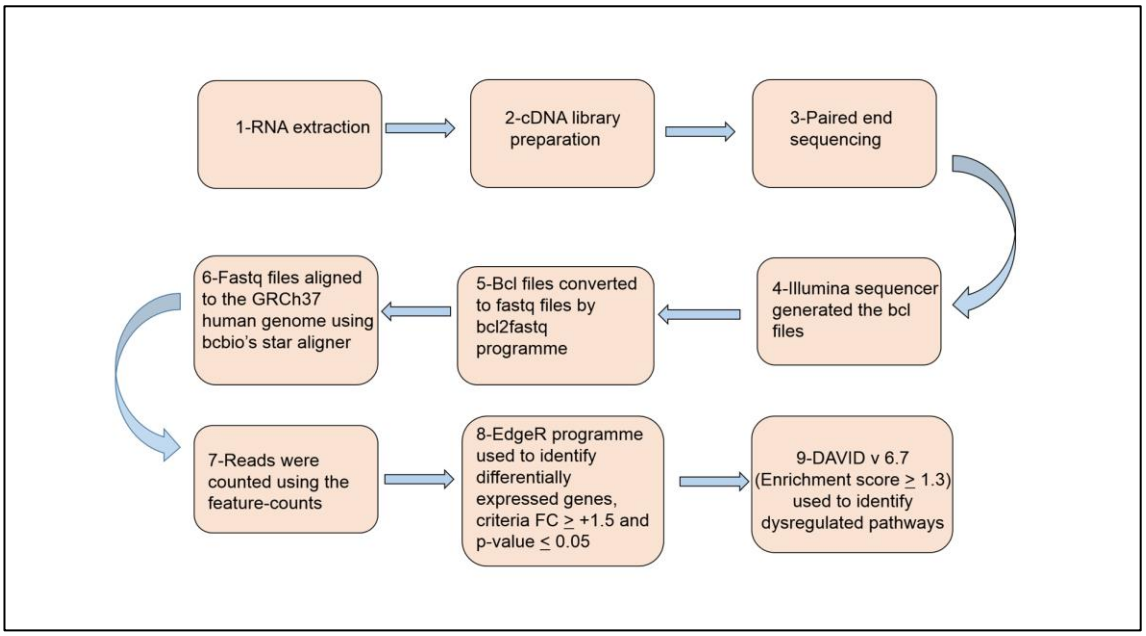

Figure 2.2: *Schematic diagram showing the analysis of the RNA sequencing data.*

2.11 Fluorescence in situ hybridization

Fluorescence in situ hybridization (FISH) is a powerful technique that reveals the location of nucleic acid inside the cell using a designed complementary labelled probe. In the current work three probes were designed by the manufacturer against potential nuclear mRNAs (Table 2.48).

Table 2.48: Labelled probe sets

Condition	Gene	Filter set
Control 155	RNU6-1	Cy5 (650)
Patient 48 (missense mutation)	MMP1	FITC (488)
Patient 192 (truncated mutation)	LUC7L3	Cy3 (550)

2.11.1 Fibroblast culture in 24 round well plate and 4% formaldehyde cell fixation

A representative fibroblast from each condition was cultured in a 24 round well plate, control 155, patient 48 missense mutation and patient 192 truncated

mutation. A pre-immersed cover slips in 70% ethanol were placed in each well prior to culture using sterile forceps. Then each fibroblast condition was placed in a well. Cells were allowed to grow in MEM and were monitored until they reached ~90% confluency.

In a fume hood, 10mL of fresh 4% formaldehyde solution was prepared by diluting 1.08mL of a 37% stock formaldehyde with 8.92mL of 1XPBS and was briefly mixed. The culture medium was carefully aspirated off, avoiding contact with cover slips and cells. Then, gently the cover slips were rinsed twice, each time with 2mL/well of 1XPBS. The final 1XPBS wash was aspirated off and 400µL/well of freshly prepared 4% formaldehyde was added, making sure that the cover slips are immersed completely. Incubated at RT for 30min. Next, the formaldehyde solution was aspirated off and gently rinsed three times each with 2mL/well of 1XPBS. Finally, fixed cells were used immediately in the in situ assay.

2.11.2 QuantiGene® ViewRNA FISH cell assay

The following were prepared prior to experiment: the dry incubator (GeneChip® Hybridization oven 640 by Affymetrix) was set at 40 ± 1°C prior, 420mL of 1XPBS was prepared by adding 42mL of 10X PBS to 378mL of H_20 and mixed well and the protease QS was placed on ice. Also, wash buffer was prepared by adding the following components in order to avoid formation of precipitates: 624.96mL H_20, 1.89mL wash comp 1 and 3.15mL wash comp 2. The probe set diluent QF, amplifier diluent QF and label probe diluent QF were pre-warm to 40°C in a water bath for 30min. The probe sets: pre-amplifier mix, amplifier mix, label probe mix and 100X DAPI were thawed at RT then placed on ice. The label probe mix was protected from light.

2.11.3 Permeabilize cells with detergent solution

The 1XPBS was aspirated and replaced with 400µL/well of detergent solution QC. The plate was covered with lid and incubated for 5 min at RT. After incubation the detergent solution QC was aspirated and cells were rinsed twice with

2mL/well of 1XPBS. The cells were allowed to sit in the final 1XPBS wash while preparing the working protease solution for the next step.

2.11.4 Digestion with working protease solution

The working protease solution was prepared by diluting the protease QS 1:4,000 in 1X PBS (Table 2.49). The mixture was mixed briefly then 1XPBS was replaced with 400µL/well of working protease solution. The plate was covered with lid and incubated for 10 min at RT. After incubation the working protease solution was aspirated off and cells were rinsed three times with 2mL/well of 1XPBS. Samples were allowed to sit in the final 1XPBS wash while preparing the working probe set solution for the next step.

Table 2.49: Working protease solution for 1 well

Component	Amount (µL)
Protease QS	0.1
1XPBS	399.9
Total volume	400.0

2.11.5 Hybridization with probe sets

The working probe set solution was prepared by diluting each Probe Set 1:100 in pre-warmed probe set diluent QF (Table 2.50). The mixture was mixed briefly, the 1XPBS was aspirated off and replaced with 400µL/well of the appropriate working probe set solution. For the “no probe” negative control, 400µL/well of pre-warmed probe set diluent QF was used. The wells were covered with lid and incubate at 40 ± 1°C for 3h.

Table 2.50: Working probe set solution for 1 well

Component	Amount (µl)
Probe set	4
Probe set diluent QF (pre-warmed at 40 °C)	396
Total volume	400

2.11.6 Cells wash

The plate was removed from the incubator and the working probe set solution was aspirated off. The cells were washed three times each with 2mL/well of wash buffer. Then cells were allowed to soak in wash buffer for 2min in each wash. Samples were left in the final washing buffer while preparing the pre-amplifier mix solution.

2.11.7 Hybridize with pre-amplifier

The working pre-amplifier mix solution was prepared by diluting pre-amplifier mix 1:25 in pre-warmed amplifier diluent QF (Table 2.51). The mixture was mixed briefly, the wash buffer was aspirated and replaced with 400µL/well of working pre-amplifier mix solution. The plate was covered with a lid and incubate at 40 ± 1°C for 30min.

Table 2.51: Working pre-amplifier mix solution for 1 well

Component	Amount (µL)
Amplifier Diluent QF (pre-warmed at 40 °C)	384
Pre-amplifier Mix	16
Total volume	400

2.11.8 Cells wash

The plate was removed from the incubator and the working pre-amplifier mix solution was aspirated off. The cells were washed three times each with 2mL/well of wash buffer. Cells were allowed to soak in wash buffer for 2min in each wash. Samples were then left in the final washing buffer while preparing the amplifier mix solution.

2.11.9 Hybridize with amplifier

The working amplifier mix solution was prepared by diluting amplifier mix 1:25 in pre-warmed amplifier diluent QF (Table 2.52).

Table 2.52: Working amplifier mix solution for 1 well

Component	Amount (µL)
Amplifier diluent QF (pre-warmed at 40 °C)	384
Amplifier mix	16
Total volume	400

2.11.10 Cells wash

The plate was removed from the incubator and the working amplifier mix solution was aspirated off. The cells were washed three times each with 2mL/well of wash Buffer. Cells were allowed to soak in wash buffer for 2min in each wash. Samples were then left in the final washing buffer while preparing the working label probe mix solution.

2.11.11 Hybridize with labelled probe

The working label probe mix solution was prepared by diluting label probe mix 1:25 in pre-warmed label probe diluent QF (Table 2.53). The mixture was mixed briefly and was protected from light. The wash buffer was aspirated and replaced with 400µL/well of working label probe. The plate was covered with a lid and incubated at 40 ± 1 °C for 30min.

Table 2.53: Working label probe mix solution for 1 well

Component	Amount (µL)
Label probe diluent QF (pre-warmed at 40 °C)	384

Label probe mix	16
Total volume	400

2.11.12 Cells wash

The plate was removed from the incubator and the working label probe mix solution was aspirated off. The cells were washed three times each with 2mL/well of wash buffer. At the first two washes cells were allowed to sock in wash buffer for 2min and the final wash was incubated for 10min. Samples were then left in the final washing buffer while preparing the working DAPI solution.

2.11.12 DAPI staining

The working DAPI solution was prepared by diluting the 100X DAPI 1:100 in 1XPBS (Table 2.54). The mixture was mixed briefly and was protected from light. The wash buffer was aspirated and replaced working DAPI solution. Cells were incubated at RT for 1min. Afterwards, DAPI working solution was aspirated off and cells were washed once with 2mL/well of 1X PBS. Then 400µL/well of fresh 1XPBS was added.

Table 2.54: Working DAPI solution for 1 well

Component	Amount (µL)
1XPBS	396
100XDAPI	4
Total volume	400

2.11.13 Mounting on glass slide

A small drop of VECTASHIELD anti-fade mounting medium was placed on a microscope slide avoiding air bubbles. Using a fine tipped forceps the cover slip was removed from the 24 round well plate and the edge of the cover slip was

gently dabbed on a dry laboratory wipe to remove excess 1XPBS. The cover slips were mounded facing down on the spot of mounting media avoiding air bubbles. Slides were left to cure overnight at RT. After that slides were stored at 2-8°C protected from light from light. The fluorescent signals were stable for up to one week.

2.11.14 Image samples using confocal microscope

Leica SP5 confocal microscope using 63x 1.20 lens along with the appropriate filter settings (Table 2.55) were applied to examine the cells.

Table 2.55: Leica SP5 confocal microscope filter settings

RNA Probe	Probe set	Filter set
Human RNU6	Type 6	Cy5 (650)
Human MMP1	Type 4	FITC (488)
Human LUC7L3	Type 1	Cy3 (550)

Chapter 3: Human Exon 1.0 ST Array GeneChip®

3.1 Human Exon 1.0 ST Array GeneChip®

Affymetrix GeneChip® Human Exon 1.0 ST Arrays were designed with better features over conventional 3' IVT microarrays as discussed in section 1.1.6.1 and 1.1.6.2. They provide the maximum information needed to understand gene expression as their aim is to detect transcripts along the entire length of an mRNA rather than the 3' end region only. Each transcript isoform of a particular gene consists of exons which can be identified by measuring the signal intensities of each exon which is presented on the GeneChip® by four probes. Measuring the combination of these signals allows the identification of known or novel alternatively spliced transcripts when compared to the current data bases (http://www.affymetrix.com).

In this chapter, RNA extracted from fibroblasts of fALS-*TARDBP* missense mutation and controls was hybridized to the Human Exon 1.0 ST Arrays and the resulting gene expression profiles were analysed in order to identify dysregulated pathways occurring in the presence of mutant *TARDBP.*

3.2 Fibroblast culture

Primary fibroblasts from three fALS-*TARDBP* cases carrying missense mutation and three aged and gender matched controls (Table 2.3 in chapter 2: materials and methods) were grown and the doubling rate was monitored carefully. Cells were evaluated under the light microscope. The goal was to achieve evenly distributed monolayer fibroblasts throughout the flasks avoiding clump formation or contamination. Cells were allowed to grow to no more than 90% confluency to avoid contact inhibition (Abercrombie, 1970).

3.3 Cytoplasmic and nuclear RNA concentrations using the Nanodrop spectrophotometer

Cell fractionation and RNA extraction was carried out using the Cytoplasmic and Nuclear RNA purification kit (Norgen Biotek). The Nanodrop spectrophotometer was used to measure the quantity of RNA in the samples. RNA yields from each cellular compartment are shown in Table 3.1. All samples presented good quantity of RNA except cytoplasmic control 11 which showed the lowest RNA concentration (yield= 7.47ng/µl). All RNA samples were eluted in 50µl of RNase free water, thus the total RNA yield of cytoplasmic control 11 was 373.5ng which was sufficient for the Human Exon 1.0 ST Array experiment which requires a total of 200ng. However, a further accurate measurement of the quantity and quality was necessary using the Agilent Bioanalyser for all samples prior to the Human Exon 1.0 ST Array RNA preparation.

The nuclear samples were DNase treated in order to eliminate any genomic DNA that might interfere with the Human Exon 1.0 ST Array experiment or in qRT-PCR validation. Table 3.2 illustrates the RNA yields post-DNase treatment. Nuclear samples demonstrated good quantity of RNA. The lowest RNA concentration post-DNase treatment was patient 51(28.86ng/µl). The total yields of patient 51 =1443ng which was sufficient.

Table 3.1: Controls and patients RNA yields using the Nanodrop spectrophotometer. ng/µl=nanograms/microliter, Con= Control, Pat= Patient, ID= identification

Cellular fraction	Mutation type	Sample ID	RNA yields (ng/µl)	Total yields (ng/µl)
Cytoplasmic	-	Con 8	68.47	3423.5
		Con 11	7.47	373.5
		Con 170	50.61	2530.5
	Missense mutation	Pat 48	10.24	512
		Pat 51	20.41	1020.5
		Pat 55	71.25	3562.5
Nuclear Pre-DNase treatment	-	Con 8	79.42	3971
		Con 11	32.99	1649.5
		Con 170	88.25	4412.5
	Missense mutation	Pat 48	84.47	4223.5
		Pat 51	13.57	678.5
		Pat 55	59.42	2971

Table 3.2: Nuclear RNA yields post-DNase treatment using the Nanodrop spectrophotometer. Cytoplasmic RNA samples were not DNase treated. ng/µl= nanograms/microliter, Con= Control, Pat= Patient, ID= identification

Cellular fraction	Mutation type	Sample ID	RNA yields (ng/µl)	Total RNA yields (ng/µl)
Nuclear Post-DNase treatment	-	Con 8	48.03	2401.5
		Con 11	36.2	1810
		Con 170	66.14	3307
	Missense mutation	Pat 48	38.3	1915
		Pat 51	28.86	1443
		Pat 55	45.64	2282

3.4 RNA quality using Agilent Bioanalyser 2100

An accurate measurement of the RNA concentrations and integrity was performed by the Agilent Bioanalyser 2100. The device separates 1µl of RNA sample into its different major species creating informative electropherograms that can be visibly interpreted. A good RNA integrity can be defined as achieving the following two characteristics: first, detecting two distinct peaks of rRNA both 18s and 28s. Second, the level of rRNA28s is required to be approximately twice the level of rRNA18s. This implies that mRNA transcripts are full length (Figure 3.1). Figure 3.1B is the cytoplasmic control 8 RNA demonstrating sharp distinct peaks of rRNA18s and rRNA28s at sizes ~2000 (nt) and ~4000 (nt) respectively and the rRNA28s was about double the level of rRNA18s. Similarly, pre-DNase treated nuclear RNA of control 8 showed the same characteristics of the cytoplasmic RNA however a peak between rRNA18s and rRNA28s was present which is suggested to be genomic DNA and degraded rRNA highlighted in a red box (see figure 3.1C). Post-DNase treated nuclear RNA of control 8 is shown in (Figure 3.1D) the graph indicates that genomic DNA was reduced effectively. However, it is clearly observed that RNA integrity was affected. This was also confirmed by the RIN values which were shown to be decreased following DNase treatment (Table 3.3). RNA sample selection for the Human Exon 1.0 ST Array experiment was based on two criteria: RIN cut-off value $\geq$5 and a minimum of ~200ng RNA yields. The cytoplasmic RNA samples yields ranged ~4000ng to 800ng and the post-DNase nuclear RNA samples ranged ~200ng to 500ng (Table 3.3). All RINs were $\geq$5, therefore, all samples were taken forward.

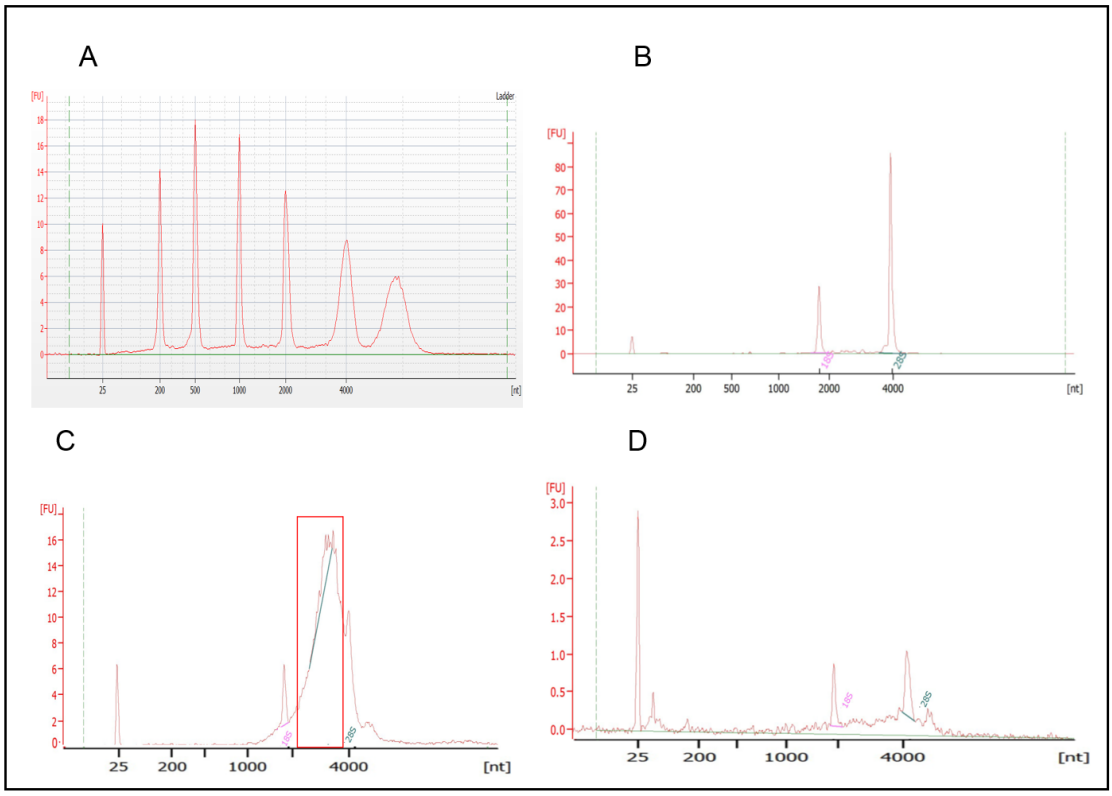

Figure 3.1: *Representative electropherograms generated by the Agilent Bioanalyser 2100 of sample (Control 8). (A) Standard ladder graph that represents the RNA markers which act as a reference for the other RNA samples. (B) Cytoplasmic RNA sample (Control 8), (C) Nuclear RNA sample (Control 8) and (D) Post-DNase treated nuclear RNA sample (Control 8). The Y axis represents the UV light absorption in fluorescence unit (FU) and the X axis represents the size in nucleotides (nt).*

Table 3.3: Cytoplasmic and post-DNase treated nuclear RNA yields using Agilent Bioanalyser. ng=nanograms, RIN= RNA integrity number, ng/µl= nanograms/ microliter, Con= Control, Pat= Patient, ID= identification

Cellular fraction	Mutation type	Sample ID	RNA yields (ng/µl)	RIN	Total RNA yields (ng)
Cytoplasmic	-	Con 8	40	10	2000
		Con11	27	5	1350
		Con 170	70	8.7	3500
	Missense mutation	Pat 48	16	8.5	800
		Pat 51	20	9.8	1000
		Pat 55	82	10	4100
Nuclear Post-DNase treatment	-	Con 8	13	6.8	260
		Con11	21	5.4	420
		Con 170	25	6.9	500
	Missense mutation	Pat 48	11	5.3	220
		Pat 51	15	5	300
		Pat 55	12	5	240

3.5 Human Exon 1.0 ST Arrays GeneChip®

Human Exon 1.0 ST Arrays GeneChip® Affymetrix were used to measure gene expression. Samples were prepared and quality checked at various stages to ensure sufficient amount of transcripts of good quality were prepared. This was achieved using both the Nanodrop spectrophotometer and the Agilent Bioanalyser (see materials and methods section 2.4 and 2.5). RNA samples were linearly amplified to obtain 10µg of cRNA that is required for the preparation of ss cDNA. RNA samples were successfully amplified and the cRNA yields were greater than the required concentration (10µg) ranging from 19.2µg to 120.4µg (Table 3.4). ss cDNA preparation was performed and the threshold was to obtain 5.5µg of ss cDNA in order to proceed with the fragmentation and labelling step. The ss cDNA was properly synthesized and high yields were achieved. Table 3.5 list the ss cDNA concentrations ranging from 7.44µg to 11.19µg.

Table 3.4: cRNA yields. µg= micrograms, ng/µl=nanograms/microliter, Con= control, Pat= Patient, ID= identification

Cellular fraction	Mutation type	Sample ID	cRNA yields (ng/µl)	Total yield (µg)
Cytoplasmic	-	Con 8	1688.73	67.5
		Con11	481.41	19.2
		Con 170	1093.68	43.7
	Missense mutation	Pat 48	718.27	28.7
		Pat 51	2406.26	96.2
		Pat 55	1412.87	56.5
Nuclear Post-DNase treatment	-	Con 8	1494.49	69.7
		Con11	2658.18	106.3
		Con 170	3010.44	120.4
	Missense mutation	Pat 48	1312.43	52.4
		Pat 51	2223.56	88.9
		Pat 55	616.55	24.6

Table 3.5: ss cDNA yields. µg= micrograms, ng/µl= nanograms/microliter, Con= Control, Pat= Patient, ID= identification

Cellular fraction	Mutation type	Sample ID	cRNA yields (ng/µl)	Total yield (µg)
Cytoplasmic	-	Con 8	373.61	11.19
		Con11	248.11	7.44
		Con 170	277.76	8.31
	Missense mutation	Pat 48	303.06	9.09
		Pat 51	308.72	9.24
		Pat 55	266.68	7.98
Nuclear Post-DNase treatment	-	Con 8	301.74	9.03
		Con11	328.37	9.84
		Con 170	300.07	9
	Missense mutation	Pat 48	270.85	8.1
		Pat 51	282.50	8.46
		Pat 55	262.75	7.86

3.5.1 Fragmentation

After preparing ss cDNA samples to the desired concentrations, they were fragmented and labelled in order to facilitate their binding to the probes on the array and for this to be detected. The recommended length is ~ 25 nt. Controls and patients fragmented ss cDNA were within the acceptable length. Figure 3.2 illustrates a representative fragmented ss cDNA (Control 8).

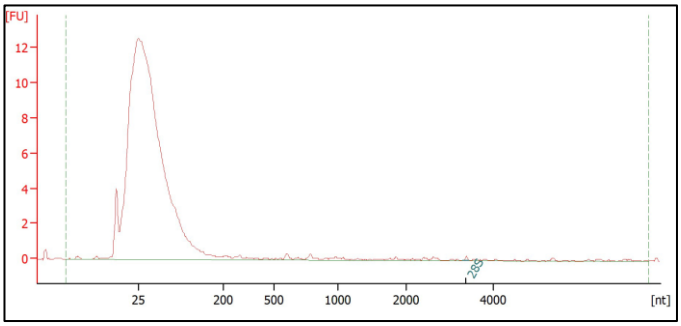

Figure 3.2: *Representative electropherogram of fragmented single stranded DNA samples (Control8). The Y axis represents the UV light absorption (FU) and the X axis represents size in (nt). The peak point of fragments can be assessed to be approximately 24-25 nucleotides in length when compared to the ladder*.

3.5.2 Gel shift assay

The gel shift assay is a procedure that assesses the efficiency of the labelling step (see materials and methods section 2.7.10). Briefly, randomly selected samples were incubated with neutravidin to facilitate its attachment to biotin labelled fragmented ss cDNA. Samples were then separated on a 4-20% gradient TBE gel by electrophoresis. The gel was stained with ethidium bromide in order to visualize the bands under UV light. All 9 of the 12 samples, were treated with neutravidin and considered the positive samples. 3 samples were treated with PBS instead of neutravidin. Positive samples showed bands at the expected position (400bp) and the negative samples did not show bands (Figure 3.3). This indicated that the labelled samples contained biotin which had hybridized to the

neutravidin and caused an altered movement of the molecules in the gel. Therefore, all the labelled samples were considered to have passed quality control and could be put on the arrays.

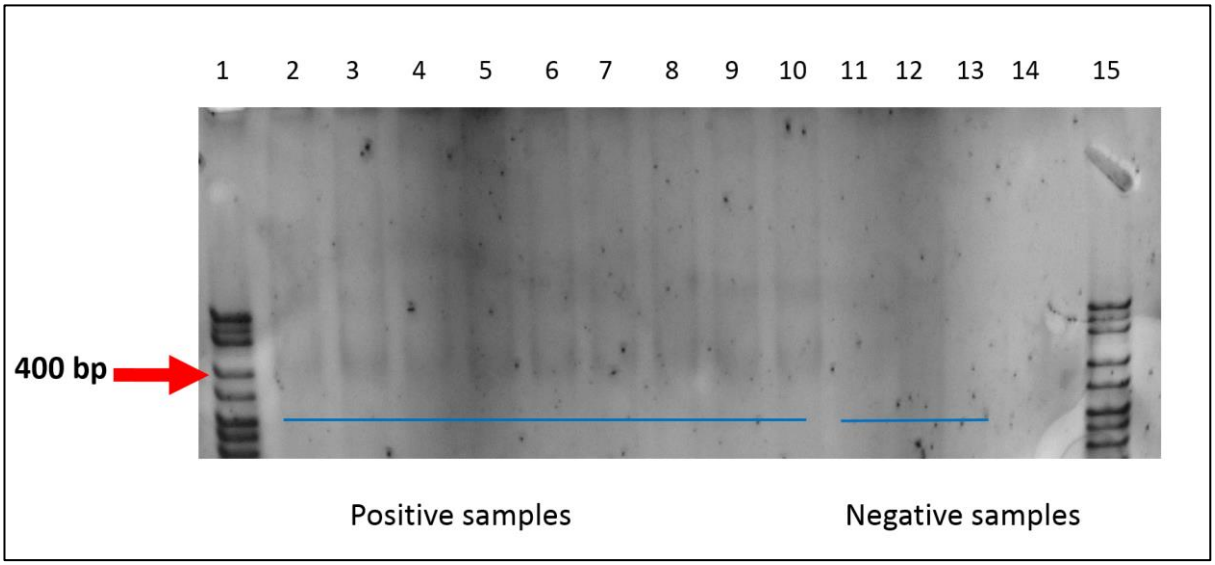

Figure 3.3: *Gel shift assay presenting 4-20% TBE gel electrophoresis stained with ethidium bromide and visualized under UV light. The positive samples showed bands at the expected positions (400 bp). The negative samples did not show any bands.*

Well no	1	2	3	4	5	6	7	8	9	10	11	12	13	14	15
Sample ID	Hyper ladder IV	Con N8	Con C8	Pat N48	Pat C48	Con N11	Con C11	Pat N51	Pat C51	Con N170	Con C170	Pat N55	Pat C55	Empty well	Hyper ladder IV
		Positive samples									Negative samples				

**Con= Control, Pat= Patient, N= Nuclear, C= Cytoplasmic*

3.5.3 Human Exon 1.0 ST Arrays quality control

The Human Exon 1.0 ST Arrays raw data was generated as CEL files using the Affymetrix GeneChip® Command Console (AGCC) software. Quality control checks of the arrays was performed through Affymetrix Expression Console v1.0 software.

The spiked in poly-A RNA controls are exogenous positive controls that are included in sample preparation (See section 2.7.2 for full description). Poly-A spiked in controls were prepared at different levels of concentrations. The *dap* gene was expected to demonstrate the highest intensity followed by *thr, phe* and *lys*. Figure 3.4 demonstrates the poly-A spiked in controls in a linear graph. As seen in figure 3.4A all cytoplasmic samples showed good quality of amplification except control 11 showed a slight flip in the concentration of (*lys*) with (*phe*). That might be due to low concentration of cytoplasmic control 11 RNA yields and the input RIN was near the lower limit (see table 3.1 & 3.3). Also there might be a technical reason i.e. inadequate spiked in poly-A control dilution preparation. Hybridization intensities of the poly-A spiked in controls of the post-DNase treated nuclear samples are shown in Figure 3.4B. Uneven hybridization intensities were demonstrated which might be due to the effect of DNase treatment on the RNA integrity.

In addition hybridization spiked in controls intensities were measured (Figure 3.5). BioB, BioC, BioD and Cre are prelabeled hybridization controls that monitor the hybridization, washing and staining process of the arrays (see section 2.7.11 for full description). It is expected that the Cre would have the highest signal intensity followed by BioD, BioC and BioB. All cytoplasmic and post-DNase treated samples showed good and even distribution of the hybridization signal intensity (Figure 3.5 A&B). The probe set intensities were measured and a box plot graph was generated to demonstrate the overall deviation of probe set signals for each array. The box represents the upper quartile, lower quartiles and median. The whiskers represent the highest and the lowest average signal intensities of the probes (Figure 3.6). The median value across samples was

detected at ~ 0.1 (red line across the boxes Figure 3.6 A&B) which is within expected range (0.1-0.2).

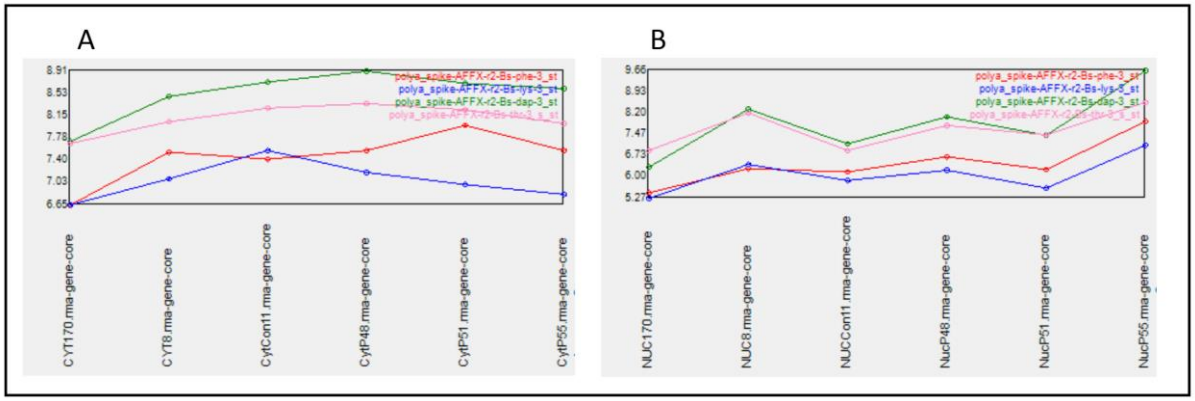

Figure 3.4: *Poly-A spiked in controls linear graph from the Human Exon 1.0 ST Array. (A)The cytoplasmic hybridization intensities of the poly-A spiked in controls. All cytoplasmic samples showed good quality of amplification except control 11 showed a slight flip in the concentration of (lys) with (phe). (B) The poly-A spiked in hybridization intensities of the post-DNase treated nuclear samples. Uneven hybridization intensities which might be due to DNase treatment.*

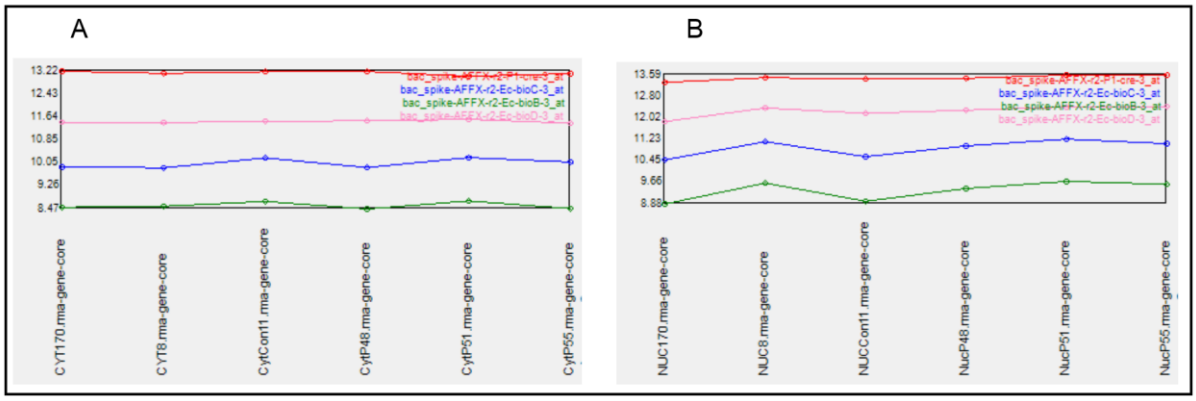

Figure 3.5: *BioB, BioC, BioD and Cre hybridization spiked in controls linear graph from the Human Exon 1.0 ST Array. (A) The cytoplasmic samples, (B) The post-DNase treated nuclear samples.*

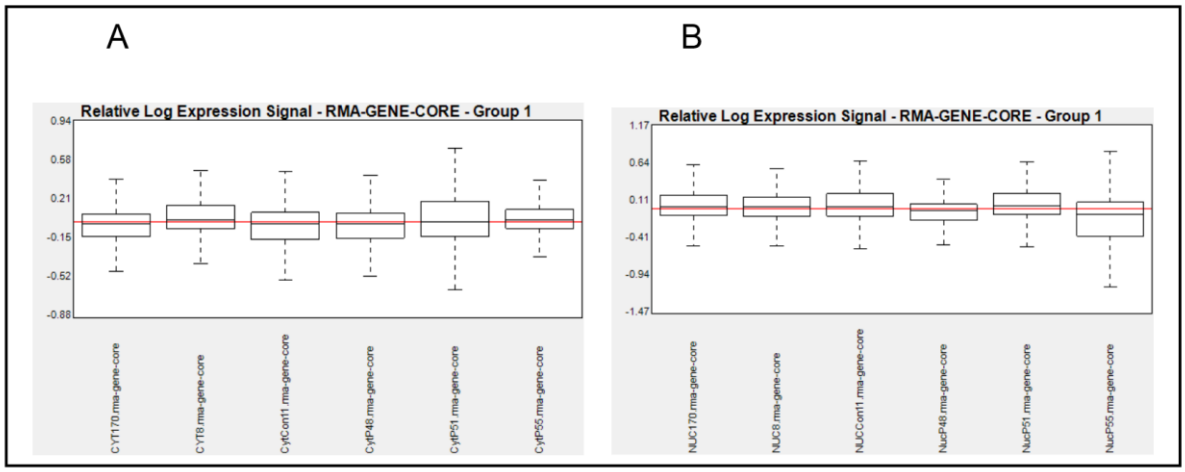

Figure 3.6: *Box plot graph of normalized relative log expression signals from the Human Exon 1.0 ST Array. Each box plot represents the mean and standard deviation of an array. The red middle line across the boxes is the median gene expression of all samples. The whiskers represent the highest and the lowest average signal intensities of the probes. (A) Cytoplasmic samples relative expression signals. (B) The post-DNase treated nuclear samples relative expression signals.*

3.6 Gene expression profiling using Partek® Genomics Suite ™ 6.6 software

CEL files from controls and patients were uploaded into Partek® Genomics Suite ™ 6.6 software. The differentially expressed genes were analysed using an ANOVA test. Genes with a significant p-value ≤ 0.05 and fold change ≥ ±1.2 were identified. These parameters were set to identify the maximum number of differentially expressed genes.

To investigate the hypothesis that, cytoplasmic and nuclear transcriptomic profile from mutant *TARDBP* fibroblasts will generate different transcriptomic profiles than control fibroblasts and will establish transcripts and pathways dysregulated in the presence of mutations in *TARDBP,* the analysis was performed as follows: cytoplasmic missense mutation MT vs. cytoplasmic controls CON and nuclear missense mutation MT vs. nuclear controls CON. This facilitates the identification of differentially expressed genes in the cellular compartments which then allows the identification of dysregulated biological processes in fALS related *TARDBP* missense mutation cases. Cytoplasmic MT vs. cytoplasmic CON showed 702 differentially expressed genes. 426 were up-regulated and 276 were down-regulated (Figure 3.7A). The nuclear MT vs. nuclear CON demonstrated 685 differentially expressed genes. 345 were up-regulated and were 340 down-regulated (Figure 3.7B).

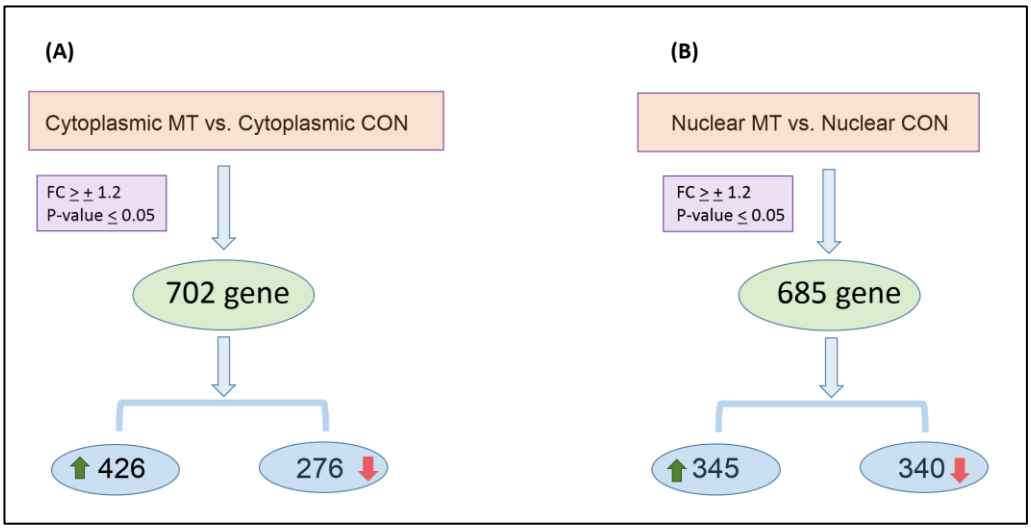

Figure 3.7: *Differentially expressed genes in cytoplasmic and nuclear fALS-TARDBP compared to controls*

3.6.1 Cytoplasmic MT vs. cytoplasmic CON gene expression profiling using the Human Exon 1.0 ST Arrays

The transcript IDs of the differentially expressed genes from cytoplasmic MT vs. cytoplasmic CON analysis were uploaded into DAVID v6.7 in order to identify the biological processes dysregulated in fALS-*TARDBP* fibroblasts. Biological pathways containing differentially expressed genes that had an enrichment score (ES) $\geq$ 1.3 were highlighted as significant which is equivalent to p-value of 0.05 (Huang da et al., 2009). The highest enrichment score hit was found in methylation, whereas the largest number of genes were clustered in RNA processing, neuron differentiation and cytoskeleton organization (Table 3.6).

3.6.1.1 Differential gene expression of cytoplasmic MT vs. CON

Table 3.6 shows that methylation, neuron differentiation, RNA processing, and cytoskeleton organization were the top four highest enriched biological processes in fALS cytoplasmic missense mutation. Thus, they were selected for further investigation.

Table 3.6: Functionally enriched biological processes generated by DAVID of the cytoplasmic MT vs. CON differentially expressed genes. GO=Gene ontology, ES=Enrichment score, no.=number

GO	Biological process	Gene no.	P-value	ES
BP_FAT	Methylation	8	3.9E-3	2
BP_FAT	Neuron differentiation	16	1.8E-1	1.81
BP_FAT	RNA processing	27	2.7E-3	1.73
BP_FAT	Cytoskeleton organization	16	1.8E-1	1.48
BP_FAT	Telencephalon development	6	2.8E-2	1.37

3.6.1.1.1 Methylation

Methylation is known to be an epigenetic modification process that can affect gene expression by silencing or activating genes (Grewal and Rice, 2004). Table 3.7 lists the methylation related genes dysregulated in the fALS-*TARDBP* cytoplasmic missense mutation. A number of genes involved in the methylation process were found to be down-regulated in the mutant *TARDBP* fibroblasts.

A reduction was found in the expression of the DNA (cytosine-5)-methyltransferase 1 (*DNMT1*) (FC=-1.5). DNMT1 is a modifying enzyme that binds to the CpG dinucleotide sequences at the promotor region to facilitate the addition of methyl group to the cytosine leading to gene silencing. In addition, it is responsible for the maintenance of DNA methylation following cell differentiation (Bonfils et al., 2000). Furthermore the GATA zinc finger domain containing 2A (*GATAD2A*) gene which belongs to the methyl-CpG-binding protein-1 complex and encodes for two proteins (p66-α and p66-β proteins) was decreased (FC=-1.2). These proteins are involved in the modulation of gene repression by the deacetylation of methylated nucleosomes (Brackertz et al., 2002). The helicase, lymphoid-specific (*HELLS*) gene was reduced (FC=-2). It encodes for the chromatin-remodelling ATPase enzyme that is involved in DNA strand separation that allows DNA methylation to take place (Lungu et al., 2015). Moreover, the coactivator-associated arginine methyltransferase 1 (*CARM1*) gene expression was down-regulated (FC=-1.2). This gene belongs to the protein arginine methyltransferase family and is involved in the methylation of the guanidine nitrogen molecules of arginine residues in a protein. It is also involved in the repression of the cAMP-dependent pathway and the activation of nuclear hormones by triggering different signalling cascades (Xu et al., 2001).

Furthermore, the euchromatic histone-lysine N-methyltransferase 1 (*EHMT1*) was decreased (FC=-1.2). It is a part of the DNA repressor complex PR domain-containing protein 16 (PRDM) which is involved in the brown adipocyte differentiation (Ohno et al., 2013). In addition, it was suggested to plays a role in silencing the *Myc* gene (Dominguez-Sola et al., 2007). Myc is a transcription factor that functions both as an activator and suppressor. It is involved in cell

proliferation, cell growth and apoptosis. It is activated through different signalling pathways including the MAP kinases (Dominguez-Sola et al., 2007). EHMT1 was also suggested to participate in cell cycle G1 phase (Ogawa et al., 2002). The RAB6C member RAS oncogene family (*RAB6C),* a member of the RAS oncogene family showed a reduction in gene expression (FC=-1.2) (Rajalingam et al., 2007).

In contrast only a single gene was up-regulated, the BTG family, member 2 (*BTG2)* (FC=1.3). BTG2 is an anti-proliferative protein which is involved in the regulation of cell cycle at the G1/S phase and is triggered by the p53 tumour suppresser protein during DNA damage (Rouault et al., 1996, Duriez et al., 2002).

Table 3.7: Genes involved in methylation in cytoplasmic missense mutation

Gene symbol	Gene names	P-value	Fold change
BTG2	BTG family, member 2	0.02	1.35
CARM1	Coactivator-associated arginine methyltransferase 1	0.05	-1.28
DNMT1	DNA (cytosine-5-)-methyltransferase 1	0.04	-1.50
EHMT1	Euchromatic histone-lysine N-methyltransferase 1	0.04	-1.29
GATAD2A	GATA zinc finger domain containing 2A	0.05	-1.28
HELLS	Helicase, lymphoid-specific	0.03	-2.02
RAB6C	RAB6C, member RAS oncogene family	0.04	-1.24
SUZ12	Suppressor of zeste 12 homolog (Drosophila)	0.006	-1.32

3.6.1.1.2 Neuron differentiation

As the model used in the current study were fibroblasts, it was surprising to find a group of genes assigned under the term neuron differentiation by DAVID and many of these genes were up-regulated (see Table 3.8). A further description of each gene is addressed below.

The BTG family member 2 (*BTG2*), as well as being involved in methylation was found to be increased (FC=1.3). It encodes for an anti-proliferative protein which is involved in the regulation of the cell cycle and is induced by the DNA damage and p53 tumour suppresser protein (Rouault et al., 1996, Duriez et al., 2002). An increased expression was observed in dopamine receptor D1 gene (*DRD1*). (FC=1.2). *DRD1* is a G-protein coupled receptor that is activated by the neurotransmitter dopamine which itself stimulates the enzyme adenylyl cyclase (Monsma et al., 1990). Adenylyl cyclase converts ATP into cyclic AMP (cAMP) which then stimulates the phosphorylation of the protein kinase A (PKA) (Sassone-Corsi, 1998). PKA is involved in several pathways however, one of the final stages of this signalling pathway is the phosphorylation of the cAMP response element-binding protein by PKA which is then diffused into the nuclear membrane and binds to the promoter region of a particular gene causing a down-regulation or up-regulation of gene expression (Dearry et al., 1990, Sassone-Corsi, 1998).

Moreover, an elevated gene expression was found in the inhibitor of DNA binding 3, dominant negative helix-loop-helix protein (*ID3*) and inhibitor of DNA binding 4, dominant negative helix-loop-helix protein (*ID4*) (FC=1.8 & FC=1.5 respectively). These encode proteins belonging to the inhibitor of DNA binding (ID) family of helix-loop-helix (HLH) proteins. They interact with helix-loop-helix transcription factors and prevent their binding to the DNA. It has been shown that ID3 is involved in neural cell differentiation, whereas ID4 was found to be highly expressed in undifferentiated cells and growing cells (Lyden et al., 1999, Shan et al., 2003).

The laminin beta 1(*LAMB1*) was increased (FC=1.8). LAMB1 belongs to the laminin protein structure which is part of the basal lamina located in the extracellular matrix and found in nearly all tissue organs. *LAMB1* expression was suggested to be associated with pial basement membrane of the brain (Radmanesh et al., 2013).

The Myosin, heavy chain 10, non-muscle (*MYH10*) is an important protein for cell division during cytokinesis and was shown to be up-regulated (FC=1.6) (Takeda et al., 2003). Moreover, the protein kinase, cGMP-dependent, type I (*PRKG1*) expression was elevated (FC=1.2). PRKG1 is essential for platelet function, cell division and smooth muscle relaxation (Li et al., 2003, Burgoyne et al., 2007). Furthermore, the protein tyrosine phosphatase, receptor type, M (*PTPRM*) which is involved in many cellular signalling cascades that result in cell differentiation, mitosis and cell growth was increased (FC=1.2) (Hendriks et al., 2013). The Septin 2 *(SEPT2)* gene was also increased (FC=1.3). It belongs to the septin family which are divided into four major groups: septin2, septin3, septin6 and septin7. They are important in activating the cellular signalling pathways in response to DNA damage (Kremer et al., 2007, Mostowy and Cossart, 2012).

On the other hand, the following genes were decreased. The LIM homeobox 2 (*LHX2*) was down-regulated (FC=-1.3). This gene encodes for a transcription factor that regulates stem cell differentiation to neuroepithelium (Mangale et al., 2008). Furthermore, the notch homolog 1, translocation-associated (drosophila) (*NOTCH1*) was reduced (FC=-1.3). *NOTCH1* is part of the notch family which are single-pass transmembrane receptors that interact with extracellular molecules that activate inner signalling pathways which control cell fate decision. The activation of *NOTCH1* has been shown to facilitate progenitor cell differentiation to astroglia (Tanigaki et al., 2001). A down-regulation of the empty spiracles homeobox 2 (*EMX2*) gene was observed (FC=-1.2). This gene is known as empty spiracles gene in drosophila however, in human this gene encodes for a homeobox-containing transcription factor which is expressed during the development of the cortical cells (Bishop et al., 2000). Finally, the plexin A3 (*PLXNA3*) was also reduced (FC=-1.2). It is a transmembrane protein which is

involved in the development of the neuronal and epithelial cells (Maestrini et al., 1996).

Interestingly, although the model used in the present work is fibroblasts, observed changes in gene expression related to the CNS in respect to cell differentiation, adhesion and DNA damage response were dysregulated. This strongly suggests that ALS-derived fibroblasts would be a good model to study neurodegenerative disorders.

Table 3.8: Genes involved in neuron differentiation in cytoplasmic missense mutation

Gene symbol	Gene names	P-value	Fold change
BTG2	BTG family, member 2	0.02	1.35
DRD1	Dopamine receptor D1	0.02	1.25
EMX2	Empty spiracles homeobox 2	0.04	-1.23
ETV4	Ets variant 4	0.01	-1.26
HOXA2	Homeobox A2	0.04	-1.64
ID3	Inhibitor of DNA binding 3, dominant negative helix-loop-helix protein	0.03	1.88
ID4	Inhibitor of DNA binding 4, dominant negative helix-loop-helix protein	0.02	1.57
LAMB1	laminin, beta 1	0.05	1.82
LHX2	LIM homeobox 2	0.01	-1.36
MYH10	Myosin, heavy chain 10, non-muscle	0.05	1.60
NOTCH1	Notch homolog 1, translocation-associated (Drosophila)	0.02	-1.32
PLXNA3	Plexin A3	0.04	-1.25
PRKG1	Protein kinase, cGMP-dependent, type I	0.03	1.28
PTPRM	Protein tyrosine phosphatase, receptor type, M	0.03	1.20
RXRA	Retinoid X receptor, alpha	0.01	-1.31
SEPT2	Septin 2	0.002	1.38

3.6.1.1.3 RNA processing

RNA processing describes mechanisms by which nascent mRNA is converted to a mature mRNA molecule. In eukaryotic cells this process takes place both during and after mRNA transcription in the nucleus and can be stepwise listed as the following: 5'capping (7-Methylguanosine), 3' polyadenylation, splicing/alternative splicing, editing and mRNA export. RNA processing has been shown to be altered in ALS and several genes involved in RNA processing were found to be mutated in some forms of fALS (Polymenidou et al., 2012, Raman et al., 2015). Table 3.9 lists the genes dysregulated in the fALS-*TARDBP* cytoplasmic missense mutation. Genes were also grouped according to functional similarity as shown below (also see figure 3.8).

3.6.1.1.3.1 RNA splicing/ alternative splicing

RNA splicing is a process by which the intronic regions of the nascent mRNA are removed and exonic regions are joined together. Alternative splicing is the mechanism that allows the production of different transcript isoforms from a single gene (Blencowe et al., 2009). Genes involved in RNA splicing/ alternative splicing were dysregulated.

The DEAD (Asp-Glu-Ala-Asp) box polypeptide 58 (*DDX58*) was increased (FC=1.2). DDX58 belongs to the DEAD box helicase family and has an RNA-dependent ATPase activity which is essential for RNA metabolism (Yoneyama et al., 2004). Furthermore, the RNA binding protein squamous cell carcinoma antigen recognized by T cells 3 (*SART-3*) showed an increase in gene expression (FC=1.4). It is involved in mRNA splicing by its association with the snRNPs U6/U4 at the recycling step of the spliceosome cycle (Harada et al., 2001, Long et al., 2014). In addition, the zinc finger CCHC-type and RNA binding motif 1 (*ZCRB1*) a part of the of the U11/U12 di-snRNP spliceosome that act in pre-mRNA splicing was increased (FC=1.3) (Wang et al., 2007). The heterogeneous nuclear ribonucleoprotein M which is a splicing regulatory factor that participates in RNA alternative splicing was increased (FC=1.8) (Hovhannisyan and Carstens, 2007). The RNA binding motif protein 39 (*RBM39*) was up-regulated (FC=1.3). RBM39 belongs to the U2AF65 family of proteins which form one of the core

spliceosomal nuclear proteins and has a role in the alternative splicing of steroid hormone receptor genes (Jung et al., 2002).

In contrast, three splicing factors were decreased, splicing factor 3a, subunit 1, 120kDa (*SF3A1*), splicing factor 3a, subunit 3, 60kDa (*SF3A3*) and splicing factor, arginine/serine-rich 15 (*SFRS15*) (FC=-1.28,-1.22 & -1.26 respectively). Moreover, U5 snRNP-specific protein, 200 kDa which is a member of the spliceosome assembly molecule and also belongs to the DEAD box helicase family showed a decrease in gene expression (FC=-1.3) (Liu and Cheng, 2015). Finally, the pre-mRNA processing factor 8 homolog (S. cerevisiae) (*PRPF8*) was decreased (FC=-1.4). PRPF8 is part of the U2 and U12 dependent spliceosomes complex that mediate mRNA splicing (Luo et al., 1999).

Whilst some genes suggests an increase in splicing this is associated with decrease in splicing factors. A further investigation is required to assess the overall effect of the missense mutation on splicing.

3.6.1.1.3.2 3’ polyadenylation

Polyadenylation is the process of adding several adenine bases to the mRNA molecule prior to mRNA export to the cytoplasm where translation takes place (Tian and Manley, 2016). Two genes involved in 3’ end processing and polyadenylation were down-regulated.

The U7 small nuclear RNA associated molecule (known as *LSM10*) which is a member of the ribonucleoproteins that are involved in 3’ end processing of non-polyadenylated histone mRNA was reduced (FC=-1.3). Although, histone mRNAs lack a poly-A tail they have a unique stem and loop structure and a histone downstream element (HDE) sequence (Marzluff et al., 2008). During 3’end processing U7 snRNA binds to the HDE sequence resulting in the recruitment of cleavage and polyadenylation specific factor 73 which is associated with a zinc finger that catalyses the cleavage reaction (Marzluff et al., 2008). Moreover, the cleavage and polyadenylation specific factor 1, 160kDa protein (*CPSF1*) gene expression was reduced (FC= -1.2). This protein is part of

a large complex protein known as cleavage and polyadenylation specific factors which are involved in the cleavage of the 3’ end of nascent mRNA and the addition of poly-A tail by recognizing the (AAUAAA) sequence (Murthy and Manley, 1995). Thus, there may be a reduction in polyadenylation.

3.6.1.1.3.3 RNA editing

RNA editing is a post-transcriptional modification step that involves a chemical alteration of the transcript bases (Schoenberg and Maquat, 2012). The adenosine deaminase, RNA-specific, B1 (*ADARB1*) encodes for a vital enzyme that participates in pre-mRNA editing was increased (FC=1.9). It is one of the adenosine deaminases acting on RNA (ADAR), a group of enzymes responsible for RNA editing (Bass, 2002). ADARB1 edits the Q/R site of GluR2 pre-mRNA converting adenosine to inosine causing an alteration of the translated codon from arginine to glycine. This has a major effect on Ca++ ion permeability through the glutamate receptor (Eckmann et al., 2001). An increased level of ADARB1 may lead to more editing which may result in disrupted intracellular Ca++ homeostasis.

3.6.1.1.3.4 Pseudouridylation

Pseudouridylation is defined as the isomerization of the nucleoside uridine by altering the chemical bond attachment of the nucleotide uracil to the ribose sugar ring from nitrogen-carbon to carbon- carbon via the pseudouridine synthases. This modification was observed to increase tRNA stability, promote the RNA recognition in the translation process and be involved in the biogenesis of spliceosome (Ge and Yu, 2013). Two enzymes from the pseudouridine synthase family were increased in fALS-*TARDBP*, the pseudouridylate synthase 10 (*PUS10*) which acts on tRNA and rRNA, and the pseudouridylate synthase 3 (*PUS3*) that catalyse the pseudouridylation of tRNA (FC=1.3 & FC=1.2 respectively) (Chen and Patton, 2000, Hamma and Ferre-D'Amare, 2006, McCleverty et al., 2007).

3.6.1.3.3.5 Other RNA processing genes

The eukaryotic translation initiation factor 2C (*EIF2C*), also known *AGO2,* which has a major impact on microRNA synthesis, was reduced (FC=-1.3) (Turchinovich and Burwinkel, 2012). In addition, the exosome component 10 (*EXOSC10*) which is a part of the exosome complex that functions in RNA processing of several RNA species as well as mediating RNA fidelity via the nonsense mediated decay pathways was decreased (FC=-1.2) (Garneau et al., 2007).

An increase in the enzyme tRNA nucleotidyl transferase, CCA-adding, 1(*TRNT1*) was observed (FC=1.2). It is responsible for the addition of the CCA nucleotides to the tRNA 3' end which is a key step for its maturation to a functional aminoacylated tRNA that can participate in polypeptide synthesis in the translation machinery (Lizano et al., 2007). In addition, ribonuclease P/MRP 21kDa subunit (*RPP21*) which is involved in the tRNA maturation process was reduced (FC= -1.3) (Jarrous et al., 2001).

Table 3.9: Genes involved in RNA processing in cytoplasmic missense mutation

Gene symbol	Gene names	P-value	Fold change
ADARB1	Adenosine deaminase, RNA-specific, B1 (RED1 homolog rat)	0.03	1.97
CLNS1A	Chloride channel, nucleotide-sensitive, 1A	0.04	1.36
CPSF1	Cleavage and polyadenylation specific factor 1, 160kDa	0.02	-1.20
DDX58	DEAD (Asp-Glu-Ala-Asp) box polypeptide 58	0.02	1.29
DGCR14	DiGeorge syndrome critical region gene 14	0.03	-1.21
EIF2C2	Eukaryotic translation initiation factor 2C, 2	0.03	- 1.38
EXOSC10	Exosome component 10	0.003	-1.29
FDXACB1	Ferredoxin-fold anticodon binding domain containing 1	0.003	1.35
GEMIN7	Gem (nuclear organelle) associated protein 7	0.03	-1.25
HNRNPM	Heterogeneous nuclear ribonucleoprotein M	0.01	1.84
LSM10	LSM10, U7 small nuclear RNA associated	0.04	- 1.37
MAGOH	Mago-nashi homolog, proliferation-associated (Drosophila)	0.03	1.28
PPP4R2	Protein phosphatase 4, regulatory subunit 2	0.014	1.27
PRPF8	PRP8 pre-mRNA processing factor 8 homolog (S. cerevisiae)	0.05	- 1.48
PUS3	Pseudouridylate synthase 3	0.01	1.21
PUS10	Pseudouridylate synthase 10	0.02	1.36
RBM6	RNA binding motif protein 6	0.01	1.25
RBM39	RNA binding motif protein 39	0.04	1.30
RPP21	Ribonuclease P/MRP 21kDa subunit	0.03	-1.37
SART-3	Squamous cell carcinoma antigen recognized by T cells 3	0.001	1.44
(*)SF3A1	Splicing factor 3a, subunit 1, 120kDa	0.05	-1.28
SF3A3	Splicing factor 3a, subunit 3, 60kDa	0.04	-1.22
(*)SNRNP200	Small nuclear ribonucleoprotein 200kDa (U5)	0.032	-1.34
SFRS15	Splicing factor, arginine/serine-rich 15	0.02	-1.26
SRSF12	Serine-arginine repressor protein (35 kDa)	0.003	- 1.29
TRNT1	tRNA nucleotidyl transferase, CCA-adding, 1	0.057	1.24
ZCRB1	Zinc finger CCHC-type and RNA binding motif 1	0.002	1.37

**selected genes for qRT-PCR validation*

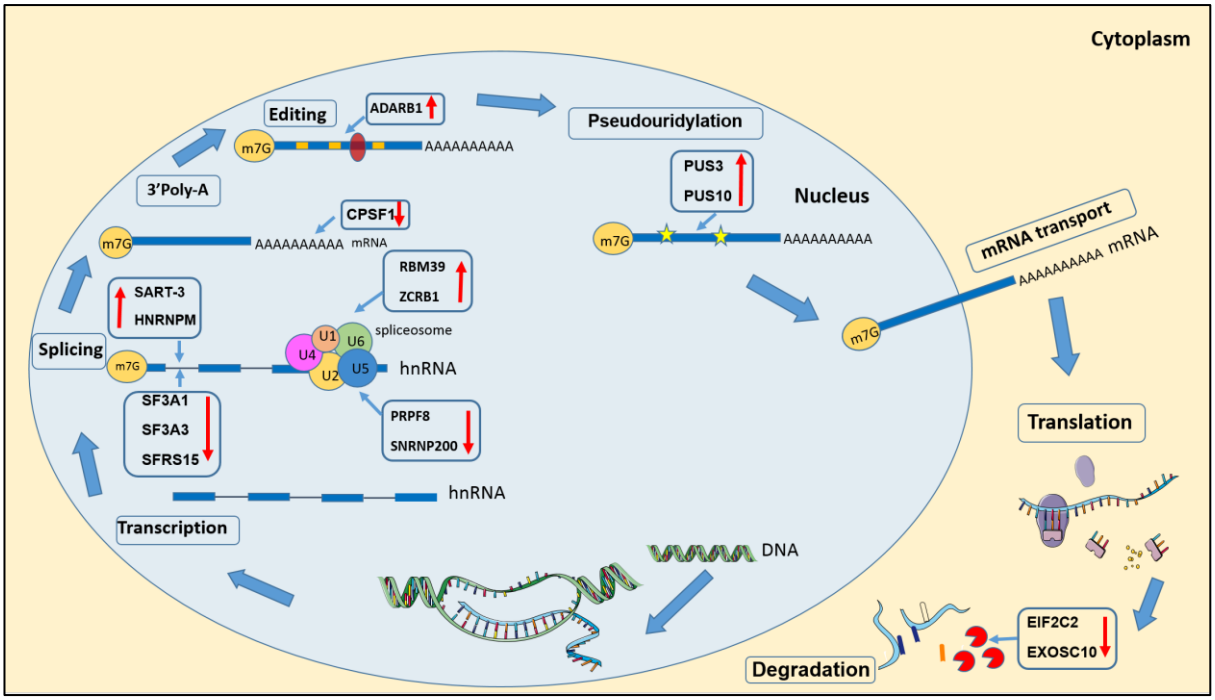

Figure 3.8: *A representative diagram showing the dysregulated RNA processing genes in fALS-TARDBP cytoplasmic missense mutation*

3.6.1.1.4 Cytoskeleton organization

The cytoskeleton is one of the most important structures of the cell as it maintains the cell shape, organelle location within the cell and cell movement. The dysregulation of the cytoskeleton has been shown to be associated with neurodegenerative disorders such as: AD, PD and ALS (McMurray, 2000). A group of genes from this structure were found to be dysregulated in fALS and are discussed below (Table 3.10).

The ATPase, Ca++ transporting, type 2C, member 1 (*ATP2C1*) expression was increased (FC=1.3). It encodes for a magnesium-dependent enzyme that is involved in transporting Ca++ ions to cells (Ton et al., 2002). Furthermore, caldesmon1 (*CALD1*) was increased (FC= 1.58). CALD1 is an actin binding protein which regulates smooth muscle and non-muscle contraction (Hayashi et al., 1992). The actin depolymerizing factor destrin (*DSTN*) showed an up-regulation (FC=1.5). It is a part of the microfilament protein component which is involved in the turnover rate of actin filaments (Hawkins et al., 1993). An increase in the dynein, light chain, LC8-type 1(*DYNLL1*) was observed (FC=1.38). DYNLL1 acts as a regulator for protein dimerization. It is involved in DNA damage response, transcription, nitric oxide signalling, and cell migration (Jurado et al., 2012). The tropomyosin 1 (alpha) (*TPM1*) is an actin-binding protein which is involved in smooth muscle, striated muscle and cytoskeletal contractile system was up-regulated (FC=1.4) (Denz et al., 2004). Two genes previously described in the neuronal differentiation biological process appeared in the cytoskeleton organization group and showed an increased gene expression, the myosin, heavy chain 10, non-muscle (*MYH10*) (FC=1.6) and the protein kinase, cGMP-dependent, type I (*PRKG1*) (FC= 1.28). Both genes were involved in cytokinesis (Li et al., 2003, Takeda et al., 2003, Burgoyne et al., 2007).

On the other hand, a group of genes were down-regulated. The CDC28 protein kinase regulatory subunit 2 (*CKS2*) has shown a reduction in gene expression (FC=-2.1). CKS2 has shown to be involved in the cell cycle process (Richardson et al., 1990). Furthermore, the FYVE, RhoGEF, PH domain containing 1 (*FGD1*) was also decreased (FC=-1.4). FGD1 has been shown to interact with actin-

binding protein-1 (mAbp1) which regulates the polymerization of the Arp2/3 cytoskeleton complex (Hou et al., 2003). The angiomotin (*AMOT*) gene was down-regulated (FC=-1.4). This gene was suggested to have a role in cell migration and motility (Troyanovsky et al., 2001). Moreover, the inverted formin, FH2 and WH2 domain containing (*INF2*) was reduced (FC=-1.2). INF2 interacts with actin in the cell to facilitate the polymerization and de-polymerization of actin filaments (Chhabra and Higgs, 2006). Talin 2 (*TLN2*) gene expression was decreased. TLN2 is highly expressed in the synapse region of brain tissue, heart and skeletal muscle. In addition, it is involved in facilitating the binding of integrin to actin filaments (Senetar et al., 2007, Debrand et al., 2009).

A group of genes involved in cytoskeleton organization were shown to be disrupted within the fibroblasts. This observation may demonstrate a similar effect of the mutation on impaired axonal transport shown in ALS.

Table 3.10: Genes involved in cytoskeleton organization in cytoplasmic missense mutation

Gene symbol	Gene names	P-value	Fold change
ABL1	C-abl oncogene 1, receptor tyrosine kinase	0.04	-1.29
AMOT	Angiomotin	0.01	-1.48
ATP2C1	ATPase, Ca++ transporting, type 2C, member 1	0.05	1.30
CALD1	Caldesmon 1	0.03	1.58
CKS2	CDC28 protein kinase regulatory subunit 2	0.03	-2.14
DSTN	Destrin (actin depolymerizing factor)	0.03	1.50
DYNLL1	Dynein, light chain, LC8-type 1	0.05	1.38
FGD1	FYVE, RhoGEF, PH domain containing 1	0.05	-1.41
FHDC1	FH2 domain containing 1	0.05	1.29
INF2	Inverted formin, FH2 and WH2 domain containing	0.02	-1.26
MYH10	Myosin, heavy chain 10, non-muscle	0.05	1.60
OFD1	Oral-facial-digital syndrome 1	0.04	1.38
PRKG1	Protein kinase, cGMP-dependent, type I	0.03	1.28
TLN2	Talin 2	0.01	-1.28
TMSB15A	Thymosin beta 15a	0.01	-1.50
TPM1	Tropomyosin 1 (alpha)	0.05	1.45

3.6.2 Nuclear MT vs. nuclear CON gene expression profiling using the Human Exon 1.0 ST Arrays

As in the cytoplasmic fALS-*TARDBP* study, the nuclear MT vs. nuclear CON transcript IDs were uploaded into DAVID v6.7 to identify the significant biological processes dysregulated in fALS fibroblasts. The criteria of selection was based on the enrichment score (ES≥ 1.3) as this is equivalent to a p-value of 0.05 (Huang da et al., 2009).

3.6.2.1 Differential gene expression of nuclear MT vs. CON

Table 3.11 illustrates that nuclear division, cellular response to stress and mRNA processing were the top three highest enriched biological processes with the highest gene number. Thus, they were selected for further discussion.

Table 3.11: Functionally enriched biological processes generated by DAVID of the nuclear MT vs. CON differentially expressed genes. GO=Gene ontology, ES=Enrichment score, no.=number

GO	Biological process	Gene no.	P-value	ES
BP_FAT	Nuclear division	22	3.1E-7	6.8
BP_FAT	Cellular response to stress	28	1.9E-3	4.3
BP_FAT	mRNA processing	15	4.3E-2	1.53
BP_FAT	Spindle organization	5	2.9E-2	1.48
BP_FAT	Chromosome segregation	9	1.2E-3	1.42

3.6.2.1.1 Nuclear division

Nuclear division is the process through which a single eukaryotic cell is divided into daughter cells during the process of mitosis or meiosis. In the nuclear fALS-*TARDBP* missense mutation, it was shown that genes involved in nuclear division were down-regulated (Table 3.12).

The DSN1, MIND kinetochore complex component, homolog (S. cerevisiae) (*DSN1*) gene was down-regulated (FC=-1.5). It is a part of the multiprotein complex kinetochore, which is known for its role in chromatin alignment and separation during mitosis (Liu et al., 2005). Furthermore, HAUS augmin-like complex, subunit 6 (*HAUS6*) was reduced (FC=-1.3). It is a component of the human augmin complex, this is a microtubule-binding complex that is involved in microtubule spindle assembly and stabilization of the kinetochore during mitosis (Lawo et al., 2009). In addition, the chromosome 13 open reading frame 34 (*C13orf34*), also known as Aurora kinase A activator, was down-regulated (FC=-1.3). It has a role in spindle assembly and centrosome development during mitosis (Seki et al., 2008). The PDZ binding kinase (*PBK*) gene was down-regulated (FC=-1.9). PBK is associated with mitotic spindles and was shown to be expressed during cytokinesis at the interphase stage (Matsumoto et al., 2004). Moreover, the kinetochore associated complex subunit 3 (*SKA3*) which is a component of the kinetochore-associated protein complex was reduced (FC=-1.6). SKA3 functions in regulating the attachment of the microtubules to the kinetochore during cell division (Gaitanos et al., 2009). Also the ZW10 interactor (*ZWINT*) was down-regulated (FC=-1.5). ZWINT is associated with the kinetochore complex (Obuse et al., 2004).

The budding uninhibited by benzimidazoles 1 homolog beta (yeast) (*BUB1B*) gene was decreased (FC=-2). It encodes for a protein that is involved in the spindle assembly checkpoint. It ensures a correct chromosome segregation prior to anaphase in mitosis (Lampson and Kapoor, 2005). Two further genes also involved in chromosomal segregation were down-regulated, the non-SMC condensin II complex, subunit D3 (*NCAPD3*) and nucleolar and spindle

associated protein 1 (*NUSAP1*) (FC=- 1.3 and FC=-1.9 respectively) (Ono et al., 2003, Raemaekers et al., 2003b). Moreover, citron (rho-interacting, serine/threonine kinase 21) (*CIT*) expression was reduced (FC=-1.7). CIT was reported to be localized in the central spindle and is involved in maintaining effective cytokinesis (Di Cunto et al., 2000, Kato, 2007).

The kinesin family member 20B (*KIF20B*) gene was down-regulated (FC=-1.4). Kinesins are mobile proteins that move along the microtubule in the cell. They mediate anterograde axonal transport of the cellular organelles such as: mitochondria, macromolecules and vesicles (De Vos et al., 2008). Defects in the *Kinesin* gene have been shown to be associated with ALS (Bosco et al., 2010). In addition, TAR DNA binding protein (*TARDBP*) was found to be down-regulated (FC=-1.5) which is involved in RNA processing (Xia et al., 2016) (see section 1.1.4.1.2 and 1.1.4.2.1 for more details). Finally, the YEATS domain containing 4 (*YEATS4*) gene was reduced (FC=-1.3). It has been suggested to be associated with RNA transcription (Zimmermann et al., 2002).

This marked reduction of nuclear division genes may explain the slow growth rate of patient's fibroblasts in the laboratory.

Table 3.12: Genes involved in nuclear division in nuclear missense mutation

Gene symbol	Gene name	P-value	Fold change
ANAPC10	Anaphase promoting complex subunit 10	0.01	-1.35
BUB1B	Budding uninhibited by benzimidazoles 1 homolog beta (yeast)	0.04	-2.10
C13orf34	Chromosome 13 open reading frame 34	0.03	-1.32
CIT	Citron(rho-interacting, serine/threonine kinase 21)	0.04	-1.73
DSN1	DSN1, MIND kinetochore complex component, homolog (S. cerevisiae)	0.02	-1.55
HAUS6	HAUS augmin-like complex, subunit 6	0.04	-1.33
HELLS	Helicase, lymphoid-specific	0.02	-1.85
KIF20B	Kinesin family member 20B	0.03	-1.49
NCAPD3	Non-SMC condensin II complex, subunit D3	0.04	-1.39
NEK4	NIMA (never in mitosis gene a)-related kinase 4	0.01	-1.25
NUP43	Nucleoporin 43kDa	0.02	-1.29
NUSAP1	Nucleolar and spindle associated protein 1	0.03	-1.93
OIP5	Opa interacting protein 5	0.01	-1.30
PBK	PDZ binding kinase	0.03	-1.98
PTTG1	Pituitary tumor-transforming 1	0.02	-1.57
SKA3	kinetochore associated complex subunit 3	0.03	-1.66
SMC2	Structural maintenance of chromosomes 2	0.0003	-1.61
TARDBP	TAR DNA binding protein	0.04	-1.55
TUBB5	Tubulin, beta; similar to tubulin, beta 5	0.006	-1.27
YEATS4	YEATS domain containing 4	0.02	-1.34
ZWILCH	Zwilch, kinetochore associated, homolog (Drosophila)	0.01	-1.37
ZWINT10	ZW10 interactor	0.03	-1.55

3.6.2.1.2 Cellular response to stress

Cellular response to stress can be defined as any exogenous or endogenous stress insult that can alter the normal cell function and activate intracellular pathways to prevent sudden cell death. There are several known cellular responses, for example: the response to oxidative stress, DNA damage response, unfolded protein response and heat shock response. Several genes involved in the DNA damage response were dysregulated in the nuclear fALS fibroblasts (see table 3.13). A further explanation is addressed below.

The RAD9A-related pathway involves several genes which can promote either cell survival or death depending on the level of cellular DNA damage that occurred (Ta and Gioeli, 2014). One of these gene is ATPase family, AAA domain containing 5 *(ATAD5*) which is activated during DNA damage to initiate DNA repair was shown to be reduced (FC= -1.5) (Sikdar et al., 2009). The down-regulation of *ATAD5* was suggested to provoke the RAD9A to associate with the oncogene B-cell lymphoma 2 (*BCL2*) which promotes cell apoptosis, was also decreased (FC=-1.2). The binding of RAD9A/ BCL2 accelerates apoptosis (Ishii et al., 2005). Also, the checkpoint kinase 1 (*CHK1*) was shown to be reduced (FC=-1.3) (Feijoo et al., 2001).

Furthermore, the RAD51 homolog C (S. cerevisiae) was reduced (FC=-1.2). It is involved in DNA repair by homologous recombination when double stranded DNA breaks occur (Park et al., 2008). In addition, the breast cancer 2, early onset gene (*BRCA2*) whose protein participates in transporting the RAD51 protein to the DNA repair site was down-regulated (FC=-1.3) (Pellegrini et al., 2002, Park et al., 2008). Two gene involved in the BRCA associated complex were reduced, the chromosome 19 open reading frame 62 which is involved in DNA repair (*C19orf62*) (FC=-1.2) and the mortality factor 4 like 1 (*MORF4L1*) (FC=-1.2). Both of these genes interact with BRCA2 and RAD51 in response to DNA damage (Feng et al., 2009, Hayakawa et al., 2010). Furthermore, the chromosome 9 open reading frame 80 (*C9orf80*) which has shown to be involved in DNA damage repair was reduced (FC=-1.4) (Huang et al., 2009).

The minichromosome maintenance complex component 7 (*MCM7*) gene which is essential during the cell cycle and mainly at the time of DNA replication was shown to be also reduced (FC=-1.4) (Spanjaard et al., 1997). Moreover, the ERO1-like (S. cerevisiae) (*ERO1L*) was down-regulated (FC=-1.4). The encoded protein is localized in the endoplasmic reticulum (ER) and belongs to the oxidation reduction reaction (Redox) family that are involved in oxidative protein folding and the formation of disulfide bonds between two cysteine residues. It has been suggested that it may have a role in ER stress induced apoptosis (Li et al., 2009). Two DNA polymerase enzymes were down-regulated, the polymerase (DNA directed), epsilon 2 (p59 subunit) (FC=-1.7) and polymerase (DNA-directed), delta 3, accessory subunit (FC=-1.5) which are both involved in the elongation of primed DNA strand (Syvaoja et al., 1990). In addition, three genes that encode for the replication factor C complex that are essential for DNA elongation, synthesis and repair were down-regulated, the replication factor C (activator 1) 2 40kDa (*RFC2*) (FC=-1.2), the replication factor C (activator 1) 3 38kDa (*RFC3*) (FC=-1.6), and replication factor C (activator 1) 5 36.5kDa (*RFC5*) (FC=-1.3) (Tsurimoto and Stillman, 1990, Wang et al., 2000). The thymidylate synthetase (*TYMS*) was reduced (FC=-1.5). TYMS functions in converting the deoxyuridine monophosphate (dUMP) to deoxythymidine monophosphate (dTMP). Reduction in the thymidylate synthetase activity results in incomplete DNA synthesis leading to DNA damage (Kaneda et al., 1990). The thyroid hormone receptor interactor 13 (*TRIP13*) which is considered a hormone-dependent transcription factor that interacts with thyroid hormone receptors to regulate their expression was reduced (FC=-1.7) (Lee et al., 1995).

In contrast, the glutathione peroxidase 3 (plasma) (*GPX3*) was shown to be up-regulated (FC=1.3). GPX3 is an important enzyme which protects the cell from oxidative damage by the elimination of hydrogen peroxide molecules (Chambers et al., 1986). Furthermore, the thyroid peroxidase was also increased (FC=1.2). Thyroid peroxidase functions in the iodination of tyrosine residues in thyroglobulin to form the thyroid hormones which are: triiodothyronine (T3) and thyroxine (T4) (Park and Chatterjee, 2005).

Overall, it has been shown that nuclear fALS-*TARDBP* fibroblasts showed a significant reduction in gene expression in response to stress.

Table 3.13: Genes involved in cellular response to stress in nuclear missense mutation

Gene symbol	Gene name	P-value	Fold change
ATAD5	ATPase family, AAA domain containing 5	0.04	-1.56
BCL2	B-cell CLL/lymphoma 2	0.005	-1.25
BRCA2	Breast cancer 2, early onset	0.02	-1.34
BTG2	BTG family, member 2	0.04	1.50
CDKN2D	Cyclin-dependent kinase inhibitor 2D (p19, inhibits CDK4)	0.003	1.23
CHAF1B	Chromatin assembly factor 1	0.03	-1.29
CHEK1	CHK1 checkpoint homolog (S. pombe)	0.006	-1.37
C19orf62	Chromosome 19 open reading frame 62	0.004	-1.24
C9orf80	Chromosome 9 open reading frame 80	0.04	-1.40
DHX9	DEAH (Asp-Glu-Ala-His) box polypeptide 9	0.01	-1.32
DTL	Denticleless homolog (Drosophila)	0.03	-1.91
ERO1L	ERO1-like (S. cerevisiae)	0.02	-1.48
GPX3	Glutathione peroxidase 3 (plasma)	0.02	1.31
MAP3K13	Mitogen-activated protein kinase kinase kinase 13	0.04	1.32
MCM7	Minichromosome maintenance complex component 7	0.02	-1.48
MORF4L1	Mortality factor 4; mortality factor 4 like 1	0.03	-1.20
NONO	Non-POU domain containing, octamer-binding	0.03	-1.35
POLD3	Polymerase (DNA-directed), delta 3, accessory subunit	0.04	-1.52
POLE2	Polymerase (DNA directed), epsilon 2 (p59 subunit)	0.04	-1.74
PTTG1	Pituitary tumor-transforming 1	0.02	-1.57
RAD51C	RAD51 homolog C (S. cerevisiae)	0.02	-1.21
RFC2	Replication factor C (activator 1) 2, 40kDa	0.02	-1.25
RFC3	Replication factor C (activator 1) 3, 38kDa	0.02	-1.69
RFC5	Replication factor C (activator 1) 5, 36.5kDa	0.02	-1.31
TDP1	Tyrosyl-DNA phosphodiesterase 1	0.007	-1.20
TPO	Thyroid peroxidase	0.03	1.27
TRIP13	Thyroid hormone receptor interactor 13	0.04	-1.7
TYMS	Thymidylate synthetase	0.04	-1.52

3.6.2.1.3 mRNA processing

It was shown that the majority of the genes in the nuclear mRNA processing list were down-regulated and were mainly involved in splicing/alternative splicing. In addition, a single gene from each of the following processes were found to be down-regulated: RNA silencing, transcription, translation, hormone response and RNA decay. Table 3.14 demonstrates the gene list and a further exploration of these genes is described below.

3.6.2.1.3.1 Splicing / alternative splicing

The FUS interacting protein (serine/arginine-rich) 1 (*SRSF10*), one of the serine-arginine (SR) family, is involved in RNA processing and in particular alternative RNA splicing was down-regulated (FC=-1.3) (Cowper et al., 2001, Shin et al., 2004). In addition the TAR DNA binding protein (*TARDBP*) is an RNA/DNA-binding protein that is involved in RNA processing including; transcription, splicing and mRNA transport was also reduced (FC=-1.5) (Xia et al., 2016) (see section 1.1.4.1.2 and 1.1.4.2.1 for more details). Moreover, the heterogeneous nuclear ribonucleoprotein K (*HNRNPK*) was down-regulated (FC=-1.3). HNRNPK is involved in mRNA splicing along with other cellular functions such as: transcription activation and repression, translation and DNA damage response (Fukuda et al., 2009). The splicing regulatory factor heterogeneous nuclear ribonucleoprotein M (*HNRNPM*) was down-regulated (FC=-1.5) and is also involved in RNA alternative splicing (Hovhannisyan and Carstens, 2007).

The KH domain containing, RNA binding, signal transduction associated 1 (*KHDRBS1*), also known as *Sam68*, was reduced (FC=-1.2). It is involved in the alternative splicing of the *CD44* gene though binding to the splice-regulatory elements of exon v5 (Matter et al., 2002). It also alternatively splices mRNAs involved in normal neuronal differentiation (Chawla et al., 2009). Furthermore, Sam68 induces exon 7 skipping of the *SMN2* gene. Mutation in the *Sam68* gene leads to the production of non-functional SMN2 protein which is known to be a feature of spinal muscular atrophy (SMA) (Pedrotti et al., 2010). The Non-POU domain containing octamer-binding (*NONO*) gene was reduced (FC=-1.3). The

NONO is involved in pre-mRNA processing including: transcription activation and repression, splicing and transport (Mircsof et al., 2015).

Three genes which are part of the spliceosomal complex involved in nascent RNA splicing were down-regulated, small nuclear ribonucleoprotein polypeptides B and B1(*SNRPB*) (FC=-1.3), PRP4 pre-mRNA processing factor 4 homolog (yeast) (*PRPF4*) (FC=-1.2) and PRP8 pre-mRNA processing factor 8 homolog (*PRPF8*) (FC=-1.2) (Luo et al., 1999, Gonzalez-Santos et al., 2002, Chari et al., 2008).

A marked reduction in RNA splicing genes was observed in the nuclear fALS missense mutation which strongly suggest an alteration in splicing regulation caused by the *TARDBP* mutation (Figure 3.9).

3.6.2.1.3.2 RNA silencing /transcription/ translation/ hormone response/ RNA decay

The DEAH (Asp-Glu-Ala-His) box polypeptide 9 (*DHX9*) was reduced (FC=-1.3). It belongs to the RNA helicase family which are generally considered transcriptional regulators involved in RNA metabolism. DHX9 is also known as RNA Helicase A and has been shown to be associated with the RNA silencing pathway i.e. the RISC complex (Robb and Rana, 2007). Furthermore, the polymerase (RNA) II (DNA directed) polypeptide B (*POLR2B*) was also reduced (FC=-1.3). The cytoplasmic polyadenylation element binding protein 1(*CPEB1*) gene expression was also down-regulated (FC=-1.4). The protein encoded by this gene binds to the 3'end of the mRNA to initiate the translation machinery (Welk et al., 2001). Moreover, the heterogeneous nuclear ribonucleoprotein C (C1/C2) (*HNRNPC*) was reduced (FC=-1.3). It is an RNA binding protein involved in RNA processing and was suggested to have a role in the regulation of hormone response elements in vitamin D resistant patients (Chen et al., 2006). Finally, the heterogeneous nuclear ribonucleoprotein D (AU-rich element RNA binding protein 1, 37kDa) (*HNRNPD)* which is a part of a complex molecule that binds to

the AU-rich element on the mRNA to initiate RNA decay was found to be down-regulated (FC=-1.3) (Grosset et al., 2000).

Table 3.14: Genes involved in mRNA processing in nuclear missense mutation

Gene symbol	Gene name	P-value	Fold change
CPEB1	Cytoplasmic polyadenylation element binding protein 1	0.02	-1.46
DHX9	DEAH (Asp-Glu-Ala-His) box polypeptide 9	0.01	-1.32
HNRNPC	Heterogeneous nuclear ribonucleoprotein C (C1/C2)	0.02	-1.31
HNRNPD	Heterogeneous nuclear ribonucleoprotein D	0.03	-1.35
HNRNPK	Heterogeneous nuclear ribonucleoprotein K	0.05	-1.30
HNRNPM	Heterogeneous nuclear ribonucleoprotein M	0.01	-1.50
KHDRBS1	KH domain containing, RNA binding, signal transduction associated 1	0.03	-1.24
NONO	Non-POU domain containing, octamer-binding	0.03	-1.35
POLR2B	Polymerase (RNA) II (DNA directed) polypeptide B, 140kDa	0.02	-1.30
PRPF4	PRP4 pre-mRNA processing factor 4 homolog (yeast)	0.02	-1.23
PRPF8	PRP8 pre-mRNA processing factor 8 homolog (S. cerevisiae)	0.04	-1.25
RBM4B	RNA binding motif protein 4B	0.01	-1.21
SNRPB	Small nuclear ribonucleoprotein polypeptides B and B1	0.01	-1.39
(*)SRSF1	FUS interacting protein (serine/arginine-rich) 1	0.02	-1.37
(*)TARDBP	TAR DNA binding protein	0.04	-1.55

**Selected genes for qRT-PCR validation.*

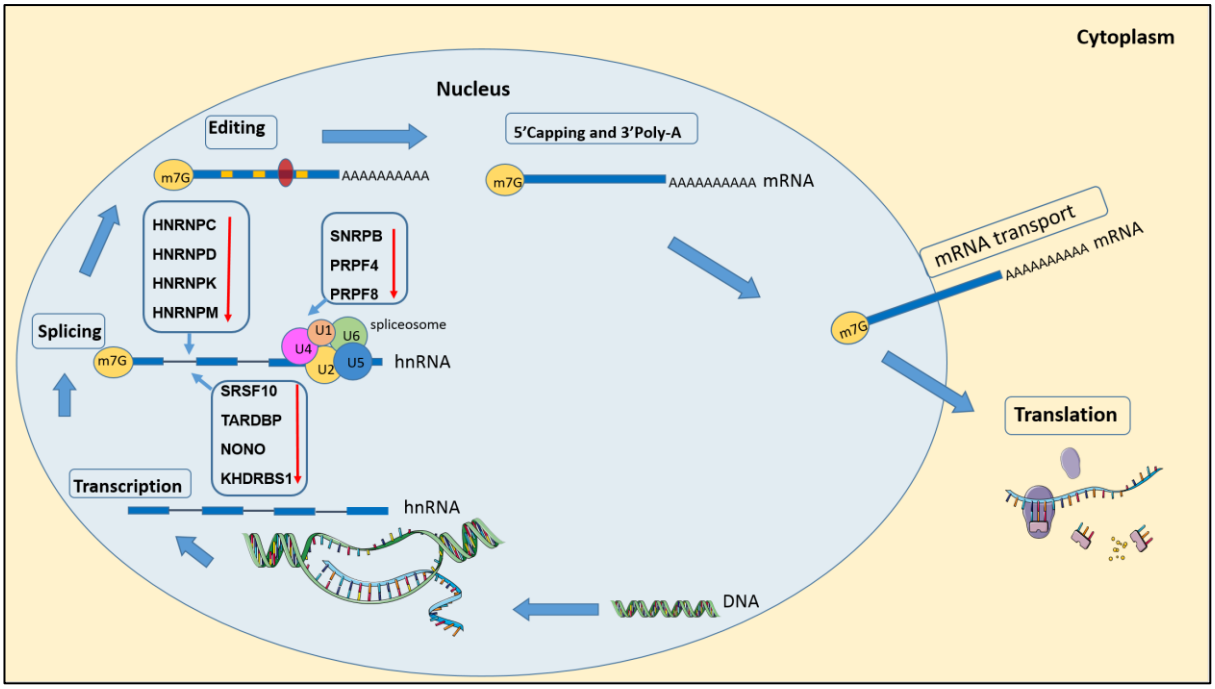

Figure 3.9: *A representative diagram showing the dysregulated RNA processing genes in fALS-TARDBP nuclear missense mutation*

3.6.3 Comparative analysis of the differentially expressed gene from the cytoplasmic and nuclear missense mutation using the Human Exon 1.0 ST Array

To further explore the effect of the *TARDBP* missense mutation on gene expression in fALS, it was interesting to find which genes were specific to each cellular component and which gene were in shared in both. Therefore, GeneVenn tool was used to identify those genes. 653 genes out of the 702 genes were cytoplasmic specific while 636 genes out of the 685 genes were nuclear specific and 49 genes were in both (Figure 3.10). The transcript IDs were uploaded into DAVID to identify the dysregulated biological process in each cellular compartment. The highest enriched in cytoplasmic missense mutation were mRNA splicing and transcription (ES= 3.5 and 1.6 respectively) and the nuclear missense mutation were enriched with mitotic nuclear division, DNA replication and mRNA splicing (ES= 7, 2.7 and 2.3 respectively). None of the 49 shared genes belonged to a biological process. The shared gene list was also investigated manually, 37 genes were annotated and 12 genes were unannotated. None of the annotated genes belonged to the mRNA splicing genes that were identified in each cellular component.

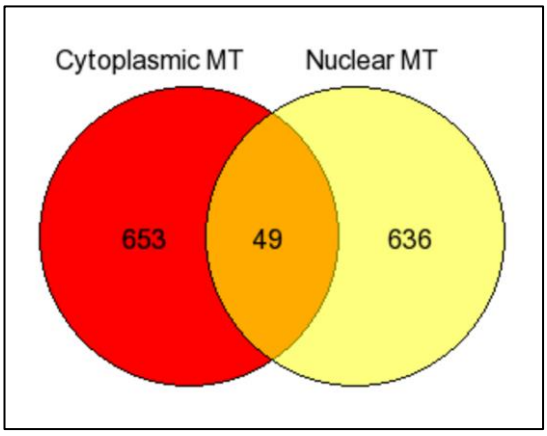

Figure 3.10: *Comparative analysis of the differentially expressed gene from the cytoplasmic and nuclear missense mutation using the Human Exon 1.0 ST Array. Venn diagram showing 653 genes specific to the cytoplasmic missense mutation while 636 genes were specific to the nuclear missense mutation and 49 genes were shared in both cellular fractions. MT= missense mutation, TT= truncated mutation*

3.7 qRT-PCR validation of fALS RNA processing genes

Key exon array differentially expressed genes were identified in order to attempt validation by qRT-PCR. Two genes involved in RNA processing were selected from each comparison study. From the cytoplasmic MT vs. cytoplasmic CON the following genes were selected: small nuclear ribonucleoprotein 200kDa (*SNRNP200*) (FC=-1.34 and p-value=0.032) and splicing factor 3a, subunit 1, 120kDa (*SF3A1*) (FC=-1.28 and p-value=0.05). From the nuclear MT vs. nuclear CON the following genes were selected: FUS interacting protein (serine/arginine-rich) 1 (*SRSF10*) (FC=-1.37 and p-value= 0.02) and TAR DNA binding protein (*TARDBP*) (FC=-1.55 and p-value= 0.04). All genes were normalized against the β-actin housekeeping gene. The statistical analysis was performed using *Graph Pad Prism* and unpaired t-test was applied.

The nuclear candidate genes confirmed the directional change of gene expression (down-regulation) compared to the Human Exon 1.0 ST Array data. However, the cytoplasmic candidate genes did not. Unfortunately, none of the four genes showed statistical significant results (p-values > 0.05) although trends were shown in the correct direction for *TARDBP* and *SRSF10* (See figure 3.11 A&B, 3.12A&B).

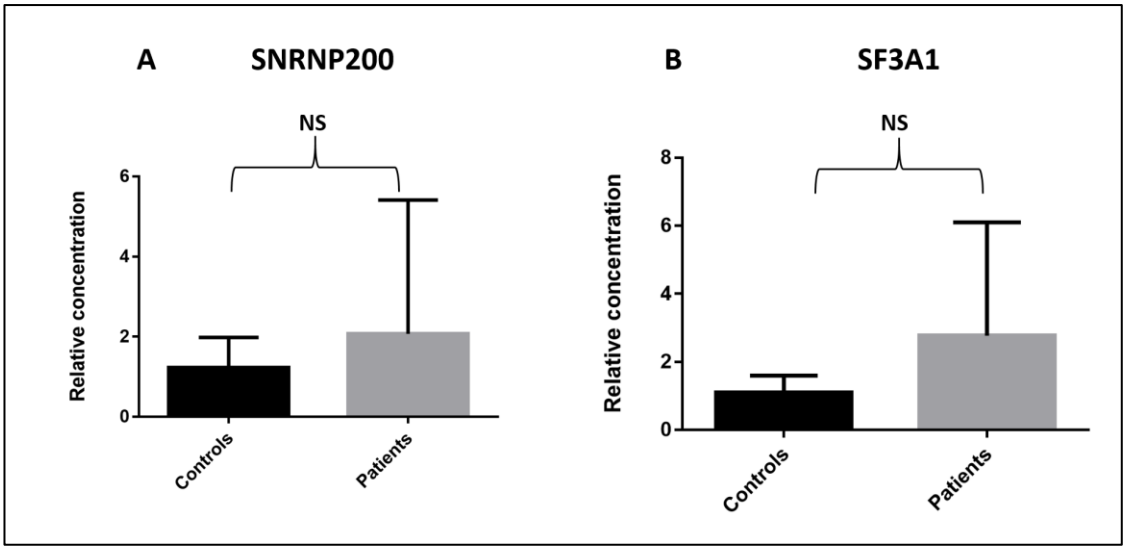

Figure 3.11: *qRT-PCR validation of the RNA processing cytoplasmic genes in fALS fibroblasts. (A)The relative expression of the SNRNP200 gene. The statistical analysis showed insignificant p-value (p-value = 0.6915) with slight increase of SNRNP200 gene expression, (n=3). (B) The relative expression of the SF3A1 gene. The statistical analysis also showed insignificant (p-value= 0.4380) with increased SF3A1 gene expression, (n=3). (n= the sample size, NS= not significant, the error bars represents the SEM).*

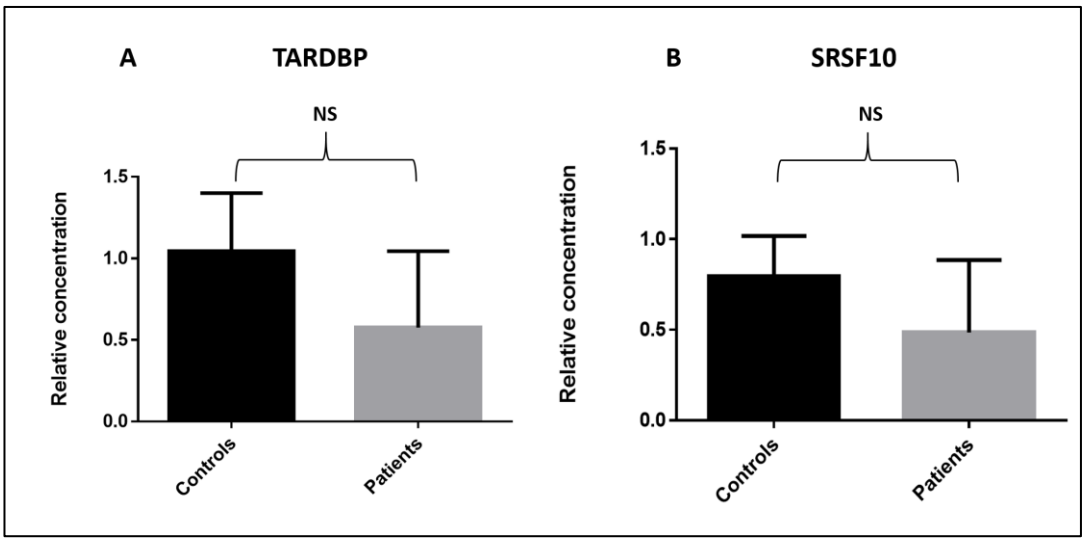

Figure 3.12*: qRT-PCR validation of the RNA processing nuclear genes in fALS fibroblasts. (A)The relative expression of the TARDBP gene. The directional change of the gene expression was confirmed (down-regulation), however the p-value was insignificant (p-value=0.2388), (n=3). (B)The relative expression of the SRSF10 gene. The directional change of the gene expression was confirmed (down-regulation), however the p-value was insignificant (p=0.3026), (n=3). (n= the sample size, NS= not significant, the error bars represents the SEM.*

3.8 Discussion

Several animal models have been generated to provide an understanding of the pathological mechanisms underlying the disease process of ALS. In particular, mammalian models of mutant *TARDBP* include transgenic mice and rats as well as genetically engineered non-mammalian models like drosophila, zebrafish and Caenorhabditis elegans *(C. elegans)* (Liu et al., 2013). In the current study, fibroblasts derived from fALS-*TARDBP* were chosen to study the pathological role of mutant TDP-43 in fALS-*TARDBP*. From a technical point of view fibroblasts are useful because they are accessible from the patient through a skin biopsy, they are easy to grow and suitable for RNA extraction. In addition, several studies on ALS and other neurodegenerative disorders such as AD and PD have shown the effectiveness of using fibroblasts to investigate the underling pathophysiological disease process (Nagasaka et al., 2005, Mortiboys et al., 2008, Highley et al., 2014, Raman et al., 2015).

In the present study, patients and controls were age and gender matched to minimize variations. The cell fractionation and RNA isolation methods were challenging. However, a good degree of separation with acceptable quality and quantity of RNA was achieved. The Nanodrop spectrophotometer measurements showed that a good quantity of RNA could be derived from all samples. Moreover, the Agilent Bioanalyser electropherograms showed two significant features; clear sharp peaks of rRNA 28s and rRNA 18s with higher RNA concentration in the cytoplasm than in nucleus and the level of rRNA 28s were approximately twice the level of rRNA 18s suggesting full length transcripts although the RIN values were of a moderate level. A clear genomic DNA peak was observed in nuclear RNA samples which was eliminated successfully by DNase treatment. The RNA quantity and quality were affected although to an acceptable degree. Peaks of genomic DNA in the cytoplasmic electropherograms were not present. This does not completely exclude the presence of DNA however it suggests a low possibility of cross contamination between cellular compartments. This was in agreement with an earlier study which demonstrated superb cell fractionation and RNA isolation results using a similar strategy (Trask et al., 2009).

The current study aimed to elucidate the possible dysregulated biological processes present in the cytoplasm and the nucleus of fALS-*TARDBP* patients. Thus, three biological replicates for each disease and controls were used. The fibroblasts were collected from three different *TARDBP* missense mutations: p.A321V, p.M337V and p.G2875. Pooling the samples as one mutation in the analysis was not the most effective method to study the effect of individual mutations, however, this strategy provided an overall view of the effect of *TARDBP* missense mutations on the disease process. Partek® Genomics Suite ™ 6.6 software was used to identify the statistically significant differentially expressed genes and the DAVID online tool facilitated the assigning of these genes into biological processes. fALS-*TARDBP* cytoplasmic differentially expressed genes fell into the following biological processes: methylation, neuronal differentiation, RNA processing, and cytoskeleton organization. Moreover, the fALS-*TARDBP* nuclear differentially expressed genes belonged to the following biological processes: nuclear division, cellular response to stress and mRNA processing. Several of these defective biological processes have been shown to be aberrant in ALS. This strongly supports the effectiveness of fibroblasts as a model to study ALS and the relevance of the experimental model used to investigate possible aberrant processes in fALS.

3.8.1 Cytoplasmic fALS-*TARDBP* fibroblasts

3.8.1.1 Methylation

It was surprising to find that DNA methylation showed the highest enriched cytoplasmic pathway in fALS-*TARDBP* related cases as this has not been observed before. The current literature focuses on understanding the effect of epigenetics on sALS cases rather than fALS. This is because familial cases are characterised as being caused by alterations in the genome, whereas, sALS is believed to be influenced by gene mutations, life style, environmental factors and epigenetic modifications.

As some gene mutations are a shared aetiology in cases of sALS and fALS, an attempt was to search the literature for studies that may have a similar pattern of dysregulated genes as in the present study. Unfortunately, only *DNMT1* was shown to be increased in the motor neurons of the motor cortex in sALS and was decreased in fALS-*TARDBP* in the current study (Chestnut et al., 2011).

All genes related to DNA methylation were down-regulated and have not been reported before, *GATAD2A, RAB6C, CARM1, EHMT1, HELLS and SUZ12* with the exception of *BTG2* which was up-regulated. This may suggest that hypomethylation is associated with fALS-*TARDBP* cases and might lead to increased level of transcription of some genes.

3.8.1.2 Neuron differentiation

It was shown in the analysis that the second highest enriched biological process in cytoplasmic fALS-*TARDBP* was neuron differentiation showing a significant number of genes. Investigating these genes revealed that the majority were increased and involved in cell cycle regulation (*BTG2* and *MYH10)*, differentiation (*ID3* and *ID4*), mitosis (*PRKG1*) and cell growth (*PTPRM)*. This was expected as the cell model in this study was primary fibroblasts which undergo continuous cell division and growth. An interesting observation was that these genes are also expressed in neurons. *PRKG1* is strongly expressed in hippocampal neurons (Hofmann, 2005). Furthermore, *MYH10* is expressed in the hippocampal neurons and involved in maintaining spine morphology (Ryu et al., 2006). A mutation in *MYH10* was suggested to be associated with brain malformations (Tuzovic et al., 2013). *ID3* and *ID4* genes were involved in neural cell differentiation and therefore are essential for normal development of the central nervous system (Lyden et al., 1999, Bedford et al., 2005).

Several genes involved in cell differentiation into cortical cells during development such as *LHX2, EMX2*, *PLXNA3* and into astroglia, *NOTCH1,* were down-regulated. These gene expression changes in ALS-derived fibroblasts strongly suggest that fibroblasts are good model to study neurodegenerative disorders, as there is an overlap in the genes that are expressed.

3.8.1.3 RNA processing

RNA processing is an umbrella term describing a range of molecular functions which are involved in the production of a mature mRNA. These include: RNA splicing, editing, transport and degradation. Studies have shown that dysregulated RNA processing was identified as a pathogenic mechanism in both fALS and sALS (Vance et al., 2006, Lagier-Tourenne et al., 2010, Polymenidou et al., 2012). In the current study, the number of genes dysregulated in RNA processing in the cytoplasmic fALS-*TARDBP* cases were significantly high. The majority of these genes were related to RNA splicing.

Dysregulated spliceosome complexes have been previously reported in sALS-*TARDBP* (Highley et al., 2014). Genes associated with spliceosome complexes were shown to be dysregulated in the present work, *SART-3, ZCRB1, RBM39* were up-regulated and *SNRNP200* and *PRPF8* were down-regulated. In addition, splicing factors were also reduced *SF3A1, SF3A3* and *SFRS15.* Furthermore, the splicing regulatory factor *HNRNPM* was shown to be expressed at low levels in sALS fibroblasts (Raman et al., 2015). In contrast, in the present work *HNRNPM* was shown to be increased in fALS, perhaps reflecting a mutant *TARDBP* specific effect.

RNA editing is one of the most important post-transcriptional modification steps that is involved in normal gene expression. The editing enzyme encoded by the *ADARB1* gene is vital for normal GluR2 function in maintaining Ca++ ion impermeability in neurons. Studies suggest that in sALS *ADARB1* expression is altered leading to reduced GluR2 editing and possibly as a result, increased Ca++ permeability (Aizawa et al., 2010, Hideyama et al., 2012, Yamashita and Kwak, 2014). In fALS-*TARDBP* the *ADARB1* expression was increased suggesting normal or perhaps increased editing of GluR2 in fALS. Two genes involved in pseudouridylation were slightly increased *PUS3* & *PUS10.* They were suggested to promote tRNA stability and RNA recognition during the translation process (Chen and Patton, 2000, Hamma and Ferre-D'Amare, 2006, McCleverty et al., 2007).

MicroRNAs are short sequences of RNA (22nt) that regulate gene expression by inhibiting translation or enhancing mRNA degradation (Nelson et al., 2003). A single gene involved in the biogenesis of microRNAs was down-regulated (*EIF2C2* also known as *AGO2*), this was also found decreased in sALS fibroblasts (Raman et al., 2015). Briefly, during microRNA transcription by RNA polymerase II a primary hairpin loop microRNA is formed. DGCR8 protein binds to the primary microRNA along with the enzyme DROSHA to cleave the primary microRNA and produce a shorter sequence known as precursor microRNA that is capable of export from the nucleus. In the cytoplasm the microRNA is bound to DICER1 which cleaves the stem loop leaving the ds-microRNA. AGO2 interacts with DICER1 and bind to the ds-microRNA. This is followed by unwinding and releasing of one strand of the microRNA. The single strand microRNA associated with AGO forms an RNA induced silencing complex (RISC). RISC plays an important role in regulating gene expression by inhibiting mRNA transcription or translation (Bartels and Tsongalis, 2009). The down-regulation of *AGO2* might cause this process to be hindered and gene expression to be dysregulated.

3.8.1.4 Cytoskeleton organization

A proper cytoskeleton organization is required for normal cell function. The cytoskeleton is mainly categorized into shapers, movers and motors. The shapers and movers maintain cell rigidity and movement of the cell. They are composed of three main types: the intermediate filaments, actin filaments and microtubules. The motors are associated with anterograde and retrograde transport of molecules and cargoes in the cell and are dynactin, kinesins and dynein. Alteration of these cellular structures has been shown to be associated with several neurodegenerative disorders such as: AD, PD and ALS (McMurray, 2000, Bamburg and Bloom, 2009, Parisiadou and Cai, 2010).

Cytoskeletal defects are an important contributor to ALS pathology. Early studies showed that both mutant transgenic mice models $SOD1^{G37R}$ and $SOD1^{G85R}$ showed evidence of dysfunctional axonal transport caused by defective neurofilament subunits and tubulin (Williamson and Cleveland, 1999). In a more

recent study, mutation in the actin binding protein Profilin1 (*PFN1*) gene was shown to inhibit axonal outgrowth of motor neurons in fALS (Wu et al., 2012). In addition, the *CRMP4* missense mutation was identified in motor neurons of ALS patients (Blasco et al., 2013). Expression of this variant in mouse motor neuron cultures showed an increased cell death and decreased axonal outgrowth (Blasco et al., 2013). Furthermore, mutations in dynactin and dynein have been shown to be associated with faulty retrograde transport in ALS (Munch et al., 2004).

In the current study, genes involved in cytoskeleton organization were also dysregulated. The actin binding proteins (*Caldesmon1, TPM1* and *MYH10*), actin depolymerizing factor destrin (*DSTN*) the protein kinase cGMP-dependent type I (*PRKG1*) and the magnesium-dependent enzyme (*ATP2C1)* which is involved in transporting Ca++, were all up-regulated. In contrast, a group of genes were down-regulated. These genes were involved in actin polymerization (*FGD1* and *INF2*), cell motility and migration (*AMOT* and *Talin2*) and cell cycle process (*CKS2*). These observations strongly support the involvement of cytoskeletal dysregulation in ALS.

3.8.2 Nuclear fALS-*TARDBP* fibroblasts

3.8.2.1 Nuclear division

Nuclear division (also known as karyokinesis) is the process by which a single cell nucleus is divided into daughter cells. This typically consists of the following stages: prophase, prometaphase, metaphase, anaphase, and telophase. Nuclear missense fALS-*TARDBP* fibroblasts showed a significant down-regulation of genes involved in nuclear division.

Genes involved in the kinetochore complex (*DSN1* and *ZWILCH*), kinetochore stabilization, (*HAUS6*), centromere development (*C13orf34*), spindle assembly and check point (*PBK* and *BUB1B*), microtubule attachment to kinetochore

(*SKA3*) and chromosome segregation (*NCAPD3* and *NUSAP1*) were decreased. Moreover, the (*CIT*) gene which is located in the central spindle and shown to be associated with CNS development was also reduced. Mutations in this gene have been shown to be associated with bipolar disorder (Di Cunto et al., 2000, Kato, 2007).

Dysregulation of kinesin was reported to be associated with ALS (Ferraiuolo et al., 2011). Here, the *KIF20B* gene was shown to be reduced which may suggest defective axonal transport (Bosco et al., 2010). Furthermore, *TARDBP* gene expression was reduced in the nuclear missense mutation (Neumann et al., 2006, Vance et al., 2006). This reduction in expression may reflect the process of degradation of mutant *TARDBP* transcripts in the nucleus. Also, the overall marked decrease in nuclear division related genes could explain the slow growth rate of missense mutated fALS-*TARDBP* fibroblasts.

3.8.2.2 Cellular response to stress

Normally, DNA lesions are continually repaired in most dividing cells. However, DNA lesions in post-mitotic neuronal cells have been shown to trigger a cell death response (Madabhushi et al., 2014). It was expected to find an increased expression of genes involved in cellular response to stress as TDP-43 sequestration and production of stress granules stimulates a stress response which leads to an immediate motor neuron cell death. In the present study a significant down-regulation in genes involved in DNA damage response was observed in ALS-*TARDBP* fibroblasts. A general reduction of expression of genes involved in DNA repair was observed (*ATAD5, RAD51C*, *BRCA2, C19orf62, MORF4L1, ERO1L, POLD3, POLE2, RFC2, RFC3, RFC5, TYMS, C9orf80* and *MCM7).* By searching the literature for a similar outcome, a single study by Yu et al., showed that TDP-43 is able to form a complex molecule with fragile X mental retardation protein (FMRP) and staufen (STAU1) to regulate several genes (Yu et al., 2012). One of these genes was the DNA damage repair gene Sirtuin 1 (*SIRT1).* The depletion of TDP-43 in the SH-SY5Y cell line showed a significant low expression of *SIRT1* (Yu et al., 2012). In contrast, overexpression of *SIRT1* was observed in both mutant *SOD1*^{G93A} ALS transgenic

mouse and AD mouse model which suggest its protective mechanism for cell survival (Kim et al., 2007).

The down-regulation effect of this alteration suggests a reduced DNA repair process in fALS-*TARDBP.* Both Yu et al., and the current study observations propose that the decrease in DNA repair genes could be a unique feature of ALS-*TARDBP* (Yu et al., 2012). Also, this data supports that fibroblasts are good model that to an extent mimics gene changes in CNS.

3.8.2.3 mRNA processing

TDP-43 is an RNA processing protein that is predominantly located in the nucleus and has a major role in RNA metabolism. Mutations in *TARDBP* were strongly linked to dysregulated RNA processing, primarily splicing (Tollervey et al., 2011). A defective TDP-43 splicing mechanism was shown in FTLD-TDP post-mortem brain tissue (Tollervey et al., 2011). Down-regulation of expression of spliceosomal complex proteins *SNRNP48* and *SNRNP25* in motor neurons of post-mortem tissue has been previously observed (Highley et al., 2014). Also, dysregulated RNA processing genes were evident in sALS-*TARDBP* fibroblasts, in which altered splicing was observed (Raman et al., 2015).

One of the aims of this project was to study the transcriptomic profile of the nuclear fALS-*TARDBP* separated from the cytoplasm to acquire a more precise view of the effect of the *TARDBP* mutation on RNA processing as this has not been examined previously. A significant reduction in genes involved in splicing was demonstrated (*TARDBP, HNRNPK, HNRNPM, KHDRBS1, NONO, PRPF4, PRPF8 SRSF10* and *SNRPB)* of which two genes *SRSF10* and *HNRNPM* had a similar pattern of regulation shown in sALS-*TARDBP* fibroblasts (Raman et al., 2015). Furthermore, a group of genes involved in mRNA processing other than splicing were down-regulated, the transcription regulator *DHX9,* transcription initiator *POLR2B*, translation initiator factor *CPEB1* and RNA decay *HNRNPD.* In addition, an interesting finding was the down-regulation of the RNA binding protein *HNRNPC* that regulates the vitamin D hormone response elements. As ALS is a multisystem disorder, speculations of vitamin D deficiency in ALS

patients has been recently proposed and suggested as a therapeutic target (Gianforcaro and Hamadeh, 2014). This observation supports the risk of fALS-*TARDBP* to vitamin D deficiency. As an overall view, it is clearly found that the presence of *TARDBP* missense mutation in fibroblasts causes alteration in the ability of these cells to process RNA.

3.8.3 qRT-PCR validation

At the time of this experimental study using Human Exon 1.0 ST Arrays to understand the possible dysregulated biological processes in 2012, the attention was narrowed to validate the predicted genes involved in RNA processing from both cellular compartments to confirm the effect of *TARDBP* missense mutation on RNA processing in fALS as there was a number of studies suggesting an impaired RNA processing associated with mutant *TARDBP*. Unfortunately, gene expression of the selected cytoplasmic fALS-*TARDBP* genes showed results in disagreement compared to the Human Exon 1.0 ST Array outcome. Both *SF3A1* and *SNRNP200* showed an opposing trend of gene expression than that observed on the arrays. The nuclear fALS-*TARDBP* candidate genes *TARDBP* and *SRSF10* confirmed the trend change although they demonstrated insignificant p-values.

This could be due to the method of quantification of gene expression and the oligonucleotide probes design on the Human Exon 1.0 ST Array. Gene expression levels are based on averaging the signal intensities of the total set of exons on the arrays to provide an expression level of that transcript. In contrast, qRT-PCR is amplifying a comparatively small and specific region of the transcript. Thus, this may be the basis of the discrepant result. Also, due to low levels of RNA concentrations obtained from fibroblasts the amount of RNA used for the reverse transcription reaction was little which may affected the correct quantification of the transcripts. In addition, there was a slight variation in the Ct values of the normalizer (β-actin) used in the qRT-PCR which may led to in the insignificant results obtained.

Arriving at a strong conclusion based on the validation results was not possible as the number of genes selected to confirm the changes that occurred on the arrays were insufficient. In addition, a general observation was that the fold changes produced from the arrays were relatively low, making validation even more difficult. Also, the robustness of the Human Exon Arrays were questioned in some studies (see section 3.8.5 below)

3.8.4 The overall effect of *TARDBP* missense mutation in fALS using the Human Exon 1.0 ST Arrays

The Human Exon 1.0 ST Arrays were used to understand the effect of the *TARDBP* missense mutation on the disease process. An overall view of the effect of the mutation on gene expression was shown. Dysregulated RNA processing was markedly affected in both cellular compartments in fALS. It was also shown that mRNA splicing regulation was significantly affected in both cellular fractions indicting that the mislocalization of TDP-43 caused by the *TARDBP* missense mutation in fALS plays a key role in splicing alteration (see section 3.6.3). This observation was in agreement with earlier studies on ALS which showed dysregulated splicing in the presence of *TARDBP* mutations (Highley et al., 2014, Raman et al., 2015).

3.8.5 The Human Exon 1.0 ST Arrays design

At the time of analysing the Human Exon 1.0 ST Array data, an enormous number of unknown gene sequences appeared in the data. As the Human Exon 1.0 ST Array GeneChip® probes were designed based on the available data libraries which contained all the known and predicted exon sequences at the time of manufacture (July, 2003), this may explain the large number of unannotated genes. Furthermore, a study was performed by Gaidatzis et al., which tested the efficiency of the Human Exon 1.0 ST Array. This was done by running RNA sequencing in parallel to the arrays and comparing results. It was shown that the

arrays contained probes that were not detected in the RNA sequencing data which may suggests faulty designed probes and poor annotation (Gaidatzis et al., 2009).

With the Gaidatzis et al., observation in mind another possible issue is raised which was the mathematical method of identifying differentially expressed genes on Human Exon 1.0 ST Arrays. It is based on averaging the signal intensities of all probes of a particular gene (http://www.affymetrix.com). This may give rise to false expression of some genes. The overall conclusion in the literature is that there are weaknesses in the design of the Human Exon 1.0 ST Arrays. To address this and specifically the detection of known splice variants, Affymetrix introduced the Affymetrix® Human Transcriptome Arrays (HTA) (Xu et al., 2011).

In summary, this work did show that the fibroblasts are a good model for studying fALS and that the separation of the two cellular components might provide some insights into the effect of the *TARDBP* missense mutation in fALS. However, at the time (April, 2013) no further analysis was performed on the arrays nor further validation experiments completed. Due to the difficulty with validation, this led to the design of a new experiment using the recently developed Affymetrix® Human Transcriptome Arrays (HTA) (Xu et al., 2011) which promised more robust results.

Chapter 4: Human Transcriptome Array 2.0 GeneChip®

4.1 Human Transcriptome Array 2.0 GeneChip®

In this current work, the Human Transcriptome Array 2.0 GeneChip® were used to study gene expression profiling in fALS-*TARDBP*. These arrays were designed with better features that the Human Exon 1.0 ST Arrays (see section 1.1.6.3).

A further aim was added into the experiment designed which was to improve the cell component separation method by monitoring cell membrane lysis under a light microscope. This was to ensure the isolation of an intact nucleus prior to RNA extraction. The cell fractionation was performed by osmotic pressure and centrifugation and the RNA extraction was achieved by the Trizol method (Refer to 2.2.2.1 for the method). In addition to the missense *TARDBP* mutation fibroblasts used in the Human Exon 1.0 ST Arrays, three truncation *TARDBP* mutation cases carrying p.Y374X mutation were also included.

4.2 Nuclear isolation

It has been previously demonstrated that studying gene expression profiling of total mRNA showed a significant contribution from nuclear polyadenylated mRNA that was characterized as cytoplasmic mRNA (Trask et al., 2009). This was based on the assumption that polyadenylated mRNA were only found in the cytoplasmic fraction. The literature shows that total mRNA does not accurately represent the steady state level of cytoplasmic mRNA. It was demonstrated that the levels of cytoplasmic mRNA were influenced by different factors, for example: the turnover time of a transcript (Trask et al., 2009).

In the current work nuclei were separated from the cytoplasm from patient and control fibroblasts to study the effect of *TARDBP* mutation on the disease process and investigate the possible dysregulated biological processes in relation to the disease. Cell lysis was monitored throughout the cell fractionation step. Cells were stained with trypan blue and visualized under the light microscope (Figure 4.1).

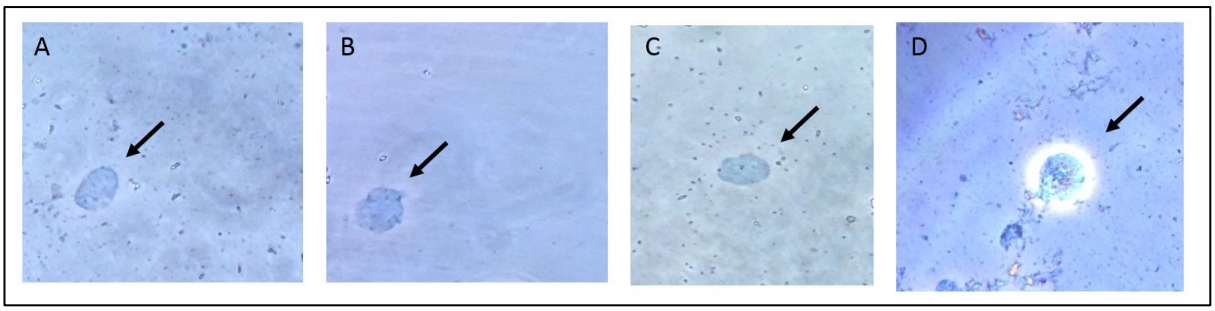

Figure 4.1: *Representative images of isolated intact nucleus stained with trypan blue and visualised under light microscope from three condition. (A) Control 2303, (B) Patient 51 MT and (C) Patient TT 192 (D) Poorly isolated nucleus demonstrating cytoplasmic material. MT=missense mutation, TT=Truncated mutation.*

4.3 Cytoplasmic and nuclear RNA concentrations and quality measurements using Agilent Bioanalyser 2100

The Agilent Bioanalyser 2100 was used to measure the quantity and quality of RNA (Table 4.1 and Figure 4.2) (*Refer to section 2.5 for Agilent Bioanalyser 2100 method of RNA quantification*).

The RNA samples from both cellular compartments showed better quality of RNA than the Human Exon 1.0 ST Arrays RNA samples. Also, the electropherograms did not show detectable levels of DNA contamination. This was achieved by modifying both, the cell fractionation and RNA extraction methods. The fibroblasts were monitored throughout the cell lysis procedure to ensure proper separation. Also, the Trizol method was used for RNA extraction. Trizol separates the lysate into a three layers, clear upper aqueous layer which contain the RNA, a middle interphase which contain the DNA and a lower layer which contains proteins. Therefore, it was easier to aspirate the RNA sample avoiding any interfering genomic DNA and proteins during RNA extraction.

The sample selection was based on RIN cut-off value$\geq$ 8 and a minimum of ~200ng yield. The cytoplasmic RNA samples yields ranged 2.5µg to 14.2µg and the nuclear samples ranged from 0.8µg to 10.8µg (Table 4.1). Thus, all samples were taken forwards.

Table 4.1: RNA yields from cytoplasmic and nuclear extractions by the Agilent Bioanalyser. µg=nanograms, RIN= RNA integrity number, ng/µl= nanograms/ microliter, Con= Control, Pat= Patient, ID= Identification

Cellular fraction	Mutation type	Sample ID	RNA yields (ng/µl)	RIN	Total RNA yield (µg)
Cytoplasmic	-	Con155	284	9.3	14.2
		Con 2303	198	9.6	9.9
		Con170	148	9	7.4
		Con159	216	9.3	10.8
	Missense mutation	Pat 48	81	9.7	4
		Pat 55	68	9.7	3.8
		Pat 51	147	9.5	7.3
	Truncated mutation	Pat192	81	9.7	4
		Pat193	128	9	6.4
		Pat194	50	9	2.5
Nuclear	-	Con 155	128	8	6.4
		Con 2303	192	9.5	9.6
		Con 170	136	9.9	6.8
		Con 159	218	9.8	10.9
	Missense mutation	Pat 48	27	8	1.35
		Pat 55	72	9.6	3.6
		Pat 51	100	8.7	5
	Truncated mutation	Pat 192	36	9.1	1.8
		Pat 193	144	9.7	7.2
		Pat 194	16	8	0.8

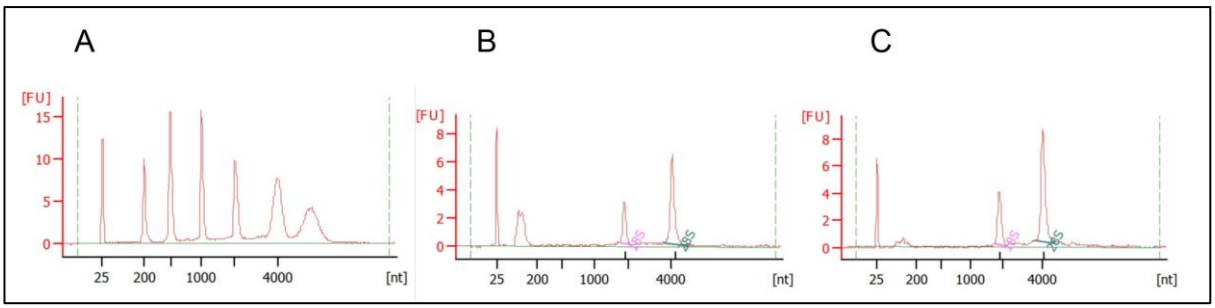

Figure 4.2: *Representative electropherograms generated by the Agilent Bioanalyser 2100 of cytoplasmic and nuclear RNA samples (A) Standard ladder graph that represents the RNA markers which act as a reference for the other RNA samples. (B) Cytoplasmic RNA sample (patient 193) and (C) Nuclear RNA sample (patient 193). The Y axis represents the UV light absorption (FU) and the X axis represents size (nt).*

4.4 Human Transcriptome Arrays 2.0 GeneChip®

Human Transcriptome Arrays 2.0 GeneChip® Affymetrix were used to determine differentially expressed genes. As a quality control of the sample preparation, sample concentrations were measured as specific stages by the Nanodrop 1000 spectrophotometer and the Agilent Bioanalyser 2100. RNA samples were linearly amplified to reach (15µg) of cRNA for the preparation of ss cDNA. A successful cRNA amplification was achieved and the yields ranged from 38.8µg to 203µg (Table 4.2). The ss cDNA was prepared and the cut-off value was to achieve (5.5µg) in order to perform the fragmentation and labelling step. Samples show satisfactory amount of ss cDNA ranging from 12µg to 23.5µg (Table 4.3).

Table 4.2: cRNA yields. µg= micrograms, RIN= RNA integrity number, ng/µl= nanograms/ microliter, Con= Control, Pat= Patient, ID= Identification

Cellular fraction	Mutation types	Sample ID	Yields (ng/µl)	Total yields (µg)
Cytoplasmic	-	Con 2302	1222.55	73
		Con170	1105.70	66
		Con159	736.39	44
		Con155	2205.89	132
	Missense mutation	Pat 48	1157.57	69
		Pat 51	888.90	53
		Pat 55	3388.94	203
	Truncated mutation	Pat 192	1833.75	110
		Pat 193	1460.08	87.6
		Pat 194	1817.46	109
Nuclear	-	Con 2302	1204.57	72
		Con170	2049.17	122.9
		Con159	1498.74	89.9
		Con155	3389.85	203
	Missense mutation	Pat 48	1721.47	103
		Pat 51	647.96	38.8
		Pat 55	1476.04	88.5
	Truncated mutation	Pat 192	2312.14	138.7
		Pat 193	3122.39	187
		Pat 194	1859.12	111.5

Table 4.3: Single-Stranded cDNA yield. µg= micrograms, RIN= RNA integrity number, ng/µl= nanograms/ microliter, Con= Control, Pat= Patient, ID= Identification

Cellular fraction	Mutation type	Sample ID	Yields (ng/µl)	Total yields (µg)
Cytoplasmic	-	Con 2302	507.98	15
		Con170	483.45	14.5
		Con159	436.75	13
		Con155	688.60	20.6
	Missense mutation	Pat 48	433.21	12.9
		Pat 51	478.45	14
		Pat 55	751.11	22.5
	Truncated mutation	Pat 192	612.10	18
		Pat 193	603.54	18
		Pat 194	543.29	16
Nuclear	-	Con 2302	486.03	14.5
		Con170	581.62	17
		Con159	530.30	15.9
		Con155	784.38	23.5
	Missense mutation	Pat 48	552.50	16.5
		Pat 51	407.36	12
		Pat 55	645.25	19
	Truncated mutation	Pat 192	649.63	19
		Pat 193	767.60	23
		Pat 194	484	14.5

4.4.1 Fragmentation

The ss cDNA samples were fragmented to enable their binding to the probes on the arrays. The recommended fragment length is 40nt to 70nt. Controls and patients samples were fragmented properly with most of the fragmented ss cDNA being ~70nt long (Figure 4.3).

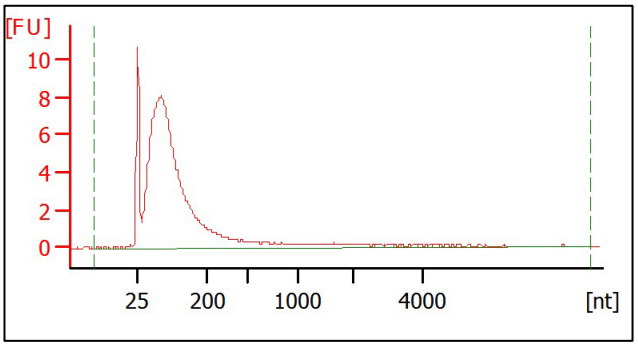

Figure 4.3: *Representative electropherogram of fragmented single stranded DNA sample (patient 193). The peak point of fragments can be assessed to be approximately ~70nt in length.*

4.4.2 Gel shift assay

The gel shift assay is a procedure that assess the efficiency of the labelling step (See section 2.7.10 for the procedure). Figure 4.4 demonstrated that positive samples showed bands at the expected position (400bp) and the negative samples did not show bands. This indicates that the samples were properly labelled.

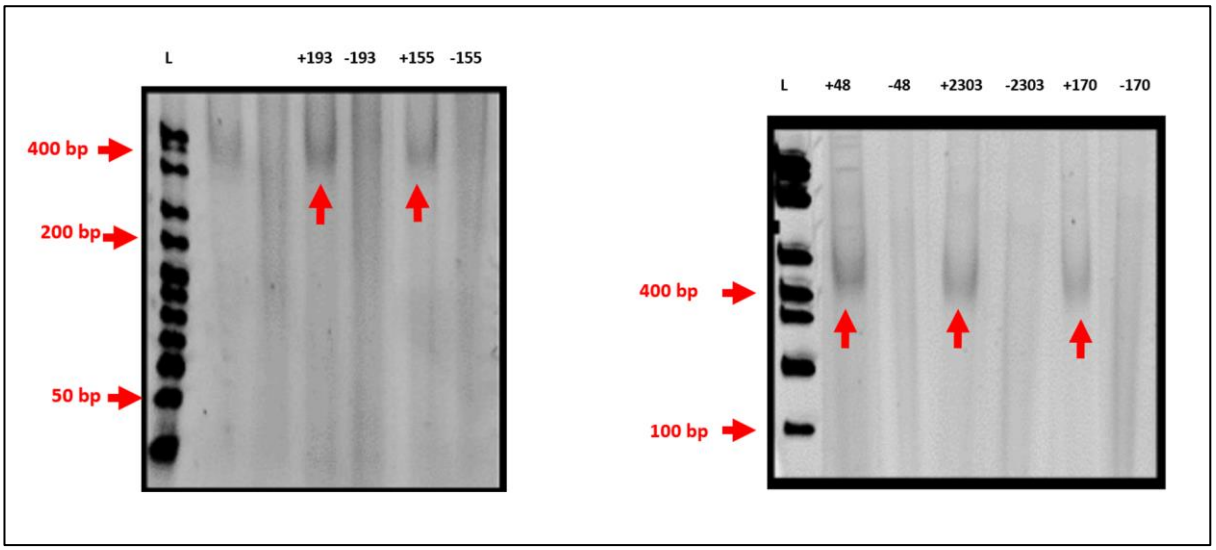

Figure 4.4: *4-20% graded TBE gel electrophoresis. The gel is stained with ethidium bromide and visualized under UV light. Avidin treated (positive) samples showed bands which corresponds to the expected bands size (400bp). Untreated samples acted as negative controls. Hyperladder V and IV were used.*

Sample type	*Control*	*Control*	*Control*	*Missense mutation*	*Truncated mutation*
Sample ID	*Nuclear 155*	*Nuclear 2303*	*Nuclear 170*	*Nuclear 48*	*Cytoplasmic 193*

4.4.3 Human Transcriptome Arrays 2.0 quality control

The Human Transcriptome Arrays raw data were converted to CEL files using the Affymetrix GeneChip Command Console (AGCC) software. The quality control check of the arrays was performed through Affymetrix Expression Console v1.0 software. The samples were monitored throughout the preparation process by the exogenous poly-A RNA positive controls (see section 2.7.2). Figure 4.5 shows a linear graph of the spiked in poly-A controls for both the cytoplasmic and nuclear samples. Cytoplasmic samples demonstrated a good quality of amplified spiked in poly-A controls except control 2303 and patient 55 which showed a slight reduction of the expression of the four spiked in poly-A controls. However the level of expression of these genes were as expected (Figure 4.5A). The hybridization intensities of the poly-A spiked in controls of the nuclear samples showed a good quality of amplification (Figure 4.5B).

The process of hybridization, washing and staining of the arrays were monitored by a set of prelabeled hybridization control which are BioB, BioC, BioD and Cre (see section 2.7.11). Cytoplasmic and nuclear samples illustrated an even distribution of the hybridization controls signal intensity (Figure 4.6A&B). In addition, the probe set intensities were measured and a box plot graph was produced to determine the overall deviation of probe set signals for each array. This was presented as a box plot diagram that shows the upper quartile, lower quartiles and median. The whiskers illustrates the highest and lowest average signal intensities of the probes. The red line across the boxes represent the median which expected to range from 0.1 to 0.2. The median value of the cytoplasmic and nuclear samples was detected at ~0.1 (Figure 4.7).

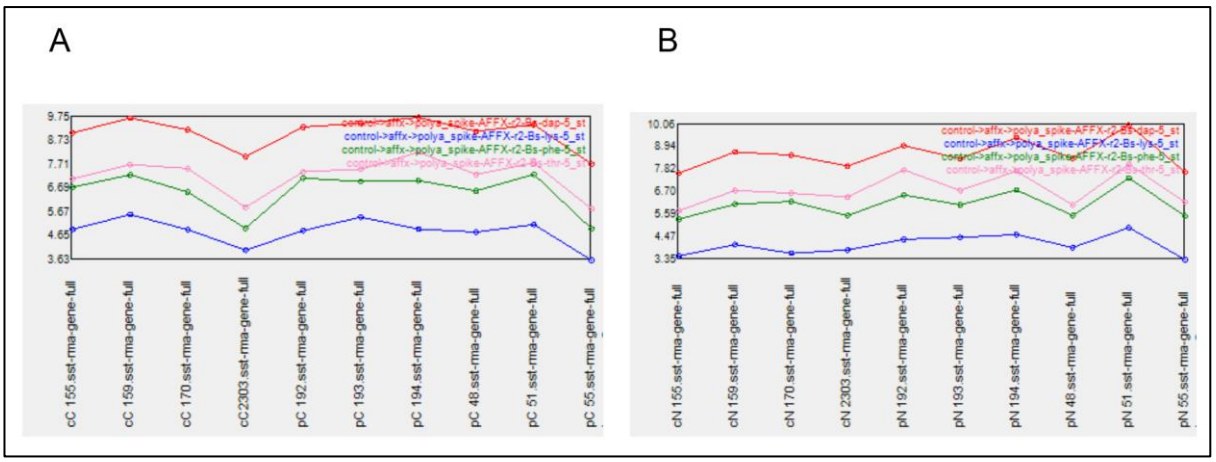

Figure 4.5: *Poly-A spiked in controls linear graph of the HTA. (A)The cytoplasmic hybridization intensities of the poly-A spiked in controls. All cytoplasmic samples demonstrated good quality of amplification except control 2303 showed a reduction of gene expression of the spiked in controls. (B) The poly-A spiked in hybridization intensities of the nuclear samples.*

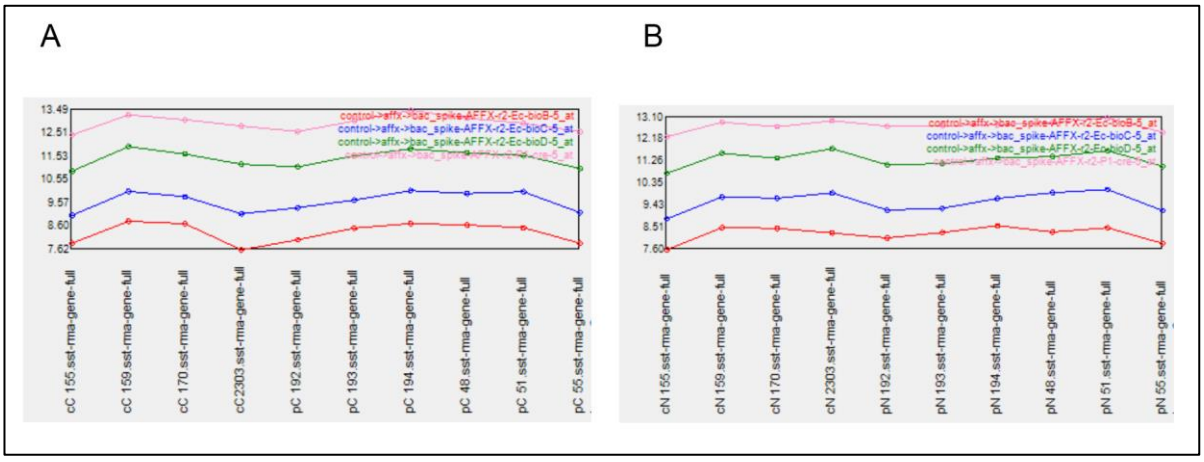

Figure 4.6: *The Hybridization controls (BioB, BioC, BioD and Cre) linear graph of HTA. (A) The cytoplasmic hybridization controls linear graph. (B) The nuclear hybridization controls linear graph. Overall all samples show even hybridization intensity.*

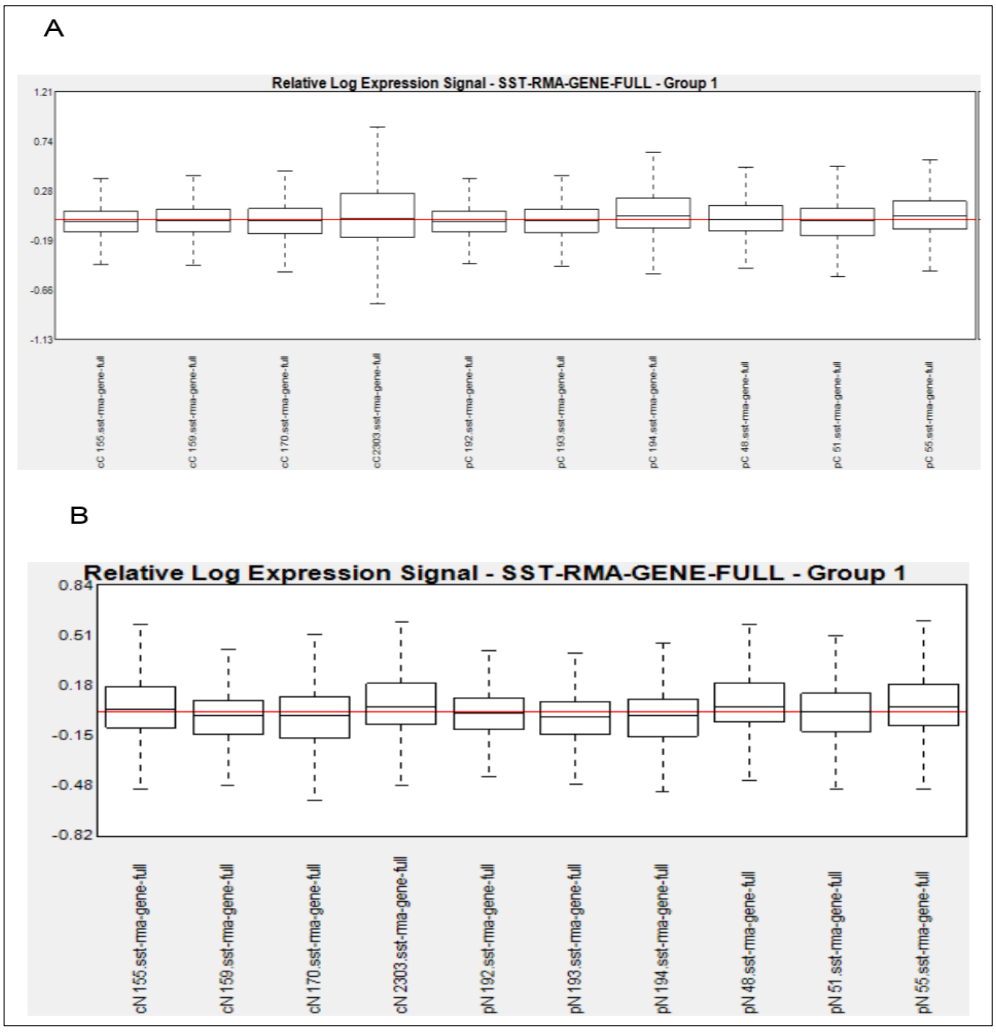

Figure 4.7: *Box plot graph of the relative expression signals after normalization of the HTA. Each box plot represents the mean and standard deviation of an array. The red middle line across the box plots is the median gene expression of all samples after normalization. The whiskers represent the highest and the lowest average signal intensities of the probes. (A) The relative log expression signal of cytoplasmic samples. (B) The relative log expression signal of the nuclear samples. They demonstrate an overall acceptable range of averaged signal intensities.*

4.5 Gene expression profiling using the Transcriptome Analysis Console (TAC) software

CHP files from controls and patients were generated from GeneChip® Command Console® (AGCC) Software and were uploaded into the TAC software. CHP files ware normalized prior to analysis. A one-way ANOVA test was carried out and the significant differentially expressed transcripts with a p-value $\leq$ 0.05 and fold change $\geq \pm$ 2 were identified. The main approaches were first to identify statistically significant genes that are differentially expressed in fALS-*TARDBP* from both missense MT vs. control CON and truncated mutations TT vs. control CON in each cellular component then to assign these genes to biological processes through available online software.

Cytoplasmic MT vs. cytoplasmic CON showed 80 differentially expressed genes; 43 were up-regulated and 37 were down-regulated. In addition, the cytoplasmic TT vs. cytoplasmic CON demonstrated 221 differentially expressed genes; 182 were up-regulated and 39 were down-regulated (Figure 4.8). Within the nuclear extract, nuclear MT vs. nuclear CON showed 73 differentially expressed genes; 45 were up-regulated and 28 were down-regulated. In addition, the nuclear TT vs. nuclear CON demonstrated differentially expressed genes 321; 263 were up-regulated and 58 were down-regulated (Figure 4.9). It was surprisingly that at FC $\geq$ 2 and a p-value $\leq$ 0.05 very few genes were identified in both mutation types and cellular compartments. The GeneVenn tool was used to determine differentially expressed genes that were specific to each type of mutation and in each cellular component. Common genes were also identified (Figure 4.10 and 4.11).

The gene lists were uploaded into DAVID v6.7 to study the biological processes involved in the disease process. The cut-off value of enrichment score was set to $\geq$ 1.3 which is considered the lowest significant value equivalent to a p-value of 0.05 (Huang da et al., 2009). Similarly, very few biological processes were identified. The differentially expressed genes from cytoplasmic MT vs. cytoplasmic CON showed that vesicle-mediated transport was the only significant biological process affected in fALS-*TARDBP* missense mutation. Furthermore,

cytoplasmic TT vs. cytoplasmic CON demonstrated that regulation of acute inflammatory response, response to nutrient and negative regulation of proteolysis were the most significant enriched biological processes. On the other hand, nuclear MT vs. nuclear CON illustrated that bone development and nucleosome assembly were both affected. Lastly, DAVID online software did not show any significant biological process for nuclear TT vs. nuclear CON with the highest enrichment score being 0.99 (Table 4.4). 6 genes were common in both the cytoplasmic MT and TT, 3 were annotated and 3 were unannotated. On the other hand, 8 gene were common in both nuclear MT and TT, 2 were annotated and 6 were unannotated (Table 4.5 and Table 4.6).

The results generated by TAC software were therefore not satisfactory. This was most probably due to two reasons, first, the normalization step prior to data analysis. CHP files from the cytoplasmic RNA and nuclear RNA were normalized together by the expression console software this may have deceased the number of genes significantly. Second was the inability to manipulate the fold change at the time of analysis at FC $\pm$ 1.2 (April 2015) which made it difficult to reduce the stringency and get higher number of differentially expressed genes and it was obvious that the number of genes in each biological process were significantly low with undetected biological process in the nuclear truncated mutation although it showed the highest number of differentially expressed genes. With the limitations of the TAC software, Qlucore Omics Explorer software was the best alternative available option to analyse the data. This had adjustable fold change setting and was easy to use.

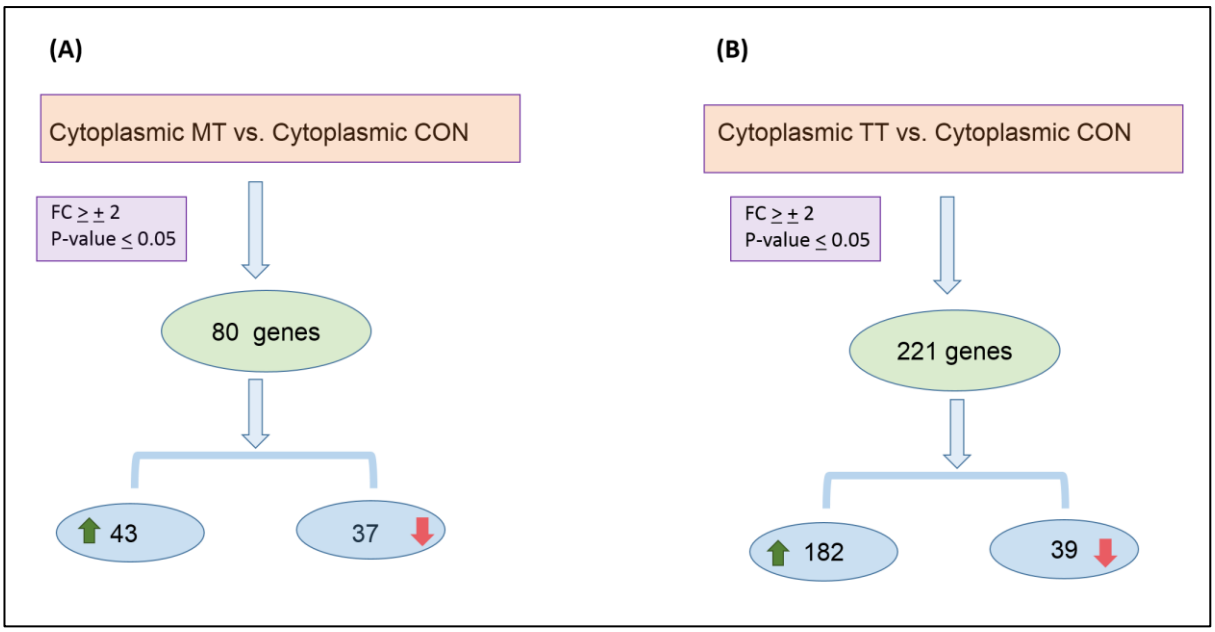

Figure 4.8: *Differentially expressed genes in cytoplasmic MT and cytoplasmic TT compared to controls using the TAC software.*

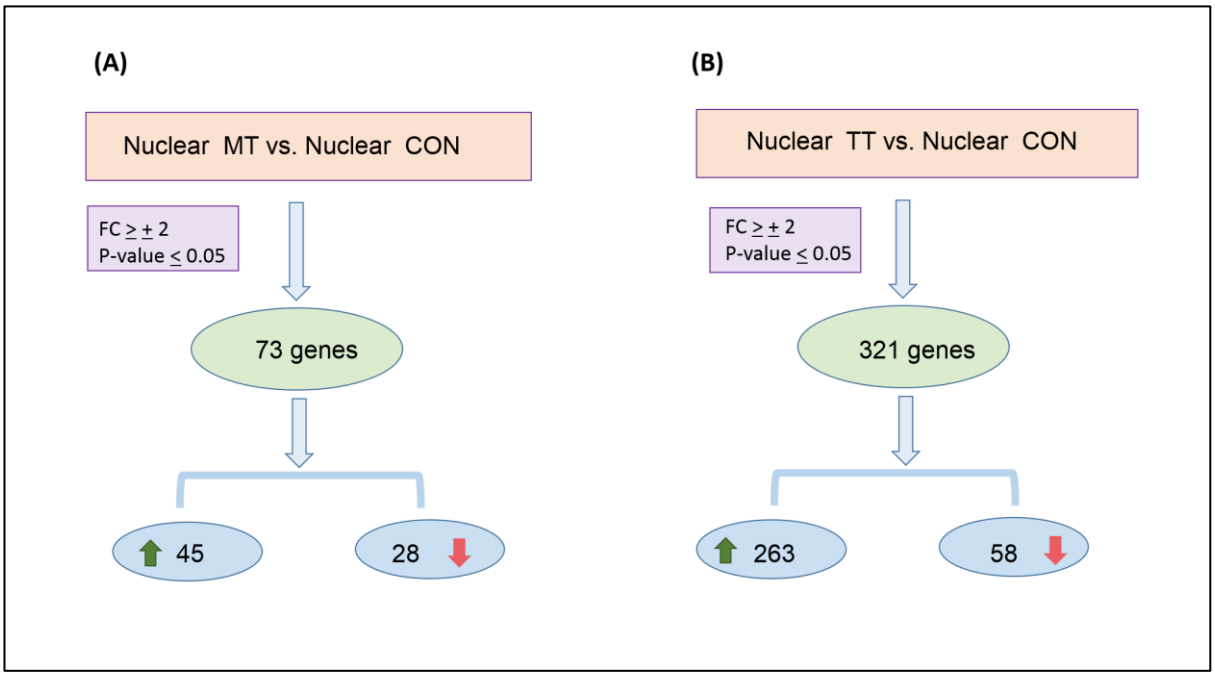

Figure 4.9: *Differentially expressed genes in nuclear MT and nuclear TT compared to controls using the TAC software.*

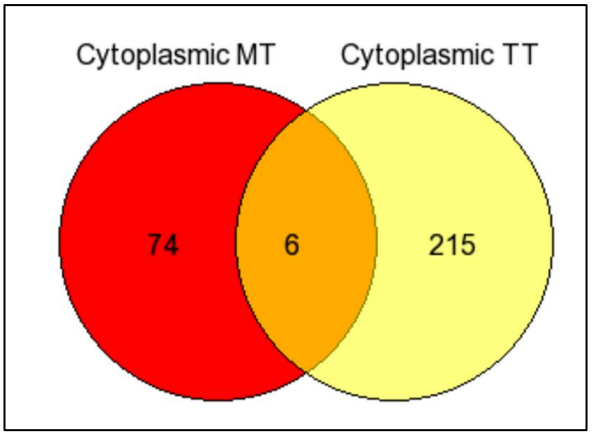

Figure 4.10: *Comparative study of differentially expressed genes in the cytoplasmic MT vs. TT. Venn diagram showing 74 genes specific to the cytoplasmic missense mutation, 215 genes specific to the cytoplasmic truncation mutation and 6 genes were found common in both types of mutations using the TAC software.*

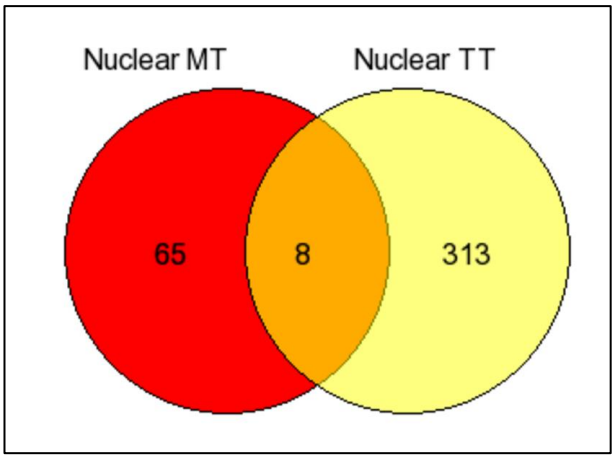

Figure 4.11: *Comparative study of differentially expressed genes in the nuclear MT vs. TT. Venn diagram showing 65 genes specific to the cytoplasmic missense mutation, 313 genes specific to the cytoplasmic truncation mutation and 8 genes were found common in both types of mutations using the TAC software.*

Table 4.4: Functionally enriched biological processes generated by DAVID for cytoplasmic MT & TT and nuclear MT & TT (TAC software). GO= Gene ontology, no.=number, ES= Enrichment score, MT= missense mutation, TT= truncated mutation

GO	Biological process	Gene no.	P- value	ES
Cytoplasmic MT vs. CON				
BP_FAT	Vesicle-mediated transport	6	2.0E-3	1.78
Cytoplasmic TT vs. CON				
BP_FAT	Regulation of acute inflammatory response	3	3.4E-3	1.57
BP_FAT	Response to nutrient	5	2.7E-3	1.47
BP_FAT	Negative regulation of proteolysis	3	3.7E-3	1.31
Nuclear MT vs.CON				
BP_FAT	Bone development	3	2.1E-2	1.69
BP_FAT	Nucleosome assembly	3	1.0E-2	1.42
Nuclear TT vs. CON				
BP_FAT	Keratinocyte differentiation	3	3.1E-2	0.99

Table 4.5: Common annotated genes in cytoplasmic MT and TT (TAC software). MT=missense mutation, TT=truncated mutation, FC=fold change

Gene symbol	Gene name	FC MT	FC TT
FSIP1	Fibrous sheath interacting protein 1	2.09	2.95
MGAT5	Mannosyl (alpha-1,6-)-glycoprotein beta-1,6-N-acetyl-glucosaminyltransferase	2.17	2.15
NAV2	Neuron navigator 2	-2.11	-2.15

Table 4.6: Common annotated genes in nuclear MT and TT (TAC software). MT=missense mutation, TT=truncated mutation, FC=fold change

Gene symbol	Gene name	FC MT	FC TT
ARL17A	ADP-ribosylation factor-like 17A	2.67	2.14
ARL17B	ADP-ribosylation factor-like 17B	2.99	2.93

4.6 Gene expression profiling using Qlucore Omics Explorer software

Gene expression profiling from the cytoplasmic and nuclear RNA fractions were studied using Qlucore Omics Explorer software. CEL files were uploaded into the Qlucore Omics Explorer software and samples were normalized according to their cellular component and mutation type prior to the analysis. The p-value was set to $\leq$ 0.05 and fold change to $\geq \pm$ 1.2. Two comparison studies were carried out on each type of mutation, fALS-*TARDBP* missense mutation MT and fALS-*TARDBP* truncated mutation TT. The analysis was set similarly to the Human Exon 1.0 ST Array with the aim to identify biological pathways dysregulated specifically and commonly in response to the *TARDBP* mutations in each RNA compartment.

The cytoplasmic MT vs. cytoplasmic CON showed 224 differentially expressed genes; 162 genes were up-regulated and 62 genes were down regulated. Cytoplasmic TT vs. cytoplasmic CON revealed 421 differentially expressed genes; 290 genes were up-regulated and 131 genes were down regulated. However, nuclear MT vs nuclear CON presented 552 differentially expressed genes; 344 genes were up-regulated and 208 genes were down regulated (Figure 4.12). The nuclear TT vs. nuclear CON illustrated 685 differentially expressed genes; 270 genes were up-regulated and 415 genes were down regulated (Figure 4.13). GeneVenn tool was also used to determine differentially expressed genes to each type of mutation and each cellular component. Common genes were also identified (This is shown further in section 4.6.1.3 and 4.6.2.3).

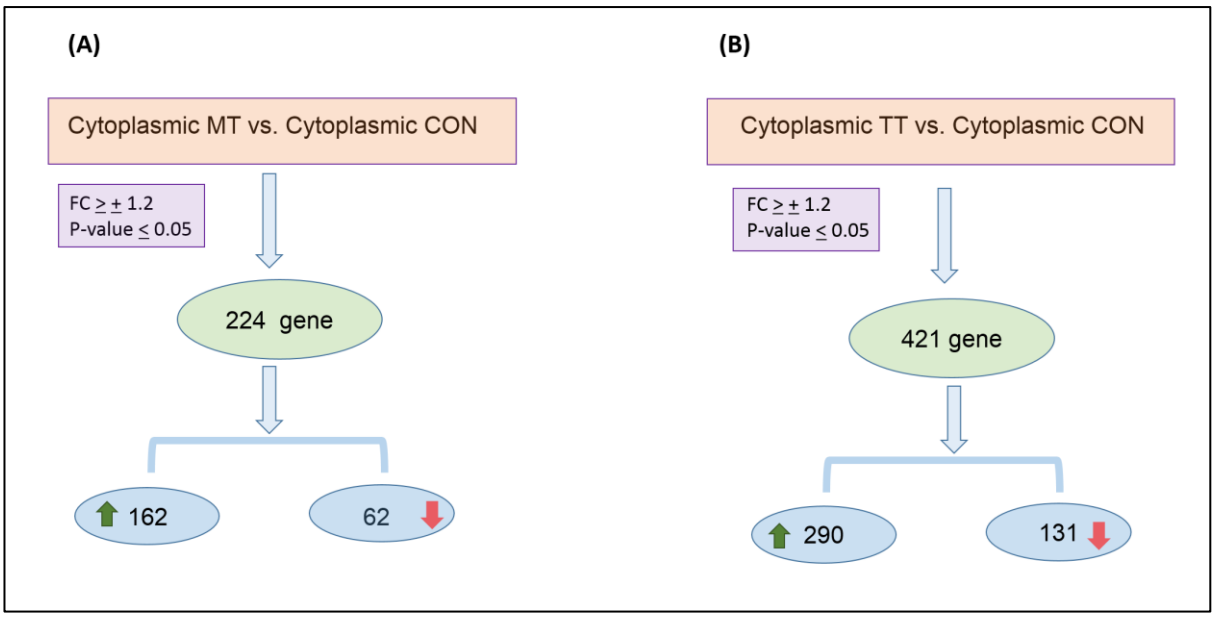

Figure 4.12: *Differentially expressed genes in cytoplasmic MT and cytoplasmic TT compared to controls using the Qlucore Omics Explorer software*

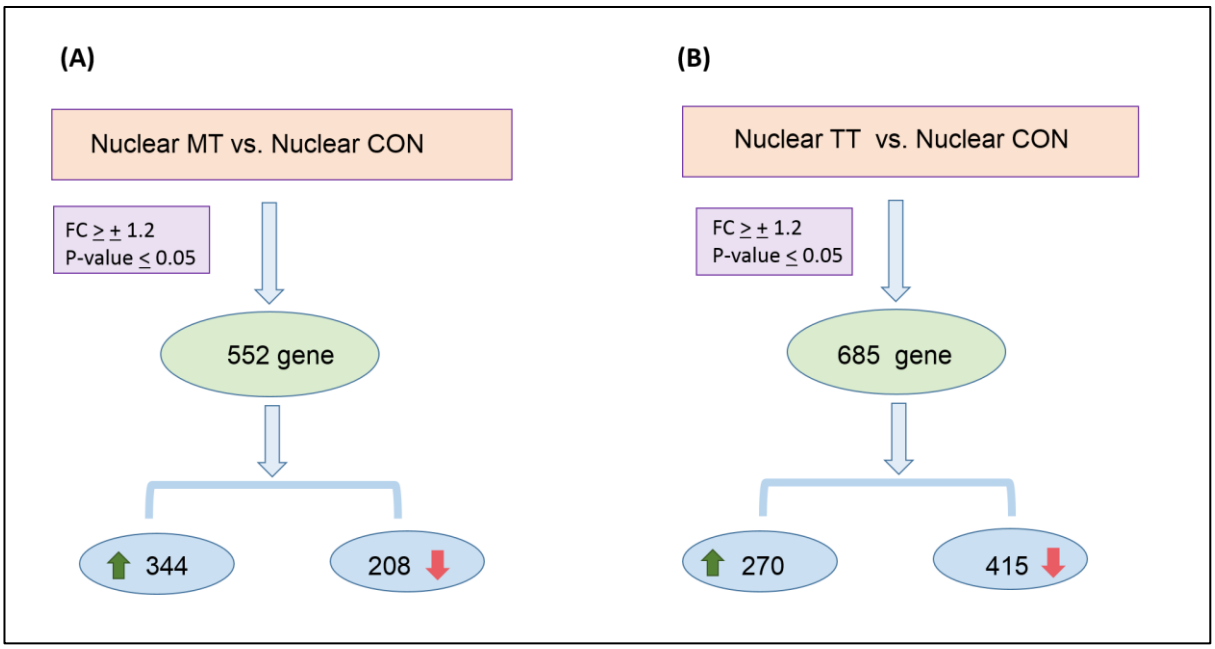

Figure 4.13: *Differentially expressed genes in nuclear MT and nuclear TT compared to controls using the Qlucore Omics Explorer software*

4.6.1 Cytoplasmic gene expression profiling using the Human Transcriptome Arrays

4.6.1.1 Differential gene expression of cytoplasmic MT vs. CON

Qlucore Omics Explorer software generated the principal component analysis (PCA) graph which is a statistical test that illustrates the variability of a set of values. The highest percentage of variability is blotted on the longest axis. The PCA graph of cytoplasmic MT vs. cytoplasmic CON showed a good separation between patients and controls (Figure 4.14). The gene list was uploaded into DAVID analysis tool to identify the biological processes to what these genes belong. Using a high stringency classification those with a significant enrichment score $\geq$ 1.3 were selected. The most significantly enriched biological processes were the following: RNA processing, angiogenesis, cell adhesion and neurological system process (Table 4.7). A more detailed examination of the genes within these significant pathways is provided below.

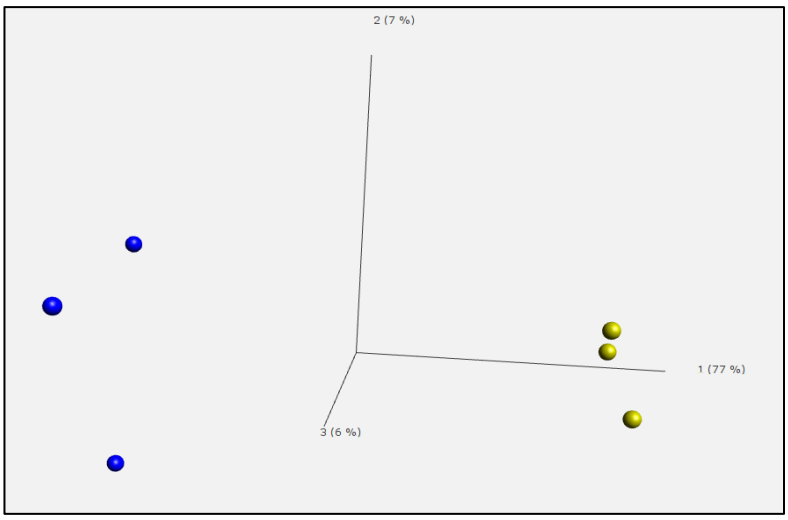

Figure 4.14: *Principal component analysis plot of cytoplasmic MT vs. cytoplasmic CON. It shows a 77% variability between patients and controls clustering at the first principal component (PC1). It demonstrates good separated cluster (Blue = MT) & (Yellow = CON)*

Table 4.7: Functionally enriched biological processes generated by DAVID of the cytoplasmic MT vs. CON differentially expressed genes (High stringency). GO= Gene ontology, no.=number, ES= enrichment score

GO	Biological process	Gene no.	P-value	ES
BP_FAT	RNA processing	7	6.0E-2	1.58
BP_FAT	Angiogenesis	4	4.0E-2	1.47
BP_FAT	Cell adhesion	8	6.5E-2	1.39
BP_FAT	Neurological system process	10	1.6E-1	1.33

4.6.1.1.1 RNA processing

As mentioned previously (section 3.6.1.1.3), RNA processing is an essential cellular metabolic process which involves a wide range of sequential events which control gene expression. These include: RNA splicing, editing, transport, translation and RNA decay. The majority of genes involved in RNA processing have been shown to be down-regulated in cytoplasmic fALS-*TARDBP* missense mutation samples (Table 4.8) and (Figure 4.15).

The U2 small nuclear RNA auxiliary factor 1-like 4 (*U2AF1L4*) is a splicing factor which is involved in RNA splicing was decreased (FC=-1.2). Northern blotting showed that the expression of *U2AF1L4* was high in the brain (Shepard et al., 2002). Furthermore, the small nuclear ribonucleoprotein polypeptide A (*SNRPA*) gene was down-regulated (FC=-1.3). It is a component of the spliceosome and binds to the U1 snRNP that is involved in pre-mRNA splicing (Sillekens et al., 1987, Nelissen et al., 1991). The methyltransferase like 1 (*METTL1)* gene was also reduced (FC=-1.2). It encodes for a methyltransferase protein which was suggested to have an S-adenosylmethionine (SAM) binding site. It is thought to be involved in transferring methyl groups from one molecule to another in the cell, and is therefore, suggested to be involved in regulating gene expression through methylation (Bahr et al., 1999). The poly (A) binding protein, nuclear 1 (*PABPN1*) was also reduced (FC=-1.2). The gene encodes for a nuclear protein which is involved in the regulation of nascent RNA polyadenylation (Fan et al., 2001). Furthermore, two pseudogenes, the proliferation-associated 2G4 (*PA2G4P4*) and the ribosomal protein L36a pseudogene (*RPL36A*) were also reduced (FC=-1.3 and -1.2 respectively). In contrast, a single gene showed a significant increase in gene expression. The adenosine deaminase, RNA specific B1 (*ADARB1*) which is responsible for the editing of the GluR2 pre-mRNA at the Q/R site converting adenosine to inosine was increased (FC= 1.6). This was suggested to have an effect the Ca++ ion permeability through the GluR2 receptor (Eckmann et al., 2001).

As the majority of RNA processing takes place in the nucleus, it is not surprising to find that genes related to RNA processing i.e. splicing, and polyadenylation and also gene related to methylation being reduced in the cytoplasmic missense mutation. However, to further investigate the expression of these gene in the nuclear missense mutation, the nuclear MT vs. CON gene list was investigated. Surprisingly none of the genes were identified. Therefore, this may suggest that as a result of TDP-43 mutation, RNA splicing factors, spliceosome complexes and other RNA binding proteins are degraded in the nucleus.

The overall observation suggests a decreased expression of genes involved in RNA processing in the fALS missense mutation. This observation indicates that less splicing regulation takes place in fALS-*TARDBP* missense mutation. Also dysregulated RNA processing genes was observed in the cytoplasmic fraction using the Human Exon 1.0 ST Arrays (see section 3.6.1.1.3).

Table 4.8: Genes involved in RNA processing in the cytoplasmic missense mutation

Gene symbol	Gene name	P-value	Fold change
ADARB1 *	Adenosine deaminase, RNA-specific, B1 (RED1 homolog rat)	0.009	1.66
METTL1 *	Methyltransferase like 1	0.04	-1.23
PABPN1	Poly(A) binding protein, nuclear 1	0.02	-1.21
PA2G4P4	Proliferation-associated 2G4, 38kDa; pseudogene 4	0.009	-1.34
RPL36A	Ribosomal protein L36a pseudogene	0.01	-1.25
SNRPA	Small nuclear ribonucleoprotein polypeptide A	0.02	-1.30
U2AF1L4	U2 small nuclear RNA auxiliary factor 1-like 4	0.02	-1.28

(*) selected candidate genes for validation by qRT-PCR

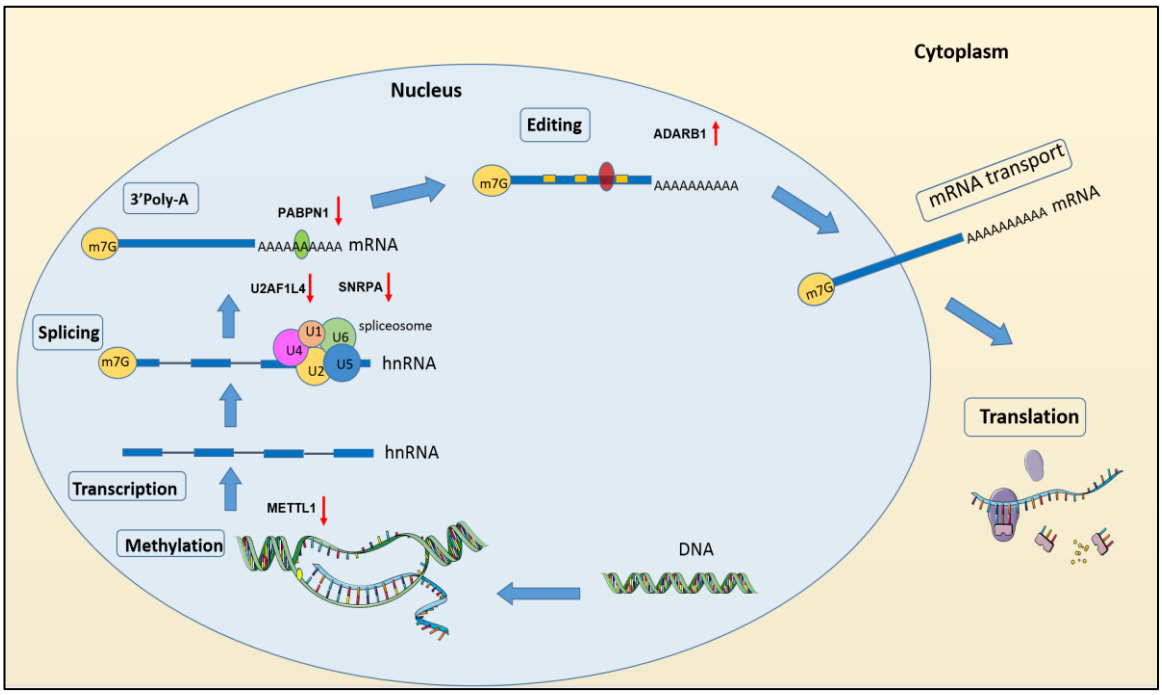

Figure 4.15: *A representative diagram showing the dysregulated RNA processing genes in fALS-TARDBP cytoplasmic missense mutation*

4.6.1.1.2 Angiogenesis

The vascular endothelial growth factor (*VEGF*) gene which is involved in angiogenesis has been suggested to be associated with the pathology of ALS (Oosthuyse et al., 2001). Normally, *VEGF* is a mitogen which has a role in angiogenesis and neurogenesis. A study showed that the depletion of *VEGF* in a mouse model resulted in low expression of *VEGF* in the brain and spinal cord producing symptoms resembling ALS (Oosthuyse et al., 2001). Furthermore, mutations in the angiogenin (*ANG*) gene are associated with ALS. ANG has a role in vessel repair, endothelial cell proliferation, migration and rRNA transcription (Gao and Xu, 2008).

In the current study, four genes associated with angiogenesis were up-regulated in the cytoplasm of the fALS missense mutation cases (Table 4.9). *VEGF* gene expression is stimulated by external factors such as hypoxia and also by internal factors such as circulating cytokines, interleukin 6 and interleukin 1β. Here, the proinflammatory cytokine interleukin 18 (interferon-gamma-inducing factor) (*IL18*) was shown to be up-regulated (FC=1.2). It is involved in immune defence and has been associated with cancer metastasis (Vidal-Vanaclocha et al., 2000, Ferrara, 2004). Furthermore, the endothelin receptor type A (*EDNRA*) was increased (FC=1.2). The *EDNRA* is activated via the binding of endothelin-1, which is produced by endothelial cells, to the receptor. This action induces blood vessel vasoconstriction (Miyamoto et al., 1996). The kruppel-like factor 5 (intestinal) (*KLF5*) belongs to the zinc finger protein Kruppel-like factor subfamily and is considered a transcription factor which is essential for normal development of arterial walls and angiogenesis. *KLF5* $^{+/-}$ knockout mice showed decreased levels of angiogenesis activity (Shindo et al., 2002). The *KLF5* gene was up-regulated (FC=1.2). Finally the transforming growth factor, alpha (*TGFA*) was also increase (FC=1.2). *TGFA* is involved in cell proliferation, differentiation and development. Overexpression of *TGFA* was shown to be associated with several types of cancer (Singh and Coffey, 2014). Overall there are few number of differentially expressed gene related to angiogenesis in fALS-*TARDBP* missense mutation. Possibly not a significant pathway however may be considered in future work (Figure 4.16).

Table 4.9: Genes involved in angiogenesis in the cytoplasmic missense mutation

Gene symbol	Gene name	P-value	Fold change
EDNRA	Endothelin receptor type A	0.01	1.24
IL18	Interleukin 18 (interferon-gamma-inducing factor)	0.02	1.26
KLF5	Kruppel-like factor 5 (intestinal)	0.03	1.26
TGFA	Transforming growth factor, alpha	0.02	1.21

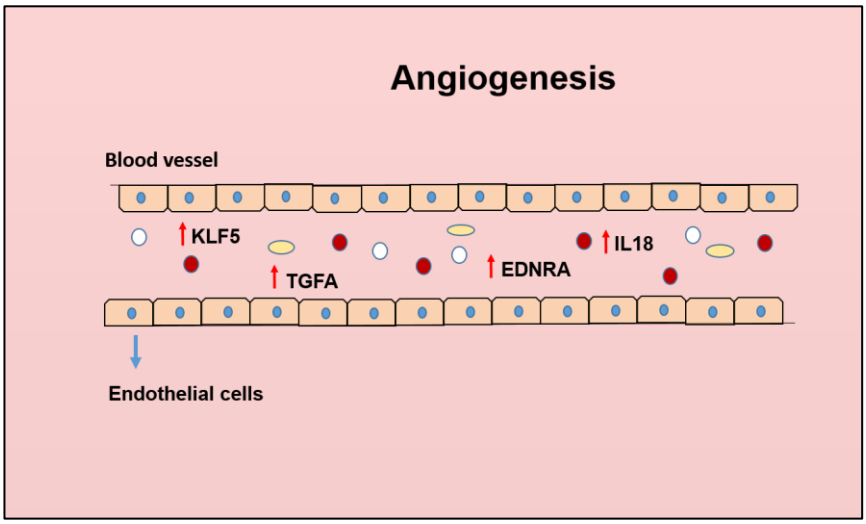

***Figure 4.16**: A representative diagram showing the dysregulated genes involved in angiogenesis in fALS-TARDBP cytoplasmic missense mutation. White circles= white blood cells, red circles= red blood cell, yellow ovals= platelet.*

4.6.1.1.3 Cell adhesion

Cell adhesion is the process by which cells are attached to each other via adhesion molecules to maintain normal cellular structure, cell integrity, protect against invading pathogens and can be involved in injury repair (Gumbiner, 1996). In the cytoplasmic fALS-*TARDBP* cell adhesion molecules were found to be dysregulated as discussed below (Table 4.10).

The CD9 molecule (*CD9*) belongs to the tetraspanin superfamily which is involved in cell adhesion and migration. It is expressed on mast cells, dendritic cells and megakaryocytes (Leung et al., 2011). Defects in the CD9 genes results in loss of its expression and associated with cancer and metastasis (Zoller, 2009). This gene was shown to be up-regulated (FC=1.2). Furthermore, the platelet/endothelial cell adhesion molecule (*PECAM1*) which facilitates endothelial cell junctions was increased (FC=1.2). It is expressed on platelets, leukocytes and T-lymphocytes (Ma et al., 2010). The protocadherin beta 15 (*PCDHB15*) belongs to a subfamily of the cadherin molecules which are Ca++ dependent adhesion molecules. *PCDHB15* has suggested to have a role in neural cell adhesion and was shown to be up-regulated (FC=1.2) (Wu and Maniatis, 1999). In contrast, cadherin 2, type 1, N-cadherin (neuronal) (*CDH2*) is involved in the maintenance of cell integrity was down-regulated (FC=-2.2). It was shown that *CDH2* is necessary to facilitate pre-synaptic and post-synaptic adhesion (Tanaka et al., 2000). The trophinin associated protein (tastin) (*TROAP*) that has a role in the attachment of the blastocyst to the endometrium during implantation was also deceased (FC=-1.2) (Fukuda et al., 1995). Finally, the tumour necrosis factor, alpha-induced protein 6 (*TNFAIP6)* was reduced (FC=-1.2). It was demonstrated that genes involved in cell adhesion were dysregulated in fALS missense mutation with a number of genes were up-regulated and down-regulated, acting across several systems (Figure 4.17).

Table 4.10: Genes involved in cell adhesion in the cytoplasmic missense mutation

Gene symbol	Gene name	P-value	Fold change
CD9	CD9 molecule	0.01	1.29
CDH2	Cadherin 2, type 1, N-cadherin (neuronal)	0.04	-2.24
PCDHB15	Protocadherin beta 15	0.02	1.21
PECAM1	Platelet/endothelial cell adhesion molecule	0.02	1.22
RPSA	Ribosomal protein SA pseudogene	0.04	-1.27
TMEM8A	NULL///Transmembrane protein 8A	0.02	1.36
TNFAIP6	Tumour necrosis factor, alpha-induced protein 6	0.03	-1.28
TROAP	Trophinin associated protein (tastin)	0.03	-1.24

**NULL=Not accurately characterized yet*

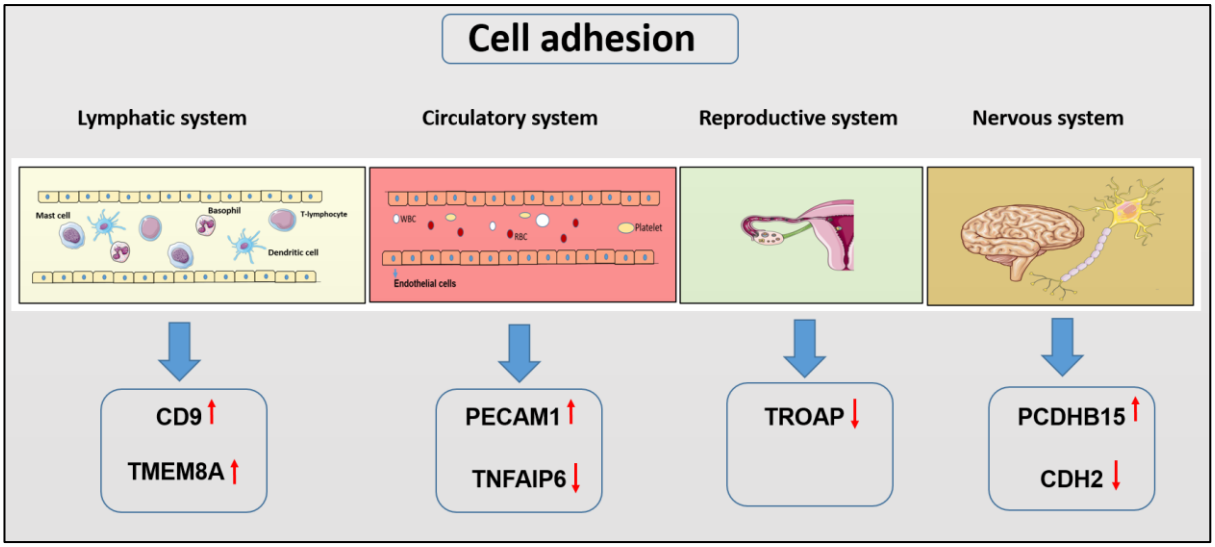

Figure 4.17: *A representative diagram showing the cell adhesion molecules in fALS-TARDBP cytoplasmic missense mutation and their previously described roles.*

4.6.1.1.4 Neurological system process

DAVID analysis tool grouped some genes under the term neurological process (Table 4.11). This was defined by the gene ontology terminology as genes carrying functions in relation to the CNS. A large group of chemoreceptors were shown to be increased in expression. They are G-protein-coupled receptors with a characteristic 7-transmembrane domain structure that are activated by exogenous stimuli (Buck and Axel, 1991). Several olfactory receptor gene were up-regulated, olfactory receptor, family 4, subfamily D, member 10 (*OR4D10*) (FC=1.2), olfactory receptor, family 5, subfamily H, member 1 (*OR5H1*) (FC=1.2), olfactory receptor, family 5, subfamily R, member 1 (*OR5R1*) (FC=1.3), olfactory receptor, family 51, subfamily B, member 4 (*OR51B4*) (FC=1.2), olfactory receptor, family 52, subfamily J, member 3 (*OR52J3*) (FC=1.3). On the other hand, the olfactory receptor, family 1, subfamily G, member 1 (*OR1G1*) was down-regulated (FC=-1.4).

The CD9 molecule (*CD9*) was up-regulated (FC= 1.2). As previously described it is involved in both cell adhesion and signal transduction (see section 4.6.1.1.3). It also was shown to be expressed in the CNS (Tole and Patterson, 1993). The LIM homeobox 8 (*LHX8*) gene which is involved in neuronal differentiation was increased (FC=2.2). Mutations in the *LHX8* gene have been suggested to be associated with defective cholinergic neuronal development (Zhao et al., 2003). Furthermore, the arrestin, beta 1 (*ARRB1*) gene was up-regulated (FC=1.4). It encodes for a cofactor that acts by inhibiting the beta-adrenergic receptor kinase (BARK) signalling pathway (Zhao et al., 2003). The regulating synaptic membrane exocytosis 1 (*RIMS1*) mediates synaptic vesicle release at the presynaptic nerve ending by creating a scaffold with other proteins that enables the transportation of synaptic vesicle to the presynaptic terminal (Schoch et al., 2002). This gene was shown to be increased (FC=2.0).

It is shown that genes involved in the neurological system process were up-regulated in the fALS-*TARDBP* missense mutation even though the work was carried out using fibroblasts. This was mainly involved in olfactory receptors, cell adhesion, exocytosis, neuronal differentiation and BARK signalling pathway.

Table 4.11: Genes involved in neurological system process in the cytoplasmic missense mutation

Gene symbol	Gene name	P-value	Fold change
ARRB1	Arrestin, beta 1	0.02	1.46
CD9	CD9 molecule	0.01	1.29
LHX8	LIM homeobox 8	0.02	2.25
OR1G1	Olfactory receptor, family 1, subfamily G, member 1	0.02	-1.40
OR4D10	Olfactory receptor, family 4, subfamily D, member 10	0.04	1.20
OR5H1	Olfactory receptor, family 5, subfamily H, member 1	0.01	1.20
OR5R1	Olfactory receptor, family 5, subfamily R, member 1	0.04	1.34
OR51B4	Olfactory receptor, family 51, subfamily B, member 4	0.008	1.22
OR52J3	Olfactory receptor, family 52, subfamily J, member 3	0.006	1.33
RIMS1	Regulating synaptic membrane exocytosis 1	0.01	2.02

4.6.1.2 Differential gene expression of cytoplasmic TT vs. CON

The PCA of cytoplasmic TT vs. cytoplasmic CON showed an acceptable separation cluster between patients and controls (Figure 4.18). The differentially expressed genes were explored using the DAVID analysis tool. Those genes with a significant enrichment score $\geq$ 1.3 were selected. The significant enriched biological processes were found in two clusters: angiogenesis and adherens junction (Table 4.12). A further description is shown below.

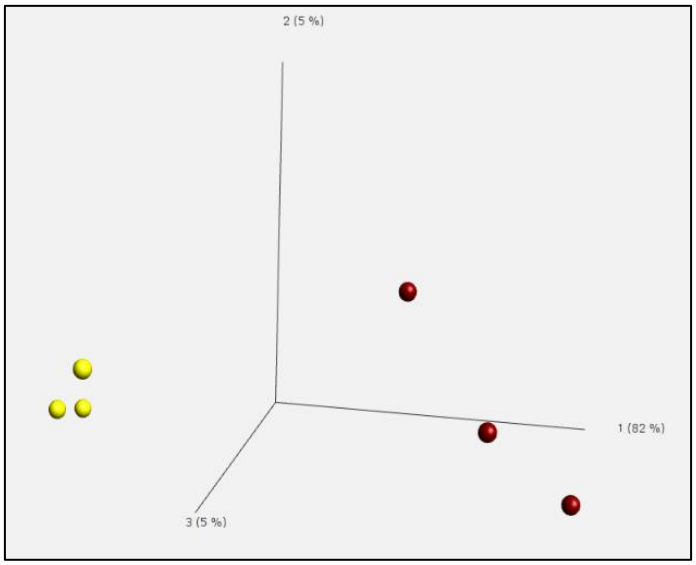

Figure 4.18: *Principal component analysis plot of cytoplasmic TT vs. cytoplasmic CON. Samples illustrate good separation with an 82 % variability between patients and controls clustering at the first principal component (PC1). (Red = TT) & (Yellow = CON).*

Table 4.12: Functionally enriched biological processes generated by DAVID of the cytoplasmic TT vs. CON differentially expressed genes. GO=Gene ontology, no.=number, ES=Enrichment score

GO	Biological process	Gene no.	P-value	ES
BP_FAT	Angiogenesis	8	1.8E-3	2.45
CC_FAT	Adherens junction	8	2.9E-3	1.89

4.6.1.2.1 Angiogenesis

Genes involved in angiogenesis were also shown to be up-regulated in fALS-*TARDBP* truncated mutation similarly to that in missense mutation however none of the same genes were identified (Table 4.13).

The epithelial mitogen homolog (mouse) (*EPGN*) was up-regulated (FC=1.2). The gene encodes for a ligand which belongs to the epidermal growth factor family. It binds to the epidermal growth factor receptor to activate cell proliferation and migration signalling pathways (Herbst and Bunn, 2003). Moreover, the fibroblast growth factor 1 (acidic) (*FGF1*) which is suggested to be an angiogenesis factor was also increased (FC=1.2) (Magnusson et al., 2007). The mesenchyme homeobox 2 (*MEOX2*) gene was up-regulated (FC=1.2) and was shown to be involved in vascular differentiation (Gorski et al., 1993, Wu et al., 2005). In addition, the sema domain, seven thrombospondin repeats (type 1 and type 1-like), transmembrane domain (TM) and short cytoplasmic domain, (semaphorin) 5A (*SEMA5A*) was increased (FC=1.6). It is involved in axon guidance in both attracting and inhibiting axonal growth during neuronal development (Kantor et al., 2004). The T-box 1 (*TBX1*) gene encodes for the TBX1 transcription factor that involves in the development of normal arterial blood. A *TBX1* mutation in mice showed phenotypic characteristics similar to DiGeorge syndrome (Jerome and Papaioannou, 2001). This gene was shown to be up-regulated (FC=1.2). The Thy-1 cell surface antigen (*THY1*) is a glycoprotein which is expressed on the cell surface. It is involved in cell proliferation, differentiation and apoptosis. It has been suggested to be a tumour suppressor for ovarian cancer (Lung et al., 2005). The tumour necrosis factor

(ligand) superfamily, member 12 (*TNFSF12*) is a member of the tumour necrosis factor (TNF) ligand family which is involved in cellular pathways such as: cell proliferation and apoptosis was increased (FC=1.2). It also was shown to be involved in angiogenesis by promoting endothelial cell proliferation and migration (Chicheportiche et al., 1997, Lynch et al., 1999). Finally the Rho GTPase activating protein 24 (*ARHGAP24*) was the only gene in the list to be down-regulated (FC=-1.3). It is involved in regulating endothelial cell proliferation and migration through the Rho signalling pathway. Knock-down of the *ARHGAP24* in mice showed an inhibition of endothelial cell migration and proliferation. This strongly suggests an *ARHGAP24* association with angiogenesis (Su et al., 2004). Genes involved in angiogenesis were increased in the cytoplasmic truncated mutation (Figure 4.19). The present observation along with the dysregulated angiogenesis related genes observed in missense mutation may suggests the association of dysregulated angiogenesis in the disease process.

Angiogenesis-related genes from both mutations were combined together and were uploaded into DAVID in order to detect any similarities or differences in angiogenesis pathway. The Kyoto Encyclopedia of Genes and Genomes (KEGG) pathway did not show any significant pathway. This may indicate distinct affected targeted genes underlying each type of mutation. It may also reflects the response to the cellular environment within the fibroblasts.

Table 4.13: Genes involved in angiogenesis in the cytoplasmic truncation mutation

Gene symbol	Gene name	P-value	Fold change
ARHGAP24	Rho GTPase activating protein 24	0.01	-1.38
EPGN	Epithelial mitogen homolog (mouse)	0.04	1.28
FGF1	Fibroblast growth factor 1 (acidic)	0.01	1.22
MEOX2	Mesenchyme homeobox 2	0.03	1.21
SEMA5A*	Sema domain, seven thrombospondin repeats (type 1 and type 1-like), transmembrane domain (TM) and short cytoplasmic domain, (semaphorin) 5A	0.01	1.65
TBX1	T-box 1	0.02	1.20
THY1	Thy-1 cell surface antigen	0.009	1.42
TNFSF12	Tumor necrosis factor (ligand) superfamily, member 12	0.03	1.21

(*) selected candidate genes for validation by qRT-PCR

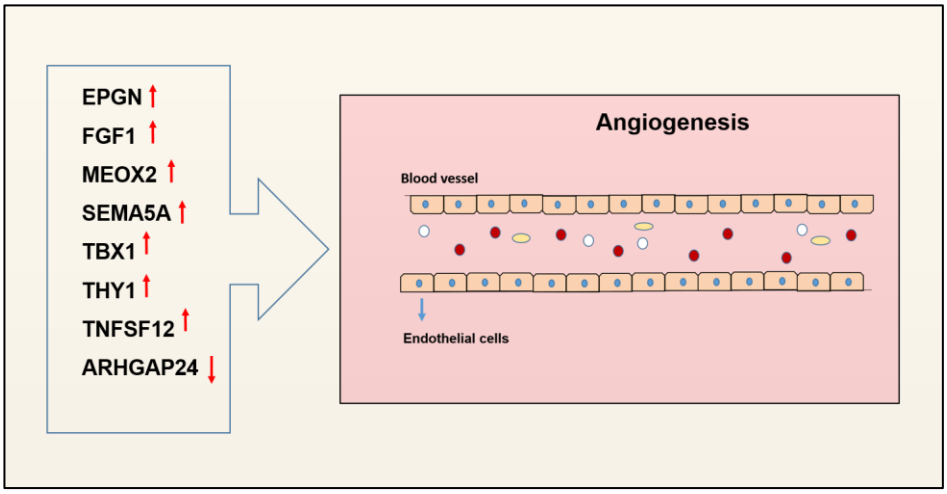

Figure 4.19: *A representative diagram showing the dysregulated genes involved in angiogenesis in fALS-TARDBP cytoplasmic truncated mutation. White circles= white blood cells, red circles= red blood cell, yellow ovals= platelet.*

4.6.1.2.2 Adherens junction

Adhesion junction molecules are anchoring proteins that are able to extend from one cell to attach to adjacent cell facilitating the adhesion process. Several genes were dysregulated in the fALS-*TARDBP* truncated mutation (Table 4.14).

The LIM domain 7 (*LMO7*) was up-regulated (FC=1.6). It has been suggested that LMO7 regulates emerin expression, a protein that facilitates the membrane anchoring of the cytoskeleton (Holaska et al., 2006). In addition, the membrane protein, palmitoylated 7 (MAGUK p55 subfamily member 7) (*MPP7*) was increased (FC=1.2). *MPP7* stimulates polarity and facilitates tight junction formation of epithelial cells (Stucke et al., 2007). In contrast some genes involved in adhesion were down-regulated. Two genes belonging to the Rho family of GTPases were reduced, the Rho GTPase activating protein 24 (*ARHGAP24*) (as seen above) and Cdc42 GTPase-activating protein (*ARHGAP31*) (FC=-1.3 &-1.3 respectively). Both genes are involved in regulating endothelial cells proliferation, migration and cytoskeletal arrangement through the Rho signalling pathway (Su et al., 2004, Tcherkezian et al., 2006). Furthermore, the enabled homolog (*ENAH*) which facilitates the movement of actin filament was down-regulated (FC=-1.5). Overexpression of *ENAH* was suggested to be associated with carcinoma cell invasion and metastasis (Philippar et al., 2008). The tensin like C1 domain containing phosphatase (tensin 2) (*TENC1*) was reduced (FC=-1.2). It belongs to the tensin family which are adhesion molecules that have been suggested to have a role in promoting cell migration (Chen et al., 2002). Both Talin 1 & Talin 2 were down-regulated (FC=-1.2 &-1.2 respectively). They are involved in cell adhesion process which facilitate the adhesion of cells through activating the connection of integrin molecules to the actin cytoskeleton (Monkley et al., 2001, Chen et al., 2002).

It was shown that genes involved in adhesion were mostly down-regulated in fALS truncated mutation. Although both fALS-*TARDBP* missense mutation and truncated mutation showed that cell adhesion/ adherens junction was dysregulated, it was interesting to find if any of the cell adhesion/ adherens junction genes from both mutations belonged to similar or distinct pathway. Thus,

genes from both mutations were combined then uploaded into DAVID and the Kyoto Encyclopedia of Genes and Genomes (KEGG) pathway was generated in order to identify significant pathways. It was shown that cell adhesion process was dysregulated similarly in both mutations, two genes; *CDH2* and *PECAM1;* from the fALS-*TARDBP* missense mutation belonged to the cell adhesion molecule pathway and the fALS-*TARDBP* truncated mutation showed that *TLN1* and *TLN2* belonged in the focal adhesion pathway (Figure 4.20 and 4.21). Therefore, dysregulated cell adhesion related pathways may be a common dysregulated biological process in fALS-*TARDBP* mutations.

Table 4.14: Genes involved in the adherens junction in the cytoplasmic truncation mutation

Gene symbol	Gene name	P-value	Fold change
ARHGAP24	Rho GTPase activating protein 24	0.01	-1.38
ARHGAP31	Cdc42 GTPase-activating protein	0.04	-1.36
ENAH *	Enabled homolog (Drosophila)	0.002	-1.58
LMO7	LIM domain 7	0.009	1.65
MPP7	Membrane protein, palmitoylated 7 (MAGUK p55 subfamily member 7)	0.01	1.24
TENC1	Tensin like C1 domain containing phosphatase (tensin 2)	0.02	-1.26
TLN1	Talin 1	0.04	-1.24
TLN2	Talin 2	0.003	-1.25

(*) selected candidate genes for validation by qRT-PCR

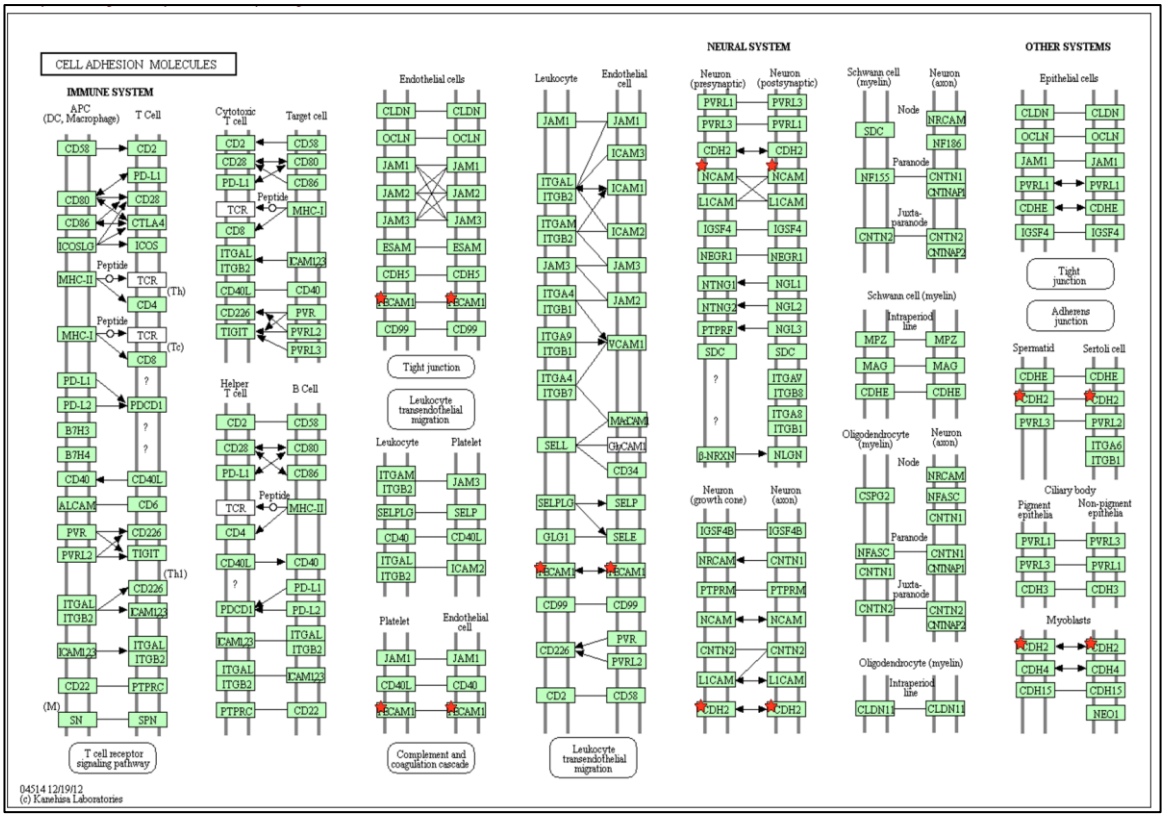

Figure 4.20: *Cell adhesion molecules pathway showing, CDH2 and PECAM1 dysregulated in fALS-TARDBP missense mutation.*

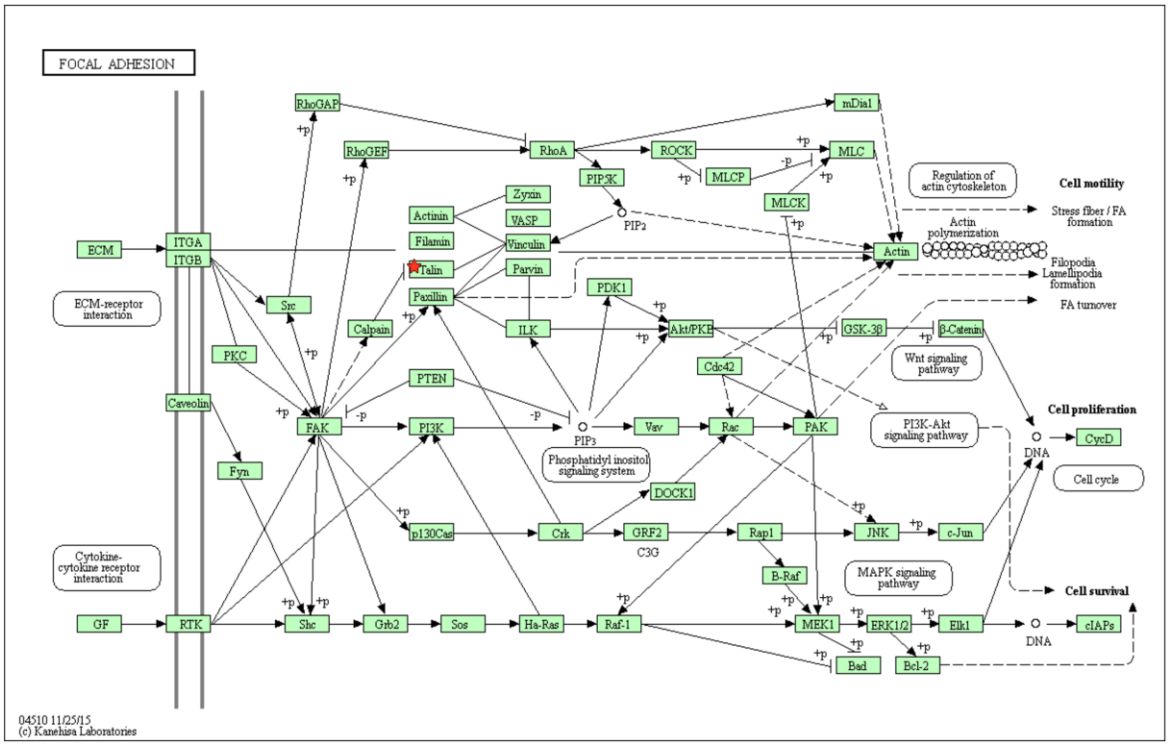

Figure 4.21: *Focal adhesion pathway showing, Talin (i.e. TLN1 and TLN2 blotted as one gene on the diagram by DAVID) dysregulated in fALS-TARDBP truncated mutation.*

4.6.1.3 Comparative analysis of differentially expressed genes in the cytoplasmic fractions of missense and truncation *TARDBP* mutation

It was interesting to distinguish genes related to each type of mutation and find genes that were common to fALS, this was performed using an online tool known as GeneVenn. The venn diagram showed 209 differentially expressed genes were specific to the cytoplasmic missense mutation, 406 differentially expressed genes were specific to the cytoplasmic truncated mutation and 15 genes were common in both (Figure 4.22).

Using DAVID online software we explored each specific list separately. Both cytoplasmic MT and cytoplasmic TT specific genes showed the same biological process to be affected which was angiogenesis however with different set of genes (enrichment score of 1.32 and 2.53 respectively). The 15 common genes did not demonstrate any clustering within a biological pathway (Table 4.15). This may suggest distinct biological processes affected by the two different types of mutations, within the cytoplasmic RNA fraction.

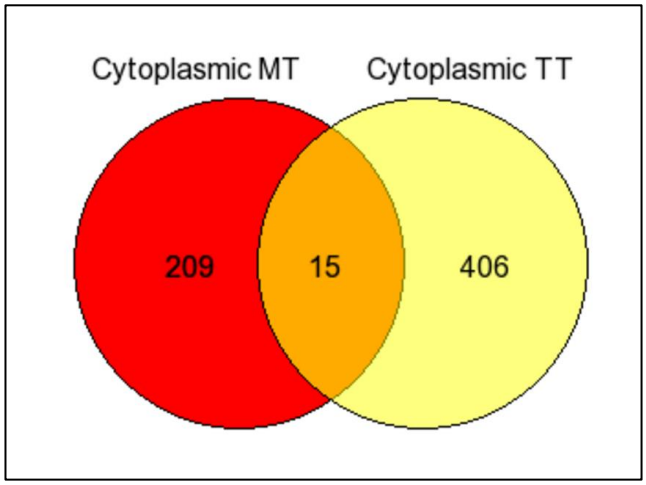

***Figure 4.22**: Comparative analysis of differentially expressed genes in the cytoplasmic fractions of missense MT and truncation TT TARDBP mutation. Venn diagram showing 209 genes specific to the cytoplasmic missense mutation, 406 genes specific to the cytoplasmic truncation mutation and 15 genes were found common in both types of mutations.*

Table 4.15: Common genes in cytoplasmic missense and truncation mutation

Gene Symbol	Gene name	FC MT	FC TT
ARL17A	ADP-ribosylation factor-like 17A	1.51	2.45
DHRS4-AS1	DHRS4 Antisense RNA 1	1.45	1.54
FSIP1	NULL/// Fibrous sheath interacting protein 1	1.85	2.11
GABARAPL1	GABA(A) receptor-associated protein like 1	1.61	1.36
HCG11	HLA complex group 11 (non-protein coding)	1.28	1.45
HCG20	NULL	1.22	1.22
MIR632	NULL /// MicroRNA 632 /// zinc finger protein 207	-1.30	-1.40
OR9A1P	Olfactory receptor, family 9, subfamily A, member 1 pseudogene	-1.32	-1.22
OTTHUMG00000007307	NULL	1.24	1.200
OTTHUMG00000157236	NULL	1.61	1.42
PABPN1	Poly(A) binding protein, nuclear 1	-1.21	-1.26
RNA5SP376	RNA, 5S ribosomal pseudogene 376	1.20	1.22
RNA5SP377	RNA, 5S ribosomal pseudogene 377	1.20	1.22
SNRPA	Small nuclear ribonucleoprotein polypeptide A	-1.30	-1.47
VSIG1	NULL/// V-set and immunoglobulin domain containing 1	1.20	1.20

**NULL= gene not annotated, NULL/// gene name= not accurately characterized yet.*

4.6.2 Nuclear gene expression profiling using the Human Transcriptome Arrays

4.6.2.1 Differential gene expression of nuclear MT vs. CON

The PCA of nuclear MT vs. nuclear CON showed a good separation of clusters between patients and controls (Figure 4.23). The differentially expressed genes were explored using DAVID. As previously mentioned, the cut-off value of enrichment score was set to $\geq$ 1.3.

The highest enrichment clustering was found in the following biological process and biological processes: nuclear mRNA splicing via spliceosome, regulation of translation, mRNA transport and nucleosome organization (Table 4.16). A further discussion of these biological processes is provided below.

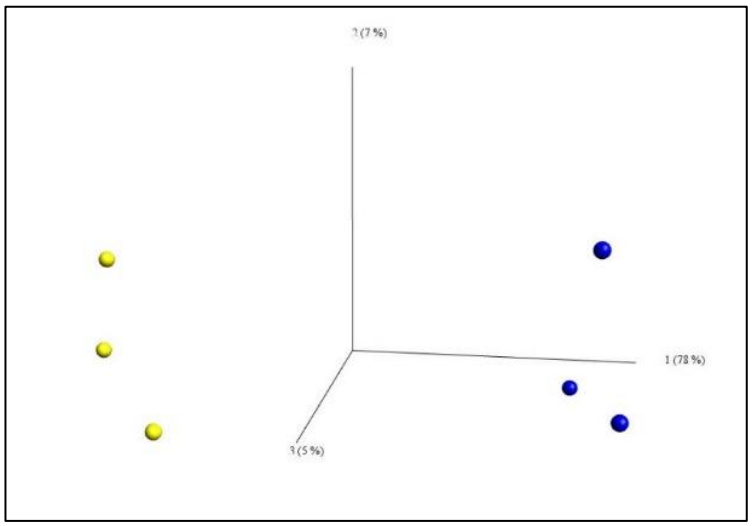

Figure 4.23: *Principal Component Analysis plot of nuclear MT vs. nuclear CON. Samples elucidate a good separation with a 78% separation between patients and controls clustering at the first principal component (PC1). (Blue = MT) & (Yellow = CON).*

Table 4.16: Functionally enriched biological processes generated by DAVID of the nuclear MT vs. nuclear CON differentially expressed genes. GO= Gene ontology, no.=number, ES= Enrichment score

GO	Biological process	Gene no.	P- value	ES
BP_FAT	Nuclear mRNA splicing via spliceosome	11	1.6E-4	4.79
BP_FAT	Regulation of translation	9	1.5E-3	2.31
BP_FAT	mRNA transport	6	1.2E-2	1.71
BP_FAT	Nucleosome organization	6	1.6E-2	1.34

4.6.2.1.1 Nuclear mRNA splicing via spliceosome

The majority of the RNA processing takes place in the nucleus and this involves RNA splicing, editing, 5' capping and polyadenylation. The analysis of nuclear MT vs. nuclear CON revealed an overall down-regulation of genes involved in mRNA splicing via the spliceosome (Table 4.17).

Three heterogeneous nuclear ribonucleoproteins were reduced. The heterogeneous nuclear ribonucleoprotein A0 (*HNRNPA0*) (FC=-1.2) which is involved in RNA splicing by its association with the HNRNP complexes (Myer and Steitz, 1995). Also, the heterogeneous nuclear ribonucleoprotein F (*HNRNPF*) was down-regulated (FC=-1.2). It is essential for proper splicing of pre-mRNA (Gamberi et al., 1997). Moreover, the heterogeneous nuclear ribonucleoprotein R (*HNRNPR*) was reduced (FC=-1.2). It is also involved in RNA processing and mainly hnRNA splicing. *HNRNPR* has been shown to interact with the *SMN* gene causing a disrupted splicing event in mouse model of spinal muscular atrophy (Rossoll et al., 2002).

A group of small nuclear ribonucleoproteins were down-regulated. The small nuclear ribonucleoprotein 40kDa (U5) (*SNRNP40*) is part of the U5 small nuclear ribonucleoprotein which is a component of the spliceosome complex. It facilitates the removal of intron sequences of nascent RNA. *SNRNP40* gene was reduced (FC=-1.2) (Achsel et al., 1998). In addition, three genes encoding for proteins belonging to the U2 ribonucleoprotein complex that were involved in pre-RNA splicing were down-regulated, the small nuclear ribonucleoprotein polypeptide B (*SNRPB2*) (FC=-1.2), the small nuclear ribonucleoprotein polypeptide E-like 1 (*SNRPE*) (FC=-1.3), and the PHD finger protein 5A (*PHF5A*) (FC=-1.2) (Habets et al., 1987, Hubert et al., 2013, Pasternack et al., 2013). The mago-nashi homolog, proliferation-associated (Drosophila) (*MAGOH*) was reduced (FC=-1.2). This gene encodes for the *MAGOH* protein which is a component of the exon junction complex (EJC). The EJC has a major role in determining the fate of the mRNA molecule towards either translation or degradation (Silver et al., 2010, Le Hir et al., 2016). Lastly, the tRNA splicing endonuclease 15 homolog (S. cerevisiae) (*TSEN15*) was also down-regulated (FC=-1.4). It encodes for the

enzyme tRNA splicing endonuclease which is involved in tRNA splicing (Paushkin et al., 2004).

Significant down-regulation of genes involved in mRNA splicing were shown in the nuclear fALS missense mutation (Figure 4.24). This may suggest that *TARDBP* missense mutation has a marked effect upon splicing regulation and it is likely to be less splicing occurring. Also, it may indicate that due to increased number of splicing alteration, these heterogeneous nuclear ribonucleoprotein and the small nuclear ribonucleoprotein are subjected to degradation within the nucleus. This observation might play a significant role in the disease process.

Table 4.17: Genes involved in nuclear mRNA splicing via spliceosome in the nuclear missense mutation

Gene symbol	Gene name	p-value	Fold change
HNRNPA0	Heterogeneous nuclear ribonucleoprotein A0	0.036	-1.24
HNRNPF	Heterogeneous nuclear ribonucleoprotein F	0.038	-1.24
HNRNPR	Heterogeneous nuclear ribonucleoprotein R	0.01	-1.23
MAGOH	Mago-nashi homolog, proliferation-associated (Drosophila)	0.032	-1.25
PHF5A	PHD finger protein 5A	0.005	-1.31
RPL36A	Ribosomal protein L36a pseudogene	0.036	-1.22
SNRNP40	Small nuclear ribonucleoprotein 40kDa (U5)	0.002	-1.23
SNRPB2	Small nuclear ribonucleoprotein polypeptide B	0.040	-1.24
*SNRPD1	Small nuclear ribonucleoprotein D1 polypeptide 16kDa, LOC100129492	0.049	-1.32
SNRPE	Small nuclear ribonucleoprotein polypeptide E-like 1	0.012	-1.36
*SNRPG	Similar to small nuclear ribonucleoprotein polypeptide G, HCG23490	0.038	-1.31
TSEN15	tRNA splicing endonuclease 15 homolog (S. cerevisiae)	0.048	-1.43

***Not accurately characterized yet*

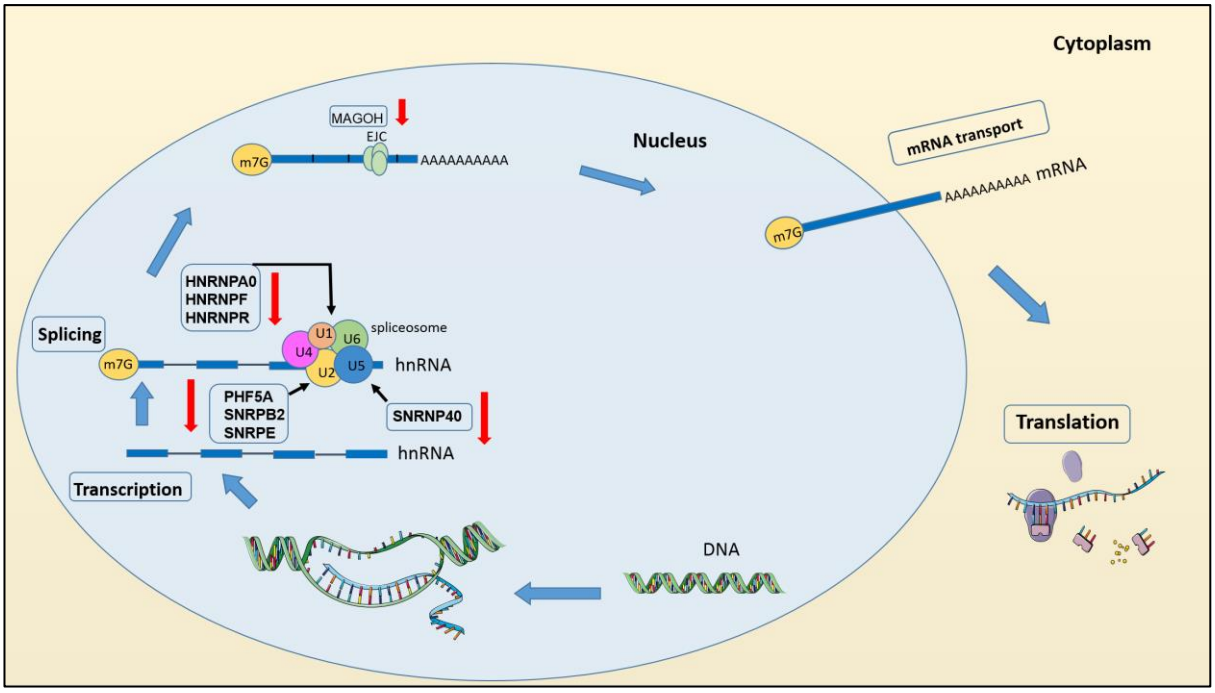

Figure 4.24: *A representative diagram showing the dysregulated RNA processing (splicing/ spliceosome) genes in fALS-TARDBP nuclear missense mutation.*

4.6.2.1.2 Regulation of translation

The central dogma that DNA is transcribed into RNA then translated into protein was established when the process of transcription and translation were discovered. It was believed that transcription took place in the nucleus and the translation machinery was located in the cytosol. Here it was shown that genes involved in the regulation of translation were dysregulated in the nuclear fALS missense mutation with the majority being down-regulated (Table 4.18).

The insulin-like growth factor 2 mRNA binding protein 3 (*IGF2BP3*) was reduced (FC=-1.9). It has been suggested that the encoded RNA binding protein binds to the Insulin-like growth factor 2 at the promotor region to repress its translation in adulthood (Nielsen et al., 1999, Jiang et al., 2006). Furthermore, the poly (A) binding protein interacting protein 2 (*PAIP2*) was down-regulated (FC=-1.2). This protein inhibits the translation process by interfering with the poly (A) binding protein (PABP) which is one of the essential molecules for translation (Khaleghpour et al., 2001). The quaking homolog, KH domain RNA binding (mouse) (*QKI*) was also reduced (FC=-1.2). It is an RNA binding protein that is involved in RNA splicing, transport and translation. In addition, it has been suggested previously that the decrease in *QKI* expression was associated with decreased oligodendrocyte-myelin genes in Schizophrenia (Lauriat et al., 2008). Moreover, the SAP domain containing ribonucleoprotein (*SARNP*) was down-regulated (FC=-1.3). *SARNP* is involved in transcription and RNA processing. It was shown that *SARNP* promotes cell proliferation (Fukuda et al., 2002). As previously mentioned, the mago-nashi homolog, proliferation-associated (Drosophila) (*MAGOH*) which is part of the EJC that controls mRNA fate in translation was also down-regulated (FC=-1.2) (Silver et al., 2010, Le Hir et al., 2016). In contrast, three genes were up-regulated. The amyloid beta (A4) precursor-like protein 1 (*APLP1*) was increased (FC=1.2). This gene encodes for the membrane bound glycoprotein which belongs to the amyloid precursor protein family. The *APLP1* was linked to Alzheimer's-like pathology (Guilarte, 2010). Moreover, the insulin-like growth factor binding protein 5 (*IGFBP5*) which is involved in the tyrosine kinase receptor pathway was significantly up-regulated (FC=4.6). The insulin-like growth factor 1 (IGF1) normally binds to Insulin-like

growth factor 1 receptor and activates the tyrosine kinase receptor pathway which promotes cell growth and proliferation. IGFBP5 binds to the Insulin-like growth factor 1 (IGF1) to inhibit its function (Mitsiades et al., 2004, Salih et al., 2004). Finally, the nanos homolog 1 (Drosophila) (*NANOS1*) which is considered a translation repressor that controls the germ line cell division was increased (FC=1.4) (Asaoka-Taguchi et al., 1999, Wang and Lin, 2004).

Genes involved in mRNA translation were dysregulated with the majority being down-regulated in fALS-*TARDBP* missense mutation (Figure 4.25). It is worth indicating that genes related to translation process are expected to be detected in the nucleus where their transcripts originally been synthesised. These transcripts are normally exported to the cytoplasm were translation takes place. However, low expression of group of genes related to translation machinery beyond normal levels may indicate a rapid turnover time of these transcripts. Also, perhaps these genes are expressed less in *TARDBP* mutation. Finally the possibility of the transcripts being degraded within the nucleus.

Table 4.18: Genes involved in the regulation of translation in the nuclear missense mutation

Gene symbol	Gene name	P-value	Fold change
APLP1	Amyloid beta (A4) precursor-like protein 1	0.008	1.26
GATC	Glutamyl-tRNA(Gln) amidotransferase, subunit C homolog (bacterial)	0.007	-1.23
IGF2BP3	Insulin-like growth factor 2 mRNA binding protein 3	0.04	-1.98
IGFBP5	Insulin-like growth factor binding protein 5	0.04	4.65
MAGOH	Mago-nashi homolog, proliferation-associated (Drosophila)	0.03	-1.25
NANOS1	Nanos homolog 1 (Drosophila)	0.006	1.40
PAIP2	Poly(A) binding protein interacting protein 2	0.002	-1.21
QKI	Quaking homolog, KH domain RNA binding (mouse)	0.008	-1.22
SARNP	SAP domain containing ribonucleoprotein	0.02	-1.34

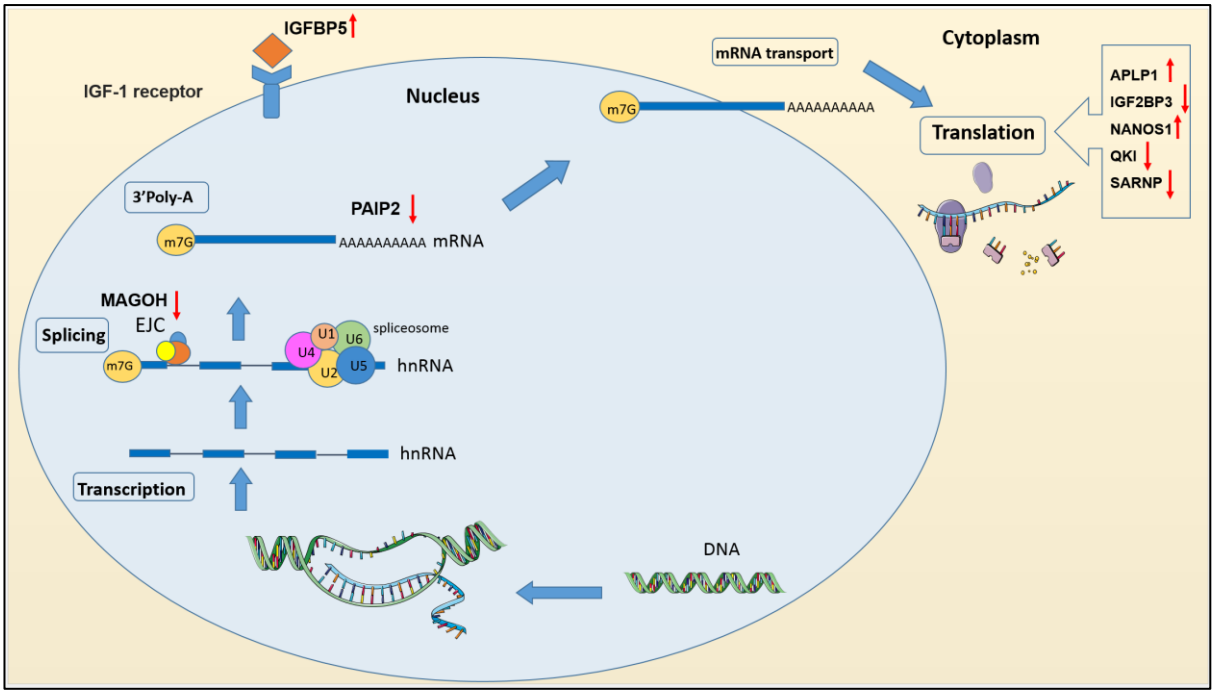

Figure 4.25: *A representative diagram showing the dysregulated genes involved in regulation of translation in fALS-TARDBP nuclear missense mutation.*

4.6.2.1.3 mRNA transport

After pre-mRNAs are transcribed and subjected to modification, mature mRNAs are generated. They are then bound to protein molecules which facilitate their transport from the nucleoplasm to the cytoplasm via the nuclear pores where they are subjected to either translation or degradation. Therefore, the main goal of mRNA synthesis is accomplished when a proper mRNA transport system is functioning within the cell (Vargas et al., 2005). TDP-43 is known to have a vital role in transporting mRNA molecules. Mutations in *TARDPB* may result in an impaired transport system. It has been shown that genes involved in mRNA transport were down-regulated (Table 4.19) and (Figure 4.26).

The mago-nashi homolog, proliferation-associated (Drosophila) (*MAGOH*) was down-regulated (FC=-1.2). It was demonstrated that *MAGOH* is involved in non-sense mediated decay and remains associated to mRNA after nuclear export (Gehring et al., 2009). Also, the mago-nashi homolog B (Drosophila) (*MAGOHB*) which has similar function to *MAGOH* was down-regulated (FC=-1.3). The DEAD (Asp-Glu-Ala-As) box polypeptide 19B (*DDX19B*) which belongs to the family of RNA helicases was reduced (FC=-1.2). The encoded protein is localized mainly at cytoplasmic side of nuclear pore (Linder and Jankowsky, 2011). The nucleoporin like 1 (*NUPL1*) gene was also reduced (FC=-1.3). It is part of the nuclear pore complex which is localized at the rim of the nucleus that facilitates molecule movement between the nucleus and the cytoplasm (Chug et al., 2015). As previously shown the quaking homolog, KH domain RNA binding (mouse) (*QKI*) which is involved in mRNA transport was also reduced (FC=-1.2) (Lauriat et al., 2008).

It appears that mRNA transport in fALS-*TARDBP* is impaired as a result of the mutation. It also may indicate that mRNA transcripts associated with these RNA binding proteins and hnRNPs are held in the nucleus as a result of impaired binding and export which may subject these transcripts to decay. This observation may also follow the previous observed down-regulation in translation.

Table 4.19: Genes involved in mRNA transport in the nuclear missense mutation

Gene symbol	Gene name	p-value	Fold change
DDX19B	DEAD (Asp-Glu-Ala-As) box polypeptide 19B	0.002	-1.25
MAGOHB	Mago-nashi homolog B (Drosophila)	0.04	-1.31
MAGOH	Mago-nashi homolog, proliferation-associated (Drosophila)	0.03	-1.25
NUPL1	Nucleoporin like 1	0.03	-1.31
QKI	Quaking homolog, KH domain RNA binding (mouse)	0.008	-1.22
*LOC728554	Similar to THO complex 3	0.03	-1.46

***Not accurately characterized yet*

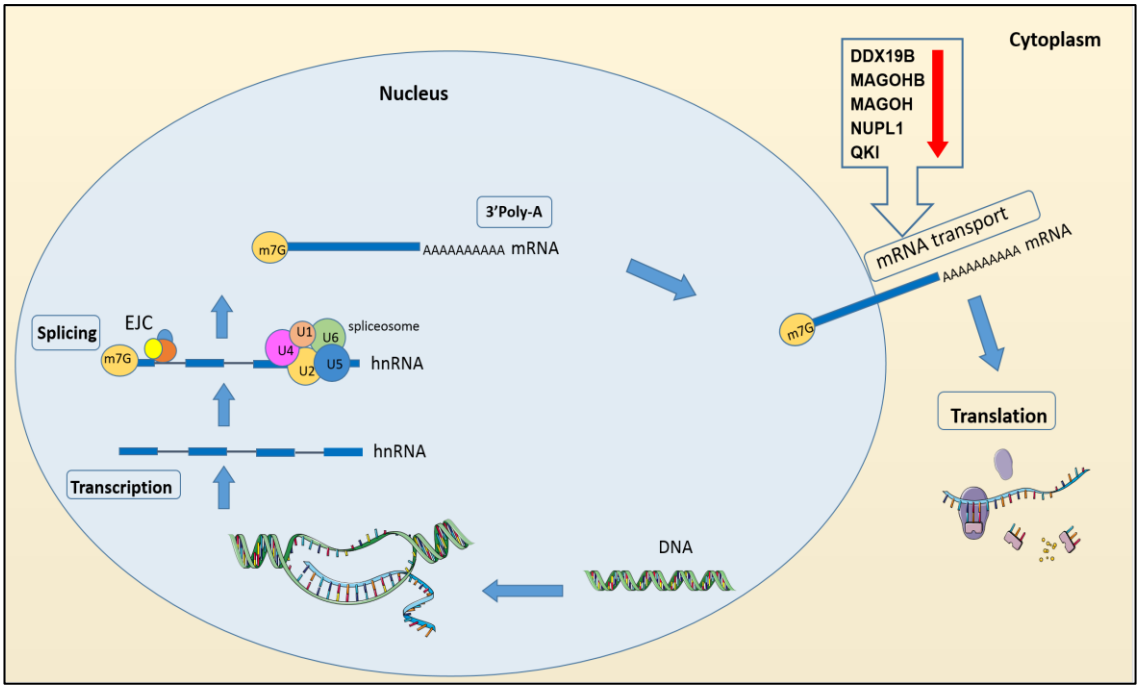

Figure 4.26: *A representative diagram showing the dysregulated genes involved in mRNA transport in fALS-TARDBP nuclear missense mutation.*

4.6.2.1.4 Nucleosome organization

Nucleosomes are unique molecular structures that are composed of approximately 200bp of DNA wrapped around histone molecules. These nucleosome units are built up to form the chromatin. Nucleosomes are known to be subjected to epigenetic modifications such as acetylation, methylation and phosphorylation which influence gene expression by enhancing or silencing the targeted gene. A group of genes involved in nucleosome organization were dysregulated with the majority down-regulated in fALS-*TARDBP* missense mutation (Table 4.20) and (Figure 4.27).

The ASF1 anti-silencing function 1 homolog A (S. cerevisiae) (*ASF1A*) was reduced (FC=-1.4). It participates in chromatin assembly during DNA replication and repair (Mello et al., 2002). Furthermore, the CCCTC-binding factor (zinc finger protein) (*CTCF*) was also down-regulated (FC=-1.3). The *CTCF* is a transcription insulator which regulates the DNA expression by creating a boundary between a silencer or an enhancer and the promotor region. Therefore, they are able to activate or repress gene expression (Jeong and Pfeifer, 2004). Three genes belonging to the core octamer histone structure that make up the nucleosome which are subjected to posttranscriptional modifications such as methylation were down-regulated, histone cluster 1, H4a (*HIST1H4A*), histone cluster 1, H4c (*HIST1H4C*) and histone cluster 2, H2ab (*HIST2H2AB*) (FC=-1.7, FC=-1.6 & FC=-1.8 respectively) (Marzluff et al., 2002). In addition, the H3 histone, family 3B (H3.3B) (*H3F3A*) was reduced (FC=-1.3). This is considered a H3 variant histone and also known as replacement histone which is essential for nucleosome assembly. It has a unique characteristic of being synthesised during any cell cycle phase and not restricted to the S phase (Tagami et al., 2004). Finally, the transition protein 1 (during histone to protamine replacement) (*TNP1*) which an essential protein for normal histone replacement with protamine during spermatogenesis was reduced (FC=-1.2) (Meistrich et al., 2003).

This suggests that nucleosome regulation is impaired in fALS-*TARDBP* missense mutation with the majority of genes being down-regulated. This may indicate a reduced DNA synthesis in fibroblasts which affects cell division and also DNA

repair. This also may explain the low growth rate of fALS-*TARDBP* fibroblasts in the laboratory.

Table 4.20: Nucleosome organization in the nuclear missense mutation

Gene symbol	Gene name	p-value	Fold change
ASF1A	ASF1 anti-silencing function 1 homolog A (S. cerevisiae)	0.03	-1.40
CTCF	CCCTC-binding factor (zinc finger protein)	0.04	-1.32
H3F3A	H3 histone, family 3B (H3.3B)	0.01	-1.35
HIST1H4A	Histone cluster 1, H4a	0.03	-1.74
HIST1H4C	Histone cluster 1, H4c	0.03	-1.67
HIST2H2AB	Histone cluster 2, H2ab	0.006	-1.84
TNP1	Transition protein 1 (during histone to protamine replacement)	0.02	1.24

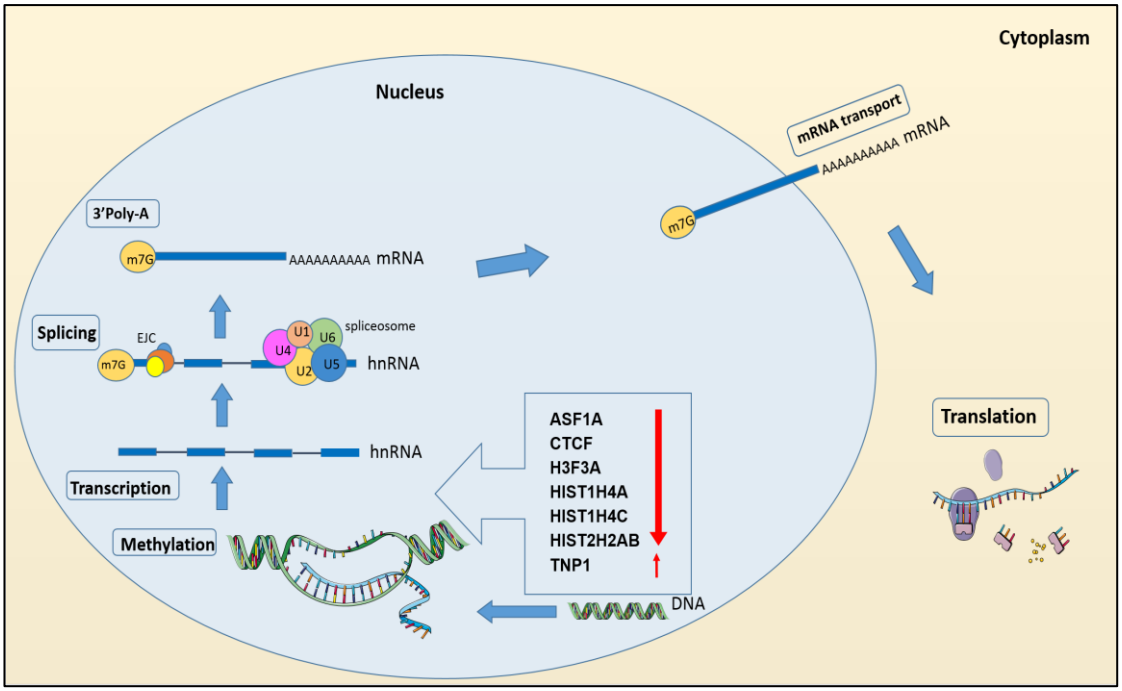

Figure 4.27: *A representative diagram showing the dysregulated genes involved in nucleosome organization in fALS-TARDBP nuclear missense mutation.*

4.6.2.2 Differential gene expression of nuclear TT vs. CON

PCA of nuclear TT vs. nuclear CON was carried out and showed a good separation of clusters between patients and controls (Figure 4.28). Differentially expressed genes were explored using DAVID. The significant enriched biological process was the G-protein coupled receptor protein signalling pathway (Table 4.21). A full description of the genes involved were described below.

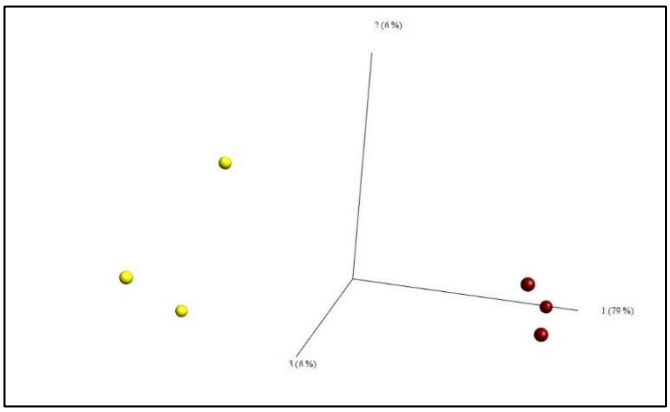

Figure 4.28: *Principal Component Analysis plot of nuclear TT vs. nuclear CON. Samples reveal a good separation with a 79% variability between patients and controls clustering at the first principal component (PC1). (Red = TT) & (Yellow = CON).*

Table 4.21: Functionally enriched biological process generated by DAVID of the nuclear TT vs. CON differentially expressed genes

Gene ontology	Biological process	Number of genes	P-value	Enrichment Score
BP_FAT	G-protein coupled receptor protein signaling pathway	30	3.7E-3	1.72

4.6.2.2.1 G-protein coupled receptor protein signalling pathway

G-protein coupled receptors are a large group of protein receptors that are expressed on the most cells. They have a common seven-transmembrane domain structure that bind to ligands causing a conformational change in the receptor structure which triggers signal transductions via the activation of G-proteins. Ligands for these receptors are a wide range of molecules such as: hormones, neurotransmitters and odours (Venkatakrishnan et al., 2013). A large number of G-protein coupled receptors were down-regulated in nuclear fALS-*TARDBP* truncated mutation (Table 4.22). A further elucidation of these genes is shown below.

The 5-hydroxytryptamine (serotonin) receptor 6 (*HTR6*) was reduced (FC=-1.2). The encoded protein is a receptor that binds the neurotransmitter serotonin which is able to activate the cAMP pathway by activating adenylate cyclase through the G-proteins (Wacker et al., 2013). Furthermore, the melanocortin 3 receptor (*MC3R*) was also reduced (FC=-1.3). The melanocortin hormone binds to the MC3R which activates the cAMP through the G-protein activation (Lee et al., 2001). Also, the cholinergic receptor, muscarinic 4 (*CHRM4*) was reduced (FC=-1.5). CHRM4 receptor was shown to bind to acetylcholine which is known to be involved in potassium channel activation (Ockenga et al., 2013). The glycine receptor, beta (*GLRB*) was down-regulated (FC=-1.5). *GLRB* is activated by several molecules including amino acids and has a role in inhibiting postsynaptic neurons. Mutation in the *GLRB* is associated with hyperekplexia (Rees et al., 2002).

The G protein-coupled receptor 3 (*GPR3*) was also down-regulated (FC=-1.2). It was shown that *GPR3* acts as a cell cycle inhibitor for oocytic meiosis, the inactivation of *GPR3* gene allows the resumption of the cell cycle. Therefore it was suggested to play a role in cell cycle arrest in oocyte (Mehlmann et al., 2004). Moreover, the chemokine (C-C motif) receptor 9 (*CCR9*) was down-regulated (FC=-1.2). *CCR9* has been suggested to activate chemokines shown to play vital role in thymocyte migration (Zabel et al., 1999).

The opiate receptor-like 1 (*OPRL1*) was reduced (FC=-1.2). It is the receptor of the nociception ligand. *OPRL1* is expressed in several areas in the brain which are responsible for learning and motivation (Mollereau and Mouledous, 2000). It was shown that *OPRL1* has a negative effect on adenylyl cyclase by etorphine and an inhibitory effect on Ca++ ion channels (Mollereau et al., 1994, Beedle et al., 2004). Furthermore, the sphingosine-1-phosphate receptor 4 (*S1PR4*) was down-regulated (FC=-1.3). *S1PR4* is a member of the sphingosine-1-phosphate receptor family which activate a plethora of pathways. S1PR4 is the receptor for the lysosphingolipid sphingosine 1-phosphate (S1P). The activation of the S1PR4 was suggested to activate Ca++ ion mobility (Villullas et al., 2003).

Furthermore, the taste receptor, type 2, member 39 (*TAS2R39*) which was recently shown to be involved in the recognition of bitterness taste of some substances such as theaflavins and soy isoflavones was reduced (FC=-1.2) (Roland et al., 2011, Yamazaki et al., 2014). The purinergic receptor P2Y, G-protein coupled, 8 (*P2RY8*) which may be involved in the purinergic signalling was also down-regulated (FC=-1.2) (Fields and Burnstock, 2006). The MAS-related GPR, member G (*MRGPRG*) was reduced (FC=-1.2). It is characterized as an itch receptor which is stimulated by some drugs like chloroquine. Administrating chloroquine to *MRGPRG* deficient mice did not cause a skin itchiness reaction. Therefore, it was suggested to be an itch receptor (Liu et al., 2009).

A large group of olfactory receptor family that belong to the G-protein coupled receptor 1 family were down-regulated. Olfactory receptor family genes were also showed to be dysregulated in the cytoplasmic missense mutation MT (see section 4.6.1.1.4). The olfactory receptor, family 10, subfamily G, member 7 (*OR10G7*) (FC=-1.2), olfactory receptor, family 10, subfamily G, member 9 (*OR10G9*) (FC=-1.2), olfactory receptor, family 2, subfamily A, member 12 (*OR2A12*) (FC=-1.2), olfactory receptor, family 2, subfamily A, member 4; olfactory receptor, family 2, subfamily A, member 7 (*OR2A4*) (FC=-1.3), olfactory receptor, family 4, subfamily C, member 5 (*OR4C5*) (FC=-1.3), olfactory receptor, family 4, subfamily M, member 2 (*OR4M2*) (FC=-1.2), olfactory receptor, family 4, subfamily N, member 2; seven transmembrane helix receptor (*OR4N2*) (FC=-1.2), olfactory receptor,

family 4, subfamily P, member 4 (*OR4P4*) (FC=-1.2), olfactory receptor, family 5, subfamily L, member 2 (*OR5L2*) (FC=-1.2), olfactory receptor, family 51, subfamily S, member 1 (*OR51S1*) (FC=-1.2), olfactory receptor, family 52, subfamily L, member 1(*OR52L1*) (FC=-1.2), olfactory receptor, family 6, subfamily C, member 4 (*OR6C4*) (FC=-1.2), olfactory receptor, family 6, subfamily C, member 70 (*OR6C70*) (FC=-1.2), olfactory receptor, family 8, subfamily J, member 1 (*OR8J1*) (FC=-1.2) and vomeronasal 1 receptor 2 (*VN1R2*) (FC=-1.3) (Young and Trask, 2002, Shirokova et al., 2008).

Moreover, the basic helix-loop-helix family, member a15 (*BHLHA15*) was down-regulated (FC=-1.2). It is also known as *Mist1* which is a transcription factor that binds to enhancer box (E-box) regions on DNA to regulate gene expression (Lemercier et al., 1997). The potassium channels, subfamily K, member 2 (*KCNK2*) was down-regulated (FC=-1.2) (Meadows et al., 2000). Potassium channels are important structures that maintain the membrane action potential. The prolactin releasing hormone (*PRLH*) was reduced (FC=-1.2). Prolactin releasing hormone (*PRLH*) stimulates the anterior pituitary gland to release the prolactin hormone which has a direct effect in binding to receptors on the mammary glands and ovaries (Yoshimura et al., 1994, Hinuma et al., 1998). Finally, the opsin 3 (*OPN3*) is an encephalic photoreception which convert the photons into signals that activate vision cascades was increased (FC=1.2) (Tarttelin et al., 2012).

The data showed that there is a significant overall down-regulation in G-protein coupled receptors in fALS-*TARDBP* truncated mutation and were mainly found in relation to the cAMP pathway and diverse chemoreceptors.

Table 4.22: Genes involved in the G-protein coupled receptor protein signalling pathway in nuclear truncation mutation

Gene symbol	Gene name	P-value	Fold change
BHLHA15	Basic helix-loop-helix family, member a15	0.04	-1.21
CCR9	Chemokine (C-C motif) receptor 9	0.03	-1.21
CHRM4	Cholinergic receptor, muscarinic 4	0.01	-1.50
GLRB	Glycine receptor, beta	0.01	-1.50
GPR3	G protein-coupled receptor 3	0.03	-1.27
HTR6	5-hydroxytryptamine (serotonin) receptor 6	0.02	-1.25
MC3R	Melanocortin 3 receptor	0.01	-1.33
MRGPRG	MAS-related GPR, member G	0.002	-1.23
KCNK2	Potassium channel, subfamily K, member 2	0.03	-1.27
OR10G7	Olfactory receptor, family 10, subfamily G, member 7	0.02	-1.21
OR10G9	Olfactory receptor, family 10, subfamily G, member 9	0.01	-1.24
OR2A12	Olfactory receptor, family 2, subfamily A, member 12	0.01	-1.21
OR2A4	Olfactory receptor, family 2, subfamily A, member 4; olfactory receptor, family 2, subfamily A, member 7	0.02	-1.30
OR4C5	Olfactory receptor, family 4, subfamily C, member 5	0.02	-1.35
OR4M2	Olfactory receptor, family 4, subfamily M, member 2	0.04	-1.23
OR4N2	Olfactory receptor, family 4, subfamily N, member 2; seven transmembrane helix receptor	0.0001	-1.20
OR4P4	Olfactory receptor, family 4, subfamily P, member 4	0.01	-1.23
OR5L2	Olfactory receptor, family 5, subfamily L, member 2	0.04	-1.24
OR51S1	Olfactory receptor, family 51, subfamily S, member 1	0.009	-1.24
OR52L1	Olfactory receptor, family 52, subfamily L, member 1	0.02	-1.23
OR6C4	Olfactory receptor, family 6, subfamily C, member 4	0.02	-1.22
OR6C70	Olfactory receptor, family 6, subfamily C, member 70	0.04	-1.25
OR8J1	Olfactory receptor, family 8, subfamily J, member 1	0.001	-1.22
OPN3	Opsin 3	0.01	1.24
OPRL1	Opiate receptor-like 1	0.004	-1.26
PRLH	Prolactin releasing hormone	0.03	-1.22
P2RY8	Purinergic receptor P2Y, G-protein coupled, 8	0.006	-1.23
S1PR4	Sphingosine-1-phosphate receptor 4	0.04	-1.31
TAS2R39	Taste receptor, type 2, member 39	0.005	-1.27
VN1R2	Vomeronasal 1 receptor 2	0.009	-1.39

4.6.2.3 Comparative analysis of differentially expressed genes in the nuclear fractions of missense and truncation *TARDBP* mutation

The identification of differentially expressed genes associated with each type of mutation was also applied to the nuclear comparison study. As previously the GeneVenn software was used. The venn diagram showed 529 differentially expressed were specific to the nuclear MT, 658 differentially expressed genes were specific to the nuclear TT and 23 genes were found common in both. It important to clarify that after generating the venn diagram of four genes from the nuclear TT gene list were missing. After investigating the gene lists it was shown that *ARL17A* gene was present in the data as five repeats. Therefore, the software pooled the repeated copies as one gene (Figure 4.29). DAVID online software showed that the highest enriched pathway of the missense mutation MT in the nuclear fraction belonged to mRNA processing and the truncated mutation TT were mostly involved in G-protein coupled receptor signalling pathway (enrichment score of 4.98 and 1.95 respectively). The common genes were: *ARL17A, GABPB1-AS1, KIRREL3, TEX2* and *THY1* (Table 4.23). The other genes were pseudogenes and not annotated gene (NULL). The common nuclear genes did not belong to any significant biological process.

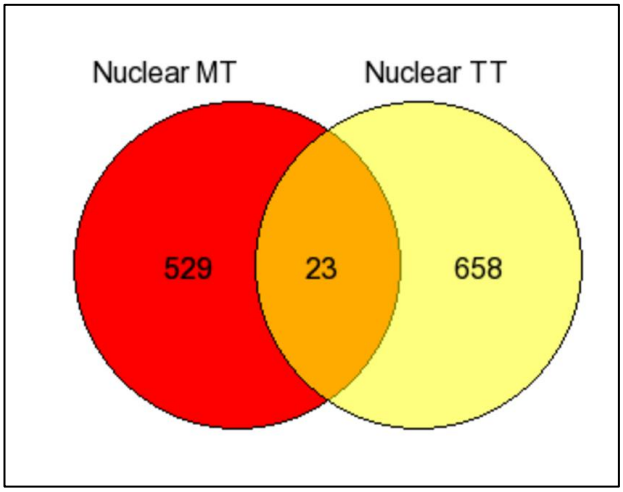

Figure 4.29: *Comparative analysis of differentially expressed genes in the nuclear fractions of missense and truncation TARDBP mutation. Venn diagram showing 529 genes specific to the nuclear missense mutation, 658 genes specific to the nuclear truncation mutation and 23 genes were found common in both types of mutations.*

Table 4.23: Common genes in missense MT and truncation mutation TT. FC= fold change

Gene Symbol	Gene Title	FC MT	FC TT
ARL17A	ADP-ribosylation factor-like 17A	1.71	1.47
CASP7	NULL /// caspase 7, apoptosis-related cysteine peptidase	-1.21	-1.21
ENOSF1	NULL /// enolase superfamily member 1	-1.29	-1.22
FAM215A	Family with sequence similarity 215, member A (non-protein coding) /// NULL	1.26	1.46
GABPB1-AS1	GABPB1 antisense RNA 1	-1.20	-1.24
GS1-5L10.1	NULL /// NULL	1.22	1.55
KIRREL3	Kin of IRRE like 3 (Drosophila)	1.33	1.23
MRPL24	NULL /// mitochondrial ribosomal protein L24	-1.30	-1.23
NEK7	NIMA-related kinase 7 /// NULL	1.25	1.35
NREP	NULL /// neuronal regeneration related protein	-1.32	-1.42
OTTHUMG00000019246	NULL	1.32	1.33
RNA5SP302	RNA, 5S ribosomal pseudogene 302	1.31	1.30
RNU4-10P	RNA, U4 small nuclear 10, pseudogene	1.20	1.25
RNU4-5P	RNA, U4 small nuclear 5, pseudogene	1.38	1.27
RNY1P8	RNA, Ro-associated Y1 pseudogene 8	1.23	1.45
RPL35A	NULL /// ribosomal protein L35a	-1.26	-1.23
RPS3AP47	Ribosomal protein S3a pseudogene 47	-1.39	-1.20
SEC23A	NULL /// Sec23 homolog A (S. cerevisiae)	-1.26	-1.25
SNRPEP4	Small nuclear ribonucleoprotein polypeptide E pseudogene 4	-1.42	-1.31
TEX2	Testis expressed 2	1.37	1.30
THY1	Thy-1 cell surface antigen	1.59	1.36
TMEM78	NULL /// transmembrane protein 78	1.29	1.28
WDFY3-AS1	NULL /// WDFY3 antisense RNA 1	1.31	1.76

NULL= not annotated gene, NULL/// gene name= not accurately annotated yet.

4.6.2.4 Comparative analysis of differentially expressed genes in the cytoplasmic vs. nuclear in missense mutation and truncation mutation

The identification of differentially expressed genes associated with cellular component within each type of mutation was also applied. As previously, the GeneVenn software was used and the following observations were found: 190 genes were specific to the cytoplasmic MT while 518 genes were specific to the nuclear MT and 34 common (Figure 4.30) and 334 genes were specific to the cytoplasmic TT while 597 genes were specific to the nuclear and 81 genes were in common (Figure 4.31).

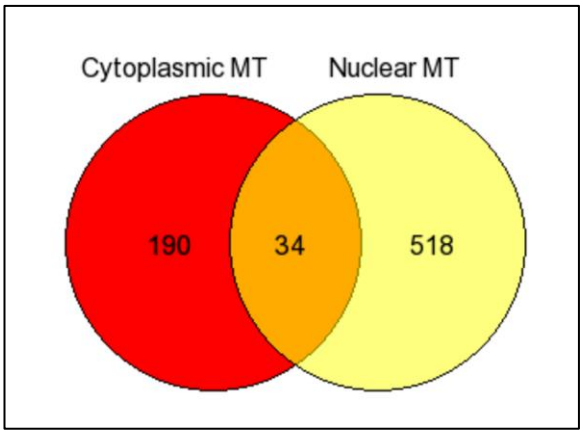

Figure 4.30: *Comparative analysis of differentially expressed genes in the cytoplasmic vs. nuclear in TARDBP missense mutation. Venn diagram showing 190 genes specific to the cytoplasmic missense mutation, 518 genes specific to the nuclear missense mutation and 34 genes were found common in both.*

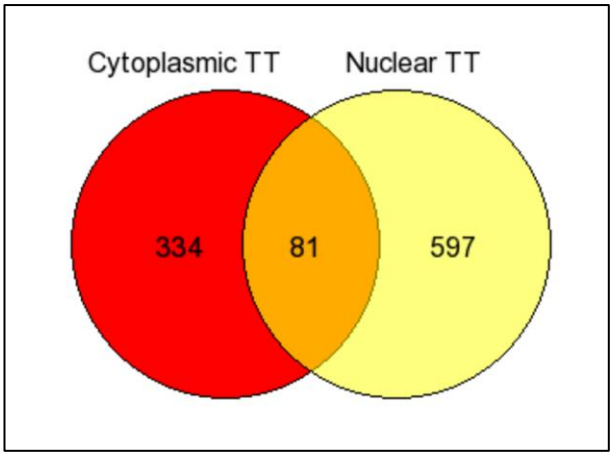

Figure 4.31: *Comparative analysis of differentially expressed genes in the cytoplasmic vs. nuclear in TARDBP truncation mutation. Venn diagram showing 334 genes specific to the cytoplasmic truncation mutation, 597 genes specific to the nuclear truncation mutation and 81 genes were found common in both.*

4.7 qRT-PCR validation of the fALS-*TARDBP* cytoplasmic MT and cytoplasmic TT genes

Candidate genes were chosen for validation using the same RNA material used in the HTA. In addition, the Q-RCR was performed using the prime time qRT-PCR method which is different to that of the Human Exon 1.0 ST Array qRT-PCR validation method (See section 2.9.3).

To validate the cytoplasmic MT and cytoplasmic TT gene changes by qRT-PCR, two candidate from the fALS cytoplasmic MT genes involved in RNA processing were selected which were the following: *ADARB1* (FC=1.6 and p-value=0.009) and *METTL1* (FC= -1.23 and a p-value=0.04). In addition, candidate from the fALS cytoplasmic TT genes were selected from both angiogenesis and adherens junction genes which were the following: *SEMA5A* (FC=1.6 and p-value=0.01) and *ENAH* (FC=-1.5 and p-value= 0.002). All genes were normalized against the housekeeping gene β-actin, as the expression of β-actin was consistent in all

samples. An unpaired t-test was applied *using Graph Pad Prism*. qRT-PCR of *ADARB1* confirmed the directional change of gene expression (up-regulation). In addition, qRT-PCR of *ENAH* also confirmed the directional change of gene expression (down-regulation). However, neither showed statistical significance. *METTL1* and *SEMA5A* did not show any noticeable changes between ALS samples. (Figure 4.32 A&B, Figure 4.33A&B).

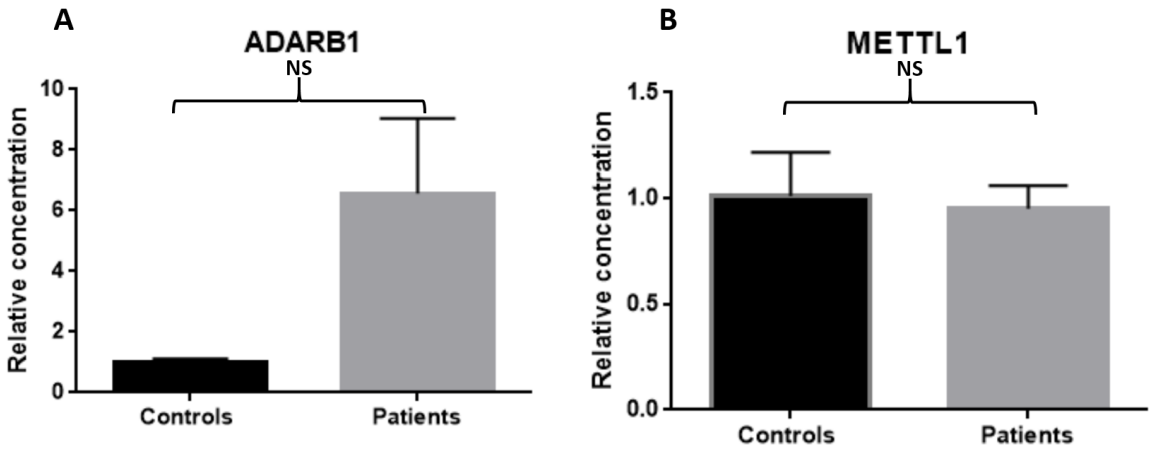

Figure 4.32: *qRT-PCR validation of the RNA processing cytoplasmic genes in fALS MT fibroblasts. (A)The relative expression of the ADARB1 gene. The statistical analysis showed insignificant p-value (p-value = 0.0869) with significant increase of ADARB1 gene expression (confirmed directional change) (B) The relative expression of the METTL1 gene. The statistical analysis also showed insignificant (p-value= 0.7572) with no significant difference METTL1 gene expression. (MT= missense mutation, NS= not significant, the error bars represents the SEM).*

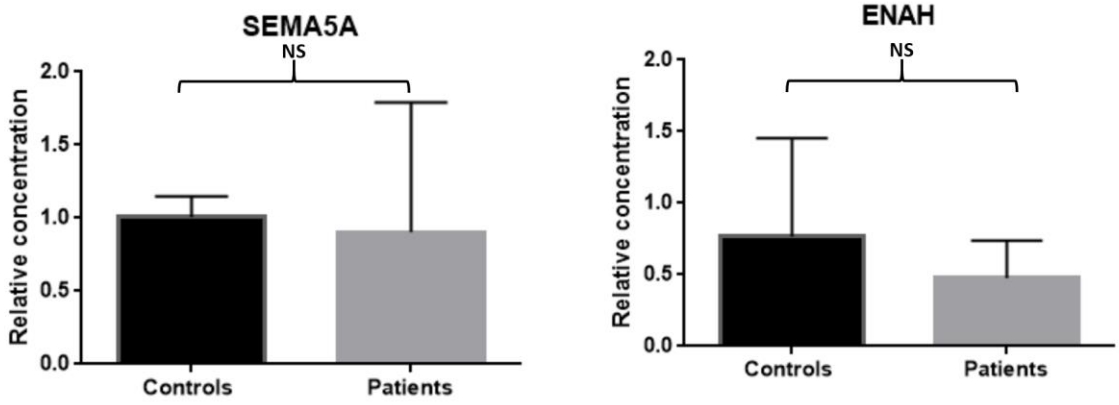

Figure 4.33: *qRT-PCR validation of the angiogenesis and adherens junction cytoplasmic genes in fALS TT fibroblasts. (A)The relative expression of the SEMA5A gene. The statistical analysis showed insignificant p-value (p-value = 0.8883) with no difference of SEMA5A gene expression, (B) The relative expression of the ENAH gene. The statistical analysis also showed insignificant (p-value= 0.6333) with significant decrease ENAH gene expression (confirmed directional change). (TT= truncated mutation, NS= not significant, the error bars represents the SEM).*

4.8 Fluorescence in situ hybridization of fALS nuclear controls, missense mutation and truncated mutation

Fluorescence in situ hybridization (FISH) is a powerful technique that reveals the location of nucleic acid inside the cell using a designed complementary labelled probe (see section 2.11 for the method).

A preliminary experiment was performed aiming to validate nuclear genes expressed in the fALS-*TARDBP* missense mutation and truncated mutation. Due to the overall low fold changes observed in the HTA data, the nuclear gene lists were investigated manually in order to pick genes with a relatively high fold change, high signal intensity and a significant p-value. This was applied to enable their visual detection using the confocal microscope. From the nuclear missense mutation matrix metalloproteinase-1 (*MMP1)* was selected (FC= 4.0, p-value= 0.03, signal intensity was high=8.4) and from the nuclear truncated mutation LUC7 like 3 pre-MRNA splicing factor (*LUC7L3)* was selected (FC= 2.0, p-value= 0.01, signal intensity was high=7.4). RNA U6 small nuclear 1 (*RNU6-1)* was used as a positive control and was the recommended gene by the manufacturer and had been designed and optimized specifically for nuclear FISH experiments.

The nuclear FISH experiment was performed twice. Unfortunately, both experiments failed to show any positive signals (Figure 4.34, 4.35 and 4.36). Although, probes were stated to be optimized by the manufacture against several tissue types including skin tissue, individual probes should have been optimized for fibroblasts which was not performed. This was due to limited reagent supply and limited time remaining for the current lab work.

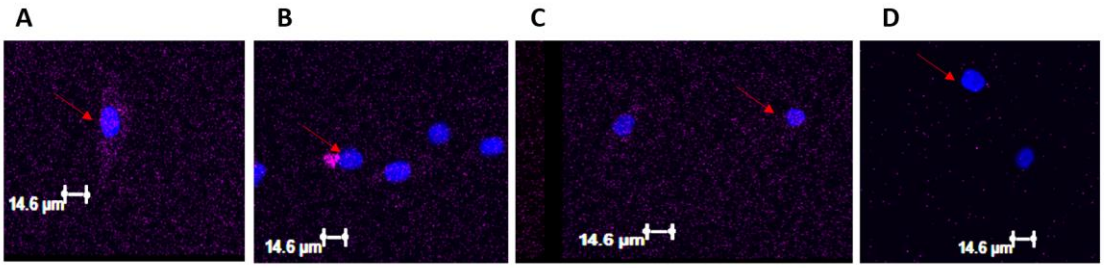

Figure 4.34: *FISH of fALS-TARDBP and control using RNU6-1 probe labelled Cy5 (filter=650nm) (A) Control (control155) showing negative detection of RNU6-1 in the nuclei. (B) fALS-TARDBP missense mutation (patient 48) showing negative detection of RNU6-1 in the nuclei. (C) fALS-TARDBP truncated mutation (patient 192) showing negative detection of RNU6-1 in the nuclei. (D) Negative control (control 155) negative detection of RNU6-1 in the nuclei. The red arrows point to nuclei.*

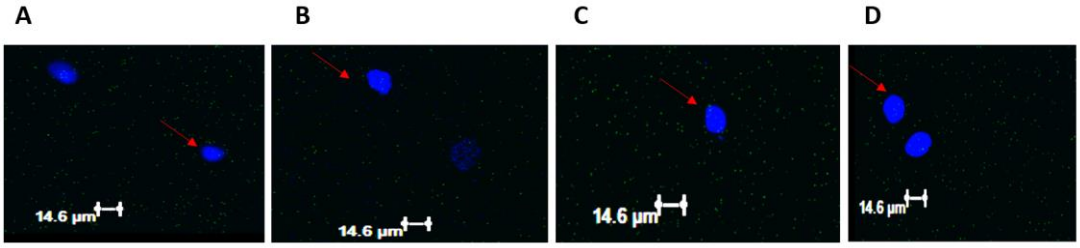

Figure 4.35: *FISH of fALS-TARDBP and control using MMP1 probe labelled FITC (filter=488nm) (A) Control (control155) showing negative detection of MMP1 1 in the nuclei. (B) fALS-TARDBP missense mutation (patient 48) showing negative detection of MMP1 in the nuclei. (C) fALS-TARDBP truncated mutation (patient 192) showing negative detection of MMP1 in the nuclei. (D) Negative control (patient 48) negative detection of MMP1 in the nuclei. The red arrows point to nuclei.*

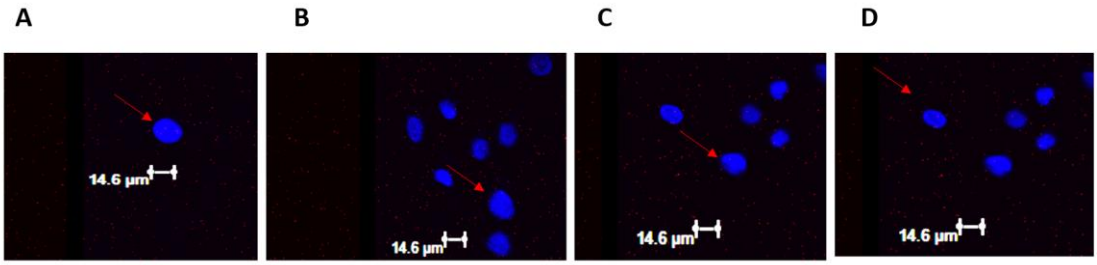

Figure 4.36: *FISH of fALS-TARDBP and control using LUC7L3 probe labelled Cy3 (filter=550nm) (A) Control (control155) showing negative detection of LUC7L3 in the nuclei. (B) fALS-TARDBP missense mutation (patient 48) showing negative detection of LUC7L3 in the nuclei. (C) fALS-TARDBP truncated mutation (patient 192) showing negative detection of LUC7L3 in the nuclei. (D) Negative control (patient 192) negative detection of LUC7L3 in the nuclei. The red arrows point to nuclei.*

4.9 Discussion

ALS is known to be a multisystem disorder and influenced by genetic and environmental factors. The current study aimed to identify the affected biological processes in two types of fALS-*TARDBP* mutations, the missense mutation and the truncation mutation. This approach has the potential to highlight possible common causes of ALS pathology which could then be targeted for therapy. In this experiment the nuclear and cytoplasmic separation method was modified in order to achieve a confident degree of separation of the two compartments. Cell membrane lysis was monitored throughout the separation step to ensure intact nuclear isolation prior to RNA extraction. In addition the RNA extraction was performed using the Trizol method. The nuclear isolation method was challenging, nevertheless it was performed successfully and clear images of intact nuclei ware obtained from control, missense mutation and truncated mutation fibroblasts. This was in agreement with an earlier study by Wang et., al who demonstrated isolated nuclei from mouse embryo fibroblasts with minimum cytoplasmic or perinuclear material (Wang et al., 2006). In addition, a high degree of RNA quality and quantity was reached. The electropherograms illustrated distinct peaks of rRNA 28s and rRNA 18s with the level of rRNA 28s were approximately twice the level of rRNA 18s suggesting full length transcripts. Furthermore, the RIN values from the extracted RNA were high ($\geq$ 8).

Although in the current work there was a minimum genomic DNA contamination in the cytoplasmic fraction, it would be helpful to perform western blots in future using cytoplasmic and nuclear markers as an additional evidence to support the cellular separation method.

This study was designed to demonstrate the possibility that dysregulated biological processes exist in the cytoplasm and the nucleus of fALS-*TARDBP* missense mutations and truncated mutations. Thus, three biological repeats from patients and age and gender matched controls were used. The Qlucore Omics Explorer software was utilized to identify the most significant differentially expressed genes in both mutation types. Grouping these genes into biological

processes was achieved using the DAVID analysis tool. Figure 4.37 shows diagram that illustrates the significantly identified biological processes in a single glance. Angiogenesis and cell adhesion/ adherens junction biological processes were present in both cytoplasmic fALS-*TARDBP* mutations and therefore will be discussed together. However, the rest of the biological processes will be discussed separately in respect to each type of mutation and cellular compartment.

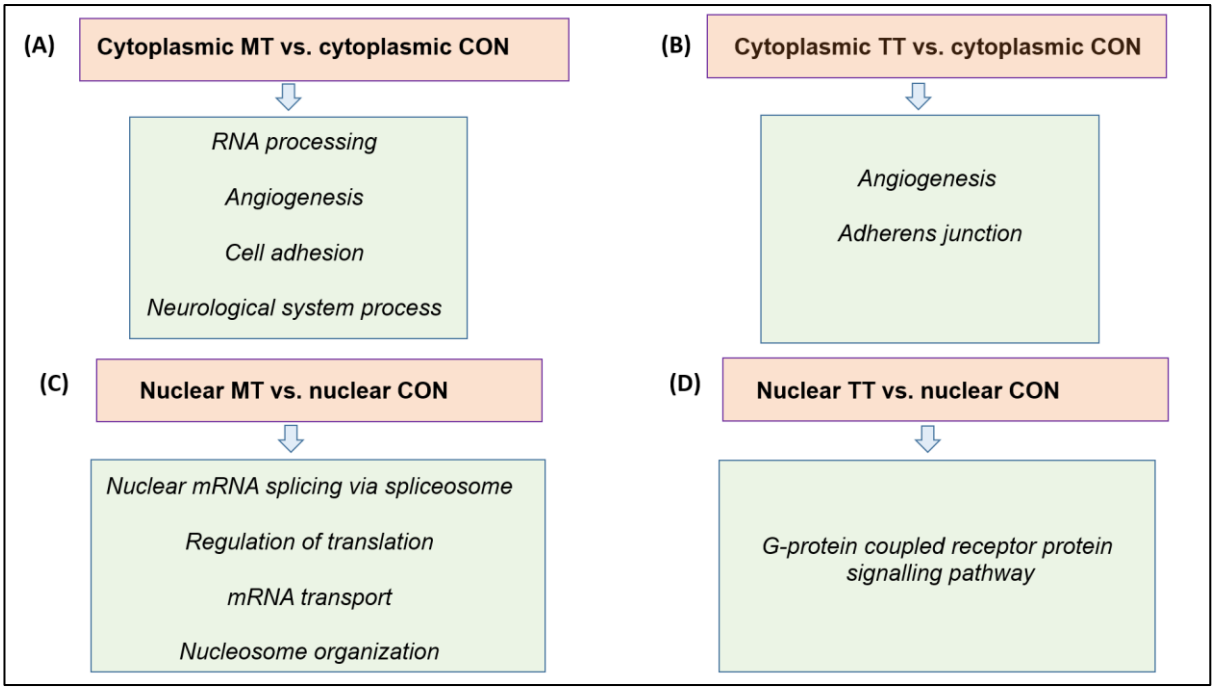

Figure 4.37: *Schematic diagram demonstrate significantly identified biological processes. (A) cytoplasmic fALS MT, (B) cytoplasmic fALS TT, (C) nuclear fALS MT and (D) nuclear fALS TT. fALS= familial amyotrophic lateral sclerosis, MT= missense mutation, TT=truncated mutation.*

4.9.1 Biological processes presented in both cytoplasmic fALS-*TARDBP* MT and TT mutations

4.9.1.1 Angiogenesis

VEGF was the first angiogenic factor that was shown to be associated with ALS. The depletion of *VEGF* in mouse model showed low levels of *VEGF* in brain and spinal cord associated with symptoms strongly linked to an ALS type disorder (Oosthuyse et al., 2001). In addition, mutations in angiogenin (*ANG*) have been associated with ALS (Greenway et al., 2006). *ANG* is known to be involved in endothelial cell proliferation, migration, synthesis of new blood vessels and enhancement of rRNA transcription. It was also shown to promote neuronal cell survival by neurovascular perfusion (Gao and Xu, 2008). In the current study, both mutations showed that angiogenesis was affected in the disease process although not all genes were shared by both. Most of these genes were involved in cell proliferation, differentiation and normal development of vessel walls. Four genes involved in angiogenesis were slightly elevated in fALS-*TARDBP* missense mutation than controls*, EDNRA, IL18, KLF5* and *TGFA.* This may indicate the fALS-*TARDBP* missense mutation may generate a relatively higher activity of angiogenesis than normal. The fALS-*TARDBP* truncated mutation also included a number of up-regulated differentially expressed genes. *MEOX2*, which is involved in vascular differentiation, was up-regulated. This observation was in contrast to *MEOX2* expression in Alzheimer's disease which showed low levels of expression (Wu et al., 2005). Furthermore, TBX1 which is involved in arterial development was increased. It was shown previously that *TBX1-/-* mice model showed a phenotype similar to DiGeorge syndrome which showed neurological abnormalities therefore, was suggested to be associated with the syndrome. In addition, it was proposed that patients with DiGeorge syndrome were at a higher risk for developing schizophrenia and early onset PD (Zinkstok and van Amelsvoort, 2005, Butcher et al., 2013). These observations illustrate that a process involving genes associated with angiogenesis is associated with fALS-*TARDBP.*

4.9.1.2 Cell adhesion/ adherens junction

Cell adhesion is a vital process that maintains cell integrity, structure, and protection against pathogens (Gumbiner, 1996). Cell adhesion molecules are important for normal cell development and migration. Also, they have a vital role in stimulating immune cell interactions (Mackay and Imhof, 1993). Defects in cell adhesion molecules were linked to several neurological diseases such as, AD which is characterized by mutations in the amyloid precursor protein (APP) and ALS which demonstrated decreased expression of plasma fibronectin (Ono et al., 2000, Liu et al., 2012). Also, mutant *SOD1*^{G93A} transgenic mice showed a significant low expression of adhesion molecules such as, gap junction protein, delta 2, 36 kDa (*GJD2*) and protocadherin beta 9 (*PCDHB9*) (Boutahar et al., 2011). Moreover, NSC34$^{SOD1\text{-}G93A}$ transfected cell lines showed low expression of the adhesion molecule, laminin, alpha 4 (*LAMA4*) (Kirby et al., 2005). In the current work fibroblasts from both the cytoplasmic missense mutation and truncated mutations showed several dysregulated adhesion molecule genes. In the fALS-*TARDBP* missense mutation four genes were up-regulated *CD9, PCDHB15, PECAM1* and *TMEM8A,* and four genes were down-regulated: *CDH2, TNFAIP6* and *TROAP.* On the other hand, the majority of fALS-*TARDBP* truncated mutation genes were reduced: *ARHGAP24, ARHGAP31, ENAH, TENC1, TLN1* and *TLN2* with only two increased; *LMO7* and *MPP7*.

Since adhesion molecules play an important role in immune responses, it was suggested that they may contribute to the occurrence of neuroinflammation in ALS patients. Neuroinflammation is the inflammation of the CNS that is triggered by factors including infections, toxins or brain injury. Studies have shown the involvement of neuroinflammation in the ALS disease process (Engelhardt and Appel, 1990, Hall et al., 1998, Alexianu et al., 2001). The development of an immune response was shown to occur at the early stage of the disease and is considered a protective immune response which then worsens to a progressive neurotoxic condition (Hooten et al., 2015). Microglial activation was shown in patients and also in the mutant *SOD1* ^{G93A} transgenic mouse which demonstrated a progressive course of the disease due to rapid neuroinflammation rather than the progression of neuronal death (Hall et al., 1998, Corcia et al., 2012). An

elevated level of proinflammatory factors such as CD3 and the intercellular adhesion molecule-1 were reported in the mutant *SOD1*^{G93A} transgenic mouse (Alexianu et al., 2001). It has been reported in ALS that activated astrocytes release soluble mediators such as IL-6, chemokine (C-C) motif ligand 2, (CCL2) and C-X-C motif chemokine 10 (CXCL10) (Farina et al., 2007, Philips and Robberecht, 2011). Also, tumour necrosis factor activated pathways (TNF) were shown to be significantly involved in ALS (Brohawn et al., 2016). These observations in the current work, along with the published literature, therefore suggest that the adhesion molecules may participate in the pathogenesis of ALS which may offer a therapeutic target to slow the progression of the disease.

4.9.2 Cytoplasmic MT vs. CON

4.9.2.1 RNA processing

Evidence on the dysregulation of RNA processing in ALS is growing in the field. Current literature shows a number of defective RNA processing genes associated with ALS. Mutations in the RNA processing genes, *TARDBP, FUS, C9ORF72, MATR3*, *hnRNPA1, ANG, SETX* and *ELP* have all been linked to ALS pathogenesis with *SMN2* being a risk factor for ALS (Sreedharan et al., 2008, Van Deerlin et al., 2008, Corcia et al., 2009, Kwiatkowski et al., 2009, Simpson et al., 2009b, Avemaria et al., 2011, Aparicio-Erriu and Prehn, 2012, Kim et al., 2013, Johnson et al., 2014, Scotter et al., 2015). Therefore, dysregulation of RNA metabolism could be a promising target for therapy. A group of RNA processing genes were dysregulated in the fALS-*TARDBP* missense mutation. Dysregulated RNA splicing and the spliceosomal components have previously been suggested to be associated with ALS and FTLD (Tollervey et al., 2011, Highley et al., 2014). In the current study genes involved in RNA splicing were down-regulated, *U2AF1L4* and *SNRPA*. The reduction in *SNRPA* expression was in agreement with an earlier study profiling sporadic ALS fibroblasts (Raman et al., 2015).

Furthermore, the *METTL1* gene that regulates DNA methylation as a posttranscriptional modification step was also reduced. The literature is scarce in studies relating methylation with fALS. Although, a single gene belonging to methylation was dysregulated, this observation along with the Human Exon Arrays result (section 3.6.1.1.1) suggest that the fALS-*TARDBP* missense mutation may be linked to hypomethylation that may lead to increased level of transcriptional activity in cells. Moreover, *ADARB1* which encodes for the RNA editing enzyme responsible for GluR2 editing was increased. This observation was also shown in Human Exon Arrays result (3.6.1.1.3.3). It is clearly shown that RNA processing and methylation are dysregulated in fALS-*TARDBP*.

4.9.2.2 Neurological system process

A group of genes involved in the neurological system which belonged to different biological processes were identified however, all were related to the CNS. Genes involved in cell adhesion (CD9), exocytosis (*RIMS1),* neuronal differentiation (*LHX8),* the BARK signalling pathway (*ARRB1)* and olfactory receptors (*OR4D10, OR5H1, OR5R1, OR51B4* and *OR52J3)* were elevated with the exception of (*OR1G1)* which was reduced. It was interesting and surprising to find a group of olfactory receptors expressed in a fibroblast model. A recent study has shown that human keratinocytes express chemoreceptors of which the majority are olfactory receptors (Busse et al., 2014). This may explain the presence of olfactory receptors in the data.

Neurotransmitters are chemical molecules that control signalling in the brain. Exocytosis is the process that facilitates the release of these chemical molecules from the presynaptic neuron into the synaptic cleft via vesicle-membrane fusion. As a result postsynaptic neuron activation occurs. Defects in glutamate receptors, glutamate uptake or release leads to disrupted signalling in the brain. This has been demonstrated in several neurological diseases such as ALS, AD and epilepsy (Hynd et al., 2004, Van den Bosch et al., 2006, Cho, 2013). One of the known causative agents in ALS is excitotoxicity which results from elevated glutamate in the synaptic cleft which leads to impaired Ca++ ions influx and neuronal death. This is proposed to be due to defects in the glutamate receptors (Ferraiuolo et al., 2011).

Controlled exocytosis and neurotransmitters levels are essential functions for normal brain signalling. Thus, increased exocytosis could lead to imbalance of neurotransmitter release leading to ALS pathology. Although, a single gene involved in exocytosis was up-regulated in this current work (*RIMS1)* and there is no current evidence of its association with ALS. This may indicate that elevated levels of neurotransmitter such as glutamate could be due to increased exocytosis which may contribute to the disease pathogenesis. Lastly, The *ARRB1* was shown to have a desensitization effect on the beta-adrenergic receptor kinase (BARK) signalling pathway and this gene was up-regulated. This

may indicate dysregulated BARK signalling pathway in fALS-*TARDBP* (Lohse et al., 1990). These observations strongly indicate that *TARDBP* missense mutation has a multiple biological effects which confirms the diversity of ALS aetiology.

4.9.3 Nuclear MT vs. CON

4.9.3.1 Nuclear mRNA splicing via spliceosome

In the current work, evidences of the association of dysregulated RNA processing with fALS-*TARDBP* missense mutation is apparent. This was previously highlighted as a significantly dysregulated biological process in the missense mutation in both cellular comparisons (see chapter 3, sections 3.6.1.1.3 and 3.6.2.1.3).

Nuclear MT vs. nuclear CON showed that the most significantly enriched biological process was nuclear mRNA splicing. Aberrant hnRNA splicing mechanism has been previously implicated in ALS (Rabin et al., 2010, Highley et al., 2014, Raman et al., 2015). Here, several genes related to hnRNA splicing were down-regulated. Heterogeneous nuclear ribonucleoproteins were decreased, including *HNRNPA0, HNRNPF* and *HNRNPR* which indicate a decreased potential for splicing events. The *HNRNPR* gene has previously been shown to also disrupt the *SMN* splicing pattern in a spinal muscular atrophy mouse model (Rossoll et al., 2002). A mutated *SMN2* gene was suggested to be a risk factor for ALS. Thus, from Rossoll et al., it is suggested that decreased levels of *HNRNPR* in the nuclear missense mutation may have an impact on lowering *SMN2* gene expression in fALS-*TARDBP* and therefore increase the risk of the disease. Furthermore, small nuclear ribonucleoproteins which are involved in hnRNA splicing were also down-regulated *SNRNP40, SNRPB2 and SNRPE. SNRPB2* gene expression was, as indicated above, in agreement with Highley et al., in which they suggested a dysfunctional spliceosomal component in ALS (Highley et al., 2014). Moreover, the U2 small nuclear ribonucleoproteins complex component *PHF5A,* the EJC protein MAGOH and the tRNA splicing enzyme TSEN15 were also down-regulated. These observations strongly support

the association of dysregulated mRNA processing in fALS-*TARDBP* missense mutation and could be a favourable area for further study and a possible therapeutic target.

4.9.3.2 Regulation of translation

Protein synthesis is a fundamental process to maintain cell viability. For the synthesis of a polypeptide the following cellular molecules are required: ribosomes, messenger RNA (mRNA) and aminoacylation of transfer RNA (tRNA). These molecules are found significantly and actively in the cytoplasm. However, several studies challenged that mRNA translation is a unique process in the cytoplasm and can also occur in the nucleus (Iborra et al., 2001, Brogna et al., 2002, Iborra et al., 2004). In the present work, three genes involved in translation inhibition were reduced, *IGF2BP3, NANOS1* and *PAIP2* suggesting elevated levels of translation. The *QKI* gene involved in RNA metabolism including translation was also reduced. Lauriat et al., suggested that reduced *QKI* might be associate with decreased oligodendrocyte-myelin in schizophrenia (Lauriat et al., 2008). Furthermore, as discussed earlier, genes involved in RNA processing were reduced (*MAGOH* and *SARNP).* Also, the *IGFBP5* gene was increased which acts as tyrosine kinase receptor pathway inhibitor. Therefore, increased levels of *IGFBP5* in fALS-*TARDBP* may suggest low cell growth and proliferation rate as a result of tyrosine kinase receptor pathway inhibition. *IGFBP5* was also suggested to co-express with the Six5 gene which is known to be linked to myotonic dystrophy-1 (Sato et al., 2002). The significant increase of *IGFBP5* gene may strongly suggest its association with fALS-*TARDBP.* Furthermore, *APLP1* which was suggested to be associated with Alzheimer's like pathology due to manganese exposure was also shown to be elevated in fALS-*TARDBP.*

4.9.3.3 mRNA transport

TDP-43 is a shuttling protein which is involved in mRNA transport from the nucleus to the cytoplasm where translation or degradation takes place (Buratti

and Baralle, 2010). Therefore, it is suggested that defects in TDP-43 possibly lead to low expression of its associated mRNA molecules and also may result in lower expression of other genes involved in the transport system within the cell. This was observed in the current work, as a group of gene involved in mRNA transport were reduced, *DDX19B, MAGOHB, MAGOH, NUPL1* and *QKI.* Although the number of genes involved in mRNA transport were low, this still may indicate a disrupted mRNA transport system in fALS-*TARDBP.* As this was not reported before, it is possibly a novel underlying aetiology in fALS-*TARDBP*.

4.9.3.4 Nucleosome organization

Nucleosomes are known molecular units that are subjected to epigenetic changes, such as: methylation, acetylation and phosphorylation which have an impact on gene expression. In the present work, it was shown that a group of histone family of genes expression were reduced in fALS-*TARDBP* missense mutation, *H3F3A, HIST1H4A, HIST1H4C* and *HIST2H2AB.* Affected DNA methylation was suggested to be associated with sALS and might impact upon histone expression (Martin and Wong, 2013). Furthermore, AD was also shown to be associated with reduced acetylation which led to reduced histone synthesis (Zhang et al., 2012). Also, hypomethylation was suggested in PD patients (Feng et al., 2015). Other genes that regulate chromatin assembly and gene expression were reduced, *ASF1A* and *CTCF.* Epigenetic modifications in fALS-*TARDBP* were also suggested in the Human Exon Array 1.0 ST chapter (*section 3.8.1.1*). Here it is shown that histone molecule synthesis was down-regulated. It suggests that epigenetic modifications on histones may contribute to the disease process.

4.9.4 Nuclear TT vs. CON

4.9.4.1 G-protein coupled receptor protein signalling pathway

Signal transduction pathways are methods of cellular communications through cell membrane receptors. Stimulation of the receptors activates a series of molecular interactions know as cascades as a response to the bound ligand.

There are two types of ligands activators and inhibitors. Signal transduction pathways controls diverse cellular processes such as cell proliferation, growth, migration and apoptosis (Venkatakrishnan et al., 2013). G-protein coupled receptors are a type of receptors that share a common characteristic which is to activate G-proteins at the early stage of the signal transduction pathway. Defective G-protein coupled receptor protein signalling has been associated with several diseases such as cancer, neuromuscular disorders and autism (Rojas Walh, 2007, Heng et al., 2013, Kanazawa et al., 2015). In ALS dysfunctional G-protein coupled receptor e.g. metabotropic glutamates receptor was associated with the disease pathogenesis (Aizawa et al., 2010).

Glutamate is the main neurotransmitter in neuronal excitation. One-way of activating the glutamate receptors is the binding of glutamate to the postsynaptic neuron after presynaptic depolarization this activates intracellular G-proteins which activate series of molecule which ends by ion channel opening. Therefore, dysfunctional glutamate receptor activity can lead to neuronal excitotoxicity (Heath and Shaw, 2002). In addition, defective G-protein coupled receptors, dopamine and metabotropic glutamate receptors were associated with PD (Jenkins et al., 2016). Furthermore, using gene expression profiling several G-protein coupled receptors have been associated with AD (Zhao et al., 2016).

In this current work a large number of G-protein coupled receptors were down-regulated in the nuclear fALS-*TARDBP* truncated mutation samples. The cAMP activators (*HTR6* and *MC3R)* and cAMP inhibitor *OPRL1* were reduced. A large number of receptors related to sensation were also decreased, the itch receptor *MRGPRG*, purinergic receptor *P2RY8* and taste receptor*, TAS2R39.* Studies showed that ALS patients score low in olfactory test which may suggested low expression of olfactory receptors (Elian, 1991, Doty, 2012). In the present work, a significant number of olfactory receptors were reduced *OR10G7*, *OR10G9*, *OR2A12*, *OR2A4*, *OR4C5*, *OR4M2*, *OR4N2*, *OR4P4*, *OR5L2*, *OR51S1*, *OR52L1*, *OR6C4*, *OR6C70*, *OR8J1* and *VN1R2* in fALS-*TARDBP* truncation mutation.

Moreover, genes involved in cell cycle arrest, *GPR3,* cell migration, *CCR9* and potassium ion channel*, KCNK2* were reduced. Furthermore, the neurotransmitter

inhibitor, *GLRB* was down-regulated. Mutation in this gene was associated with hyperekplexia which is characterized by stiffness of voluntary muscles and excessive startle reaction (Rees et al., 2002). The transcription factor *BHLHA15* was down-regulated. Also, the *PRLH* was reduced. The data shows a marked reduction of the G-protein coupled receptor proteins affected by the fALS-*TARDPB* truncated mutation. It would be interesting to investigate the downstream effect of these G-protein coupled receptor proteins which might be a scope for therapeutic targets.

4.10 Gene expression validation

Gene expression studies require validation steps to confirm the results of the arrays. Two methods were used to validate the HTA data. The cytoplasmic genes were validated using qPCR while the nuclear genes were attempted to validate by a new approach which was FISH.

4.10.1 qRT-PCR fALS cytoplasmic MT and cytoplasmic TT genes validation

From the fALS-*TARDBP* missense mutation only *ADARB1* confirmed the directional change of expression compared to the HTA outcome. However, the *METTL1* gene expression did not show any difference. Similarly, in fALS-*TARDBP* the truncated mutation samples, the directional change of *ENAH* was confirmed while the *SEMA5A* gene did not show any difference. However, the two genes showing a directional change in correlation with that of the HTA data did not show a statistical significant result. This observation might be due to the low fold changes that were generally seen in the data (Fold changes: *ADARB1= 1.6, METTL1= -1.2, ENAH =-1.5 and SEMA5A = 1.6*). Therefore, it was difficult to demonstrate the change in gene expression. However, by comparing the results generated from the Human exon arrays 1.0 ST with the HTA it was obvious that the fALS-*TARDBP* showed some similar biological process. The reproducibility of similar outcomes by different microarray GeneChips® may be

suggested as a method of validation of the current results to an extent. This was shown in the *ADARB1* gene*,* it was up-regulated in both Human exon arrays 1.0 ST and HTA cytoplasmic fALS-*TARDBP* missense mutation (FC=1.9, p-value=0.03 and FC=1.6, p-value=0.009 respectively). None of the other differentially expressed cytoplasmic fALS-*TARDBP* genes within the RNA processing were shared with the Human exon arrays. However, in the nuclear fALS-*TARDBP* missense mutation*, SNRPB/B2* gene, was shared with the Human exon 1.0 ST arrays nuclear fraction.

4.10.2 Fluorescence in situ hybridization of fALS nuclear controls, missense mutation and truncated mutation

As mentioned previously, FISH is a powerful technique that can aid in the localization of RNA molecules within the cell using designed complementary labelled probes (see section 2.11 for the method). In the present work, a preliminary experiment was performed aiming to validate nuclear genes expressed in both types of fALS-*TARDBP* mutation. Although the experiment was attempted twice, both failed to show positive results. The reasons behind that could be improper optimization of individual probes which was necessary prior to the actual testing. Optimization would set the threshold concentrations required of each probes, set the actual time needed for fibroblast permeabilization and also can suggest any faulty manufacture design of probes or reagents. The experiments were carried out towards the end of the available time in the laboratory and hence were not carried out with the usual levels of integrity. There was not enough time, or finances, to carry out further experiments.

4.11 The overall effect of the *TARDBP* mutation on the biological processes in fALS using the HTA

ALS is a complex neurodegenerative disorder caused by several underlying aetiologies and therefore is considered a multifactorial disorder though patients

present with progressive muscle wasting with symptoms varying according to the muscle groups affected. However, it is proposed that patients go through a similar disease process. The literature shows that in ALS-*TARDBP* studies that aimed to investigate the possible affected pathways, researchers do not always differentiate between the mutation types, assuming that the effects of mutations are the same. However, the current work showed that cytoplasmic fALS-*TARDBP* missense mutation were presented with defective RNA processing in the form of RNA editing, mRNA polyadenylation and splicing via spliceosome complex. However, the truncated mutation showed angiogenesis to be the most affected biological process.

The nuclear fALS-*TARDBP* missense mutation also demonstrated that RNA processing was the most affected pathway, while the nuclear truncated mutation showed the G-protein coupled receptor signalling pathway to be affected. This current work strongly suggests that different types of fALS-*TARDBP* mutations may affect different underlying biological processes and this should be in consideration when developing targeted treatments for fALS-*TARDBP* patients.

Furthermore, gene expression profiling using microarray GeneChips® has shown to be effective in identifying gene signature biomarkers that might help in stratifying disease types. Also, in identifying prognostic biomarkers, this may help monitoring disease progression and predict survival. The present work shows that distinct dysregulated genes were shown in different fALS-*TARDBP* mutation types.

4.12 Comparative analysis of differently expressed genes in the cytoplasm vs. nucleus in both missense mutation and truncated

A comparative analysis of differently expressed genes in the cytoplasm and the nucleus was performed as shown previously in section 4.6.2.4. It was shown that there is a significant number of differentially expressed nuclear genes in both mutation types. ~71% of the total identified transcripts in the missense mutation

were found in the nuclear component and ~62% of the total transcripts identified in the truncation mutation were from the nucleus. Only ~4% from the total transcripts identified in the missense mutation were common in both cellular components and ~7% from the total transcripts identified in the truncated mutation were common in both cellular components. This indicates that the number of shared genes is low.

It is worth noting that this initial comparative study demonstrate the possible effect of the *TARDBP* mutation on the disease process. The large number of genes in the nuclear fraction in both mutation types may suggest that there are significant number of transcripts being synthesised in the nucleus however, they do not reach their final destination i.e. the cytoplasm. These might be faulty transcripts or spliced transcripts as a result of *TARDBP* mutation and therefore were held in the nucleus and subjected to degradation. Another possible reason is the loss of TDP-43 functional role in mRNA transport due to the *TARDBP* mutation and therefore these transcripts are being also held in the nucleus.

This observation strongly supports that mutant *TARDBP* disrupts the RNA processing mechanism in the fALS. However, further analysis of this comparative study remain to be established. Also, due to time constraint alternative splicing analysis was not performed in the current work.

However, due to the low levels of gene expression changes using both the Human Exon 1.0 ST arrays and the newly designed HTA it was proposed to study the gene expression of fALS-*TARDBP* using RNA sequencing since this has been purported to provide a more robust analysis. An experimental design was established for RNA sequencing which was applied on the cytoplasmic fALS-*TARDBP* missense mutation and the truncation mutation (see chapter 5).

Chapter 5: Next generation sequencing (RNA sequencing)

5.1 Next generation sequencing (RNA sequencing)

In this work, RNA sequencing technology was chosen to study the effect of *TARDBP* mutation on the disease process in only the cytoplasmic fractions of both *TARDBP* mutations (refer to section 1.1.6.4 for RNA sequencing technology). This allows the identification of an underlying biological process and pathways affected in fALS-*TARDBP*. Also comparing the data outcome of the sequencing with the microarrays results from the previous experiments i.e. chapter 3: Human Exon Arrays 1.0 ST and chapter 4: Human Transcriptome Arrays may highlight the identification of specific dysregulated biological processes in each type of mutation.

5.2 Sample preparation and quality control

In this experiment cDNA libraries from the cytoplasmic fALS-*TARDBP* missense mutation (n=3) MT, fALS-*TARDBP* truncated mutation TT (n=3) and controls (n=4) were prepared for RNA sequencing as described in (section 2.10). The peak distribution of the fragmented DNA libraries was expected to be ~ 300bp. This was achieved efficiently as shown in (Figure 5.1). Two samples of the fALS-*TARDBP* truncated mutation had the lowest concentration; patient 192 and 194. However, the required total cDNA concentration in each library was 10nM. cDNA libraries were kept in a final volume of 25µl of water thus the total cDNA library concentration of patient 192 and 194 were 60nM and 62.5nM receptively which was sufficient and were taken forward to be sequenced (Table 5.1).

The Sequence Analysis Viewer Software from Illumina assessed the quality control of the run. The quality control output graphs generated by the software offered essential quality control checks of the data accuracy and reliability. These include an overall accuracy of the library preparation, base calling, variant calling and read alignment. The most well-known metric that is measured is the Phred quality score (Q score). The Q-score can be defined as the predicted probability value of a base sequence call being incorrect. The higher the Q-score the most

likely base calling error is low. Table 5.2 summaries the Q-scores and the corresponding predicted base calling error. The results showed a Q30=90.6% of all libraries (Figure 5.2)

The cluster density and passing filter box plot was generated to assess how optimal the reads were. The cluster density and the passing filter showed a good overlapping which indicate a low base call error (Figure 5.3 lane 6 & 7). The signal intensity of the bases are shown in (Figure 5.4). The bases were visualised at high intensity levels at the beginning of the sequencing procedure where the first strand DNA is sequenced however at cycle 50 a loss of the signals occurred due to laser energy drop. At the 100 cycle the second strand DNA is sequenced where more chemical material is added to boost the synthesis cycle.

The bioinformatics analysis was performed in collaboration with Dr Wenbin Wei/ Professor Winston Hide group. The RNA sequencing was paired end reads. The Illumina sequencer generated the bcl files which then were converted to fastq files by bcl2fastq program. The fastq files were then aligned to the GRCh37 human genome using bcbio's star aligner. The reads were counted using the feature Counts. The total number of reads, mapped reads and the percentage of mapped reads of the cytoplasmic samples are shown in table (http://bcbionextgen.readthedocs.io/en/latest/contents/introduction.html)

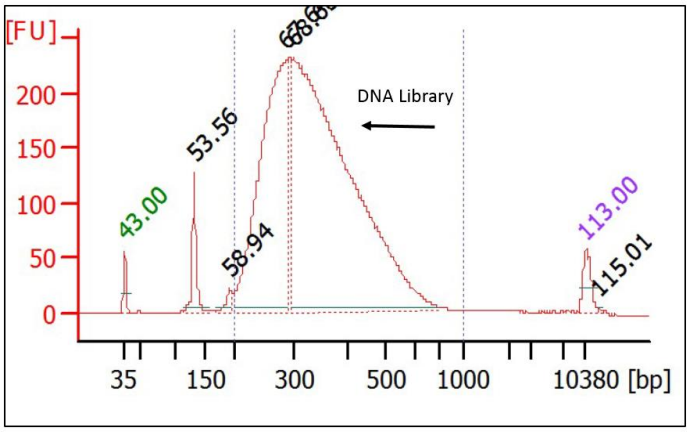

Figure 5.1. ***:*** *Representative electropherogram of a DNA library preparation. The peak point can be assessed to be approximately 300 bp in length as expected for the libraries.*

Table 5.1: DNA library concentration. FU= fluorescence unite, nmol/µl= nanomole/microliter, nM=nanomoles.

Sample type	Mutation type	Sample	Qubit (FU)	nM
Cytoplasmic	None	Con 2303	3.72	16.35164835
		Con 155	8.43	37.05495
		Con 170	1.95	8.571429
		Con 159	2.67	11.73626
	Missense	Pat 48	7.44	32.7033
		Pat 51	2.91	12.79121
		Pat 55	1.03	4.527473
	Truncated	Pat 192	0.546	2.4
		Pat 193	1.4	6.153846
		Pat 194	0.586	2.575824
Nuclear	None	Con 2303	4.28	18.81319
		Con 155	2.13	9.362637
		Con 170	3.83	16.83516
		Con 159	1.11	4.879121
	Missense	Pat 48	5.08	22.32967
		Pat 51	4.52	19.86813
		Pat 55	4.66	20.48352
	Truncated	Pat 192	3.09	13.58242
		Pat 193	1.8	7.912088
		Pat 194	3.65	16.04396

Table 5.2: Phred Quality scoring

Phred Quality Score (Q-score)	Predicted base calling error	Base calling accuracy %
Q 10	1 in 10	90
Q 20	1 in 100	99
Q 30	1 in 1000	99.9
Q 40	1 in 10,000	99.99
Q 50	1 in 100,000	99.999

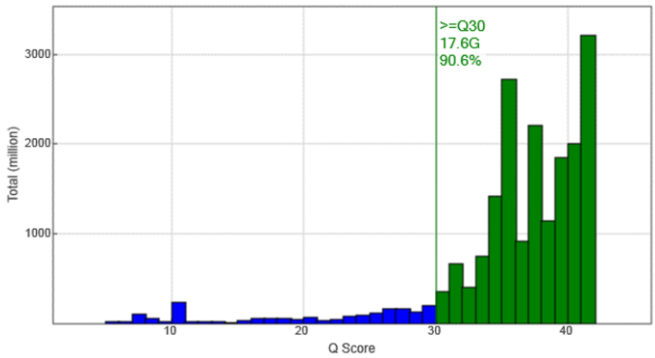

Figure 5.2: *Illumina Hi scan SQ system generated the Q-score of the overall libraries (the Q30= 90.6%).*

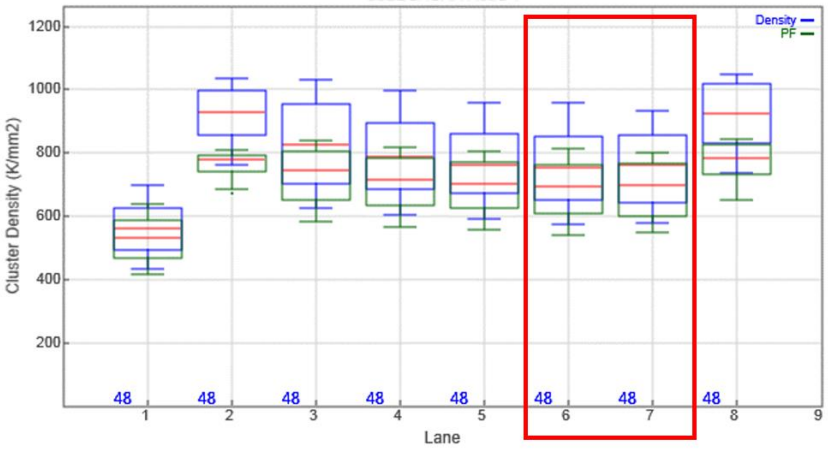

Figure 5.3: *Cluster density and passing filter box plot quality control. The (X) axis represents the lanes 1-8. The Y axis represents the cluster density. The image shows the cluster density and passing filter for the 8 lanes. The samples were loaded on lane 6 and 7 (10 samples in each lane). The blue box is the density cluster box, the green box is the passing filter box and the red line is the median. The density and the passing filter boxes are overlapping which indicate that they are optimal.*

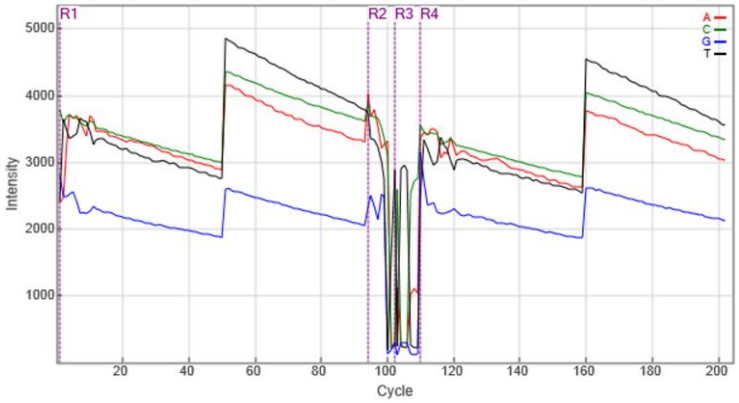

Figure 5.4: *The signal intensity of the bases of the 8 lanes. The (X) axis is the number of synthesis cycles and the (Y) axis is the signal intensity. Bases are coloured differently for easy identification. The bases was maintained at a high levels at the beginning of the sequencing procedure where the first strand DNA is sequenced however at cycle 50 a drop of the signals occurred due to laser energy loss. At the 100 cycle the second strand DNA is sequenced where more chemical material is added to boost the synthesis cycle.*

Table 5.3: The total number of reads, mapped reads and the percentage of mapped read of the cytoplasmic fractions

Condition	Cytoplasmic samples	Total reads	Mapped reads	% Mapped reads
Controls	155	17189777	16487970	95.92%
	159	26466289	25667408	96.98%
	170	22047680	20905844	94.82%
	2303	47879824	47083438	98.34%
Missense mutation	48	33927329	32963378	97.16%
	51	19798829	18581774	93.85%
	55	14730221	14296927	97.06%
Truncated mutation	192	18093922	17612955	97.34%
	193	23911777	23222052	97.12%
	194	23436050	21898231	93.44%

5.3 Gene expression profiling

The differentially expressed genes were identified using the edgeR program with the criteria of a fold change ≥ ±1.5 and p-value ≤0.05 of only the cytoplasmic fraction of each type of mutation. Two comparisons were performed, cytoplasmic MT vs. cytoplasmic CON which revealed 868 differentially expressed genes; 377 were up-regulated and 491 were down-regulated; and cytoplasmic MT vs. cytoplasmic CON which showed 1437 differentially expressed genes; 747 were up-regulated and 690 were down-regulated (Figure 5.5).

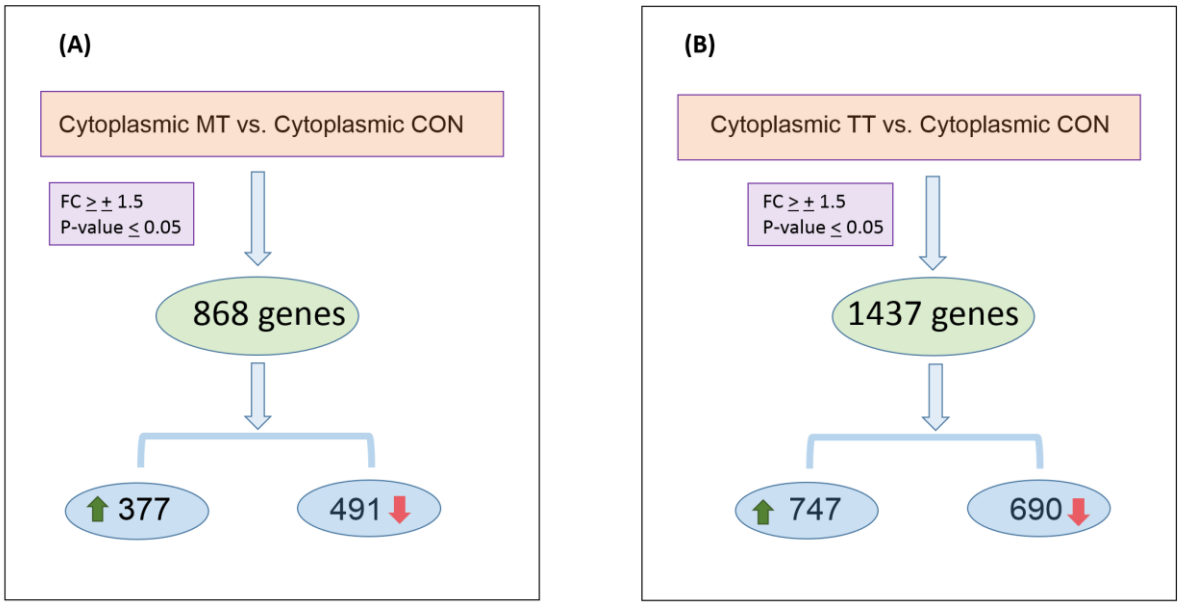

Figure 5.5: *Differentially expressed genes in cytoplasmic MT and cytoplasmic TT compared to controls using the edgeR software.*

5.3.1 Cytoplasmic MT vs. CON

DAVID analysis tool was used to identify significantly enriched biological processes (enrichment score $\geq$ 1.3) that were dysregulated in the cytoplasmic fALS-*TARDBP* missense mutation. The most significantly enriched biological processes were the following: response to steroid hormone stimulus, cell adhesion, anterior/posterior pattern formation and angiogenesis (Table 5.4). A further detailed examination of the genes within these biological processes is demonstrated below.

Table 5.4: Functionally enriched biological processes generated by DAVID of cytoplasmic MT vs. CON. GO=Gene ontology, no.=number, ES= Enrichment score

GO	Biological process	Gene no.	P-value	ES
BP_FAT	Response to steroid hormone stimulus	18	3.2E-8	4.4
BP_FAT	Cell adhesion	43	4.7E-4	3.19
BP_FAT	Anterior/posterior pattern formation	14	1.3E-3	3.17
BP_FAT	Angiogenesis	14	2.1E-3	2.29
BP_FAT	Reproductive developmental process	20	2.3E-3	2.17
BP_FAT	In utero embryonic development	23	3.5E-3	2
BP_FAT	Response to organic nitrogen	8	6.3E-3	1.97
BP_FAT	Regulation of apoptosis	42	2.2E-3	1.68
BP_FAT	Response to insulin stimulus	11	2.6E-3	1.5
BP_FAT	Regulation of growth	20	3.2E-2	1.48
BP_FAT	Positive regulation of macromolecule metabolic process	43	1.7E-2	1.47
BP_FAT	Urogenital system development	12	1.6E-3	1.43
BP_FAT	Response to extracellular stimulus	16	1.1E-2	1.41
BP_FAT	Regulation of neurological system process	10	4.3E-2	1.38
BP_FAT	Tube development	20	2.8E-4	1.35
BP_FAT	Embryonic limb morphogenesis	9	1.1E-2	1.34

5.3.1.1 Response to steroid hormone stimulus

The highest enriched biological process observed in the fALS-*TARDBP* missense mutation was the response to steroid hormone stimulus. Genes that belonged to this biological process were believed to be influenced by steroid hormones. Steroid hormones are lipid soluble molecules that are able to diffuse through the plasma membrane lipid bilayer and bind directly to the targeted receptor forming a hormone-receptor complex which is capable of inducing a change in gene expression (Schwartz et al., 2016). Dysregulated genes associated with their susceptibility to steroid hormones were shown in the fALS-*TARDBP* cytoplasmic missense mutation and will be discussed below (Table 5.5).

Alkaline phosphatase, liver/bone/kidney (*ALPL*) was up-regulated (FC=6.2). It is also known as tissue-nonspecific alkaline phosphatase (*TNSAP*). The gene encodes an enzyme which is expressed on mineralizing cells such as osteoblasts. Mutations in ALPL are associated with hypophosphatasia. $ALPL^{-/-}$ mice showed a similar phenotype, severe skeletal abnormalities due to hypomineralization and developed seizures (Liu et al., 2014). Furthermore, the butyrylcholinesterase (*BCHE*) was increased (FC= 51.8). It is also known as pseudocholinesterase and acts on the hydrolysis of the neurotransmitter acetylcholine. It has been shown that an elevated levels of BCHE was associated with AD (Greig et al., 2002b). The angiopoietin 1 (*ANGPT1*) was up-regulated (FC=2). ANGPT1 was shown to activate the MAPK pathway via the tyrosine-protein kinase receptor TIE-2. This promotes differentiation and migration of endothelial cells (Uebelhoer et al., 2012). Moreover, *ANGPT1* is highly expressed in cancers such as, neuroblastoma, multiple myeloma and prostate cancer (Hayes et al., 2000, Metheny-Barlow and Li, 2003).

In addition, cyclin D2 (*CCND2*) was increased (FC=4.2). It belongs to the cyclin family which is involved in regulating the cell cycle. CCND2 forms complexes with the cyclin-dependent kinases CDK4/CDK6 which regulate G1/S transition phase specifically. Uncontrolled activation of *CCND2* was shown to be associated with tumours such as glioblastoma, breast cancer and lymphoma (Koyama-Nasu et al., 2013). The GATA binding protein 3 (*GATA3*) was up-regulated (FC= 17.9).

GATA3 is a transcription factor which is involved in the regulation of T-cell development. It is also involved in the normal growth of the mammary glands however, overexpression *GATA3* was shown to be associated with poor prognosis of breast cancer (Chou et al., 2010).

Also, the glutathione S-transferase mu 3 (*GSTM3*) which is an enzyme that is involved in the detoxification of toxicants was shown to be increased (FC= 3.8) (Shin et al., 2016). The insulin-like growth factor binding protein 2, 36kDa (*IGFBP2*) was up-regulated (FC= 20). IGFBP2 is an essential protein that binds to the GF-I with a high affinity. It promotes cell proliferation, adhesion and survival (Shen et al., 2012). The oxytocin receptor (*OXTR*) was also increased (FC=5.3). This receptor binds the oxytocin peptide which can activate the cAMP signalling pathway through G-protein activation. OXTRs are expressed on mammary gland and myometrium. It is also found in the CNS where it regulates social behaviours (Bale et al., 2001). In addition, the platelet-derived growth factor beta polypeptide (simian sarcoma viral (v-sis) oncogene homolog) (*PDGFB*) was increased (FC=10). PDGFB is a tyrosine kinase receptor which can activate downstream signalling pathways that involve cell differentiation, migration and survival (Nicolas et al., 2013). In addition, regulator of G-protein signalling 9 (*RGS9*) was upregulated (FC=11.6). RGS9 belongs to the RGS family of proteins that are involved in inhibiting the G-protein by increasing the GTP hydrolysis thereby deactivating the adenylate cyclase enzyme (He et al., 1998). Moreover, the suppressor of cytokine signalling 2 (*SOCS2*) was increased (FC=2.7). SOCS2 was shown to inhibit the cytokine receptor activity through the JAK/STAT pathway (Minamoto et al., 1997). Furthermore, somatostatin (*SST*) was increased (FC=22). Somatostatin is a hormone which has an inhibitory effect on other secondary hormones like insulin, glycogen, thyroid stimulating hormone and growth hormone. It is also a neurotransmitter which promotes neuronal excitability by activating G protein-coupled receptors. It was shown that somatostatin decreases with age and was shown to be associated with AD (Saito et al., 2005, Liguz-Lecznar et al., 2016) . The tumour necrosis factor receptor superfamily, member 11b (*TNFRSF11B*) was up-regulated (FC=2). It is also known as osteoprotegerin (*OPG*) and, as stated, belongs to the TNF-receptor superfamily. It is considered a decoy receptor which inhibits osteoclastogenesis

by binding to the RANK ligand and thereby inhibits the RANK / RANKL pathway. Mutation in *TNFRSF11B* were suggested to associate with idiopathic hyperphosphatasia (Cundy et al., 2002, Janssens et al., 2005). The WAP four-disulfide core domain 1 (*WFDC1*) was significantly increased (FC=118.6). WFDC1 is a protease inhibitor which was reported to be expressed at a low levels in prostate cancer but no mutation in the gene was detected (Watson et al., 2004).

In contrast a group of genes were down-regulated. The carbonic anhydrase IX (*CA9*) was reduced (FC=-5.3). CA9 belongs to the carbonic anhydrase family which has a major role in normal cell proliferation and is also considered a tumour suppresser. Low levels of CA9 were associated with poor prognosis of renal cell carcinoma (Bui et al., 2003). Furthermore, the v-fos FBJ murine osteosarcoma viral oncogene homolog (*FOS*) was decreased (FC=-4.7). *FOS* It is a proto-oncogene which encodes the for FOS protein. The FOS protein is capable of binding to the JUN protein to form the activator protein 1 (AP-1) complex. The AP-1 complex promotes cell proliferation via the activation MAPK pathway (Milde-Langosch, 2005). In addition, the serpin peptidase inhibitor, clade A (alpha-1 antiproteinase, antitrypsin), member 1 (*SERPINA1*) was reduced (FC=-14.6). SERPINA1 is a protease inhibitor which acts in protecting the cells from harmful enzymes especially those produced in inflammation such as neutrophil elastase (Churg et al., 2001). Finally the solute carrier family 6 (neurotransmitter transporter, GABA), member 1 (*SLC6A1*) was down-regulated (FC=-13.9). SLC6A1 is involved in the reuptake of the neurotransmitter gamma-aminobutyric acid (GABA) from the synaptic cleft into the presynaptic neuron. It was suggested that the dysregulation of the *SLC6A1* was may disturb the GABA status in the brain which may result in seizures (Carvill et al., 2015).

It was shown that the steroid hormones have a significant effect on gene expression. This was clearly observed in fALS-*TARDBP* missense mutation with the majority of the genes being up-regulated with the top highest up-regulated genes were *BCHE, GATA3, IGFBP2, PDGFB, RGS9, SST* and *WFDC1*.

Table 5.5: Genes involved in response to steroid hormone stimulus in the cytoplasmic missense mutation

Gene symbol	Gene name	P-value	Fold change
ALPL	Alkaline phosphatase, liver/bone/kidney	0.02	6.24
ANGPT1	Angiopoietin 1	0.03	2.08
BCHE	Butyrylcholinesterase	0.01	51.81
CA9	Carbonic anhydrase IX	0.04	-5.31
CCND2	Cyclin D2	0.01	4.26
FOS	V-fos FBJ murine osteosarcoma viral oncogene homolog	0.03	-4.76
GATA3	GATA binding protein 3	0.01	17.92
GSTM3	Glutathione S-transferase mu 3 (brain)	0.0003	3.88
IGFBP2	Insulin-like growth factor binding protein 2, 36kDa	0.007	20.08
OXTR	Oxytocin receptor	0.003	5.32
PDGFB	Platelet-derived growth factor beta polypeptide (simian sarcoma viral (v-sis) oncogene homolog)	0.0008	10.20
RGS9	Regulator of G-protein signalling 9	0.03	11.60
SERPINA1	Serpin peptidase inhibitor, clade A (alpha-1 antiproteinase, antitrypsin), member 1	0.02	-14.68
SLC6A1	Solute carrier family 6 (neurotransmitter transporter, GABA), member 1	0.04	-13.91
SOCS2	Suppressor of cytokine signalling 2	0.007	2.74
SST	Somatostatin	0.03	22.04
TNFRSF11B	Tumour necrosis factor receptor superfamily, member 11b	0.04	2.08
WFDC1	WAP four-disulfide core domain 1	4.86E-05	118.62

5.3.1.2 Cell adhesion

Cell adhesion was previously shown to be associated with fALS (refer to section 4.6.1.1.3 and 4.6.1.2.2). Here, by studying gene expression profiling using RNA sequencing the data revealed that the largest number of dysregulated genes in fALS-*TARDBP* missense mutation belonged to cell adhesion biological process with the majority being significantly down-regulated though some were up-regulated (Table 5.6). A further elaboration is shown below.

Laminin, alpha 3 (*LAMA3*) was up-regulated (FC=6). LAMA3 belongs to the laminin family and was shown to be involved in epithelial basement membranes adhesion (Ryan et al., 1994). Furthermore, endomucin (*EMCN*) was increased (FC=16). EMCN is a mucin-like sialoglycoprotein which has been suggested to negatively control cell adhesion by preventing the formation of focal adhesion complexes (Kinoshita et al., 2001). In addition the CD9 molecule (*CD9*) was also up-regulated (FC=6.6). It is expressed on dendritic cells and megakaryocytes. It is involved in cell adhesion and migration (Leung et al., 2011). Mutation in the *CD9* gene was shown be associated with cancer and metastasis (Zoller, 2009). The ALX homeobox 1 gene (*ALX1*) was increased (FC=12). ALX1 is a transcription factor that is involved in cartilage synthesis. Mutations in *ALX1* were suggested to be associated with frontonasal dysplasia (FND) (Dee et al., 2013). Moreover, three genes belonging to the cadherin superfamily were up-regulated, tumour suppressor homolog 3 (Drosophila) (*FAT3*) (FC=5), cadherin 10, type 2 (T2-cadherin) (*CDH10*) (FC=5.7) and protocadherin 17 (*PCDH17*) (FC=11). Cadherins are transmembrane glycoproteins that are expressed on several types of cells and have a major role in cell-cell adhesion. (Brasch et al., 2012).

The L1 cell adhesion molecule (*L1CAM*) was up-regulated (FC=14). L1CAM is an adhesion molecule that has a major role in the CNS development including neuronal cell differentiation and migration (Schafer and Frotscher, 2012). Plakophilin 3 (*PKP3*) expression was also increased (FC=3.4). It is involved in cell adhesion by promoting the adhesion of cadherins to the cytoskeleton (Schmidt et al., 1999). The sorbin and SH3 domain containing 1 (*SORBS1*) which is involved in focal cell adhesion complexes was increased (FC=10) (Aakula et

al., 2016). Furthermore, the protein tyrosine phosphatase, receptor type, C (*PTPRC*) which belongs to the protein tyrosine phosphatase family was up-regulated (FC=4). PTPRC is able to activate signalling pathways such as the JAK pathway which promote cell cycle, cell differentiation and growth (Porcu et al., 2012). Thy-1 cell surface antigen (*THY1*) was increased (FC=1.9). THY1 is involved in cell proliferation, differentiation and apoptosis. It is also mediates cell adhesion and was considered a tumour suppressor for ovarian cancer (Lung et al., 2005, Rege and Hagood, 2006). The calsyntenin 2 (*CLSTN2*) gene was up-regulated (FC=35.7). CLSTN2 has been shown to be involved in cell adhesion and also was demonstrated to be highly expressed in GABAergic neurons (Hintsch et al., 2002). Furthermore, the roundabout, axon guidance receptor, homolog 2 (Drosophila) (*ROBO2*) was elevated (FC=7.7). ROBO2 is involved in axonal guidance (Fricke et al., 2001). Mutations in this gene have been associated with familial vesicoureteral reflux (Bertoli-Avella et al., 2008). Also the signal-regulatory protein alpha (*SIRPA*) was increased (FC=1.5). It is expressed mainly on myeloid cells which maintain cell migration and phagocytosis by interacting with the CD47 ligand (Matozaki et al., 2009).

As indicated above the majority of genes in this category were down-regulated. The polycystic kidney disease 1 (autosomal dominant) was reduced (*PKD1*) (FC=-1.9). PKD1 is considered an integral protein involved in cell to cell adhesion. Mutations in *PKD1* are known to be associated with autosomal dominant polycystic kidney disease (ADPKD) (Song et al., 2009). Also the WNT1 inducible signalling pathway protein 1 (*WISP1*) was down-regulated (FC=-4). It is a member of the connective tissue growth factor family which is involved in cell adhesion and cell proliferation via the WNT signalling pathway (Xu et al., 2000). Furthermore, the AE binding protein 1 (*AEBP1*) was decreased (FC=-3). AEBP1 is a transcriptional repressor which was suggested to be associated with adipogenesis through the MAP-kinase pathway (Bost et al., 2005). The SCO-spondin homolog (Bos taurus) (*SSPO*) was down-regulated (FC=-19). It was shown that *SSPO* is involved in the normal development of the CNS and especially in axon guidance (Goncalves-Mendes et al., 2003). The Adhesion molecule with Ig-like domain 2 (*AMIGO2*) was reduced (FC=-6). It encodes for a transmembrane protein that is involved in cell-cell adhesion (Kuja-Panula et al.,

2003). The amine oxidase, copper containing 3 (vascular adhesion protein 1) (*AOC3*) was down-regulated (FC=-22.8). AOC3 is expressed on the endothelial cell surface and is also involved in white blood cell migration and adhesion (Koskinen et al., 2007).

Four genes from the collagen family were down regulated. The collagen, type V, alpha 1 (*COL5A1*) (FC=-2.4). COL5A1 It is involved in the assembly of fibres synthesised by type V and type I collagens. Mutation in *COL5A1* gene have been associated with Ehlers-Danlos syndromes (DePaepe et al., 1997). The three other genes have previously been described as mainly expressed in the epidermal keratinocytes and to be involved in the adhesion of the epithelial cells to the basement membrane, they are collagen, type XV, alpha 1 (*COL15A*) (FC=-2.5), collagen, type XVI, alpha 1 (*COL16A1*) (FC=-4) and collagen type VII, alpha 1(*COL7A1*) (FC=-5.9). Mutations in the *COL7A1* gene have been associated with Bart syndrome and epidermolysis bullosa (Pan et al., 1992, Christiano et al., 1996, Ee et al., 2007).

A group of genes belonging to the cadherin superfamily were also down-regulated. The cadherin 2, type 1, N-cadherin (neuronal) (*CDH2*) was down-regulated (FC=-2.8). CDH2 is involved in neuronal cell adhesion. Mutations in this gene have been associated with obsessive-compulsive disorder (Moya et al., 2013). Also the calsyntenin 3 (*CLSTN3*) was reduced (FC=-5.4). It is involved in cell adhesion and was shown to be expressed in GABAergic neurons (Hintsch et al., 2002, Ortiz-Medina et al., 2015). In addition the dachsous 1 (Drosophila) (*DCHS1*) was reduced (FC=-7). Along with other adhesion molecules, DCHS1 forms adhesion complexes during neurogenesis which are essential for CNS development (Cappello et al., 2013). Furthermore, three more genes also belonging to the cadherin superfamily were down-regulated, the mucin-like protocadherin (*CDHR5*) (FC=-9), protocadherin 9 (*PCDH9*) (FC=-3) and protocadherin gamma subfamily C, 5 (*PCDHGC5*) (FC=-6.7) (Paris and Williams, 2000, Wu et al., 2001, Wang et al., 2012).

Chondroadherin (*CHAD*) gene expression was also decreased (FC=-18.7). CHAD has been shown to have an inhibitory effect on cartilage synthesis by reducing chondrocyte differentiation (Tillgren et al., 2015). Moreover, the fibronectin leucine rich transmembrane protein 1 (*FLRT1*) was decreased (FC=-3.5). FLRT1 is a member of the leucine rich repeat superfamily which is involved in cell adhesion through the activation of the Ras/Raf/ERK pathway (Wheldon et al., 2010). The NME/NM23 nucleoside diphosphate kinase 2 (*NME2*) was also reduced (FC=-5). The encoded protein was shown to be associated with tumour suppression in several cancers such as ovarian, breast and lung cancer (Thakur et al., 2011). The periostin, osteoblast specific factor (*POSTN*) was down-regulated (FC=-14). It has been shown that *POSTN* acts as a ligand for α-V/beta-5 and α-V/beta-3 integrin therefore it was suggested to have a role in cell adhesion of the ovarian epithelium (Gillan et al., 2002). The expression of the sushi, nidogen and EGF-like domains 1(*SNED1*) gene was decreased (FC=-2). It is known to be highly expressed in the kidney stroma (Leimeister et al., 2004). Furthermore, tenascin C (*TNC*) gene expression was reduced (FC=-3.6). It was previously shown that TNC inhibits integrin dependent adhesion (Probstmeier and Pesheva, 1999). In addition, tophinin associated protein (tastin) (*TROAP*) was down-regulated (FC=-2.5). It has been suggested to have a role in facilitating the blastocyst attachment to the endometrium (Fukuda et al., 1995). The trophinin (*TRO*) was decreased (FC=-1.9). The encoded protein is vital for the adhesion of the trophoblast to maternal epithelium (Harada et al., 2007). The lectin, galactoside-binding, soluble, 4 (*LGALS4*) was reduced (FC=-28.5). LGALS4 promotes cell adhesion by binding to the extracellular matrix (Huflejt et al., 1997). Finally, the tuberous sclerosis 1 (*TSC1*) gene was down-regulated (FC=-1.7). It is a tumour suppressor which has previously been shown to inhibit the mTORC1 signalling pathway (Inoki et al., 2002).

It is clearly shown that cell adhesion process is disrupted in fALS-*TARDBP* missense mutation and there is a marked reduction in gene expression. This strongly suggests less cell adhesion is undergoing which may leads to serious consequences. Less cell adhesion in fibroblasts possibly infer to the blood brain barrier breakdown observed in ALS patients especially that the skin biopsies in this study were collected at the active stage of the disease.

Table 5.6: Genes involved in cell adhesion in the cytoplasmic missense mutation

Gene symbol	Gene name	P-value	Fold change
AEBP1	AE binding protein 1	0.04	-3.09
ALX1	ALX homeobox 1	0.04	12.23
AMIGO2	Adhesion molecule with Ig-like domain 2	0.008	-6.06
AOC3	Amine oxidase, copper containing 3 (vascular adhesion protein 1)	0.008	-22.89
CD9	CD9 molecule	0.04	6.68
CDH2	Cadherin 2, type 1, N-cadherin (neuronal)	0.002	-2.82
CDH10	Cadherin 10, type 2 (T2-cadherin)	0.01	5.78
CDHR5	Mucin-like protocadherin	0.02	-9.05
CHAD	Chondroadherin	0.03	-18.70
CLSTN2	Calsyntenin 2	0.001	35.79
CLSTN3	Calsyntenin 3	0.01	-5.41
COL5A1	Collagen, type V, alpha 1	0.04	-2.47
COL7A1	Collagen, type VII, alpha 1	0.01	-5.94
COL15A1	Collagen, type XV, alpha 1	0.04	-2.52
COL16A1	Collagen, type XVI, alpha 1	0.01	-4.09
DCHS1	Dachsous 1 (Drosophila)	0.001	-7.16
EFS	Embryonal Fyn-associated substrate	0.02	-1.99
EMCN	Endomucin	0.001	16.26
FAT3	FAT tumor suppressor homolog 3 (Drosophila)	0.02	5.02
FLRT1	Fibronectin leucine rich transmembrane protein 1	0.01	-3.58
LAMA3	Laminin, alpha 3	0.009	6.27
LGALS4	Lectin, galactoside-binding, soluble, 4	0.01	-28.53
L1CAM	L1 cell adhesion molecule	0.01	14.35
NME2	NME/NM23 nucleoside diphosphate kinase 2	0.003	-5.29
PCDH9	Protocadherin 9	0.04	-3.07
PCDH17	Protocadherin 17	0.04	11.12
PCDHGC5	Protocadherin gamma subfamily C, 5	0.009	-6.79
PKD1	Polycystic kidney disease 1 (autosomal dominant)	0.02	-1.98
PKP3	Plakophilin 3	0.02	3.41
POSTN	Periostin, osteoblast specific factor	0.01	-14.45
PTPRC	Protein tyrosine phosphatase, receptor type, C	0.03	4.20
ROBO2	Roundabout, axon guidance receptor, homolog 2 (Drosophila)	0.03	7.74
SIRPA	Signal-regulatory protein alpha	0.04	1.59
SNED1	Sushi, nidogen and EGF-like domains 1	0.04	-2.10

SORBS1	Sorbin and SH3 domain containing 1	0.001	10.42
SSPO	SCO-spondin homolog (Bos taurus)	0.006	-19.03
THY1	Thy-1 cell surface antigen	0.009	1.95
TMEM8A	Transmembrane protein 8A	0.007	1.87
TNC	Tenascin C	0.005	-3.60
TRO	Trophinin	0.03	-1.95
TROAP	Trophinin associated protein (tastin)	0.01	-2.57
TSC1	Tuberous sclerosis 1	0.04	-1.76
WISP1	WNT1 inducible signaling pathway protein 1	0.01	-4.11

5.3.1.3 Anterior/posterior pattern formation

A group of genes were grouped under the banner of anterior/posterior pattern formation by DAVID. These are defined as genes that have a role in cellular development and differentiation that were located anatomically at the anterior-posterior axis of the body. No specific pattern of dysregulation was observed as there was an equal number of genes up-regulated and down-regulated in fALS-*TARDBP* missense mutation (Table 5.7).

The ALX homeobox 1(*ALX1*) gene was up-regulated (FC=12). It belongs to the homeobox protein family which are group of transcription factors that control the expression of genes responsible for organ structure. Mutations in *ALX1* were previously shown to cause frontonasal dysplasia which is uncontrolled cell proliferation and migration during embryonic development (Dee et al., 2013). Furthermore, the homeobox B9 (*HOXB9*) gene was increased (FC=53.7). It is a transcription factor that promotes cell proliferation, growth and differentiation. Elevated levels of HOXB9 have been shown to be associated with breast cancer and lung metastasis (Hayashida et al., 2010). The homeobox D13 (*HOXD13*) was also increased (FC=3.5) which is a transcription factor that promotes cell proliferation and growth of the limbs. Mutations in *HOXD13* gene were previously shown to be associated with hand-foot-genital syndrome (HFGS) (Goodman et al., 2000). The BTG family, member 2 (*BTG2*) was up-regulated (FC=2.5). It has been shown to be involved in the cell cycle regulation of at the G1 and S phase (Duriez et al., 2002) and is induced by the p53 tumour suppresser protein and DNA damage (Rouault et al., 1996). The presenilin 2 (Alzheimer disease 4) (*PSEN2*) was up-regulated (FC= 2.2). Mutations in *PSEN2* are linked to AD and have been suggested to be involved in the production of increased levels of APP in AD pathology (Levy-Lahad et al., 1996). The secreted frizzled-related protein 1 (*SFRP1*) was also increased (FC=4.3). It is involved in cell growth and also can activate the Wnt-dependent signalling pathway which is essential for cell development (Taketo, 2004). Furthermore, the zinc finger and BTB domain containing 16 (*ZBTB16*) was increased (FC= 28.5). It is a zinc finger transcription factor shown to be involved in osteoblastic differentiation (Ikeda et al., 2005). On the other hand, the secreted frizzled-related protein 2 (*SFRP2*) was down-

regulated (FC= -20.6). Similar to SFRP1, SFRP2 is involved in the activation of the Wnt-dependent signalling pathway which is essential for cell development (Taketo, 2004). The homeobox B3 (*HOXB3*) (FC= -2) was also reduced. HOXB3 is a transcription factor that promotes cell development and was shown to be associated with acute myeloid leukemia (AML) (Lindblad et al., 2015). The homeobox C6 (*HOXC6*) was decreased (FC=-2.2). HOXC6 was shown to be expressed in prostate cancer and was suggested to have a lower expression in breast cancer (Chariot et al., 1996, Hamid et al., 2015) Furthermore, the homeobox C8 (*HOXC8*) was down-regulated (FC=-2). HOXC8 is a prognostic factor for epithelial ovarian cancer (EOC). Elevated levels of HOXC8 were suggested to associate with poor prognosis of the disease (Lu et al., 2016). The activity-regulated cytoskeleton-associated protein (*ARC*) was also reduced (FC= -8.4). It is involved in brain plasticity by promoting long term potentiation and memory by increasing the AMPAR population on the postsynaptic neuron (Pevzner et al., 2012). The hematopoietically expressed homeobox (*HHEX*) was decreased (FC=-5). HHEX is a transcription factor that controls endothelial cell development (Donaldson et al., 2005). Finally, the homeobox D9 (*HOXD9*) was down-regulated (FC=-2.4). HOXD9 is a transcription factor that is involved in proliferation, migration and apoptosis. It was recently been associated with hepatocellular carcinoma (Lv et al., 2015).

Table 5.7: genes involved in anterior/posterior pattern formation in the cytoplasmic missense mutation

Gene ontology	Biological process	P-value	Fold change
ALX1	ALX homeobox 1	0.04	12.23
ARC	Activity-regulated cytoskeleton-associated protein	0.01	-8.49
BTG2	BTG family, member 2	0.03	2.56
HHEX	Hematopoietically expressed homeobox	0.02	-5.13
HOXB3	Homeobox B3	0.03	-2.08
HOXB9	Homeobox B9	0.002	53.75
HOXC6	Homeobox C6	0.01	-2.29
HOXC8	Homeobox C8	0.03	-2.08
HOXD9	Homeobox D9	0.04	-2.42
HOXD13	Homeobox D13	0.008	3.52
PSEN2	Presenilin 2 (Alzheimer disease 4)	0.03	2.26
SFRP1	Secreted frizzled-related protein 1	0.006	4.38
SFRP2	Secreted frizzled-related protein 2	0.001	-20.65
ZBTB16	Zinc finger and BTB domain containing 16	0.006	28.55

5.3.1.4 Angiogenesis

As mentioned previously, dysregulated angiogenesis related genes were shown to associate with ALS (see section 4.6.1.1.2 and 4.6.1.2.1). A large group of genes related to angiogenesis were up-regulated in the fALS-*TARDBP* missense mutation (Table 5.8) similar to the observation in the HTA data.

The endomucin (*EMCN*) was increased (FC=16.2). It is a mucin-like sialoglycoprotein which was suggested to negatively control cell adhesion by the inhibition of the focal adhesion complexes. This was demonstrated by interfering with the binding of the cells to the extracellular matrix (ECM) (Kinoshita et al., 2001). In addition, *EMCN* was shown to be highly expressed in endothelial cells and significantly up-regulated during cell proliferation, therefore it was suggested to be an angiogenic tumour marker (Liu et al., 2001). Furthermore, the HIV-1 Tat interactive protein 2, 30kDa (*HTATIP2*) was up-regulated (FC=1.7). It was first identified in small cell lung carcinoma cell lines (SCLC) and was suggested to have a suppressive effect on cancer metastasis (Shtivelman, 1997, Whitman et al., 2000). The T-box 4 (*TBX4*) was also increased (FC=11.4). *TBX4* encodes a transcription factor which is important for the development of the lower limbs. Mutations in *TBX4* have been shown to be associated small patella syndrome (SPS) (Agulnik et al., 1996, Bongers et al., 2004). Moreover, the tumour necrosis factor (ligand) superfamily, member 12 (*TNFSF12*) was up-regulated (FC=1.8). The *TNFSF12* is a cytokine that belongs to the tumour necrosis factor ligand family. It is involved in angiogenesis by mediating endothelial cell proliferation and migration. Also it can prompt cell death by activating apoptotic pathways (Chicheportiche et al., 1997, Lynch et al., 1999). The Thy-1 cell surface antigen (*THY1*) was increased (FC=1.9). Thy-1 is a cell surface glycoprotein which may induce cell proliferation, differentiation and apoptosis. In addition it was suggested to act as a tumour suppressor for ovarian cancer (Lung et al., 2005). As mentioned previously, angiopoietin 1 (*ANGPT1*) was also increased (FC=2). ANGPT1 binds to the tyrosine-protein kinase receptor TIE-2 which activates the MAPK pathway. This promotes differentiation and migration of the endothelial cells (Uebelhoer et al., 2012). In addition, *ANGPT1* was shown to be highly expressed in cancers such as prostate cancer, multiple myeloma and

neuroblastoma (Hayes et al., 2000, Metheny-Barlow and Li, 2003). The heart and neural crest derivatives expressed 2 (*HAND2*) was up-regulated (FC=2.7). It is a transcription factor that is essential for cardiogenesis (McFadden et al., 2005). In addition, the placental growth factor (PGF) was increased (FC=4.3). PGF is a cytokine that binds to VEGFR1 which results in the activation of endothelial cell migration, growth and survival (Fischer et al., 2007). It is considered a prognostic marker for several tumours therefore, it has an important role in determining tumour progression (Kim et al., 2012). The interleukin 18 (interferon-gamma-inducing factor) (*IL18*) was increased (FC= 8). It is a proinflammatory cytokine that binds to its IL18 receptor which activates an immune response. It is also an angiogenic factor that is involved in endothelial cell proliferation. Elevated levels of IL18 have been shown to be associated with cancers such melanoma and renal cancer (Park et al., 2001, Palma et al., 2013). The transforming growth factor, alpha (*TGFA*) was also up-regulated (FC=4.5). It induces cell signalling transduction and activates pathways that mediate cell proliferation, differentiation and angiogenesis (Singh and Coffey, 2014). In contrast a group of genes were down-regulated. Angiopoietin 2 (*ANGPT2*) was reduced (FC=-22.7). It acts as an antagonist for the *ANGPT1*. It competes for the binding to the TIE-2 receptor. Similar to ANGPT1, ANGPT2 can activate the MAPK pathway which results in endothelial cell differentiation and migration. *ANGPT2* was shown to be highly expressed in cancers such as lung cancer, breast cancer and hepatocellular carcinoma (Metheny-Barlow and Li, 2003, Sfiligoi et al., 2003, Hu and Cheng, 2009). Furthermore, angiopoietin-like 6 (*ANGPTL6*) was down-regulated (FC=-5.6). It belongs to the angiopoietin family proteins and is involved in vascular endothelial cell chemotaxis (Oike et al., 2003, Oike et al., 2004). The collagen, type XV, alpha 1 (*COL15A1*) was also reduced (FC=-2.5). *COL15A1* was suggested to have an anti-angiogenic function and to be a tumour suppresser (Sasaki et al., 2000). Finally, the vascular endothelial growth factor A (*VEGFA*) was reduced (FC=-3.2). VEGFA is involved in vascular formation this includes angiogenesis and vasculogenesis. It also promotes endothelial cell migration. It has a major role in the CNS as it stimulates the development of blood vessels. Furthermore, transgenic mice$^{-/-}$ for hypoxia response element of the *VEGFA* gene showed a phenotype similar to ALS (Oosthuyse et al., 2001, Mackenzie and Ruhrberg, 2012).

This data shows, again, that genes previously associated with angiogenesis are dysregulated in fALS-*TARDBP* missense mutation with the majority being up-regulated. However, it is possible that these changes are as a result of increased oxygen demand in fibroblast.

Table 5.8: Genes involved in angiogenesis in the cytoplasmic missense mutation

Gene symbol	Gene name	P-value	Fold change
ANGPT1	Angiopoietin 1	0.03	2.08
ANGPT2	Angiopoietin 2	0.005	-22.77
ANGPTL6	Angiopoietin-like 6	0.01	-5.60
COL15A1	Collagen, type XV, alpha 1	0.04	-2.52
EMCN	Endomucin	0.001	16.26
HAND2	Heart and neural crest derivatives expressed 2	0.01	2.71
HTATIP2	HIV-1 Tat interactive protein 2, 30kDa	0.03	1.71
IL18	Interleukin 18 (interferon-gamma-inducing factor)	0.003	8.09
PGF	Placental growth factor	0.001	4.36
TBX4	T-box 4	0.04	11.40
THY1	Thy-1 cell surface antigen	0.009	1.95
TGFA	Transforming growth factor, alpha	0.01	4.58
TNFSF12	Tumor necrosis factor (ligand) superfamily, member 12	0.04	1.82
VEGFA	Vascular endothelial growth factor A	0.02	-3.25

5.3.2 Cytoplasmic TT vs. CON

As in the missense mutation study, the DAVID analysis tool was used to identify significantly enriched biological processes (enrichment score $\geq$ 1.3) that were dysregulated in cytoplasmic fALS-*TARDBP* truncated mutation. The most significantly enriched biological processes were the following: response to vitamins, regulation of mitotic cell cycle, response to steroid hormone stimulus, blood vessel development and vesicle-mediated transport (Table 5.9). A more detailed examination of the genes within these biological processes is demonstrated below.

Table 5.9: Functionally enriched biological processes generated by DAVID of cytoplasmic TT vs. CON. GO=Gene ontology, no.=number, ES= Enrichment sore

GO	Biological process	Gene no.	P-value	ES
BP_FAT	Response to vitamins	12	2.1E-3	4.04
BP_FAT	Regulation of mitotic cell cycle	16	8.1E-2	3.12
BP_FAT	Response to steroid hormone stimulus	23	3.6E-3	2.74
BP_FAT	Blood vessel development	25	1.6E-2	2.42
BP_FAT	Vesicle-mediated transport	52	5.4E-3	2.26
BP_FAT	Stem cell development	7	4.2E-3	2.02
BP_FAT	Tissue morphogenesis	24	6.8E-4	1.63
BP_FAT	Tube development	22	3.0E-2	1.6
BP_FAT	Positive regulation of vascular endothelial growth factor receptor signalling pathway	4	6.7E-3	1.53
BP_FAT	Positive regulation of protein kinase cascade R	17	5.2E-2	1.47
BP_FAT	Response to amine stimulus	8	8.9E-3	1.46
BP_FAT	Morphogenesis of a polarized epithelium	4	1.5E-2	1.43
BP_FAT	Reproductive process in a multicellular organism	49	4.0E-3	1.4
BP_FAT	Regulation of hormone levels	16	4.5E-2	1.35
BP_FAT	Circulatory system process	20	2.0E-2	1.31
BP_FAT	Regulation of synaptic transmission	15	4.0E-2	1.25

5.3.2.1 Response to vitamins

The highest enriched biological process was the response to vitamins. Vitamins are organic compounds that are essential for normal development. Studies have shown that vitamins capable of altering gene expression such are vitamin K, vitamin A and vitamin E (Wang et al., 1995, Landes et al., 2003, McGrane, 2007). A group of genes that were up-regulated in fALS-*TARDBP* truncated mutation and are involved in vitamin metabolism are indicated in Table 5.10.

The aldehyde dehydrogenase 1 family, member A2 was up-regulated (*ALDH1A2*) (FC=3.8). *ALDH1A2* is a member of the aldehyde dehydrogenase family. It is involved in the synthesis of retinoic acid (vitamin A) from retinaldehyde which is vital for the development of the spinal cord (Deak et al., 2005).The retinol binding protein 4, plasma (*RBP4*) was increased (FC=4.4). RBP4 binds to retinoic acid in the blood to properly deliver the retinoic acid from the liver to other sites in the body and preventing it being filtered by the renal system (Folli et al., 2005). Two genes involved in embryonic development and bone and cartilage synthesis were up-regulated, the bone morphogenetic protein 4 (*BMP4*) (FC=43.5) and bone morphogenetic protein 7 (*BMP7*) (FC=16.6) (Bakrania et al., 2008). Furthermore, the butyrylcholinesterase (*BCHE*) was up-regulated (FC=23.4). It was previously shown that it has a role in the hydrolysis of the neurotransmitter acetylcholine. In addition, elevated levels of BCHE were shown to be associated with AD (Greig et al., 2002b). Two proinflammatory cytokines that are involve in inflammation were up-regulated, chemokine (C-C motif) ligand 2 (*CCL2*) (FC=2.7) and interleukin 1, beta (*IL1B*) (FC=4.2) (Corrigall et al., 2001). Also, the imprinting gene mesoderm specific transcript homolog (mouse) (*MEST*) which is expressed mainly in the mesodermal tissues during embryonic development was increased (FC=7) (Kobayashi et al., 1997). The hydroxysteroid (17-beta) dehydrogenase 2 (*HSD17B2*) was up-regulated (FC=11.6). The encoded protein is an enzyme which negatively regulates estradiol hormone activity (Plourde et al., 2008). The oxytocin, prepropeptide (*OXT*) was elevated (FC=49). OXT is a hormone and a neurotransmitter that is produced by the hypothalamus and has an effect on the uterus and mammary gland. It is also found in the CNS wherein it regulates social

behaviours (Bale et al., 2001). The kruppel-like factor 4 (gut) (*KLF4*) was increased (FC=1.8). KLF4 is a member of the krüppel like factor family, is a transcription factor and a tumour suppresser. It has roles in proliferation, development, inflammation and apoptosis (Rowland and Peeper, 2006). Finally, only a single gene was reduced, the prostaglandin-endoperoxide synthase 2 (prostaglandin G/H synthase and cyclooxygenase) (*PTGS2*) (FC=-4.6). PTGS2 is known to have a major role during injury and inflammation (Yamauchi et al., 2013).

As an overall, a high number of genes influenced by vitamins was observed in fALS-*TARDBP* truncated mutation and also the highest enriched biological process. This observation may reflects ALS patients' diet. As the disease progress, a high nutritional supplements are given to ALS patients to compensate the body mass loss. This may alter expression of some genes as seen above. Also, this observation could be as a result of the vitamin supplement added to the fibroblast culture media to maintain their growth.

Table 5.10: Genes involved in response to vitamin in the cytoplasmic truncation mutation

Gene symbol	Gene name	P-value	Fold change
ALDH1A2	Aldehyde dehydrogenase 1 family, member A2	0.01	3.88
BCHE	Butyrylcholinesterase	0.01	23.48
BMP4	Bone morphogenetic protein 4	0.002	43.56
BMP7	Bone morphogenetic protein 7	0.01	16.66
CCL2	Chemokine (C-C motif) ligand 2	0.04	2.78
HSD17B2	Hydroxysteroid (17-beta) dehydrogenase 2	0.01	11.60
IL1B	Interleukin 1, beta	0.003	4.27
KLF4	Kruppel-like factor 4 (gut)	0.01	1.83
MEST	Mesoderm specific transcript homolog (mouse)	3.51513E-05	7.36
OXT	Oxytocin, prepropeptide	0.002	49.14
PTGS2	Prostaglandin-endoperoxide synthase 2 (prostaglandin G/H synthase and cyclooxygenase)	0.01	-4.68
RBP4	Retinol binding protein 4, plasma	0.04	4.43

5.3.2.2 Regulation of the mitotic cell cycle

In the fALS-*TARDBP* truncated mutation comparison a number of dysregulated genes related to the mitotic cell cycle were identified with equal numbers of up-regulated and down-regulated gene expression (Table 5.11).

The CD28 molecule (*CD28*) was up-regulated (FC=10.5). It is a surface protein that can co-stimulate T-cells and is important for their proliferation and survival (Mikolajczak et al., 2004). Furthermore, the epithelial mitogen homolog (mouse) (*EPGN*) was increased (FC=12). *EPGN* belongs to the epidermal growth factor family which encodes for a legend that binds to the epidermal growth factor receptor and can activate cell migration and proliferation signalling pathways (Herbst and Bunn, 2003). In addition, the transforming growth factor, alpha (*TGFA*) was up-regulated (FC=8). The TGFA is involved in cell proliferation, differentiation and development. Overexpression of *TGFA* was shown to be associated with several types of cancer (Singh and Coffey, 2014). The insulin-like growth factor 2 (somatomedin A) (*IGF2*) was also increased (FC=40). IGF2 binds to the IGF1 receptor which stimulates cell proliferation therefore is considered a mitogenic signalling molecule (Morrione et al., 1997). The nuclear factor of kappa light polypeptide gene enhancer in B-cells inhibitor-like 1(*NFKBIL1*) was up-regulated (FC=1.7). It is involved in the regulation of the innate immune response and is considered a tumour suppressor (Pajerowski et al., 2009). In addition, two proinflammatory cytokines were up-regulated, interleukin 1, alpha (*IL1A*) (FC=7) and interleukin 1, beta (*IL1B*) (FC=4.2).

On the other hand, a group of genes were down-regulated. The Mdm2, transformed 3T3 cell double minute 2, p53 binding protein (mouse) binding protein, 104kDa (*MTBP*) was reduced (FC=-2.6). MTBP may regulate cell growth and was suggested to be a tumour suppressor gene (Boyd et al., 2000). Also the sphingosine kinase 1(*SPHK1*) was down-regulated (FC=-2). SPHK1 is involved in the phosphorylation of sphingosine to form sphingosine-1-phosphate that has a role in cell growth and proliferation (Wang et al., 2013). The hect domain and RLD 2 (*HERC2*) was also reduced (FC=-7.4). HERC2 is a shuttling protein that

is involved in the ubiquitination of several proteins and therefore, mediates protein degradation (Wang et al., 2009a).

The nucleolar and spindle associated protein 1 (*NUSAP1*) was reduced (FC=-2.7). NUSAP1 interact with cellular microtubule proteins which are involved in cell mitosis (Raemaekers et al., 2003a). Also the extra spindle pole bodies homolog 1 (S. cerevisiae) (*ESPL1*) was down-regulated (FC=-2.7). ESPL1 is involved in the control of proper cell division by promoting the cleavage of the sister chromatin during anaphase (Sun et al., 2009). The NIMA (never in mitosis gene a)-related kinase 2 (*NEK2*) was reduced (FC=-4.9) NEK2 was shown to be involved in centromere separation during cell division and was detectable at the S phase and reached its highest expression at the G2 phase (Cappello et al., 2014). The centromere protein F, 350/400ka (mitosin) (*CENPF*) was also down-regulated (FC=-3). It is part of the centromere kinetochore complex. Therefore, it was suggested to play a role in cell division and especially during chromosome segregation (Eisch et al., 2016). Finally, the discs, large (Drosophila) homolog-associated protein 5 (*DLGAP5*) was decreased (FC=-3.5). DLGAP5 is a kinetochore protein which is involved in cell division by promoting microtubule stabilization and chromosome alignment (Wong and Fang, 2006).

It can be observed that the majority of the down-regulated genes were related to mitotic cell division while the up-regulate genes were related to cell proliferation pathways. This may indicated that some of the fibroblasts are subjected to death as a result of the *TARDBP* mutation and also a compensatory process is established by activating the proliferation pathways.

Table 5.11: Genes involved in regulation of mitotic cell cycle in the cytoplasmic truncation mutation

Gene symbol	Gene name	P-value	Fold change
CD28	CD28 molecule	0.04	10.54
CENPF	Centromere protein F, 350/400ka (mitosin)	0.007	-3.10
DLGAP5	Discs, large (Drosophila) homolog-associated protein 5	0.03	-3.54
EPGN	Epithelial mitogen homolog (mouse)	0.002	12.21
ESPL1	Extra spindle pole bodies homolog 1 (S. cerevisiae)	0.007	-2.71
HERC2	Hect domain and RLD 2	0.01	-7.40
IGF2	Insulin-like growth factor 2 (somatomedin A); insulin	6.3434E-08	40.15
IL1A	Interleukin 1, alpha	0.01	7.22
IL1B	Interleukin 1, beta	0.003	4.27
MTBP	Mdm2, transformed 3T3 cell double minute 2, p53 binding protein (mouse) binding protein, 104kDa	0.02	-2.69
NEK2	NIMA (never in mitosis gene a)-related kinase 2	0.01	-4.98
NFKBIL1	Nuclear factor of kappa light polypeptide gene enhancer in B-cells inhibitor-like 1	0.02	1.79
NUSAP1	Nucleolar and spindle associated protein 1	0.03	-2.78
SBDSP1	Shwachman-Bodian-Diamond syndrome pseudogene	0.01	1.78
SPHK1	Sphingosine kinase 1	0.04	-2.07
TGFA	Transforming growth factor, alpha	0.007	8.20

5.3.2.3 Response to steroid hormone stimulus

The third highest enriched biological process demonstrated in the fALS-*TARDBP* truncated mutation comparison was the response to steroid hormone stimulus. This was a similar observation to the ALS-*TARDBP* missense mutation. Genes that belonged to this biological process were also supposed to be stimulated by steroid hormones. As mentioned previously, steroid hormones are lipid soluble molecules which are capable to diffuse though plasma membrane lipid bilayer to bind to targeted receptor forming complexes which are then able to induce gene expression changes (Schwartz et al., 2016). Dysregulated genes associated with steroid hormone susceptibility were demonstrated in fALS-*TARDBP* cytoplasmic truncated mutation and are discussed below (Table 5.12).

The WAP four-disulfide core domain 1 (*WFDC1*) was up-regulated (FC= 26). WFDC1 is a protease inhibitor and is considered a tumour marker. It is expressed at low levels in prostate cancer and breast cancer however no mutation has been detected (Watson et al., 2004, Madar et al., 2009). Furthermore, the aldehyde dehydrogenase 1 family, member A2 (*ALDH1A2*) was increased (FC=3.8). ALDH1A2 is involved in the formation of retinoic acid from retinaldehyde that is vital for the development and maturation of the spinal cord (Deak et al., 2005). Moreover, three genes belong to the transforming growth factor-β superfamily were up-regulated, bone morphogenetic protein 4 (*BMP4*) (FC=43.5), bone morphogenetic protein 7 (*BMP7*) (FC=16.6) and myostatin (*MSTN*) (FC=3.8). Both BMP4 and BMP7 are involved in bone and cartilage formation and embryonic development while MSTN was shown to inhibit skeletal muscle development (Bakrania et al., 2008, Gu et al., 2016). The tumour necrosis factor receptor superfamily, member 11b (*TNFRSF11B*) was increased (FC=2.7). It is also known as osteoprotegerin (*OPG*) which is considered a decoy receptor which inhibits osteoclast synthesis by binding to the RANK ligand therefore inhibits the RANK / RANKL pathway. Mutation in this gene was suggested to associate with idiopathic hyperphosphatasia (Cundy et al., 2002, Janssens et al., 2005). The cyclin D2 (*CCND2*) was also increased (FC=3.4). CCND2 regulates the cell division process by forming complexes with the cyclin-dependent kinases

CDK4/CDK6. CCND2-CDK4/CDK6 complexes regulate the G1/S transition phase. Uncontrolled regulation of *CCND2* has been shown to be associated with tumours such as lymphoma, glioblastoma and breast cancer (Koyama-Nasu et al., 2013). Also the cyclin-dependent kinase inhibitor 1A (p21, Cip1) (*CDKN1A*) was increased (FC=2). CDKN1A is a cell cycle regulator that functions mainly at the G1 phase. It was shown that it promote cell arrest by inhibiting the CDK2/CDK4 complex formation (Bendjennat et al., 2003).

In addition, two peptide hormones were up-regulated. Adrenomedullin (*ADM*) was increased (FC=2.4). This peptide hormone has a variety of functions, these include growth, angiogenesis and smooth muscle dilatation (Fernandez et al., 2008). Also the oxytocin, prepropeptide (*OXT*) was also elevated (FC=49). Oxytocin is a hormone and a neurotransmitter which is synthesised in the hypothalamus and has an effect on the mammary gland and uterus. It is also expressed in the CNS and was shown to regulate social behaviours (Bale et al., 2001). Furthermore, three genes involved in inflammation were up-regulated. The chemokine (C-C motif) ligand 2 (*CCL2*) was increased (FC=2.7). CCL2 binds to its receptor chemokine C-C motif receptor to initiate the recruitment of monocytes and macrophages to the site of inflammation. Elevated levels of CCL2 were associated with a poor prognosis of late stage metastatic breast cancer (Qian et al., 2011). In addition, the prostaglandin-endoperoxide synthase 2 (prostaglandin G/H synthase and cyclooxygenase) was also increased (*PTGS2*) (FC=-4.6). PTGS2 is shown to have a major role in tissue injury and inflammation (Yamauchi et al., 2013). Also the interleukin 1, beta (IL1B) was up-regulated (FC=4). The butyrylcholinesterase (*BCHE*) was up-regulated (FC=23.4). BCHE acts on the hydrolysis of the acetylcholine and was shown to be highly expressed in AD (Greig et al., 2002b).

A group of enzymatic genes were up-regulated. The cytochrome P450, family 11, subfamily A, polypeptide 1(*CYP11A1*) was up-regulated (FC=2.4). This gene encodes for a monooxygenase enzyme that is involved in the synthesis of lipids and steroids (Sahakitrungruang et al., 2011). The glutathione peroxidase 4 (phospholipid hydroperoxidase) (*GPX4*) was increased (FC=2). GPX4 belongs to the glutathione peroxidases family which are antioxidant enzymes. It reduces

hydroperoxide radicals generated from cholesterol and phospholipid metabolism (Liang et al., 2007). Furthermore, the alpha-2-macroglobulin (*A2M*) was up-regulated (FC=6). A2M is a protease inhibitor which is able to inactivate several proteins and is able to prevent fibrinolysis by inhibiting plasmin, it also binds to thrombin which results in the inhibition of coagulation (de Boer et al., 1993). On the other hand, two enzymatic genes were down-regulated. The nitric oxide synthase 3 (endothelial cell) (*NOS3*) was decreased (FC=-7.8). NOS3 is an enzyme that promotes the synthesis of nitric oxide which has a major role in vasodilatation. Polymorphisms in the NOS3 have been suggested to be associated with AD (Dasar et al., 2012). Moreover, carbamoyl-phosphate synthetase 1, mitochondrial (*CPS1*) was also decreased (FC=-2.7). CPS1 is an essential enzyme that is involved in the elimination of the toxic effect of ammonia by converting ammonia to carbamoyl phosphate. This is the initial step of the urea cycle which takes place in the mitochondria (Haberle et al., 2003).

The aryl-hydrocarbon receptor nuclear translocator 2 (*ARNT2*) was down-regulated (FC=-1.5). ARNT2 was shown to be expressed in the CNS and mutations in this gene were associated with Webb-Dattani syndrome (Haberle et al., 2003). The cortactin binding protein 2 (*CTTNBP2*) was down-regulated (FC=-12.175). The encoded protein was suggested to play a role in dendritic spinogenesis (Chen et al., 2012). Finally the oestrogen receptor 1 (*ESR1*) was reduced (FC=-3.7). ESR1 is a steroid receptor and is a member of a nuclear receptor family which is activated by oestrogen hormone. The activation of ESR1 by oestrogen involves in the development female sexual system (Kos et al., 2001).

The majority of genes that were influenced by steroid hormones were increased in the fALS-*TARDBP* truncated mutation with only five genes being shared with the fALS-*TARDBP* missense mutation, *BCHE, WFDC, CCND2, GSTM3* and *TNFRSF11B* (Figure 5.6). Although both mutations were harbouring the same biological processes in name, a large number of distinct genes were observed.

It was shown that genes involved in response to steroid hormone stimulus were dysregulated and the majority were up-regulated in both the fALS-*TARDBP*

missense mutation and truncated mutation. It was interesting to find if any of the cell genes from both mutations belonged to a similar or distinct pathway. Thus, response to steroid hormone gene list from both mutations were combined then uploaded into DAVID and the KEGG pathway was generated in order to identify the significant pathways. A number of pathways were highlighted, the MAP kinase pathway showing, *Fos* and *PDGF* dysregulated genes specifically to fALS-*TARDBP* missense mutation while *IL1* was specifically to the fALS-*TARDBP* truncated mutation (Figure 5.7). Furthermore, the cytokine-cytokine receptor interaction pathway was demonstrated, *PDGFB* was a dysregulated gene specific to the fALS-*TARDBP* missense mutation and *CCL2, BMP7* and *IL1B* genes were specific to the fALS-*TARDBP* truncated mutation, *TNFRSF11B* was found a common gene in both mutations (Figure 5.8).

Two pathways specfic to the fALS-*TARDBP* truncated mutation were dysregulated, the TGF beta signalling pathway showing, *BMP4* and *BMP7* dysregulated gene specifically and the VEGF signalling pathway showing, *NOS3* and *PTGS2* dysregulated gene (Figure 5.9 and 5.10).

Table 5.12: Genes involved in response to steroid hormone stimulus in the cytoplasmic truncation mutation

Gene symbol	Gene name	P-value	Fold change
ADM	Adrenomedullin	0.01	2.43
ALDH1A2	Aldehyde dehydrogenase 1 family, member A2	0.01	3.88
ARNT2	Aryl-hydrocarbon receptor nuclear translocator 2	0.05	-1.53
A2M	Alpha-2-macroglobulin	0.002	6.06
BCHE	Butyrylcholinesterase	0.01	23.48
BMP4	Bone morphogenetic protein 4	0.002	43.56
BMP7	Bone morphogenetic protein 7	0.01	16.66
CCL2	Chemokine (C-C motif) ligand 2	0.04	2.78
CCND2	Cyclin D2	0.006	3.48
CDKN1A	Cyclin-dependent kinase inhibitor 1A (p21, Cip1)	0.01	2.14
CPS1	Carbamoyl-phosphate synthetase 1, mitochondrial	0.001	-2.76
CTTNBP2	Cortactin binding protein 2	0.03	-12.17
CYP11A1	Cytochrome P450, family 11, subfamily A, polypeptide 1	0.03	2.42
ESR1	Estrogen receptor 1	0.04	-3.79
GPX4	Glutathione peroxidase 4 (phospholipid hydroperoxidase)	0.02	2.02
GSTM3	Glutathione S-transferase mu 3 (brain)	1.70603E-05	3.83
IL1B	Interleukin 1, beta	0.003	4.27
MSTN	Myostatin	0.01	3.83
NOS3	Nitric oxide synthase 3 (endothelial cell)	0.009	-7.83
OXT	Oxytocin, prepropeptide	0.002	49.14
PTGS2	Prostaglandin-endoperoxide synthase 2 (prostaglandin G/H synthase and cyclooxygenase)	0.016	-4.68
TNFRSF11B	tumor necrosis factor receptor superfamily, member 11b	7.46286E-05	2.70
WFDC1	WAP four-disulfide core domain 1	0.0001	26.02

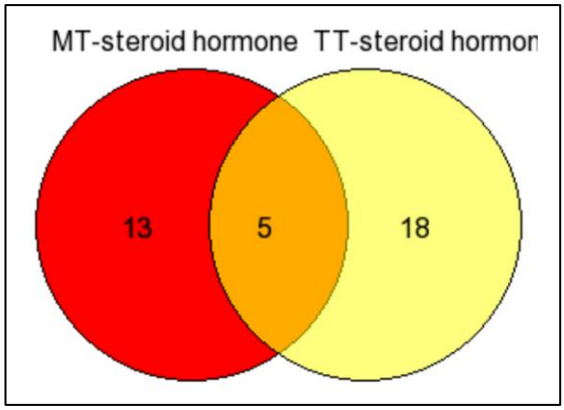

Figure 5.6: *Comparative analysis of the steroid hormone differentially expressed genes in MT and TT mutations. Venn diagram showing 13 genes specific to response to steroid hormone stimulus in fALS-TARDBP missense mutation while 18 genes were specific to fALS-TARDBP truncated mutation and 5 genes were in common.*

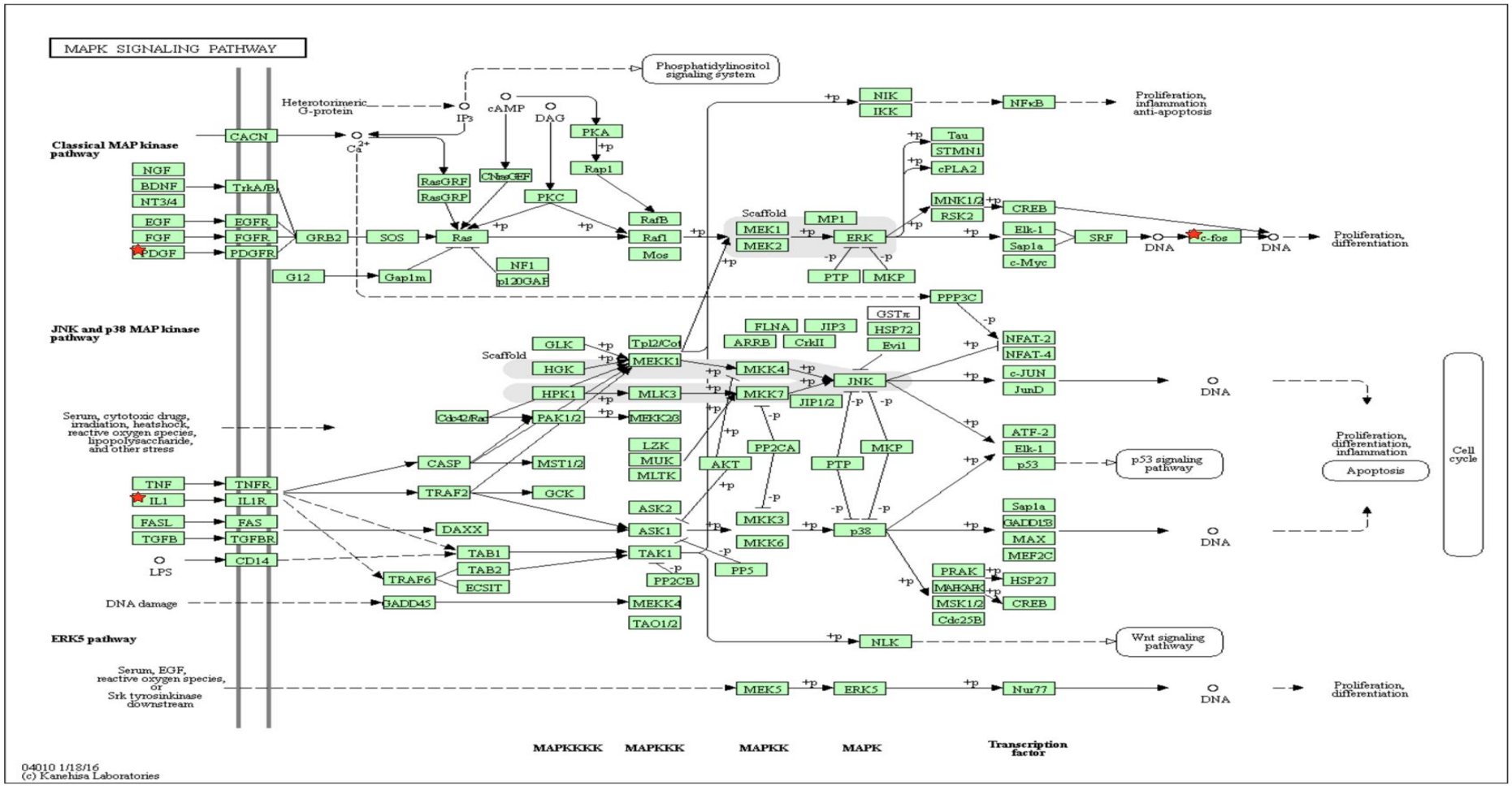

Figure 5.7: *MAP kinase pathway showing, Fos and PDGF dysregulated gene specifically to fALS-TARDBP missense mutation and IL1 specifically to the fALS-TARDBP truncated mutation. Thus, the MAP kinase pathway is possibly a common dysregulated pathway in both mutation types.*

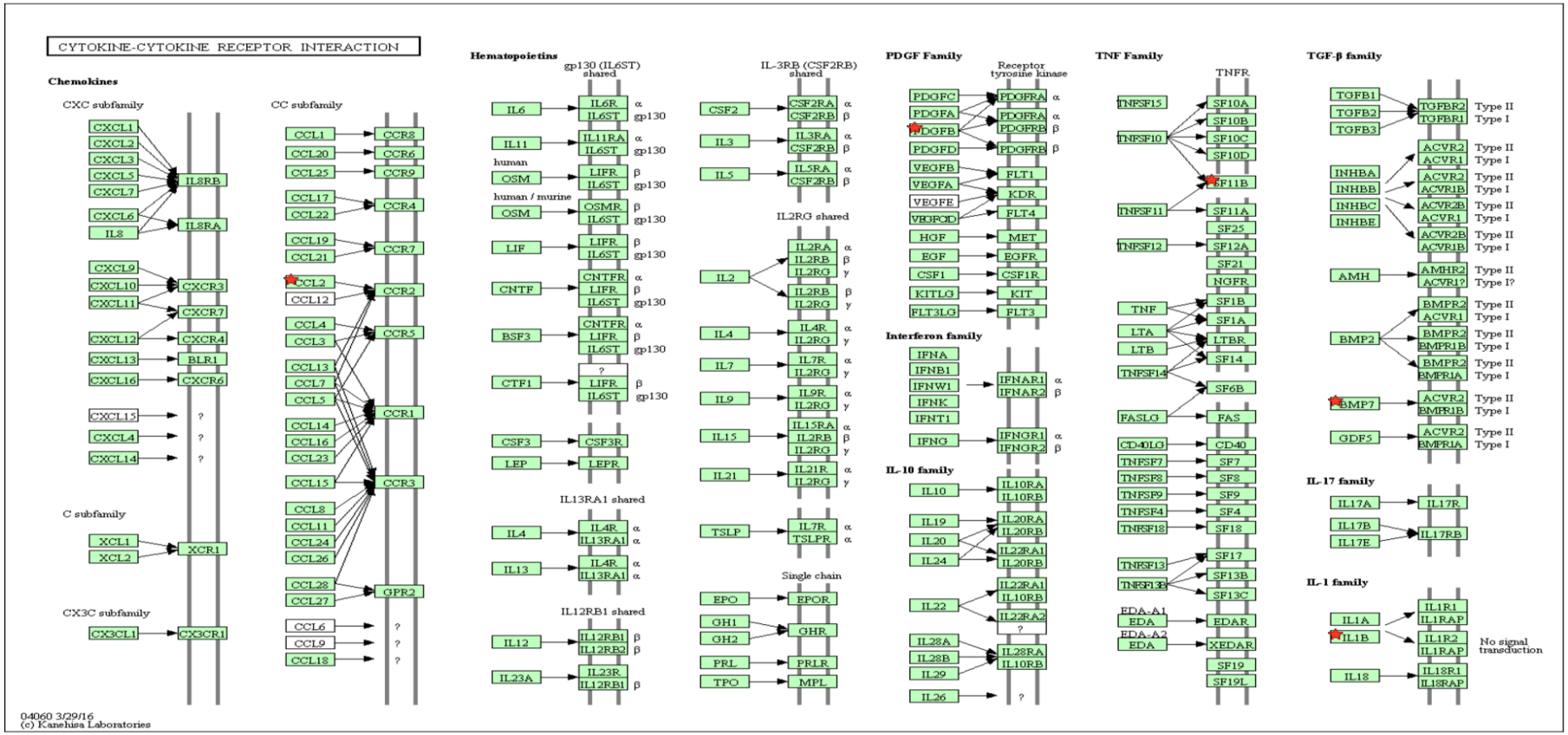

Figure 5.8: *Cytokine- cytokine receptor interaction pathway showing, PDGFB dysregulated gene specifically to fALS-TARDBP missense mutation and CCL2, BMP7, IL1B genes specifically to the fALS-TARDBP truncated mutation. TNFRSF11B is a common gene in both mutations. Thus, the cytokine- cytokine receptor interaction pathway is possibly a common dysregulated pathway in both mutation types.*

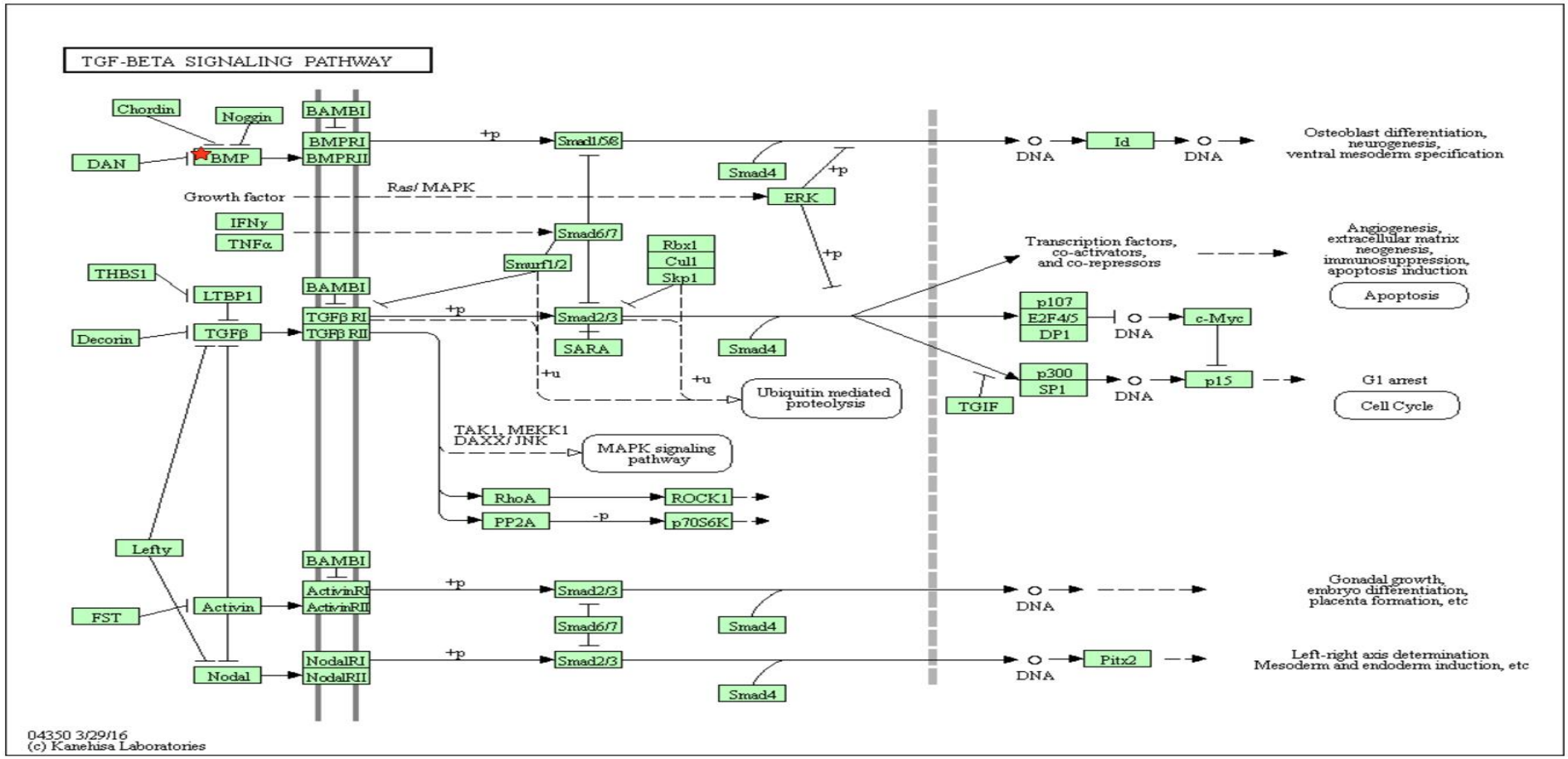

Figure 5.9: *TGF beta signalling pathway showing, BMP4, BMP7 dysregulated gene in TARDBP truncated mutation. This may suggest that the TGF beta signalling pathway is dysregulated in fALS-TARDBP truncated mutation.*

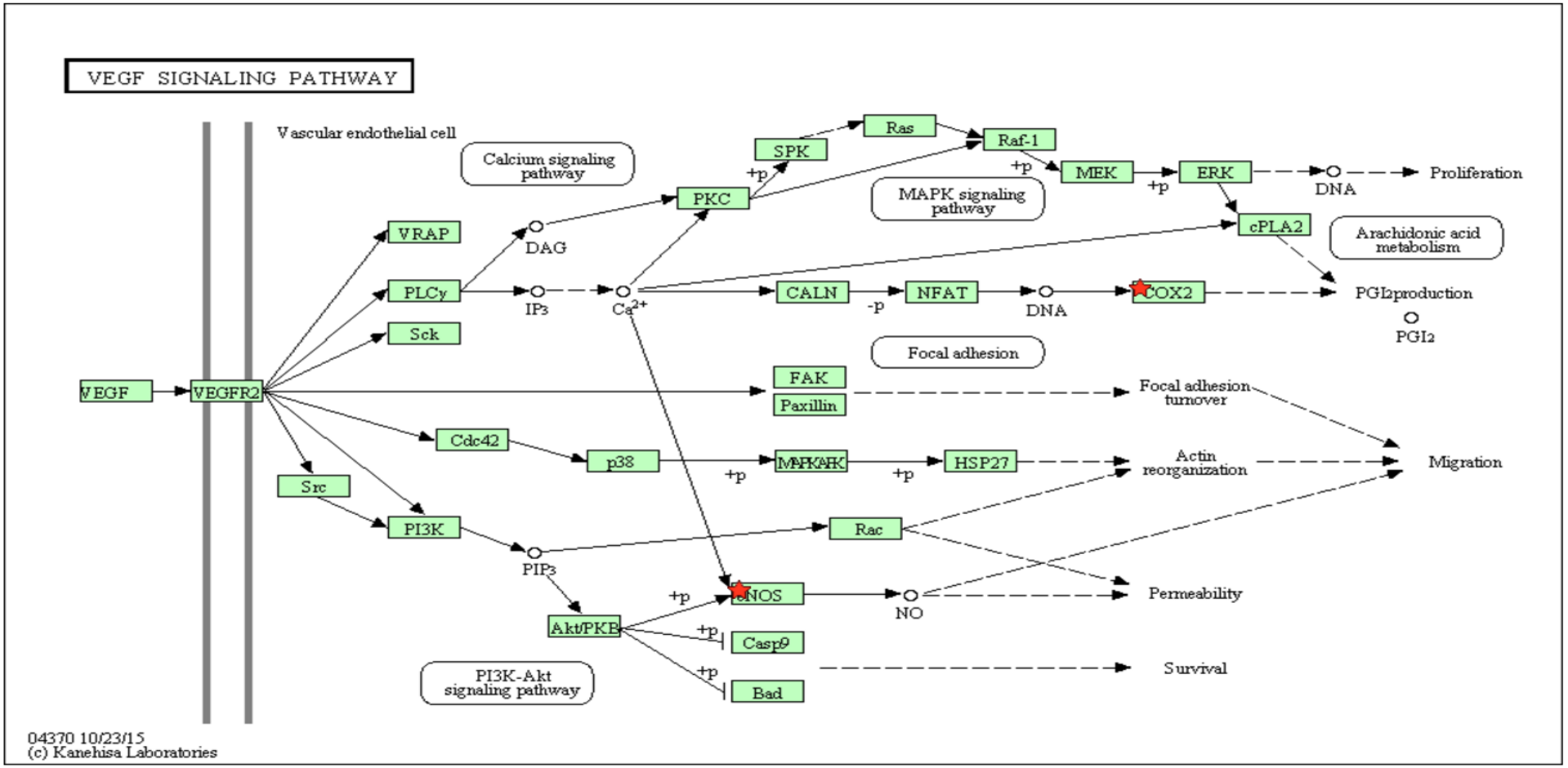

Figure 5.10: *VEGF signalling pathway showing, NOS3 and PTGS2 dysregulated gene specifically to TARDBP truncated mutation. This may suggest that the VEGF signalling pathway is dysregulated in fALS-TARDBP truncated mutation.*

5.3.2.4 Blood vessel development

The biological process blood vessel development was also shown to be dysregulated in the fALS-*TARDBP* truncated mutation with the majority of genes being up-regulated (Table 5.13). A further discussion of the dysregulated genes is shown below.

Rho GTPase activating protein 24 (*ARHGAP24*) was down-regulated (FC=-1.9). ARHGAP24 regulates endothelial cell migration and proliferation. Mice knocked-down for the *ARHGAP24* gene showed a suppression of endothelial cell migration and proliferation. This strongly supports the association of *ARHGAP24* with angiogenesis (Su et al., 2004). The tumour necrosis factor (ligand) superfamily, member 12 (*TNFSF12*) was increased (FC=1.9). The encoded cytokine is involved in angiogenesis by mediating endothelial cell migration and proliferation. Also it may initiate cell death by activating apoptotic pathways (Chicheportiche et al., 1997, Lynch et al., 1999). In addition the EGF-like-domain, multiple 7 (*EGFL7*) was elevated (FC=2.5). EGFL7 is also known as vascular endothelial statin has a role in promoting vasculogenesis (Parker et al., 2004). The mesenchyme homeobox 2 (*MEOX2*) was up-regulated (FC=5). MEOX2 has been shown to be involved in vascular differentiation. It was also previously suggested to be linked with Alzheimer's disease (Gorski et al., 1993, Wu et al., 2005). The transforming growth factor, alpha (*TGFA*) was up-regulated (FC=8). TGFA is a signalling molecule that activates pathways involved in proliferation, differentiation and angiogenesis (Singh and Coffey, 2014). Also the anti-angiogenic factor, collagen, type XV (*COL15A1*), alpha 1, (*COL15A1*) was increased (FC=2) (Sasaki et al., 2000). In addition, the plasminogen activator, tissue (*PLAT*) was up-regulated (FC=2). PLAT is produced by the vascular endothelial cells which is considered a fibrinolytic enzyme that converts plasminogen to plasmin maintaining blood viscosity (Ny et al., 1984).

Three fibroblast growth factors were up-regulated. These proteins have diverse cellular functions which are best characterized as mitogenic and especially during

embryonic development. Each of these genes were found to predominate in function in particular tissues, the fibroblast growth factor 10 (*FGF10*) was shown to have a role in keratinocyte development (FC=8.6) and was up-regulated (Sun et al., 2015). Also the fibroblast growth factor 18 (*FGF18*) was shown to participate in bone and cartilage synthesis (FC=5) (Moore et al., 2005). Whilst the fibroblast growth factor 9 (glia-activating factor) (*FGF9*) was shown to function as male sex determining factor (FC=2.8) (Colvin et al., 2001). Two transcription factors that belong to the T-box family were up-regulated, the T-box 1(*TBX1*) (FC=4.5) which is involved in the maturation of normal arterial blood. Mutant *TBX1* in mice showed phenotypic features of DiGeorge syndrome (Jerome and Papaioannou, 2001). Also, the T-box 4 (*TBX4*) was increased (FC=10.5). T-box 4 is essential for the development of the lower limbs. A *TBX4* mutation was associated small patella syndrome (SPS) (Agulnik et al., 1996, Bongers et al., 2004). Furthermore, genes involved in cell proliferation and migration were up-regulated. The Thy-1 cell surface antigen (*THY1*) was increased (FC=2). THY1 was shown to mediate cell differentiation, proliferation and apoptosis. It is also involved in adhesion and was considered a tumour suppressor for ovarian cancer (Lung et al., 2005, Rege and Hagood, 2006). Also, the bone morphogenetic protein 4 (*BMP4*) which is important for the development of bone and cartilage synthesis was up-regulated (FC=43.5) (Bakrania et al., 2008). Also, the epithelial mitogen homolog (mouse) (*EPGN*) was increased (FC=12). EPGN binds to the epidermal growth factor receptor which activates cell migration and proliferation signalling pathways (Herbst and Bunn, 2003).

The adrenergic, alpha-1B-, receptor (*ADRA1B*) was up-regulated (FC=3). ADRA1B is a G protein-coupled receptor which is capable of binding to the phospholipase C enzyme to facilitate the hydrolysis of the compound phosphatidylinositol 4, 5-bisphosphate into diacylglycerol and inositol 1,4,5-trisphosphate. Both diacylglycerol and inositol 1, 4, 5-trisphosphate act as second messengers that activate other proteins in the cell. One of the outcomes of the activation of these molecules is the elevation of Ca++ ion concentration in the cytoplasm along with protein kinases. The phospholipase C, delta 3 (*PLCD3*) was also shown to be increased (FC=1.7) (Haenisch et al., 2010, Jungmichel et al.,

2014). Finally, the proinflammatory cytokine interleukin 1, beta (*IL1B*) was also up-regulated (FC=4).

In contrast, a lower number of genes involved in blood vessel development were down-regulated. The vasodilator enzyme nitric oxide synthase 3 (endothelial cell) (*NOS3*) was shown to be down-regulated (FC=-7.8) (Dasar et al., 2012). Furthermore, the hypoxia inducible factor 1, alpha subunit (basic helix-loop-helix transcription factor) (*HIF1A*) was reduced (FC=-1.8). HIF1A is a transcription factor that is induced in response to oxygen levels. It is involved in transcribing several gene associated with angiogenesis such as erythropoietin and VEGF (Lee et al., 2004). In addition, endothelial cell-specific chemotaxis regulator (*ECSCR*) was down-regulated (FC=-6.6). The encoded gene is capable of initiating endothelial cell signalling transduction which promotes cell migration (Verma et al., 2010). The Integrin, alpha 4 (antigen CD49D, alpha 4 subunit of VLA-4 receptor) (*ITGA4*) was decreased (FC=-3.5). It was suggested that ITGA4 is involved in endothelial cell adhesion and proliferation (Garmy-Susini et al., 2005). The inhibitor of DNA binding 1, dominant negative helix-loop-helix protein (*ID1*) was reduced (FC=-3). The ID1 is a member of the Inhibitor of DNA binding family which they inhibit DNA transcription by binding to the transcription factors (Lyden et al., 1999). Moreover, neuropilin 2 (*NRP2*) was down-regulated (FC=-3.7). It has been reported that the NRP2 receptors were involved in neuronal migration during brain development by determining their destinations. Neurons that express NRP2 were shown to be directed to the cortex region (Marin et al., 2001).

Comparing the genes related to angiogenesis in the cytopasmic missense mutation to the genes related to blood vessel development in truncated mutation revealed that the majority of genes were distinct to each muation with only five gene being shared, *COL15A1, TBX4, TGFA, THY1* and *TNFSF12* (Figure 5.11). It was shown that genes involved in angiogenesis and blood vessel development were dysregulated and mostly up-regulated in the fALS-*TARDBP* missense mutation and truncated mutation respectively. It was interesting to find if any of the genes form both mutations belonged to similar or distinct pathway. Thus, genes from both mutations were combined then uploaded into DAVID and KEGG pathway was generated in order to identify the significant pathways. It was shown

that *FGF9, FGF10, FGF18* and *IL1B* from the fALS-*TARDBP* truncated mutation were dysregulated in the MAP signalling pathway (Figure 5.12). None of the genes from the missense mutation list belonged to a particular pathway.

Table 5.13: Genes involved in blood vessel development in the cytoplasmic truncation mutation

Gene symbol	Gene name	P-value	Fold change
ADRA1B	Adrenergic, alpha-1B-, receptor	0.04	3.42
ARHGAP24	Rho GTPase activating protein 24	0.02	-1.90
BMP4	Bone morphogenetic protein 4	0.002	43.56
COL15A1	Collagen, type XV, alpha 1	0.04	2.30
ECSCR	Endothelial cell-specific chemotaxis regulator	0.01	-6.62
EGFL7	EGF-like-domain, multiple 7	0.01	2.56
EPGN	Epithelial mitogen homolog (mouse)	0.002	12.21
FGF9	Fibroblast growth factor 9 (glia-activating factor)	0.01	2.84
FGF10	Fibroblast growth factor 10	0.01	8.64
FGF18	Fibroblast growth factor 18	0.01	5.45
HIF1A	Hypoxia inducible factor 1, alpha subunit (basic helix-loop-helix transcription factor)	0.01	-1.84
ID1	Inhibitor of DNA binding 1, dominant negative helix-loop-helix protein	0.02	-3.36
IL1B	Interleukin 1, beta	0.003	4.27
ITGA4	Integrin, alpha 4 (antigen CD49D, alpha 4 subunit of VLA-4 receptor)	0.001	-3.53
MEOX2	Mesenchyme homeobox 2	0.04	5.04
NOS3	Nitric oxide synthase 3 (endothelial cell)	0.009	-7.83
NRP2	Neuropilin 2	0.008	-3.79
PLAT	Plasminogen activator, tissue	0.03	2.06
PLCD3	Phospholipase C, delta 3	0.03	1.79
TBX1	T-box 1	0.002	4.55
TBX4	T-box 4	0.04	10.59
THY1	Thy-1 cell surface antigen	0.002	2.23
TGFA	Transforming growth factor, alpha	0.007	8.20
TGFBR3	Transforming growth factor, beta receptor III	0.002	2.45
TNFSF12	Tumor necrosis factor (ligand) superfamily, member 12	0.01	1.98

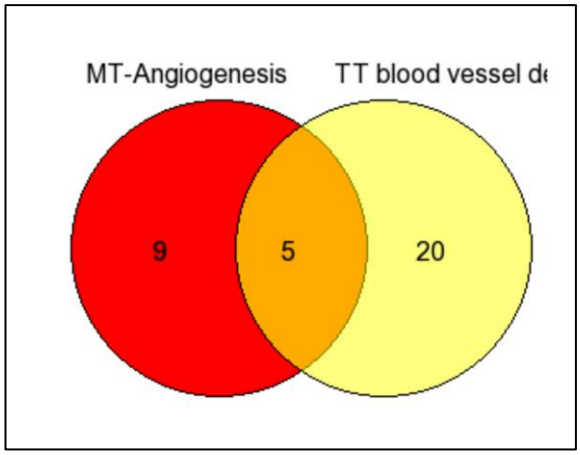

Figure 5.11: *Comparative analysis of the angiogenesis/blood vessel development differentially expressed genes in both MT and TT mutations. Venn diagram showing 9 genes specific to angiogenesis in fALS-TARDBP missense mutation while 20 genes were specific to blood vessel development in fALS-TARDBP truncated mutation and 5 genes were in common.*

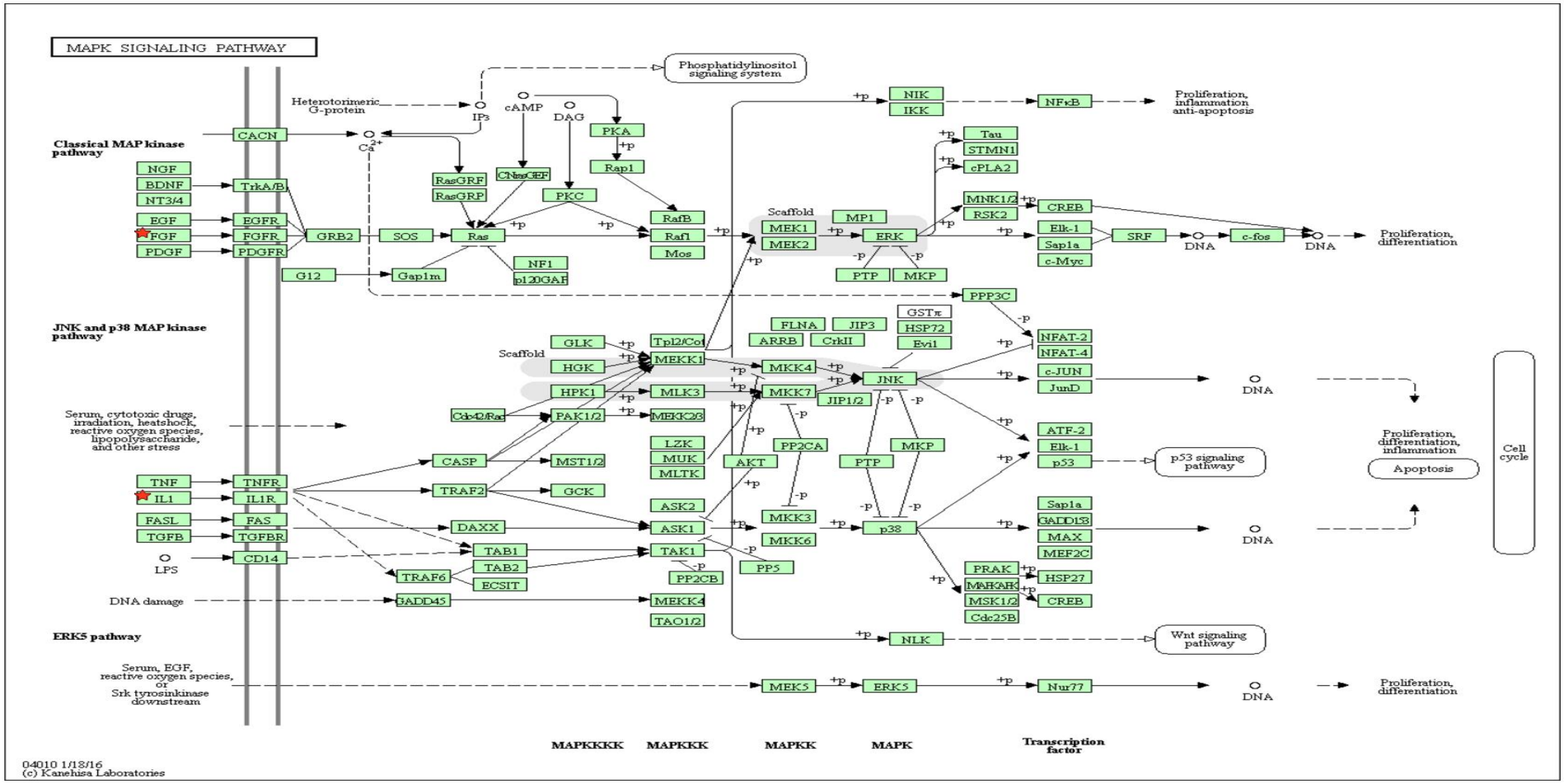

Figure 5.12: *MAP kinase pathway showing, FGF9, FGF10, FGF18 and IL1B dysregulated gene specifically to TARDBP truncated mutation. MAP kinase pathway perhaps a dysregulated pathway in fALS-TARDBP truncated mutation.*

5.3.2.5 Vesicle-mediated transport

The axonal transport system in neuronal cells is mediated by the motor proteins, kinesins and dyneins, which are essential molecules for cargo, organelle and vesicle movement along the axon in both directions i.e. anterograde and retrograde. Studies showed that defective axonal transport is strongly linked to ALS. Here, it is shown that the largest number of dysregulated genes were related to vesicle-mediated transport in the fALS-*TARDBP* truncated mutation (Table 5.14). A further elucidation of the genes involved is described below.

Clathrins are a family of protein receptors that mediate endocytosis via receptor mediated endocytosis. Two genes belonging to the clathrins were up-regulated. The adaptor-related protein complex 1, mu 2 subunit (*AP1M2*) (FC=10). AP1M2 is expressed mainly in the epithelium and is involved in cargo endocytosis from the plasma membrane to the Golgi apparatus where molecules are modified (Robinson and Pimpl, 2014). Also the clathrin light chain subunit, clathrin, light chain (Lcb) (*CLTB*) was increased (FC=2) (Wu et al., 2016). Furthermore, three members of the vesicle associated membrane proteins that are involved in the docking and fusion process of the synaptic vesicles were increased, vesicle-associated membrane protein 2 (synaptobrevin 2) (*VAMP2*) (FC=1.6), vesicle-associated membrane protein 5 (myobrevin) (*VAMP5*) (FC=2) and syntaxin 8 (*STX8*) (FC=1.7) (McNew et al., 2000). Protein kinase C and casein kinase substrate in neurons 3 (*PACSIN3*) was increased (FC=2.5). PACSIN3 is involved in vesicle trafficking by associating the actin filaments with the vesicles (Roach and Plomann, 2007).

Membrane associated ring-CH proteins are enzymes that are involved in protein degradation by adding ubiquitin to the lysine residues of protein molecules. As a result, signalling pathways which end by protein elimination are activated. Recently, these proteins were shown to be involved in other functions such as endocytosis and protein transport (Samji et al., 2014). Two members of the membrane associated ring-CH proteins were up-regulated, membrane-associated ring finger (C3HC4) 2 (*MARCH2*) (FC=1.8) and membrane-associated ring finger (C3HC4) 3 (*MARCH3*) (FC=2.6). The coatomer protein

complex, subunit zeta 2 (*COPZ2*) was also up-regulated (FC=1.7). COPZ2 is part of the coatomer protein complex which is involved in the synthesis of the coat protein I (COPI). COPI is essential for Golgi-to-ER retrograde transport (Moelleken et al., 2007). Also the regulating synaptic membrane exocytosis 1(*RIMS1*) gene which creates a scaffold with other exocytotic proteins that mediate vesicles release at the synaptic cleft was increased (FC=3) (Schoch et al., 2002). The chemokine (C-X-C motif) ligand 16 (*CXCL16*) was increased (FC=2.6). CXCL16 is a cytokine that is a member of the CXC chemokine family. CXCL16 is involved in leukocyte trafficking. Also it is activated in angiogenesis and is activated in immune response (Zlotnik and Yoshie, 2000).

The B-cell receptor-associated protein 31 (*BCAP31*) was up-regulated (FC=1.5) BCAP31 is expressed on the surface of the endoplasmic reticulum and highly expressed in neurons. It is involved in vesicle export and also directs defective proteins to the degradation pathway (Cacciagli et al., 2013). Also, the low density lipoprotein receptor-related protein associated protein 1 (*LRPAP1*) was increased (FC=2). This protein is the ligand for the low density lipoprotein (LDL) receptor. LRPAP1 binds to members of the low density lipoprotein receptor family and interferes with the other ligand molecules to bind to the low density lipoprotein receptor (Korenberg et al., 1994). The naked cuticle homolog 2 (Drosophila) (*NKD2*) was up-regulated (FC=9).

The encoded protein negatively regulated Wnt receptor signalling (Wharton et al., 2001). Moreover, the v-Ha-ras Harvey rat sarcoma viral oncogene homolog (*HRAS*) was increased (FC=10.6). HRAS is a GTPase enzyme that is activated under the influence of growth factors. Therefore, it is involved in cell proliferation and growth though the activation of the MAPK signalling pathway (Zhang et al., 2006). The glutamate receptor, ionotropic, AMPA 1 (*GRIA1*) was up-regulated (FC=2.8). *GRIA1* encodes for the ionotropic AMPA 1 receptor that is activated upon the binding to glutamate which stimulate the opening of the ion channels in the neuronal cells (Anggono and Huganir, 2012). Also the amyloid beta (A4) precursor-like protein 1 (*APLP1*) was increased (FC=3). *APLP1* encodes for the membrane bound glycoprotein which is similar in structure to the amyloid beta

precursor the hallmark for AD (Guilarte, 2010). The ferritin light polypeptide (*FTL*) was increased (FC=1.8). The gene encodes for the light peptide chain of the iron storage protein ferritin (Carmona et al., 2014).

In contrast, a group of genes were down-regulated. Four genes associated with the COPII-coated vesicles that are involved in the protein transport were down-regulated, SEC24 family, member A (S. cerevisiae) (*SEC24A*) (FC=-1.7), SEC24 family, member D (S. cerevisiae) (*SEC24D*) (FC=-2), SEC23 homolog A (S. cerevisiae) (*SEC23*) (FC=-1.7) and the ADP-ribosylation factor GTPase activating protein (*ARFGAP1*) (FC=-1.9) (Bigay et al., 2003, Mancias and Goldberg, 2008). Also, the USO1 homolog, vesicle docking protein (yeast) (*USO1*) was reduced (FC= -1.5). This protein was shown to bind to the COP2 which mediates vesicle exiting from the endoplasmic reticulum and targeting to the Golgi apparatus (Allan et al., 2000).

Furthermore, the component of oligomeric Golgi complex 3 (*COG3*) was decreased (FC=-1.7). COG3 is a member of the conserved oligomeric Golgi complex which is essential for glycoprotein modifications and transport (Ungar et al., 2002). Also the dedicator of cytokinesis 1 (*DOCK1*) was decreased (FC=-2.8). DOCK1 is a protein that controls the Rac-GTPase enzyme during the G-protein activation through signalling transduction. Therefore, it is involved in several processes including phagocytosis (Bagci et al., 2014). The dopey family member 1(*DOPEY1*) was reduced (FC=-2). DOPEY1 was suggested to be involved in vesicle transport within the cell (Tanaka et al., 2014). Moreover, the kinesin family member 20A (*KIF20A*) was down-regulated (FC=-4.7). As has been stated previously kinesins are proteins that mediate the movement of cellular organelles including vesicles within the cell (Bosco et al., 2010).

Four genes related to clathrins were down-regulated. The phosphatidylinositol binding clathrin assembly protein (*PICALM*) was decreased (FC=-1.5). It is involved in the clathrin-vesicle assembly which mediates endocytosis. Reduced levels of PICALM have been associated with AD (Thomas et al., 2016). Also, the clathrin interactor 1 (*CLINT1*) was reduced (FC=-2). CLINT1 is part of the clathrin-coated vesicles which are involved in retrograde transport from the endosomes

to the trans-Golgi (Saint-Pol et al., 2004). The two other genes were component of the clathrin-coated vesicles which facilitate the transport of proteins from the plasma membrane to the Golgi apparatus and hence to the lysosomes were down-regulated, adaptor-related protein complex 1, gamma 1 subunit (*AP1G1*) (FC=-1.7) and adaptor-related protein complex 3, beta 2 subunit (*AP3B2*) (FC=-6) (Robinson and Bonifacino, 2001). Furthermore, the dynamin 1 (*DNM1*) gene was down regulated (FC=-1.7). It was suggested that dynamin 1 is an essential protein for the dissociation of the newly formed endocytosed vesicle from the plasma membrane (Razzaq et al., 2001). Also, the protein amphiphysin (*AMPH*) was decreased (FC=-3) which has been suggested to play a role in directing the DNM1 protein to the site of vesical cleavage (Razzaq et al., 2001). In addition, the Ca++-dependent secretion activator 2 (*CADPS2*) was reduced (FC=-4). CADPS2 mediates exocytosis of vesicles and has been suggested to be associated with autism. *CADPS2*$^{-/-}$ mice showed phenotypic characteristics similar to autism (Sadakata et al., 2007).

Huntingtin (*HTT*) was reduced (FC=-1.7). HTT is a nuclear protein that is involved in regulating gene expression by binding to transcription factors. Mutations in this gene cause Huntington's disease (Futter et al., 2009). Two cellular receptors were down-regulated. The adenosine A2a receptor (*ADORA2A*) was one (FC=-11). ADORA2A is a G protein coupled receptor which was shown to increase cAMP levels. Therefore, it has a role in cardiac rhythm, inflammation and blood flow (Raskovalova et al., 2005). Also, the low density lipoprotein receptor-related protein 4 (*LRP4*) (FC=-2). Also known as multiple epidermal growth factor-like domains 7, it was shown to be strongly associated with the activation of the Wnt signalling pathway (Barik et al., 2014).

Other genes that were involved in protein trafficking were down-regulated. ADP-ribosylation factor guanine nucleotide-exchange factor 2 (brefeldin A-inhibited) (*ARFGEF2*) (FC=-2), phosphoinositide kinase, FYVE finger containing (*PIKFYVE*) (FC=-1.7), Golgi associated PDZ and coiled-coil motif containing (*GOPC*) (FC=-1.7), zinc finger, FYVE domain containing 16 (*ZFYVE16*) (FC=-1.6), the N-ethylmaleimide-sensitive factor attachment protein, gamma (*NAPG*)

(FC=-1.6), secretory carrier membrane protein 5 (*SCAMP5*) (FC=-3.9) and synuclein, alpha (non A4 component of amyloid precursor) (*SNCA*) (FC=-5).

Three genes were grouped by DAVID under vesicle-mediated transport which were more related to the immune response. The elastase, neutrophil expressed (*ELANE*) was increased (FC=8). ELANE is an enzyme that is secreted by the neutrophils and monocytes as a response to inflammation (Chua and Laurent, 2006). Also, the pentraxin-related gene, rapidly induced by IL-1 beta (*PTX3*) was elevated (FC=2). PTX3 is an acute phase protein which is has a major role in immune defense against pathogens (Bozza et al., 2006). Furthermore, the CD36 molecule (thrombospondin receptor) (*CD36*) was increased (FC=14). CD36 is an integral membrane protein that is expressed on different types of cells and capable to bind to several ligands, therefore can activate diverse cellular pathways such as: atherogenesis, lipid metabolism and inflammation (Park, 2014).

Table 5.14: Genes involved in vesicle-mediated transport in the cytoplasmic truncation mutation

Gene symbol	Gene name	P-value	Fold change
ADORA2A	Adenosine A2a receptor	0.04	-11.40
AMPH	Amphiphysin	0.009	-3.12
AP1G1	Adaptor-related protein complex 1, gamma 1 subunit	0.02	-1.77
AP1M2	Adaptor-related protein complex 1, mu 2 subunit	0.04	10.40
AP3B2	Adaptor-related protein complex 3, beta 2 subunit	0.04	-6.18
APLP1	Amyloid beta (A4) precursor-like protein 1	0.01	3.12
ARFGAP1	ADP-ribosylation factor GTPase activating protein 1	0.04	-1.96
ARFGEF2	ADP-ribosylation factor guanine nucleotide-exchange factor 2 (brefeldin A-inhibited)	0.006	-2.06
BCAP31	B-cell receptor-associated protein 31	0.04	1.56
BLOC1S1	Biogenesis of lysosomal organelles complex-1, subunit 1	0.02	1.81
CADPS2	Ca++-dependent secretion activator 2	0.01	-4.22
CD36	CD36 molecule (thrombospondin receptor)	0.001	14.46
CLINT1	Clathrin interactor 1	0.006	-2.04
CLTB	Clathrin, light chain (Lcb)	0.006	2.05
COG3	Component of oligomeric golgi complex 3	0.04	-1.71
COPZ2	Coatomer protein complex, subunit zeta 2	0.01	1.74
CXCL16	Chemokine (C-X-C motif) ligand 16	0.04	2.62
DOCK1	Dedicator of cytokinesis 1	0.01	-2.82
DOPEY1	Dopey family member 1	0.02	-2.44
DNM1	Dynamin 1	0.03	-1.79
ELANE	Elastase, neutrophil expressed	0.002	8.22
FTL	Ferritin, light polypeptide	0.03	1.89
GOPC	Golgi associated PDZ and coiled-coil motif containing	0.02	-1.77
GRIA1	Glutamate receptor, ionotropic, AMPA 1	0.006	2.80
HRAS	v-Ha-ras Harvey rat sarcoma viral oncogene homolog	0.04	10.61
HTT	Huntingtin	0.03	-1.71
KIF20A	Kinesin family member 20A	0.004	-4.74
LRP4	Low density lipoprotein receptor-related protein 4	0.04	-2.08
LRPAP1	Low density lipoprotein receptor-related protein associated protein 1	0.02	2.04

LRRN3	Leucine rich repeat neuronal 3	0.01	5.92
MARCH2	Membrane-associated ring finger (C3HC4) 2	0.03	1.81
MARCH3	Membrane-associated ring finger (C3HC4) 3	0.01	2.64
MON2	MON2 homolog (S. cerevisiae)	0.04	-2.15
NAPG	N-ethylmaleimide-sensitive factor attachment protein, gamma	0.04	-1.60
NKD2	Naked cuticle homolog 2 (Drosophila)	0.04	9.29
NME2	Non-metastatic cells 1, protein (NM23A) expressed in; NME1-NME2 readthrough transcript; non-metastatic cells 2, protein (NM23B) expressed in	0.02	-3.41
PACSIN3	Protein kinase C and casein kinase substrate in neurons 3	0.0006	2.52
PICALM	Phosphatidylinositol binding clathrin assembly protein	0.04	-1.57
PIKFYVE	Phosphoinositide kinase, FYVE finger containing	0.04	-1.72
PTX3	Pentraxin-related gene, rapidly induced by IL-1 beta	0.02	2.02
RIMS1	Regulating synaptic membrane exocytosis 1	0.01	3.02
SCAMP5	Secretory carrier membrane protein 5	0.005	-3.97
SEC23A	SEC23 homolog A (S. cerevisiae)	0.04	-1.75
SEC24A	SEC24 family, member A (S. cerevisiae)	0.02	-1.75
SEC24D	SEC24 family, member D (S. cerevisiae)	0.004	-2.09
SNCA	Synuclein, alpha (non A4 component of amyloid precursor)	0.01	-5.08
STON1-GTF2A1L	Stonin 1; STON1-GTF2A1L readthrough transcript; general transcription factor IIA, 1-like	0.04	10.40
STX8	Syntaxin 8	0.03	1.74
USO1	USO1 homolog, vesicle docking protein (yeast)	0.03	-1.58
VAMP2	Vesicle-associated membrane protein 2 (synaptobrevin 2)	0.01	1.68
VAMP5	Vesicle-associated membrane protein 5 (myobrevin)	0.01	2.11
ZFYVE16	Zinc finger, FYVE domain containing 16	0.03	-1.69

5.3.3 Comparative analysis of differentially expressed genes in the cytoplasmic fractions of missense and truncation *TARDBP* mutation

It was interesting to identify which genes belonged to each mutation type and which were common in all of the fALS-*TARDBP* cases examined. Therefore, a venn diagram was generated using the online GeneVenn programme (Figure 5.13). The venn diagram showed 609 differentially expressed genes were specific to the missense mutation, 1178 differentially expressed genes were specific to the truncated mutation and 259 genes were common. The genes were explored using the DAVID analysis tool. The fALS-*TARDBP* missense mutation showed that the largest number of genes were belonged to cell adhesion while the fALS-*TARDBP* truncated mutation showed the highest enriched and largest number of genes were found in vesicle-mediated transport. A small group of the common genes were related to response to organic substance (Tables 5.15, 5.16 & 5.17). Therefore, it is clearly shown that distinct biological processes affected by the two types of mutation in fALS-*TARDBP* within the cytoplasmic fraction.

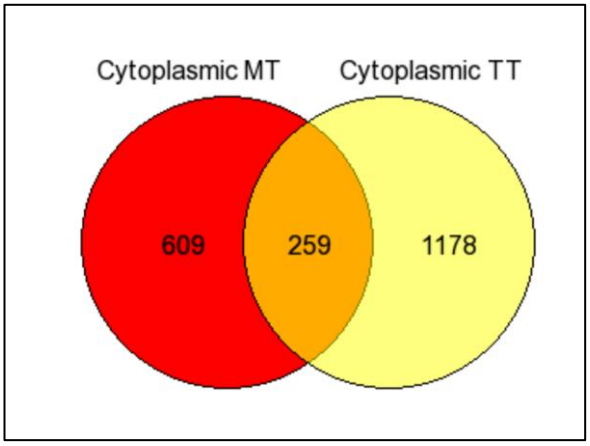

Figure 5.13: *Comparative analysis of differentially expressed genes in the cytoplasmic fractions of missense and truncation TARDBP mutation. Venn diagram showing 609 genes specific to the cytoplasmic missense mutation, 1178 genes specific to the cytoplasmic truncation mutation and 259 genes were found common in both types of mutations.*

Table 5.15: Functionally enriched biological processes generated by DAVID of cytoplasmic specific missense mutation genes. GO= gene ontology, no.=number, ES=Enrichment score

GO	Biological process	Gene no.	P-value	ES
BP_FAT	In utero embryonic development	11	1.3E-2	3.04
BP_FAT	Cell adhesion	30	4.9E-3	2.86
BP_FAT	Response to endogenous stimulus	27	9.6E-6	2.84
BP_FAT	Regulation of RNA metabolic process	61	1.2E-2	2.32
BP_FAT	Pattern specification process	18	3.7E-4	1.81
BP_FAT	Tube development	18	1.2E-4	1.55
BP_FAT	Cytoskeleton organization	20	1.3E-2	1.52
BP_FAT	Kidney development	7	3.2E-2	1.35
BP_FAT	Angiogenesis	9	3.1E-2	1.32

Table 5.16: Functionally enriched biological processes generated by DAVID of cytoplasmic specific truncated mutation genes. GO= gene ontology, no.=number, ES=Enrichment score

GO	Biological process	Gene no.	P- value	ES
BP_FAT	Vesicle-mediated transport	46	3.2E-3	2.43
BP_FAT	Stem cell differentiation	7	5.1E-3	2.39
BP_FAT	Positive regulation of cell cycle	12	3.2E-2	2.12
BP_FAT	Response to organic substance	28	3.8E-2	2.05
BP_FAT	Regulation of cytokine production	7	1.4E-3	1.81

Table 5.17: Functionally enriched biological processes generated by DAVID of the cytoplasmic common genes. GO= gene ontology, no.=number, ES=Enrichment score

GO	Biological process	Gene no.	P-value	ES
BP_FAT	Response to organic substance	15	1.4E-2	1.65

5.4 Discussion

RNA sequencing has been shown to provide more accurate and precise detection and measurements of the transcriptome as it can identify mutations, alternative splicing and posttranscriptional modifications (Morozova and Marra, 2008). RNA sequencing was performed on the cytoplasmic fALS-*TARDBP* missense mutation and truncated mutation in order to generate an in depth understanding of the effect of mutant TDP-43 from both types of mutation and to confirm previous genes identified as deregulated by the other experimental paradigms; the Human Exon 1.0 ST Array and the HTA.

In the present study, three biological repeats from patients and controls age and gender matched were studied. The differentially expressed genes in the cytoplasm of fALS-*TARDBP* missense mutation and truncated mutation were grouped into biological processes using the online DAVID analysis tool. Figure 5.14 shows a diagram that demonstrates the significantly identified biological processes in both mutations. The response to steroid hormone stimulus and angiogenesis / blood vessel development were the biological processes that are present in both cytoplasmic fALS-*TARDBP* mutations therefore they are discussed together below. However, the rest of the biological processes are discussed further individually in respect to each type of mutation.

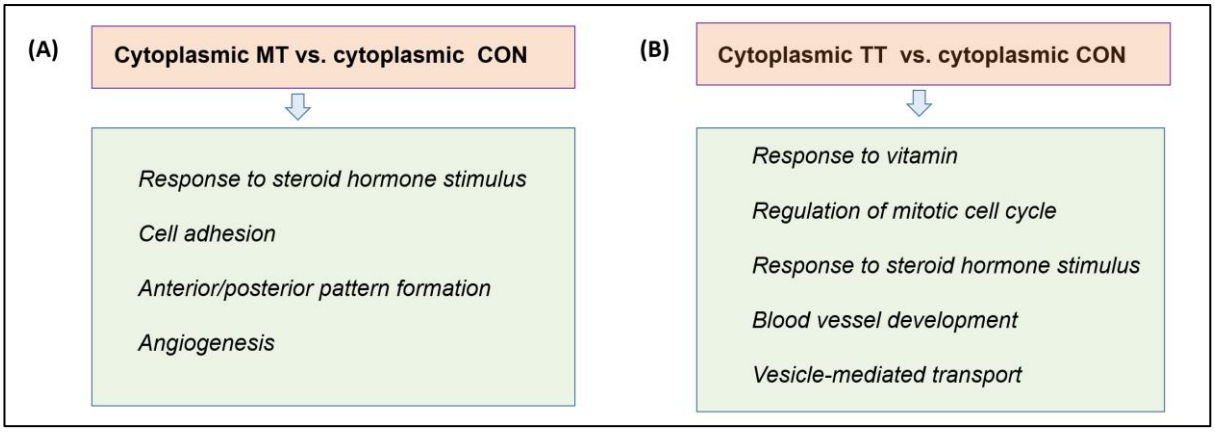

Figure 5.14: *A diagram illustrating significantly identified biological processes. (A) Cytoplasmic fALS-TARDBP MT and (B) Cytoplasmic fALS-TARDBP TT. MT=missense mutation, TT truncation mutation.*

5.4.1 Biological processes presented in both cytoplasmic fALS-*TARDBP* MT and TT mutations

5.4.1.1 Response to steroid hormone stimulus

As the incidence of patients diagnosed with ALS is higher in males than in females, several studies suggested the role of steroid sex hormones in the pathogenesis of ALS (Jones, 1988). A qualitative analysis was performed on female ALS patients which showed that the longer exposure to oestrogen throughout life was associated with a higher survival rate compared to females with lower exposure to oestrogen (de Jong et al., 2013). Furthermore, the serum levels of free testosterone hormone was reported to be significantly lower in ALS male patients than in controls (Militello et al., 2002). Patacchioli et al., assessed the adrenal activity of ALS patients by measuring the salivary cortisol levels which were reported to be higher in ALS patients that controls (Patacchioli et al., 2003). Also, morning cortisol plasma levels were shown to be higher in ALS patients (Spataro et al., 2015). In addition, ALS mouse models showed dysregulated hormonal changes. An elevated level of serum corticosterone was observed in

SOD1^{G93A} transgenic mice (Fidler et al., 2011). Reduced plasma levels of testosterone and elevated levels of corticosterone were observed in Wobbler mouse (Deniselle et al., 2016). Therefore, a disrupted endocrine system is suggested to be associated with ALS and may account of the higher incidence of ALS in males compared to females.

Steroid hormones are lipid soluble molecules that are able to diffuse through the plasma membrane and bind to the targeted receptor forming hormone-receptor complexes that are able to induce gene expression change (Schwartz et al., 2016). In the current study, dysregulated genes related to steroid hormones were demonstrated. The highest significantly up-regulated genes in fALS-*TARDBP* missense mutation were *BCHE, WFDC1*, *GATA3, GFBP2, PDGFB* and *SST* while the highest increased genes in the fALS-*TARDBP* truncated mutation were *BCHE, WFDC1, BMP4, BMP7* and *OXT*. In contrast, the significantly down-regulated genes in fALS-*TARDBP* missense mutation were *SERPINA1* and *SLC6A1*. However, in fALS-*TARDBP* truncated mutation these were *CTTNBP2* and *NOS3*. It would be interesting to further investigate the hormonal status of fALS patients in the present study (if available) at the time of skin biopsy collection and/or clinical history of hormonal measurements during their lifetime. This may help to obtain an indication of how these genes were influenced by hormones.

However, the literature shows that some of the dysregulated genes in the present study have been investigated previously and were related to steroid hormone changes. The BCHE enzyme levels were studied in chick enterocytes in both gender types. Interestingly, BCHE enzyme level was significantly higher in females than males. This may suggest the involvement of sex hormones in *BCHE* expression (Sine et al., 1991). Also, the same observation was demonstrated in female rats which showed higher BCHE plasma levels than males (Alves-Amaral et al., 2010). Furthermore, the marked elevation of *BCHE* in the current study may indicate that more cleavage of the neurotransmitter acetylcholine is occurring in the motor neurons (Greig et al., 2002a).

Moreover, the *GFBP2* was shown also to be markedly increased. A study has shown that under the influence of high oestrogen levels the *GFBP2* expression in rat hippocampus was significantly increased compared to controls (Takeo et al., 2009).

Also an elevated levels of *GFBP2* in spinal motor neurons was shown in sALS (Wilczak et al., 2003). Moreover, Zhang et al., reported that *TARDBP*^{A315T} mice model demonstrated a hyperactive SST in the cortical region of the mice model brain which may have a role in motor neurons excitotoxicity observed in the disease (Zhang et al., 2016). The SST gene was also shown to be elevated in fALS-*TARDBP* missense mutation. The *OXT* was shown to be markedly increased in the fALS-*TARDBP* truncated mutation. *OXT* expression was shown to be influenced by oestrogen (Ivell and Walther, 1999).

In the current study, the majority of genes that were influenced by steroid hormones were markedly increased with only five genes being shared, *BCHE, WFDC1, CCND2, GSTM3* and *TNFRSF11B.* Although both mutations were harbouring the same biological processes, distinct genes were observed. Thus, it may be suggested that fALS-*TARDBP* patients should not be treated similarly as the underlying affected pathways may be different.

5.4.1.2 Angiogenesis / Blood vessel development

The current literature illustrates that defective genes related to angiogenesis have been strongly associated with ALS (Oosthuyse et al., 2001, Gao and Xu, 2008). Also, the chapter 4: HTA experiment showed genes associated to angiogenesis in both fALS-*TARDBP* mutation types being dysregulated (Refer to section 4.9.1.1). Here, using RNA sequencing technology to study gene expression in both mutations revealed angiogenesis / blood vessel development biological processes to be affected with a higher number of dysregulated gene and significantly higher fold changes compared to HTA.

Oosthuyse et al., reported that the deletion of the hypoxia-response element of the *VEGF* gene in a mouse model resulted in low expression of the VEGF in

brain and spinal cord with symptoms resembling an ALS type disorder. Therefore, dyregulated *VEGF* was strongly associated with ALS. In the current study, a member of the *VEGF* family, *VEGFA*, was shown to be decreased in the fALS-*TARDBP* missense mutation. This strongly supports Oosthuyse et al., observation that *VEGFA* could be a significant candidate gene associated with the fALS-*TARDBP* missense mutation. Furthermore, the majority of the fALS-*TARDBP* missense genes were increased, *ANGPT1, EMCN, HAND, HTATIP2, IL18, PGF, TBX4, THY1, TGFA* and *TNFSF12.* Only four genes were decreased, *ANGPT2, ANGPTL6, COL15A1* and *VEGFA.* Also it was interesting to find that *IL18* was shared with the HTA experiment which may indicate its association with fALS-*TARDBP* missense mutation.

The fALS-*TARDBP* truncated mutation revealed a higher number of genes compared to the missense mutation, this was also observed in the HTAs. The majority of the genes in the fALS-*TARDBP* truncated mutation were also increased, *ADRA1B, BMP4, COL15A1, EGFL7, EPGN, FGF9, FGF10, FGF18, IL1B, MEOX2, PLAT, PLCD3, TBX1, TBX4, THY1, TGFA, TGFBR3* and *TNFSF12.* The decreased genes were *ARHGAP24, ECSCR, HIF1A, ID1, ITGA4, NOS3* and *NRP2.* Also, a several genes were shared with the HTA experiment, *EPGN, MEOX2, TBX1,THY1* and *TNFSF12* with a similar increased trend.

Furthermore, comparing the genes related to angiogenesis in the cytoplasmic missense mutation to the blood vessel development in the truncated mutation showed that the majority of gene were distinct to each mutation with only five genes being shared. Therefore, approaching each type of fALS-*TARDBP* mutation separately may be required when designing treatments for patients.

5.4.2 Cytoplasmic MT vs. CON

5.4.2.1 Cell adhesion

Current literature illustrates a limited number of observations linking ALS to dysregulated adhesion molecules. Ono et al., reported decreased levels of collagen IV in both skin and serum of ALS patients and the levels of collagen IV were shown to progressively decrease with the progress of ALS. Therefore, it was strongly suggested to be correlated with ALS pathogenesis (Ono et al., 1998). Ono et al., also reported a significant reduction in plasma fibronectin in ALS patients (Ono et al., 2000). Using a whole human genome oligo microarray, Aronica et al, demonstrated dysregulated collagens and integrins in sALS (Aronica et al., 2015). In the present work, studying gene expression using RNA sequencing revealed a large number of genes that belonged to a cell adhesion group were significantly affected in the fALS-*TARDBP* missense mutation with the majority being significantly down-regulated.

Cadherins are important cell surface molecules that have a role in signal transduction and promote normal cell development and morphogenesis (Maitre and Heisenberg, 2013). A large group of members of the cadherin superfamily were significantly reduced, *CDH2*, *CLSTN3*, *DCHS1*, *CDHR5*, *PCDH9* and *PCDHGC5*. Furthermore, members of the collagen family were also reduced, *COL5A1, COL15A*, *COL16A1* and *COL7A1.* Also integrins that facilitate focal adhesion*, PKD1, TNC, DCHS1* and *AMIGO2* were down-regulated. Decreased expression of integrins such as: *ITGA1, ITGB4, ITGA3, ITGB1 ITGA5, ITGAV* and *ITGA11* and the extracellular matrix molecules such as collagens including collagen IV and fibronectin have been previously demonstrated in sALS (Aronica et al., 2015).

Furthermore, a couple of genes that belonged to cellular pathways that mediate cell adhesion were also down-regulated. *WISP1* which activates the WNT pathway was reduced, the *AEBP1* which negatively regulated the MAP kinase pathway was also decreased, the *FLRT1* which is involved in the RAS/RAF/ERK pathway was down-regulated and *TSC1* which promotes the mTORC1 signalling

pathway was decreased. Moreover, *SSPO* which is involved in axonal guidance was decreased. Two genes that facilitate uterine cell adhesion were also reduced, *POSTN* and *TROAP.*

Several members of the cadherin superfamily were shown to be up-regulated in fALS-*TARDBP* missense mutation, *FAT3*, *CDH10* and *PCDH17.* Also *PKP3* that facilitates the binding of cadherins to intracellular actin filaments was increased. Other cell adhesion molecules that mediate cell adhesion, migration and proliferation were also up-regulated, *CD9, L1CAM, THY1, ALX1* and *SIRPA.* Furthermore, focal adhesion molecules which are cell surface proteins that mediate adhesion though binding to the extracellular matrix were up-regulated, *EMCN* and *SORBS1*.

The laminin family of proteins are involved in the adhesion to the extracellular matrix. Laminin 1 was previously shown to be expressed in astrocytes of sALS-*SOD1* spinal cord. In the current work, *LAMA3* a member of the laminin family was highly expressed (Wiksten et al., 2007). Interestingly, genes that are normally expressed in the CNS were also shown to be expressed in fibroblasts, *CLSTN2* which is expressed on GABAergic neurons and *ROBO2* that mediates axonal guidance were up-regulated. This observation along with the previously shown results (section 3.6.1.1.2) demonstrates that fibroblasts are good models that may mimic some of the changes on the CNS and therefore would be a favourable model to study ALS.

The majority of the effect of *TARDBP* mutation is fALS was shown to involve down-regulation cell adhesion molecules. Dysregulated cadherins, integrins and collagens were strongly suggested to be linked with the fALS-*TARDBP* missense mutation.

5.4.2.1 Anterior/posterior pattern formation

A group of genes related to the anterior/posterior pattern formation were dysregulated in the fALS-*TARDBP* missense mutation.

The transcription factors *ALX1, HOXB9, HOXD13* were increased. Mutations in *ALX1* have been linked to frontonasal dysplasia (Dee et al., 2013). In addition, *HOXB9* was shown to be expressed at a high level in breast cancer and lung metastasis (Hayashida et al., 2010). Mutations in *HOXD13* have been shown to be linked with hand-foot-genital syndrome (HFGS) (Goodman et al., 2000). *PSEN2* was increased, mutations in *PSEN2* are associated with AD and have been thought to cause the increased levels of APP in AD (Levy-Lahad et al., 1996). On the other hand, several transcription factors that promote cell proliferation were decreased *HOXB3, HOXC6*, *HOXC8, HOXD9* and *HHEX*. Also the *ARC* gene has shown to be reduced. It was suggested that ARC plays a role in promoting long term potentiation and memory by increasing the AMPAR on the postsynaptic neuron (Pevzner et al., 2012).

5.4.3 Cytoplasmic TT vs. CON

5.4.3.1 Response to vitamins

Vitamins are vital organic compounds that mediate normal cell development though their effect on gene expression (Wang et al., 1995, Landes et al., 2003, McGrane, 2007). Surprisingly, a group of up-regulated genes were categorised under response to vitamin and were the highest enriched biological process in fALS-*TARDBP* truncated mutation.

Two genes involved in bone and cartilage synthesis *BMP4* and *BMP7* were up-regulated. BMP7 was shown to be positively influenced by vitamin D (Nobili and Reif, 2015). Furthermore, vitamin A was shown to induce an increased expression of *HSD17B2* which also was increased in the fALS-*TARDBP* truncated mutation (Su et al., 2007). In addition, two genes involved in vitamin A synthesis were up-regulated, *ALDH1A2* and *RBP4.* Vitamin C was suggested to be involved in cellular reprogramming by activating four genes one of which was the *KLF4* which showed increased expression in fALS-*TARDBP* truncated mutation (Shi et al., 2010).

The overall elevated levels of genes influenced by vitamins could be due to the effect of the vitamin supplement added to the fibroblasts culture media to maintain their growth, and although these supplements are added to all fibroblast cultures, the ALS fibroblasts may be responding differently due to their genetic background. It also could reflect ALS patients' diet which is high in supplements which leaves epigenetic changes on patient derived cells (Rosenfeld and Ellis, 2008).

5.4.3.2 Regulation of mitotic cell division

Genes involved in cell division were shown to be dysregulated in the fALS-*TARDBP* truncated mutation. The most apparent reason for detecting these genes was that fibroblasts used in this project as a model to study fALS-*TARDBP*. Fibroblasts are known to undergo continuous cell division therefore it is possible to identify genes related to mitotic cell division. However, it was shown that neuronal cell cycle genes continue to be active during neurogenesis until full maturation is reached. Afterwards, cell cycle arrest occurs and neurons become post-mitotic however some cell division proteins are detectable and the reason for that is still not fully understood. Also, DNA repair enzymes continue to be active (Herrup and Yang, 2007).

A couple of studies have reported an increased expression of genes related to cell cycle in ALS. Mutant *SOD1*^{G93A} transgenic mouse showed an increased expression of cell cycle genes in motor neurons, protein phosphatase 3 catalytic subunit (*PPP3CA*), cyclin L1 (*CCNL1*), cyclin E2 (*CCNE2*) and cyclin D2 (*CCND2*) (Ferraiuolo et al., 2007). Furthermore, the cell cycle checkpoint kinases (*CHK1/CHK2*) was also shown to be increased in sALS (Aronica et al., 2015). In the current study a group of genes related to cell division were up-regulated. Genes that were involved in cell proliferation were increased *EPGN, CD28*, *TGFA* and *IGF2*. Interestingly, *EPGN* was also shown to be up-regulated in the fALS-*TARDBP* truncated mutation using the HTA (section 4.6.1.2.1). A study have shown that DNA damage in post-mitotic neurons activates cell cycle re-entry which may be responsible for the neuronal death (Kruman et al., 2004).

Therefore, the increased expression of genes related to mitotic cell division may contribute to the neuron loss in the disease.

Moreover, genes involved in cell proliferation *MTBP, SPHK1* were down-regulated. Also, genes involved in cellular microtubule *NUSAP1*, centromere and kinetochore separation *ESPL1, NEK2, CENPF* and *DLGAP5* were reduced. *NUSAP1* was shown to be decreased in fALS-*TARDBP* missense mutation using the Human Exon Array 1.0 ST (section 3.8.2.1).

5.4.3.3 Vesicle-mediated transport

Axonal transport consists of three main structures which are: the cytoskeleton, the motor proteins and the carried cargo/vesical/organelle. Defects in any of these structures may result in failure to complete the transportation process effectively and be deleterious to the health of the neuron. Defective axonal transport has been reported by many studies and was strongly suggested to be associated with ALS, especially in the ALS-*SOD1* mutation (De Vos et al., 2008). In 1999, Williamson and Cleveland studied the possible effect of *SOD1* mutation on axonal transport. Interestingly, both mutant *SOD1*^{G85R} and *SOD1*^{G37R} mouse models revealed slow axonal transport at an early stage of the disease (Williamson and Cleveland, 1999). Furthermore, deficient retrograde axonal transport was reported in *SOD1*^{G93A} mice (Bilsland et al., 2010). Also, the inhibition of kinesin-1 was reported in a mutant *SOD1*^{G93A} mouse model (Morfini et al., 2013). In the current work, the largest number of dysregulated genes were related to vesicle-mediated transport in the fALS-*TARDBP* truncated mutation and the majority were down-regulated.

Mutations in kinesin have been linked to ALS-*SOD1*, and here a member of the kinesin family, *KIF20A* was reduced (Bosco et al., 2010). Also, a mutation in *DNM1* was suggested to be associated with ALS. *DNM1* levels were reduced in the fALS-*TARDBP* truncated mutation (Munch et al., 2004). Furthermore, clathrin related genes were also down-regulated; *AP1G1, AP3B2, CLINT1* and *PICALM.*

It has been shown that reduced levels of *PICALM* might be associated with AD (Thomas et al., 2016). The membrane trafficking gene *SNCA* was reduced. Mutations in *SNCA* have been reported in PD (Siddiqui et al., 2016). Also, the neuronal vesicle trafficking genes were decreased. Genes involved in Golgi to ER retrograde transport and in the oligomeric Golgi complex were also decreased. There is a significant reduction in the membrane trafficking genes in fALS-*TARDBP* truncated mutation which may have a serious consequences on motor neurons. Deficit in axonal transport is one of the major underlying aetiology in ALS which contribute to cell death and this was also observed in the current work.

5.4.4 The overall effect of the *TARDBP* mutations on the biological processes in fALS and the possibility of identifying biomarkers

ALS is a multifactorial complex disease and is nowadays categorized into several subgroups depending on the underlining genetic risk factor. Therefore, developing a generalized treatment for ALS patients is not the best approach and personalized medicine is highly recommended for proper treatment, prognostic and diagnostic biomarkers development (Picher-Martel et al., 2016). As this will provide a better prediction to patient survival.

Gene expression profiling using RNA sequencing highlighted significant dysregulated biological processes in respect to each mutation type. In the cytoplasmic fALS-*TARDBP* missense mutation, marked dysregulation in cell adhesions was observed showing the largest number of differentially expressed genes. Moreover, the cytoplasmic fALS-*TARDBP* truncated mutation showed significant changes in gene involved in vesical-mediated transport and were also harbouring the highest number of genes. Furthermore, gene influenced by steroid hormones and genes related to angiogenesis/ blood vessel development were shared by both mutations however the majority of the genes were distinct to mutation type. The outcome of the present work strongly supports the possibility of identifying biomarkers as a diagnostic test to differentiate between fALS-

TARDBP subtypes as well prognostic biomarkers to help in monitoring and predicting fALS-*TARDBP* patient survival. Also, the current work could shed light on possible targeted therapies for fALS-*TARDBP* patients which may significantly reduce the tragic motor neuron loss observed in the d fALS-*TARDBP*. However, further validation steps remain to be established.

5.4.5. Microarray GeneChip® vs. RNA sequencing

In the current work gene expression profiling was approached by both microarray GeneChip® and RNA sequencing technologies. The current work showed that these tools varies in their robustness to detect gene expression. Advantages and disadvantages of each technology is shown in Table 5.17 (Wang et al., 2009b).

Table 5.17: The advantages and disadvantages of microarray GeneChip® and RNA sequencing

	Microarray GeneChip®	RNA sequencing
Advantages	1-Identify alternative spliced transcripts and novel transcripts to an extent.	1-Robust in identifying alternative spliced transcripts and novel transcripts although this was not performed in this work due to time constraint. 2-Accurate measurement of the RNA transcript expression, as reads are counted precisely. 3-Identify all known and unknown genes. 4-Identify abnormal transcript structure such as insertion, deletion and inversion. 5-Do not require normalization as the reads are mapped to the human genome reference sequence. 6-Higher reproducibility. 7-RNA concentration required for sequencing is low.
Disadvantages	1-Probes were designed according to previously identified genes in databases. 2-Inaccurately measurement of gene expression due to averaging signal intensity of all probes. 3-Require normalization. 4-In some instances fail reproducibility by other gene expression method such as qRT-PCR 4-RNA concentration required is high.	1-Large data to handle. 2-Required sophisticated bioinformatics skills in order to handle with data.

Chapter 6: Discussion

ALS is a devastating chronic progressive disorder with an average survival rate 2-5 years. To date, there is no definitive underlying cellular pathway identified in ALS that can be targeted for therapy (Cooper-Knock et al., 2012a). The present work aimed to investigate the possible effects of *TARDBP* mutations on gene expression in fALS using fibroblasts as a surrogate model. The hypothesis was that cytoplasmic and nuclear transcriptomic profile from mutant *TARDBP* fibroblasts will generate different transcriptomic profiles than control fibroblasts and will establish the transcripts and pathways dysregulated in the presence of mutations in *TARDBP*. To test the hypothesis, the specific aims were set. The first aim was to obtain a good separation of the cytoplasm and nuclear compartments before extracting RNA. A good degree of RNA separation from each cellular component was achieved. It was shown that the cell fractionation method using osmotic pressure and centrifugation and RNA extraction by Trizol method was significantly better than the commercially available kit (Cell fractionation for Cytoplasmic and Nuclear RNA Purification by Norgen). Monitoring the cell fractionation under the light microscope allowed proper timing for the cellular component separation. Although fibroblasts in this project were cultured up to passage 12, it is worth noting that the higher the passage the more time was required for optimal fractionation. Therefore, using a standardized kit protocol may underestimate the actual separation process and could produce low RNA yields or poor separation.

The current work also aimed to compare the expression profiles of the cytoplasmic and nuclear compartments from control and *TARDBP* mutations fibroblasts and to determine the possible effect of the mutations on the disease process. Transcriptome profiling was approached by GeneChip® microarrays and RNA sequencing. An interesting observation was that although there were a limited number of common significant differentially expressed genes across the GeneChip® microarrays and RNA sequencing, dysregulated RNA processing was repeatedly shown to be affected in the missense mutation in both cellular

compartments. Dysregulated spliceosome complexes have been previously reported in sALS-*TARDBP* (Highley et al., 2014). Genes associated with spliceosome complexes were shown to be dysregulated in the present work, *SART-3, ZCRB1, RBM39*, *SNRNP200* and *PRPF8.* In addition, splicing factors were also dysregulated such as: *SF3A1, SF3A3* and *SFRS15.* Furthermore, the splicing regulatory factor *HNRNPM* was shown to be expressed at low levels in sALS fibroblasts (Raman et al., 2015). In contrast, in the present work *HNRNPM* was shown to be increased in fALS, perhaps reflecting a mutant *TARDBP* specific effect. This strongly suggests the association of dysregulated RNA processing with fALS-*TARDBP* missense mutations.

Whilst literature has shown that the Human Exon Arrays 1.0 ST low robustness due to manufacture design (Gaidatzis et al., 2009), they were still able to detect differentially expressed genes related to RNA processing in both cellular compartment of fALS-*TARDBP* missense mutation. Although, a limited number of differentially expressed genes were identified by the newly designed HTA, RNA processing was shown to be affected in both cellular compartments of fALS-*TARDBP* missense mutation and dysregulated RNA splicing regulation was therefore common in both array types. Furthermore, the HTA recognized novel dysregulated RNA processing related biological processes in the missense mutations such as: mRNA transport, nucleosome organization and regulation of translation. In contrast, the fALS-*TARDBP* truncation mutation did not show RNA processing related pathways in both cellular compartments which may indicate that dysregulated RNA processing is more specific to the missense mutations. Moreover, in the current work there was a reduction in *TARDBP* gene expression in the fALS-*TARDBP* missense mutation. Therefore, it can be predicted that the reason there was marked down-regulation in genes related to RNA splicing, polyadenylation, transport, translation, olfactory receptors, cell adhesion and vesicle-mediated transport could be that their transcripts are associated with TDP-43 in normal conditions. However when *TARDBP* is mutated TDP-43 loses its functional role in RNA processing this result in a disruption of the binding of TDP-43 to transcripts.

Initially, the olfactory receptors were previously categorized as smell sensory receptors and thought to be expressed exclusively in the nose. Recently, olfactory receptors were shown to be expressed all over the human body which may indicate that they have vital roles other than smell (Nguyen et al., 2016). Olfactory receptors were shown to be expressed in the skin, lungs, heart, muscles, kidneys and sperm (Ferrer et al., 2016). Furthermore, it was shown that the activation of olfactory receptors in of the skin allowed cell viability, proliferation and migration. Down-regulation of olfactory receptors were observed in PD frontal cortex (Garcia-Esparcia et al., 2013). In addition, AD, PD and ALS patients achieved low scores in an olfaction test (scratch and sniff test) (Devanand et al., 2000, Doty, 2012, Nguyen et al., 2016). In the current study, the fALS-*TARDBP* truncation mutation showed an enormous number of down-regulated olfactory receptors genes in the nuclear compartment using the HTA. This marked reduction in olfactory receptors in fibroblasts could indicate also their loss in motor neurons in fALS-*TARDBP* truncation mutation which may lead to early cell loss in the disease. As the olfactory receptors were shown specifically in the truncated mutation, an olfactory test could be offered to fALS-*TARDBP* to differentiate between subtypes and aid in the diagnosis.

RNA sequencing is believed to generate the most accurate and precise identification of the transcripts by mapping them to the human genome. In the present work RNA sequencing technology uncovered novel pathways in both the fALS missense mutation and the truncated mutation, such as: dysregulated genes influenced by steroid hormones. This observation may justify to an extent male predominance in the disease. Another interesting observation was the identification of a large number of dysregulated cell adhesion genes in fALS-*TARDBP* missense mutation fibroblasts which may translate to possible defective blood and CNS barrier breakdown proposed in the disease process (Garbuzova-Davis and Sanberg, 2014). Furthermore, both mutations shared commonality in angiogenesis which has been proposed to be associated with ALS (Oosthuyse et al., 2001, Greenway et al., 2006).

Moreover, some dysregulated biological processes identified in the present work have been previously identified in ALS as a defective mechanism such as: the

defective cytoskeleton organization in the cytoplasmic fALS-*TARDBP* missense mutation (McMurray, 2000) and the dysregulated vesicle mediated transport system in the cytoplasmic fALS-*TARDBP* truncated mutation which have also been observed in the *SOD1* mutation (De Vos et al., 2008). It is clearly shown that the new approach of cellular separation in gene expression profiling allowed the identification of interesting possible dysregulated biological processes in the fALS-*TARDBP* mutations that could have been masked as a result of studying global gene expression from whole cell RNA extractions.

The comparative analysis of the cytoplasmic vs. nuclear gene expression of the fALS missense mutation revealed that mRNA splicing genes were dysregulated in both cellular fractions using the Human Exon Array 1.0 ST. Also a comparative analysis of the cytoplasmic vs. nuclear gene expression was performed on both mutation types using the HTA. This showed that a substantial number of nuclear genes were differentially expressed and a low number of genes were shared with the cytoplasmic fraction in both mutation types. As TDP-43 is predominantly a nuclear protein that gets mislocated to the cytoplasm when mutated this significant number of differentially expressed genes in the nucleus may indicate the loss of TDP-43 functional role in mRNA splicing which may result in faulty transcripts that are subjected to degradation. It was shown previously in this work that a group of genes related to mRNA transport were down-regulated which supports the increased levels of transcripts in the nucleus as a result of disruptive transport system caused by the mutation.

Moreover, the current project showed a lack of statistically significant validation results of the selected candidate gene in the Human Exon Arrays 1.0 ST and the HTA, although some did confirm the directional change. Since the HTA and the RNA sequencing material used were the same samples it was interesting to cross-compare the expression levels of the genes by both technologies as this may indicate the reasons for lack of validation for some genes. Gene expression of *ADARB1* and *ENAH* which showed a correct directional change by qRT-PCR from the HTA results also showed similar fold changes and significant p-values compared in the RNA sequencing data. In contrast, the *METTL1* and *SEMA5A* showed no difference in qRT-PCR compared to the HTA results. Analysis of the RNA sequencing data showed *METTL1* did not show any difference in gene

expression compared to controls and insignificant p-value (FC=1, p-value= 0.9). In addition the *SEMA5A* showed a lower gene expression than the HTA and insignificant p-value (FC=1.5, p-value=0.07). This observation may explain the reason of not achieving validation of the HTA results. However, more genes should have been selected for validation. Also validating the arrays from additional RNA material would have been favourable.

Most studies aiming for identifying therapeutic targets for disease apply their studies on large cohorts which contain a wide range of variability leading to poor applications of treatments on individualized cases. In the case of ALS, a single drug to a multifactorial disease is perhaps not the best approach for patients. Genetic risk factors and environmental factors both play a vital role in patient response to treatment. Precise understanding of the disease subtypes provides a better understanding of the defective mechanisms to which treatments can be designed. Therefore, personalized medicine would appear to be a promising approach in modern medicine for better therapeutic outcome. It might reduce the serious consequences of generalized treatment to patients such as: toxicity, organ damage and subsequently treatment failure (Mini and Nobili, 2009, Ashley, 2016). The present work showed dysregulated pathways in fALS-*TARDBP* mutations which might possibly be targeted for therapy such as: the dysregulated RNA processing in fALS-*TARDBP* missense mutation and the dysregulated olfactory receptors in the fALS-*TARDBP* truncation mutation. Also the current work sheds light on the possibility of identifying biomarkers for fALS-*TARDBP* subtypes which may help in predicting patient survival. However, further investigation and analysis to confirm these observations is required.

Furthermore, fibroblasts have been shown to be a good model to study fALS-*TARDBP* mutations, as several dysregulated biological processes that were identified mimic changes that occur in motor neurons and therefore make them a favourable model to represent the disease. The truncated TDP-43 has been shown to be expressed in the fibroblasts used in this project (Mead et al., *in preparation*). Recently, there has been a significant development in the feasibility of using induced pluripotent stem cells (iPSC) and subsequent differentiation to motor neurons as a model for neurodegenerative disease (Hedges et al., 2016).

There are advantages and limitations of using iPSC as a model to study ALS. The major advantage of these over fibroblasts is the unlimited self-renewal. However reprograming fibroblasts to iPSC and then motor neurons does have some limitations. Whether or not gene expression profiling of genetically engineered cells will reflect the actual active form of the disease or it will reflect a pre-symptomatic stage of the disease is still unknown. Another concern is whether there will be a loss of epigenetic changes in the iPSC and motor neurons as a result of reprograming. Also, cell reprograming is labour intensive and requires a long period of time to generate the cell type of interest. Lastly, the possibility of altering other genes in iPSC as a result of the genetic manipulation my lead to false gene expression levels but this currently remains unclear (Dolmetsch and Geschwind, 2011, Hedges et al., 2016). In this project fibroblasts were shown to be a good surrogate model for fALS-*TARDBP*. They are easy to collect from patients via skin biopsies, also were easy to grow in the laboratory and showed similarity to motor neurons changes in ALS.

Future work

Future work that could be completed is additional qRT-PCR validation of the differential expressed RNA processing genes in fALS-*TARDBP* missense mutation from the Human Exon Array 1.0 ST results. Genes such as *HNRNPM, HNRNPC, HNRNPD, HNRNPK, SSF3A3, SFRS15, CPSF1* and *LSM10* could be validated as this will support the dysregulation of RNA processing in fALS-*TARDBP* in missense mutation and will evaluate the robustness of the arrays in detecting gene expression. Also, further validation of RNA processing genes shown in fALS-*TARDBP* missense mutation from the HTA could be validated by qRT-PCR. This includes genes related to RNA splicing such as*: SNRPA, U2AF1L4, PABPN1, HNRNPA0, HNRNPF, HNRNPR, SNRNP40, SNRPB2, SNRPE and PHF5A.* Also it would be interesting to attempt the validation by qRT-PCR of the dysregulated mRNA transport genes such as: *MAGOH, MAGOHB, DDX19B, NUPL1* and *QKI.*

It would be interesting to investigate the differentially expressed genes at the alternative splicing level from both the HTA Genechips® and RNA sequencing. This may allow for the identification novel defective transcripts that are associated with the disease pathogenesis. It is also important to validate these alternatively spliced transcripts by PCR and their defective role at the protein level to be investigated by western blot. Moreover, confocal microscopy is a remarkable tool that helps in identifying the localization of transcripts and proteins expressed in the cells. The application of FISH and using the confocal microscope will help in identifying the precise location of the defective transcripts and their proteins in the cell. It may also help in showing the specificity of some genes to each type of mutation such as visualizing the loss of olfactory receptors in fALS-*TARDBP* truncated mutation.

Furthermore, it would be interesting to also analyse the nuclear missense mutations vs. controls and the nuclear truncation mutation vs. controls data that were generated by RNA sequencing. This could also uncover possible dysregulated pathways related to the disease. Moreover, in depth analysis of the cytoplasmic vs. nuclear comparison in both HTA and RNA sequencing. This may highlight the possibility of identifying dysregulated transcripts as a result of the mutation specific to a cellular component. Subsequently, functional analysis of the defective transcripts in other cell models such as NSC34 could be applied.

In summary, although there was some commonality in the fALS-*TARDBP* missense mutation and truncation mutation, the current work strongly supports the dysregulation of RNA processing is more related to the fALS-*TARDBP* missense mutation which was not observed in the truncation mutation. Also, the fALS-*TARDBP* truncation mutation showed other interesting pathways such as dysregulated olfactory receptors. This strongly highlights the importance of personalized medicine for better patient care.

References

Aakula A, Kohonen P, Leivonen SK, Makela R, Hintsanen P, Mpindi JP, Martens-Uzunova E, Aittokallio T, Jenster G, Perala M, Kallioniemi O, Ostling P (2016) Systematic Identification of MicroRNAs That Impact on Proliferation of Prostate Cancer Cells and Display Changed Expression in Tumor Tissue. Eur Urol 69:1120-1128.

Abercrombie M (1970) Contact inhibition in tissue culture. In Vitro 6:128-142.

Abhyankar MM, Urekar C, Reddi PP (2007) A novel CpG-free vertebrate insulator silences the testis-specific SP-10 gene in somatic tissues: role for TDP-43 in insulator function. J Biol Chem 282:36143-36154.

Achsel T, Ahrens K, Brahms H, Teigelkamp S, Luhrmann R (1998) The human U5-220kD protein (hPrp8) forms a stable RNA-free complex with several U5-specific proteins, including an RNA unwindase, a homologue of ribosomal elongation factor EF-2, and a novel WD-40 protein. Mol Cell Biol 18:6756-6766.

Agulnik SI, Garvey N, Hancock S, Ruvinsky I, Chapman DL, Agulnik I, Bollag R, Papaioannou V, Silver LM (1996) Evolution of mouse T-box genes by tandem duplication and cluster dispersion. Genetics 144:249-254.

Aizawa H, Sawada J, Hideyama T, Yamashita T, Katayama T, Hasebe N, Kimura T, Yahara O, Kwak S (2010) TDP-43 pathology in sporadic ALS occurs in motor neurons lacking the RNA editing enzyme ADAR2. Acta Neuropathol 120:75-84.

Al-Saif A, Al-Mohanna F, Bohlega S (2011) A mutation in sigma-1 receptor causes juvenile amyotrophic lateral sclerosis. Ann Neurol 70:913-919.

Alexianu ME, Kozovska M, Appel SH (2001) Immune reactivity in a mouse model of familial ALS correlates with disease progression. Neurology 57:1282-1289.

Allan BB, Moyer BD, Balch WE (2000) Rab1 recruitment of p115 into a cis-SNARE complex: Programming budding COPII vesicles for fusion. Science 289:444-448.

Allen SP, Rajan S, Duffy L, Mortiboys H, Higginbottom A, Grierson AJ, Shaw PJ (2014) Superoxide dismutase 1 mutation in a cellular model of amyotrophic lateral sclerosis shifts energy generation from oxidative phosphorylation to glycolysis. Neurobiol Aging 35:1499-1509.

Alves-Amaral G, Pires-Oliveira M, Andrade-Lopes AL, Chiavegatti T, Godinho RO (2010) Gender-related differences in circadian rhythm of rat plasma acetyl- and butyrylcholinesterase: effects of sex hormone withdrawal. Chem Biol Interact 186:9-15.

Anggono V, Huganir RL (2012) Regulation of AMPA receptor trafficking and synaptic plasticity. Curr Opin Neurobiol 22:461-469.

Aparicio-Erriu IM, Prehn JHM (2012) Molecular mechanisms in amyotrophic lateral sclerosis: the role of angiogenin, a secreted RNase. Front Neurosci-Switz 6.

Aronica E, Baas F, Iyer A, ten Asbroek AL, Morello G, Cavallaro S (2015) Molecular classification of amyotrophic lateral sclerosis by unsupervised clustering of gene expression in motor cortex. Neurobiol Dis 74:359-376.

Asaoka-Taguchi M, Yamada M, Nakamura A, Hanyu K, Kobayashi S (1999) Maternal Pumilio acts together with Nanos in germline development in Drosophila embryos. Nat Cell Biol 1:431-437.

Ashley EA (2016) Towards precision medicine. Nat Rev Genet 17:507-522.

Avemaria F, Lunetta C, Tarlarini C, Mosca L, Maestri E, Marocchi A, Melazzini M, Penco S, Corbo M (2011) Mutation in the senataxin gene found in a patient

affected by familial ALS with juvenile onset and slow progression. Amyotroph Lateral Sc 12:228-230.
Ayala YM, De Conti L, Avendano-Vazquez SE, Dhir A, Romano M, D'Ambrogio A, Tollervey J, Ule J, Baralle M, Buratti E, Baralle FE (2011) TDP-43 regulates its mRNA levels through a negative feedback loop. EMBO J 30:277-288.
Bagci H, Laurin M, Huber J, Muller WJ, Cote JF (2014) Impaired cell death and mammary gland involution in the absence of Dock1 and Rac1 signaling. Cell Death Dis 5:e1375.
Bahr A, Hankeln T, Fiedler T, Hegemann J, Schmidt ER (1999) Molecular analysis of METTL1, a novel human methyltransferase-like gene with a high degree of phylogenetic conservation. Genomics 57:424-428.
Bakrania P, Efthymiou M, Klein JC, Salt A, Bunyan DJ, Wyatt A, Ponting CP, Martin A, Williams S, Lindley V, Gilmore J, Restori M, Robson AG, Neveu MM, Holder GE, Collin JR, Robinson DO, Farndon P, Johansen-Berg H, Gerrelli D, Ragge NK (2008) Mutations in BMP4 cause eye, brain, and digit developmental anomalies: overlap between the BMP4 and hedgehog signaling pathways. Am J Hum Genet 82:304-319.
Bale TL, Davis AM, Auger AP, Dorsa DM, McCarthy MM (2001) CNS region-specific oxytocin receptor expression: Importance in regulation of anxiety and sex behavior. J Neurosci 21:2546-2552.
Bamburg JR, Bloom GS (2009) Cytoskeletal pathologies of Alzheimer disease. Cell Motil Cytoskeleton 66:635-649.
Banci L, Bertini I, Boca M, Girotto S, Martinelli M, Valentine JS, Vieru M (2008) SOD1 and amyotrophic lateral sclerosis: mutations and oligomerization. PLoS One 3:e1677.
Bannwarth S, Ait-El-Mkadem S, Chaussenot A, Genin EC, Lacas-Gervais S, Fragaki K, Berg-Alonso L, Kageyama Y, Serre V, Moore DG, Verschueren A, Rouzier C, Le Ber I, Auge G, Cochaud C, Lespinasse F, N'Guyen K, de Septenville A, Brice A, Yu-Wai-Man P, Sesaki H, Pouget J, Paquis-Flucklinger V (2014) A mitochondrial origin for frontotemporal dementia and amyotrophic lateral sclerosis through CHCHD10 involvement. Brain 137:2329-2345.
Barik A, Lu Y, Sathyamurthy A, Bowman A, Shen C, Li L, Xiong WC, Mei L (2014) LRP4 is critical for neuromuscular junction maintenance. J Neurosci 34:13892-13905.
Bartels CL, Tsongalis GJ (2009) MicroRNAs: novel biomarkers for human cancer. Clin Chem 55:623-631.
Bass BL (2002) RNA editing by adenosine deaminases that act on RNA. Annu Rev Biochem 71:817-846.
Bayatti N, Cooper-Knock J, Bury JJ, Wyles M, Heath PR, Kirby J, Shaw PJ (2014) Comparison of Blood RNA Extraction Methods Used for Gene Expression Profiling in Amyotrophic Lateral Sclerosis. Plos One 9.
Bedford L, Walker R, Kondo T, van Cruchten I, King ER, Sablitzky F (2005) Id4 is required for the correct timing of neural differentiation. Dev Biol 280:386-395.
Beedle AM, McRory JE, Poirot O, Doering CJ, Altier C, Barrere C, Hamid J, Nargeot J, Bourinet E, Zamponi GW (2004) Agonist-independent modulation of N-type calcium channels by ORL1 receptors. Nat Neurosci 7:118-125.
Bendjennat M, Boulaire J, Jascur T, Brickner H, Barbier V, Sarasin A, Fotedar A, Fotedar R (2003) UV irradiation triggers ubiquitin-dependent degradation of p21(WAF1) to promote DNA repair. Cell 114:599-610.

Bertoli-Avella AM, Conte ML, Punzo F, de Graaf BM, Lama G, La Manna A, Polito C, Grassia C, Nobili B, Rambaldi PF, Oostra BA, Perrotta S (2008) ROBO2 gene variants are associated with familial vesicoureteral reflux. J Am Soc Nephrol 19:825-831.

Bigay J, Gounon P, Robineau S, Antonny B (2003) Lipid packing sensed by ArfGAP1 couples COPI coat disassembly to membrane bilayer curvature. Nature 426:563-566.

Bilsland LG, Sahai E, Kelly G, Golding M, Greensmith L, Schiavo G (2010) Deficits in axonal transport precede ALS symptoms in vivo. Proc Natl Acad Sci U S A 107:20523-20528.

Bishop KM, Goudreau G, O'Leary DD (2000) Regulation of area identity in the mammalian neocortex by Emx2 and Pax6. Science 288:344-349.

Blasco H, Bernard-Marissal N, Vourc'h P, Guettard YO, Sunyach C, Augereau O, Khederchah J, Mouzat K, Antar C, Gordon PH, Veyrat-Durebex C, Besson G, Andersen PM, Salachas F, Meininger V, Camu W, Pettmann B, Andres CR, Corcia P, French ALSSG (2013) A rare motor neuron deleterious missense mutation in the DPYSL3 (CRMP4) gene is associated with ALS. Hum Mutat 34:953-960.

Blencowe BJ, Ahmad S, Lee LJ (2009) Current-generation high-throughput sequencing: deepening insights into mammalian transcriptomes. Genes Dev 23:1379-1386.

Bonfils C, Beaulieu N, Chan E, Cotton-Montpetit J, MacLeod AR (2000) Characterization of the human DNA methyltransferase splice variant Dnmt1b. J Biol Chem 275:10754-10760.

Bongers EM, Duijf PH, van Beersum SE, Schoots J, Van Kampen A, Burckhardt A, Hamel BC, Losan F, Hoefsloot LH, Yntema HG, Knoers NV, van Bokhoven H (2004) Mutations in the human TBX4 gene cause small patella syndrome. Am J Hum Genet 74:1239-1248.

Bosco DA, Morfini G, Karabacak NM, Song Y, Gros-Louis F, Pasinelli P, Goolsby H, Fontaine BA, Lemay N, McKenna-Yasek D, Frosch MP, Agar JN, Julien JP, Brady ST, Brown RH, Jr. (2010) Wild-type and mutant SOD1 share an aberrant conformation and a common pathogenic pathway in ALS. Nat Neurosci 13:1396-1403.

Bost F, Aouadi M, Caron L, Binetruy B (2005) The role of MAPKs in adipocyte differentiation and obesity. Biochimie 87:51-56.

Boutahar N, Wierinckx A, Camdessanche JP, Antoine JC, Reynaud E, Lassabliere F, Lachuer J, Borg J (2011) Differential effect of oxidative or excitotoxic stress on the transcriptional profile of amyotrophic lateral sclerosis-linked mutant SOD1 cultured neurons. J Neurosci Res 89:1439-1450.

Boyd MT, Vlatkovic N, Haines DS (2000) A novel cellular protein (MTBP) binds to MDM2 and induces a G1 arrest that is suppressed by MDM2. J Biol Chem 275:31883-31890.

Bozza S, Bistoni F, Gaziano R, Pitzurra L, Zelante T, Bonifazi P, Perruccio K, Bellocchio S, Neri M, Iorio AM, Salvatori G, De Santis R, Calvitti M, Doni A, Garlanda C, Mantovani A, Romani L (2006) Pentraxin 3 protects from MCMV infection and reactivation through TLR sensing pathways leading to IRF3 activation. Blood 108:3387-3396.

Brackertz M, Boeke J, Zhang R, Renkawitz R (2002) Two highly related p66 proteins comprise a new family of potent transcriptional repressors interacting with MBD2 and MBD3. J Biol Chem 277:40958-40966.

Brasch J, Harrison OJ, Honig B, Shapiro L (2012) Thinking outside the cell: how cadherins drive adhesion. Trends in Cell Biology 22:299-310.
Brogna S, Sato TA, Rosbash M (2002) Ribosome components are associated with sites of transcription. Mol Cell 10:93-104.
Brohawn DG, O'Brien LC, Bennett JP, Jr. (2016) RNAseq Analyses Identify Tumor Necrosis Factor-Mediated Inflammation as a Major Abnormality in ALS Spinal Cord. PLoS One 11:e0160520.
Bruijn LI, Houseweart MK, Kato S, Anderson KL, Anderson SD, Ohama E, Reaume AG, Scott RW, Cleveland DW (1998) Aggregation and motor neuron toxicity of an ALS-linked SOD1 mutant independent from wild-type SOD1. Science 281:1851-1854.
Buck L, Axel R (1991) A novel multigene family may encode odorant receptors: a molecular basis for odor recognition. Cell 65:175-187.
Bui MH, Seligson D, Han KR, Pantuck AJ, Dorey FJ, Huang YD, Horvath S, Leibovich B, Chopra S, Liao SY, Stanbridge E, Lerman M, Palotie A, Figlin R, Belldegrun AS (2003) Carbonic anhydrase IX is an independent predictor of survival in advanced renal clear cell carcinoma: Implications for prognosis and therapy. J Urology 169:172-172.
Buratti E, Baralle FE (2010) The multiple roles of TDP-43 in pre-mRNA processing and gene expression regulation. RNA Biol 7:420-429.
Buratti E, Dork T, Zuccato E, Pagani F, Romano M, Baralle FE (2001) Nuclear factor TDP-43 and SR proteins promote in vitro and in vivo CFTR exon 9 skipping. EMBO J 20:1774-1784.
Burgoyne JR, Madhani M, Cuello F, Charles RL, Brennan JP, Schroder E, Browning DD, Eaton P (2007) Cysteine redox sensor in PKGIa enables oxidant-induced activation. Science 317:1393-1397.
Bury JJ, Highley JR, Cooper-Knock J, Goodall EF, Higginbottom A, McDermott CJ, Ince PG, Shaw PJ, Kirby J (2016) Oligogenic inheritance of optineurin (OPTN) and C9ORF72 mutations in ALS highlights localisation of OPTN in the TDP-43-negative inclusions of C9ORF72-ALS. Neuropathology 36:125-134.
Butcher NJ, Kiehl TR, Hazrati LN, Chow EW, Rogaeva E, Lang AE, Bassett AS (2013) Association between early-onset Parkinson disease and 22q11.2 deletion syndrome: identification of a novel genetic form of Parkinson disease and its clinical implications. JAMA Neurol 70:1359-1366.
Cacciagli P, Sutera-Sardo J, Borges-Correia A, Roux JC, Dorboz I, Desvignes JP, Badens C, Delepine M, Lathrop M, Cau P, Levy N, Girard N, Sarda P, Boespflug-Tanguy O, Villard L (2013) Mutations in BCAP31 cause a severe X-linked phenotype with deafness, dystonia, and central hypomyelination and disorganize the Golgi apparatus. Am J Hum Genet 93:579-586.
Cappello P, Blaser H, Gorrini C, Lin DC, Elia AJ, Wakeham A, Haider S, Boutros PC, Mason JM, Miller NA, Youngson B, Done SJ, Mak TW (2014) Role of Nek2 on centrosome duplication and aneuploidy in breast cancer cells. Oncogene 33:2375-2384.
Cappello S, Gray MJ, Badouel C, Lange S, Einsiedler M, Srour M, Chitayat D, Hamdan FF, Jenkins ZA, Morgan T, Preitner N, Uster T, Thomas J, Shannon P, Morrison V, Di Donato N, Van Maldergem L, Neuhann T, Newbury-Ecob R, Swinkells M, Terhal P, Wilson LC, Zwijnenburg PJG, Sutherland-Smith AJ, Black MA, Markie D, Michaud JL, Simpson MA, Mansour S, McNeill H, Gotz M, Robertson SP (2013) Mutations in genes encoding the cadherin receptor-ligand

pair DCHS1 and FAT4 disrupt cerebral cortical development. Nature Genetics 45:1300-+.
Carmona U, Li L, Zhang L, Knez M (2014) Ferritin light-chain subunits: key elements for the electron transfer across the protein cage. Chem Commun (Camb) 50:15358-15361.
Carvill GL, McMahon JM, Schneider A, Zemel M, Myers CT, Saykally J, Nguyen J, Robbiano A, Zara F, Specchio N, Mecarelli O, Smith RL, Leventer RJ, Moller RS, Nikanorova M, Dimova P, Jordanova A, Petrou S, Helbig I, Striano P, Weckhuysen S, Berkovic SF, Scheffer IE, Mefford HC, Syndro ERE (2015) Mutations in the GABA Transporter SLC6A1 Cause Epilepsy with Myoclonic-Atonic Seizures. American Journal of Human Genetics 96:808-815.
Chambers I, Frampton J, Goldfarb P, Affara N, McBain W, Harrison PR (1986) The structure of the mouse glutathione peroxidase gene: the selenocysteine in the active site is encoded by the 'termination' codon, TGA. EMBO J 5:1221-1227.
Chari A, Golas MM, Klingenhager M, Neuenkirchen N, Sander B, Englbrecht C, Sickmann A, Stark H, Fischer U (2008) An assembly chaperone collaborates with the SMN complex to generate spliceosomal SnRNPs. Cell 135:497-509.
Chariot A, Castronovo V, Le P, Gillet C, Sobel ME, Gielen J (1996) Cloning and expression of a new HOXC6 transcript encoding a repressing protein. Biochem J 319 (Pt 1):91-97.
Chawla G, Lin CH, Han A, Shiue L, Ares M, Jr., Black DL (2009) Sam68 regulates a set of alternatively spliced exons during neurogenesis. Mol Cell Biol 29:201-213.
Chen H, Duncan IC, Bozorgchami H, Lo SH (2002) Tensin1 and a previously undocumented family member, tensin2, positively regulate cell migration. Proc Natl Acad Sci U S A 99:733-738.
Chen H, Hewison M, Adams JS (2006) Functional characterization of heterogeneous nuclear ribonuclear protein C1/C2 in vitamin D resistance: a novel response element-binding protein. J Biol Chem 281:39114-39120.
Chen J, Patton JR (2000) Pseudouridine synthase 3 from mouse modifies the anticodon loop of tRNA. Biochemistry 39:12723-12730.
Chen S, Sayana P, Zhang X, Le W (2013) Genetics of amyotrophic lateral sclerosis: an update. Mol Neurodegener 8:28.
Chen YK, Chen CY, Hu HT, Hsueh YP (2012) CTTNBP2, but not CTTNBP2NL, regulates dendritic spinogenesis and synaptic distribution of the striatin-PP2A complex. Mol Biol Cell 23:4383-4392.
Chen YZ, Bennett CL, Huynh HM, Blair IP, Puls I, Irobi J, Dierick I, Abel A, Kennerson ML, Rabin BA, Nicholson GA, Auer-Grumbach M, Wagner K, De Jonghe P, Griffin JW, Fischbeck KH, Timmerman V, Cornblath DR, Chance PF (2004) DNA/RNA helicase gene mutations in a form of juvenile amyotrophic lateral sclerosis (ALS4). Am J Hum Genet 74:1128-1135.
Chestnut BA, Chang Q, Price A, Lesuisse C, Wong M, Martin LJ (2011) Epigenetic regulation of motor neuron cell death through DNA methylation. J Neurosci 31:16619-16636.
Chhabra ES, Higgs HN (2006) INF2 Is a WASP homology 2 motif-containing formin that severs actin filaments and accelerates both polymerization and depolymerization. J Biol Chem 281:26754-26767.
Chicheportiche Y, Bourdon PR, Xu H, Hsu YM, Scott H, Hession C, Garcia I, Browning JL (1997) TWEAK, a new secreted ligand in the tumor necrosis factor family that weakly induces apoptosis. J Biol Chem 272:32401-32410.

Cho CH (2013) New mechanism for glutamate hypothesis in epilepsy. Front Cell Neurosci 7.
Chou J, Provot S, Werb Z (2010) GATA3 in development and cancer differentiation: cells GATA have it! J Cell Physiol 222:42-49.
Chow CY, Landers JE, Bergren SK, Sapp PC, Grant AE, Jones JM, Everett L, Lenk GM, McKenna-Yasek DM, Weisman LS, Figlewicz D, Brown RH, Meisler MH (2009) Deleterious variants of FIG4, a phosphoinositide phosphatase, in patients with ALS. Am J Hum Genet 84:85-88.
Christiano AM, Bart BJ, Epstein EH, Jr., Uitto J (1996) Genetic basis of Bart's syndrome: a glycine substitution mutation in the type VII collagen gene. J Invest Dermatol 106:1340-1342.
Chua F, Laurent GJ (2006) Neutrophil elastase: mediator of extracellular matrix destruction and accumulation. Proc Am Thorac Soc 3:424-427.
Chug H, Trakhanov S, Hulsmann BB, Pleiner T, Gorlich D (2015) Crystal structure of the metazoan Nup62*Nup58*Nup54 nucleoporin complex. Science 350:106-110.
Churg A, Dai J, Zay K, Karsan A, Hendricks R, Yee C, Martin R, MacKenzie R, Xie CS, Zhang L, Shapiro S, Wright JL (2001) Alpha-1-antitrypsin and a broad spectrum metalloprotease inhibitor, RS113456, have similar acute anti-inflammatory effects. Lab Invest 81:1119-1131.
Cleary JD, Ranum LP (2013) Repeat-associated non-ATG (RAN) translation in neurological disease. Hum Mol Genet 22:R45-51.
Colvin JS, Green RP, Schmahl J, Capel B, Ornitz DM (2001) Male-to-female sex reversal in mice lacking fibroblast growth factor 9. Cell 104:875-889.
Cooper-Knock J, Bury JJ, Heath PR, Wyles M, Higginbottom A, Gelsthorpe C, Highley JR, Hautbergue G, Rattray M, Kirby J, Shaw PJ (2015a) C9ORF72 GGGGCC Expanded Repeats Produce Splicing Dysregulation which Correlates with Disease Severity in Amyotrophic Lateral Sclerosis. Plos One 10.
Cooper-Knock J, Hewitt C, Highley JR, Brockington A, Milano A, Man S, Martindale J, Hartley J, Walsh T, Gelsthorpe C, Baxter L, Forster G, Fox M, Bury J, Mok K, McDermott CJ, Traynor BJ, Kirby J, Wharton SB, Ince PG, Hardy J, Shaw PJ (2012a) Clinico-pathological features in amyotrophic lateral sclerosis with expansions in C9ORF72. Brain 135:751-764.
Cooper-Knock J, Kirby J, Ferraiuolo L, Heath PR, Rattray M, Shaw PJ (2012d) Gene expression profiling in human neurodegenerative disease. Nat Rev Neurol 8:518-530.
Cooper-Knock J, Kirby J, Highley R, Shaw PJ (2015c) The Spectrum of C9orf72-mediated Neurodegeneration and Amyotrophic Lateral Sclerosis. Neurotherapeutics 12:326-339.
Corcia P, Camu W, Praline J, Gordon PH, Vourch P, Andres C (2009) The importance of the SMN genes in the genetics of sporadic ALS. Amyotroph Lateral Sc 10:436-440.
Corcia P, Mayeux-Portas V, Khoris J, de Toffol B, Autret A, Muh JP, Camu W, Andres C, Grp FAR (2002) Abnormal SMN1 gene copy number is a susceptibility factor for amyotrophic lateral sclerosis. Annals of Neurology 51:243-246.
Corcia P, Tauber C, Vercoullie J, Arlicot N, Prunier C, Praline J, Nicolas G, Venel Y, Hommet C, Baulieu JL, Cottier JP, Roussel C, Kassiou M, Guilloteau D, Ribeiro MJ (2012) Molecular imaging of microglial activation in amyotrophic lateral sclerosis. PLoS One 7:e52941.

Corrigall VM, Arastu M, Khan S, Shah C, Fife M, Smeets T, Tak PP, Panayi GS (2001) Functional IL-2 receptor beta (CD122) and gamma (CD132) chains are expressed by fibroblast-like synoviocytes: activation by IL-2 stimulates monocyte chemoattractant protein-1 production. J Immunol 166:4141-4147.
Cowper AE, Caceres JF, Mayeda A, Screaton GR (2001) Serine-arginine (SR) protein-like factors that antagonize authentic SR proteins and regulate alternative splicing. J Biol Chem 276:48908-48914.
Cundy T, Hegde M, Naot D, Chong B, King A, Wallace R, Mulley J, Love DR, Seidel J, Fawkner M, Banovic T, Callon KE, Grey AB, Reid IR, Middleton-Hardie CA, Cornish J (2002) A mutation in the gene TNFRSF11B encoding osteoprotegerin causes an idiopathic hyperphosphatasia phenotype. Hum Mol Genet 11:2119-2127.
D'Ambrogio A, Buratti E, Stuani C, Guarnaccia C, Romano M, Ayala YM, Baralle FE (2009) Functional mapping of the interaction between TDP-43 and hnRNP A2 in vivo. Nucleic Acids Res 37:4116-4126.
D'Mello V, Lee JY, MacDonald CC, Tian B (2006) Alternative mRNA polyadenylation can potentially affect detection of gene expression by affymetrix genechip arrays. Appl Bioinformatics 5:249-253.
Dasar N, Ghaderian SM, Azargashb E (2012) Human Evaluation of the Glu298Asp Polymorphism in NOS3 Gene and its Relationship with Onset age of ESRD in Iranian Patients Suffering from ADPKD. Int J Mol Cell Med 1:105-112.
de Boer JP, Creasey AA, Chang A, Abbink JJ, Roem D, Eerenberg AJ, Hack CE, Taylor FB, Jr. (1993) Alpha-2-macroglobulin functions as an inhibitor of fibrinolytic, clotting, and neutrophilic proteinases in sepsis: studies using a baboon model. Infect Immun 61:5035-5043.
De Conti L, Akinyi MV, Mendoza-Maldonado R, Romano M, Baralle M, Buratti E (2015) TDP-43 affects splicing profiles and isoform production of genes involved in the apoptotic and mitotic cellular pathways. Nucleic Acids Res.
de Jong S, Huisman M, Sutedja N, van der Kooi A, de Visser M, Schelhaas J, van der Schouw Y, Veldink J, van den Berg L (2013) Endogenous female reproductive hormones and the risk of amyotrophic lateral sclerosis. J Neurol 260:507-512.
De Vos KJ, Grierson AJ, Ackerley S, Miller CC (2008) Role of axonal transport in neurodegenerative diseases. Annu Rev Neurosci 31:151-173.
Deak KL, Dickerson ME, Linney E, Enterline DS, George TM, Melvin EC, Graham FL, Siegel DG, Hammock P, Mehltretter L, Bassuk AG, Kessler JA, Gilbert JR, Speer MC, Group NTDC (2005) Analysis of ALDH1A2, CYP26A1, CYP26B1, CRABP1, and CRABP2 in human neural tube defects suggests a possible association with alleles in ALDH1A2. Birth Defects Res A Clin Mol Teratol 73:868-875.
Dearry A, Gingrich JA, Falardeau P, Fremeau RT, Jr., Bates MD, Caron MG (1990) Molecular cloning and expression of the gene for a human D1 dopamine receptor. Nature 347:72-76.
Debrand E, El Jai Y, Spence L, Bate N, Praekelt U, Pritchard CA, Monkley SJ, Critchley DR (2009) Talin 2 is a large and complex gene encoding multiple transcripts and protein isoforms. FEBS J 276:1610-1628.
Dee CT, Szymoniuk CR, Mills PE, Takahashi T (2013) Defective neural crest migration revealed by a Zebrafish model of Alx1-related frontonasal dysplasia. Hum Mol Genet 22:239-251.
DeJesus-Hernandez M, Mackenzie IR, Boeve BF, Boxer AL, Baker M, Rutherford NJ, Nicholson AM, Finch NA, Flynn H, Adamson J, Kouri N, Wojtas A, Sengdy P,

Hsiung GY, Karydas A, Seeley WW, Josephs KA, Coppola G, Geschwind DH, Wszolek ZK, Feldman H, Knopman DS, Petersen RC, Miller BL, Dickson DW, Boylan KB, Graff-Radford NR, Rademakers R (2011) Expanded GGGGCC hexanucleotide repeat in noncoding region of C9ORF72 causes chromosome 9p-linked FTD and ALS. Neuron 72:245-256.

Deng HX, Chen W, Hong ST, Boycott KM, Gorrie GH, Siddique N, Yang Y, Fecto F, Shi Y, Zhai H, Jiang H, Hirano M, Rampersaud E, Jansen GH, Donkervoort S, Bigio EH, Brooks BR, Ajroud K, Sufit RL, Haines JL, Mugnaini E, Pericak-Vance MA, Siddique T (2011) Mutations in UBQLN2 cause dominant X-linked juvenile and adult-onset ALS and ALS/dementia. Nature 477:211-215.

Deniselle MC, Liere P, Pianos A, Meyer M, Aprahamian F, Cambourg A, Di Giorgio NP, Schumacher M, De Nicola AF, Guennoun R (2016) Steroid profiling in male Wobbler mouse, a model of amyotrophic lateral sclerosis. Endocrinology en20161244.

Denz CR, Narshi A, Zajdel RW, Dube DK (2004) Expression of a novel cardiac-specific tropomyosin isoform in humans. Biochem Biophys Res Commun 320:1291-1297.

DePaepe A, Nuytinck L, Hausser I, AntonLamprecht I, Naeyaert JM (1997) Mutations in the COL5A1 gene are causal in the Ehlers-Danlos syndromes I and II. American Journal of Human Genetics 60:547-554.

Devanand DP, Michaels-Marston KS, Liu X, Pelton GH, Padilla M, Marder K, Bell K, Stern Y, Mayeux R (2000) Olfactory deficits in patients with mild cognitive impairment predict Alzheimer's disease at follow-up. Am J Psychiatry 157:1399-1405.

Di Cunto F, Imarisio S, Hirsch E, Broccoli V, Bulfone A, Migheli A, Atzori C, Turco E, Triolo R, Dotto GP, Silengo L, Altruda F (2000) Defective neurogenesis in citron kinase knockout mice by altered cytokinesis and massive apoptosis. Neuron 28:115-127.

Dolmetsch R, Geschwind DH (2011) The human brain in a dish: the promise of iPSC-derived neurons. Cell 145:831-834.

Dominguez-Sola D, Ying CY, Grandori C, Ruggiero L, Chen B, Li M, Galloway DA, Gu W, Gautier J, Dalla-Favera R (2007) Non-transcriptional control of DNA replication by c-Myc. Nature 448:445-451.

Donaldson IJ, Chapman M, Kinston S, Landry JR, Knezevic K, Piltz S, Buckley N, Green AR, Gottgens B (2005) Genome-wide identification of cis-regulatory sequences controlling blood and endothelial development. Hum Mol Genet 14:595-601.

Doty RL (2012) Olfaction in Parkinson's disease and related disorders. Neurobiol Dis 46:527-552.

Duriez C, Falette N, Audoynaud C, Moyret-Lalle C, Bensaad K, Courtois S, Wang Q, Soussi T, Puisieux A (2002) The human BTG2/TIS21/PC3 gene: genomic structure, transcriptional regulation and evaluation as a candidate tumor suppressor gene. Gene 282:207-214.

Eckmann CR, Neunteufl A, Pfaffstetter L, Jantsch MF (2001) The human but not the Xenopus RNA-editing enzyme ADAR1 has an atypical nuclear localization signal and displays the characteristics of a shuttling protein. Mol Biol Cell 12:1911-1924.

Ee HL, Liu L, Goh CL, McGrath JA (2007) Clinical and molecular dilemmas in the diagnosis of familial epidermolysis bullosa pruriginosa. J Am Acad Dermatol 56:S77-S81.

Eggert C, Chari A, Laggerbauer B, Fischer U (2006) Spinal muscular atrophy: the RNP connection. Trends Mol Med 12:113-121.
Eisch V, Lu X, Gabriel D, Djabali K (2016) Progerin impairs chromosome maintenance by depleting CENP-F from metaphase kinetochores in Hutchinson-Gilford progeria fibroblasts. Oncotarget 7:24700-24718.
Elian M (1991) Olfactory impairment in motor neuron disease: a pilot study. J Neurol Neurosurg Psychiatry 54:927-928.
Engelhardt JI, Appel SH (1990) IgG reactivity in the spinal cord and motor cortex in amyotrophic lateral sclerosis. Arch Neurol 47:1210-1216.
Fan X, Dion P, Laganiere J, Brais B, Rouleau GA (2001) Oligomerization of polyalanine expanded PABPN1 facilitates nuclear protein aggregation that is associated with cell death. Hum Mol Genet 10:2341-2351.
Farina C, Aloisi F, Meinl E (2007) Astrocytes are active players in cerebral innate immunity. Trends Immunol 28:138-145.
Fecto F, Yan J, Vemula SP, Liu E, Yang Y, Chen W, Zheng JG, Shi Y, Siddique N, Arrat H, Donkervoort S, Ajroud-Driss S, Sufit RL, Heller SL, Deng HX, Siddique T (2011) SQSTM1 mutations in familial and sporadic amyotrophic lateral sclerosis. Arch Neurol 68:1440-1446.
Feijoo C, Hall-Jackson C, Wu R, Jenkins D, Leitch J, Gilbert DM, Smythe C (2001) Activation of mammalian Chk1 during DNA replication arrest: a role for Chk1 in the intra-S phase checkpoint monitoring replication origin firing. J Cell Biol 154:913-923.
Feng L, Huang J, Chen J (2009) MERIT40 facilitates BRCA1 localization and DNA damage repair. Genes Dev 23:719-728.
Feng Y, Jankovic J, Wu YC (2015) Epigenetic mechanisms in Parkinson's disease. J Neurol Sci 349:3-9.
Fernandez AP, Serrano J, Tessarollo L, Cuttitta F, Martinez A (2008) Lack of adrenomedullin in the mouse brain results in behavioral changes, anxiety, and lower survival under stress conditions. Proc Natl Acad Sci U S A 105:12581-12586.
Ferraiuolo L, Heath PR, Holden H, Kasher P, Kirby J, Shaw PJ (2007) Microarray analysis of the cellular pathways involved in the adaptation to and progression of motor neuron injury in the SOD1 G93A mouse model of familial ALS. J Neurosci 27:9201-9219.
Ferraiuolo L, Kirby J, Grierson AJ, Sendtner M, Shaw PJ (2011) Molecular pathways of motor neuron injury in amyotrophic lateral sclerosis. Nat Rev Neurol 7:616-630.
Ferrara N (2004) Vascular endothelial growth factor as a target for anticancer therapy. Oncologist 9 Suppl 1:2-10.
Ferrer I, Garcia-Esparcia P, Carmona M, Carro E, Aronica E, Kovacs GG, Grison A, Gustincich S (2016) Olfactory Receptors in Non-Chemosensory Organs: The Nervous System in Health and Disease. Front Aging Neurosci 8:163.
Fidler JA, Treleaven CM, Frakes A, Tamsett TJ, McCrate M, Cheng SH, Shihabuddin LS, Kaspar BK, Dodge JC (2011) Disease progression in a mouse model of amyotrophic lateral sclerosis: the influence of chronic stress and corticosterone. FASEB J 25:4369-4377.
Fields RD, Burnstock G (2006) Purinergic signalling in neuron-glia interactions. Nat Rev Neurosci 7:423-436.
Figueroa KP, Farooqi S, Harrup K, Frank J, O'Rahilly S, Pulst SM (2009) Genetic Variance in the Spinocerebellar Ataxia Type 2 (ATXN2) Gene in Children with Severe Early Onset Obesity. Plos One 4.

Fischer C, Jonckx B, Mazzone M, Zacchigna S, Loges S, Pattarini L, Chorianopoulos E, Liesenborghs L, Koch M, De Mol M, Autiero M, Wyns S, Plaisance S, Moons L, van Rooijen N, Giacca M, Stassen JM, Dewerchin M, Collen D, Carmeliet P (2007) Anti-PlGF inhibits growth of VEGF(R)-inhibitor-resistant tumors without affecting healthy vessels. Cell 131:463-475.

Folli C, Viglione S, Busconi M, Berni R (2005) Biochemical basis for retinol deficiency induced by the I41N and G75D mutations in human plasma retinol-binding protein. Biochem Biophys Res Commun 336:1017-1022.

Fratta P, Mizielinska S, Nicoll AJ, Zloh M, Fisher EM, Parkinson G, Isaacs AM (2012) C9orf72 hexanucleotide repeat associated with amyotrophic lateral sclerosis and frontotemporal dementia forms RNA G-quadruplexes. Sci Rep 2:1016.

Freibaum BD, Chitta RK, High AA, Taylor JP (2010) Global analysis of TDP-43 interacting proteins reveals strong association with RNA splicing and translation machinery. J Proteome Res 9:1104-1120.

Freischmidt A, Wieland T, Richter B, Ruf W, Schaeffer V, Muller K, Marroquin N, Nordin F, Hubers A, Weydt P, Pinto S, Press R, Millecamps S, Molko N, Bernard E, Desnuelle C, Soriani MH, Dorst J, Graf E, Nordstrom U, Feiler MS, Putz S, Boeckers TM, Meyer T, Winkler AS, Winkelman J, de Carvalho M, Thal DR, Otto M, Brannstrom T, Volk AE, Kursula P, Danzer KM, Lichtner P, Dikic I, Meitinger T, Ludolph AC, Strom TM, Andersen PM, Weishaupt JH (2015) Haploinsufficiency of TBK1 causes familial ALS and fronto-temporal dementia. Nat Neurosci 18:631-636.

Fricke C, Lee JS, Geiger-Rudolph S, Bonhoeffer F, Chien CB (2001) astray, a zebrafish roundabout homolog required for retinal axon guidance. Science 292:507-510.

Fukuda MN, Sato T, Nakayama J, Klier G, Mikami M, Aoki D, Nozawa S (1995) Trophinin and Tastin, a Novel Cell-Adhesion Molecule Complex with Potential Involvement in Embryo Implantation. Gene Dev 9:1199-1210.

Fukuda S, Wu DW, Stark K, Pelus LM (2002) Cloning and characterization of a proliferation-associated cytokine-inducible protein, CIP29. Biochem Biophys Res Commun 292:593-600.

Fukuda T, Naiki T, Saito M, Irie K (2009) hnRNP K interacts with RNA binding motif protein 42 and functions in the maintenance of cellular ATP level during stress conditions. Genes Cells 14:113-128.

Futter M, Diekmann H, Schoenmakers E, Sadiq O, Chatterjee K, Rubinsztein DC (2009) Wild-type but not mutant huntingtin modulates the transcriptional activity of liver X receptors. J Med Genet 46:438-446.

Gaidatzis D, Jacobeit K, Oakeley EJ, Stadler MB (2009) Overestimation of alternative splicing caused by variable probe characteristics in exon arrays. Nucleic Acids Res 37:e107.

Gaitanos TN, Santamaria A, Jeyaprakash AA, Wang B, Conti E, Nigg EA (2009) Stable kinetochore-microtubule interactions depend on the Ska complex and its new component Ska3/C13Orf3. EMBO J 28:1442-1452.

Gamberi C, Izaurralde E, Beisel C, Mattaj IW (1997) Interaction between the human nuclear cap-binding protein complex and hnRNP F. Mol Cell Biol 17:2587-2597.

Gao X, Xu Z (2008) Mechanisms of action of angiogenin. Acta Biochim Biophys Sin (Shanghai) 40:619-624.

Garbuzova-Davis S, Sanberg PR (2014) Blood-CNS Barrier Impairment in ALS patients versus an animal model. Front Cell Neurosci 8:21.

Garcia-Esparcia P, Schluter A, Carmona M, Moreno J, Ansoleaga B, Torrejon-Escribano B, Gustincich S, Pujol A, Ferrer I (2013) Functional genomics reveals dysregulation of cortical olfactory receptors in Parkinson disease: novel putative chemoreceptors in the human brain. J Neuropathol Exp Neurol 72:524-539.
Garmy-Susini B, Jin H, Zhu Y, Sung RJ, Hwang R, Varner J (2005) Integrin alpha4beta1-VCAM-1-mediated adhesion between endothelial and mural cells is required for blood vessel maturation. J Clin Invest 115:1542-1551.
Garneau NL, Wilusz J, Wilusz CJ (2007) The highways and byways of mRNA decay. Nat Rev Mol Cell Biol 8:113-126.
Ge J, Yu YT (2013) RNA pseudouridylation: new insights into an old modification. Trends Biochem Sci 38:210-218.
Gehring NH, Lamprinaki S, Hentze MW, Kulozik AE (2009) The hierarchy of exon-junction complex assembly by the spliceosome explains key features of mammalian nonsense-mediated mRNA decay. PLoS Biol 7:e1000120.
Gianforcaro A, Hamadeh MJ (2014) Vitamin D as a potential therapy in amyotrophic lateral sclerosis. CNS Neurosci Ther 20:101-111.
Gillan L, Matei D, Fishman DA, Gerbin CS, Karlan BY, Chang DD (2002) Periostin secreted by epithelial ovarian carcinoma is a ligand for alpha(V)beta(3) and alpha(V)beta(5) integrins and promotes cell motility. Cancer Res 62:5358-5364.
Goncalves-Mendes N, Simon-Chazottes D, Creveaux I, Meiniel A, Guenet JL, Meiniel R (2003) Mouse SCO-spondin, a gene of the thrombospondin type 1 repeat (TSR) superfamily expressed in the brain. Gene 312:263-270.
Gonzalez-Santos JM, Wang A, Jones J, Ushida C, Liu J, Hu J (2002) Central region of the human splicing factor Hprp3p interacts with Hprp4p. J Biol Chem 277:23764-23772.
Goodman FR, Bacchelli C, Brady AF, Brueton LA, Fryns JP, Mortlock DP, Innis JW, Holmes LB, Donnenfeld AE, Feingold M, Beemer FA, Hennekam RC, Scambler PJ (2000) Novel HOXA13 mutations and the phenotypic spectrum of hand-foot-genital syndrome. Am J Hum Genet 67:197-202.
Gorski DH, LePage DF, Patel CV, Copeland NG, Jenkins NA, Walsh K (1993) Molecular cloning of a diverged homeobox gene that is rapidly down-regulated during the G0/G1 transition in vascular smooth muscle cells. Mol Cell Biol 13:3722-3733.
Greenway MJ, Andersen PM, Russ C, Ennis S, Cashman S, Donaghy C, Patterson V, Swingler R, Kieran D, Prehn J, Morrison KE, Green A, Acharya KR, Brown RH, Jr., Hardiman O (2006) ANG mutations segregate with familial and 'sporadic' amyotrophic lateral sclerosis. Nat Genet 38:411-413.
Greig NH, Lahiri DK, Sambamurti K (2002a) Butyrylcholinesterase: An important new target in Alzheimer's disease therapy. International Psychogeriatrics 14:77-91.
Greig NH, Lahiri DK, Sambamurti K (2002b) Butyrylcholinesterase: an important new target in Alzheimer's disease therapy. Int Psychogeriatr 14 Suppl 1:77-91.
Grewal SI, Rice JC (2004) Regulation of heterochromatin by histone methylation and small RNAs. Curr Opin Cell Biol 16:230-238.
Grosset C, Chen CY, Xu N, Sonenberg N, Jacquemin-Sablon H, Shyu AB (2000) A mechanism for translationally coupled mRNA turnover: interaction between the poly(A) tail and a c-fos RNA coding determinant via a protein complex. Cell 103:29-40.
Gu H, Cao Y, Qiu B, Zhou Z, Deng R, Chen Z, Li R, Li X, Wei Q, Xia X, Yong W (2016) Establishment and phenotypic analysis of an Mstn knockout rat. Biochem Biophys Res Commun 477:115-122.

Guilarte TR (2010) APLP1, Alzheimer's-like pathology and neurodegeneration in the frontal cortex of manganese-exposed non-human primates. Neurotoxicology 31:572-574.
Gumbiner BM (1996) Cell adhesion: the molecular basis of tissue architecture and morphogenesis. Cell 84:345-357.
Gurney ME, Pu HF, Chiu AY, Dalcanto MC, Polchow CY, Alexander DD, Caliendo J, Hentati A, Kwon YW, Deng HX, Chen WJ, Zhai P, Sufit RL, Siddique T (1994) Motor-Neuron Degeneration in Mice That Express a Human Cu,Zn Superoxide-Dismutase Mutation. Science 264:1772-1775.
Haberle J, Schmidt E, Pauli S, Rapp B, Christensen E, Wermuth B, Koch HG (2003) Gene structure of human carbamylphosphate synthetase 1 and novel mutations in patients with neonatal onset. Hum Mutat 21:444.
Habets WJ, Sillekens PT, Hoet MH, Schalken JA, Roebroek AJ, Leunissen JA, van de Ven WJ, van Venrooij WJ (1987) Analysis of a cDNA clone expressing a human autoimmune antigen: full-length sequence of the U2 small nuclear RNA-associated B" antigen. Proc Natl Acad Sci U S A 84:2421-2425.
Haenisch B, Walstab J, Herberhold S, Bootz F, Tschaikin M, Ramseger R, Bonisch H (2010) Alpha-adrenoceptor agonistic activity of oxymetazoline and xylometazoline. Fundam Clin Pharmacol 24:729-739.
Hall ED, Oostveen JA, Gurney ME (1998) Relationship of microglial and astrocytic activation to disease onset and progression in a transgenic model of familial ALS. Glia 23:249-256.
Hamid AR, Hoogland AM, Smit F, Jannink S, van Rijt-van de Westerlo C, Jansen CF, van Leenders GJ, Verhaegh GW, Schalken JA (2015) The role of HOXC6 in prostate cancer development. Prostate 75:1868-1876.
Hamma T, Ferre-D'Amare AR (2006) Pseudouridine synthases. Chem Biol 13:1125-1135.
Hand CK, Khoris J, Salachas F, Gros-Louis F, Lopes AA, Mayeux-Portas V, Brewer CG, Brown RH, Jr., Meininger V, Camu W, Rouleau GA (2002) A novel locus for familial amyotrophic lateral sclerosis, on chromosome 18q. Am J Hum Genet 70:251-256.
Harada K, Yamada A, Yang D, Itoh K, Shichijo S (2001) Binding of a SART3 tumor-rejection antigen to a pre-mRNA splicing factor RNPS1: a possible regulation of splicing by a complex formation. Int J Cancer 93:623-628.
Harada O, Suga T, Suzuki T, Nakamoto K, Kobayashi M, Nomiyama T, Nadano D, Ohyama C, Fukuda MN, Nakayama J (2007) The role of trophinin, an adhesion molecule unique to human trophoblasts, in progression of colorectal cancer. International Journal of Cancer 121:1072-1078.
Hawkins M, Pope B, Maciver SK, Weeds AG (1993) Human actin depolymerizing factor mediates a pH-sensitive destruction of actin filaments. Biochemistry 32:9985-9993.
Hayakawa T, Zhang F, Hayakawa N, Ohtani Y, Shinmyozu K, Nakayama J, Andreassen PR (2010) MRG15 binds directly to PALB2 and stimulates homology-directed repair of chromosomal breaks. J Cell Sci 123:1124-1130.
Hayashi K, Yano H, Hashida T, Takeuchi R, Takeda O, Asada K, Takahashi E, Kato I, Sobue K (1992) Genomic structure of the human caldesmon gene. Proc Natl Acad Sci U S A 89:12122-12126.
Hayashida T, Takahashi F, Chiba N, Brachtel E, Takahashi M, Godin-Heymann N, Gross KW, Vivanco M, Wijendran V, Shioda T, Sgroi D, Donahoe PK,

Maheswaran S (2010) HOXB9, a gene overexpressed in breast cancer, promotes tumorigenicity and lung metastasis. Proc Natl Acad Sci U S A 107:1100-1105.
Hayes AJ, Huang WQ, Yu J, Maisonpierre PC, Liu A, Kern FG, Lippman ME, McLeskey SW, Li LY (2000) Expression and function of angiopoietin-1 in breast cancer. Br J Cancer 83:1154-1160.
He W, Cowan CW, Wensel TG (1998) RGS9, a GTPase accelerator for phototransduction. Neuron 20:95-102.
Heath PR, Shaw PJ (2002) Update on the glutamatergic neurotransmitter system and the role of excitotoxicity in amyotrophic lateral sclerosis. Muscle Nerve 26:438-458.
Hedges EC, Mehler VJ, Nishimura AL (2016) The Use of Stem Cells to Model Amyotrophic Lateral Sclerosis and Frontotemporal Dementia: From Basic Research to Regenerative Medicine. Stem Cells Int 2016:9279516.
Heller MJ (2002) DNA microarray technology: devices, systems, and applications. Annu Rev Biomed Eng 4:129-153.
Hendriks WJ, Elson A, Harroch S, Pulido R, Stoker A, den Hertog J (2013) Protein tyrosine phosphatases in health and disease. FEBS J 280:708-730.
Heng BC, Aubel D, Fussenegger M (2013) An overview of the diverse roles of G-protein coupled receptors (GPCRs) in the pathophysiology of various human diseases. Biotechnol Adv 31:1676-1694.
Herbst RS, Bunn PA, Jr. (2003) Targeting the epidermal growth factor receptor in non-small cell lung cancer. Clin Cancer Res 9:5813-5824.
Hewitt C, Kirby J, Highley JR, Hartley JA, Hibberd R, Hollinger HC, Williams TL, Ince PG, McDermott CJ, Shaw PJ (2010) Novel FUS/TLS mutations and pathology in familial and sporadic amyotrophic lateral sclerosis. Arch Neurol 67:455-461.
Hideyama T, Yamashita T, Aizawa H, Tsuji S, Kakita A, Takahashi H, Kwak S (2012) Profound downregulation of the RNA editing enzyme ADAR2 in ALS spinal motor neurons. Neurobiol Dis 45:1121-1128.
Highley JR, Kirby J, Jansweijer JA, Webb PS, Hewamadduma CA, Heath PR, Higginbottom A, Raman R, Ferraiuolo L, Cooper-Knock J, McDermott CJ, Wharton SB, Shaw PJ, Ince PG (2014) Loss of nuclear TDP-43 in amyotrophic lateral sclerosis (ALS) causes altered expression of splicing machinery and widespread dysregulation of RNA splicing in motor neurones. Neuropathol Appl Neurobiol 40:670-685.
Hintsch G, Zurlinden A, Meskenaite V, Steuble M, Fink-Widmer K, Kinter J, Sonderegger P (2002) The calsyntenins - A family of postsynaptic membrane proteins with distinct neuronal expression patterns. Molecular and Cellular Neuroscience 21:393-409.
Hinuma S, Habata Y, Fujii R, Kawamata Y, Hosoya M, Fukusumi S, Kitada C, Masuo Y, Asano T, Matsumoto H, Sekiguchi M, Kurokawa T, Nishimura O, Onda H, Fujino M (1998) A prolactin-releasing peptide in the brain. Nature 393:272-276.
Hofmann F (2005) The biology of cyclic GMP-dependent protein kinases. J Biol Chem 280:1-4.
Holaska JM, Rais-Bahrami S, Wilson KL (2006) Lmo7 is an emerin-binding protein that regulates the transcription of emerin and many other muscle-relevant genes. Hum Mol Genet 15:3459-3472.
Hooten KG, Beers DR, Zhao W, Appel SH (2015) Protective and Toxic Neuroinflammation in Amyotrophic Lateral Sclerosis. Neurotherapeutics 12:364-375.

Hosler BA, Siddique T, Sapp PC, Sailor W, Huang MC, Hossain A, Daube JR, Nance M, Fan C, Kaplan J, Hung WY, McKenna-Yasek D, Haines JL, Pericak-Vance MA, Horvitz HR, Brown RH, Jr. (2000) Linkage of familial amyotrophic lateral sclerosis with frontotemporal dementia to chromosome 9q21-q22. JAMA : the journal of the American Medical Association 284:1664-1669.

Hou P, Estrada L, Kinley AW, Parsons JT, Vojtek AB, Gorski JL (2003) Fgd1, the Cdc42 GEF responsible for Faciogenital Dysplasia, directly interacts with cortactin and mAbp1 to modulate cell shape. Hum Mol Genet 12:1981-1993.

Hovhannisyan RH, Carstens RP (2007) Heterogeneous ribonucleoprotein m is a splicing regulatory protein that can enhance or silence splicing of alternatively spliced exons. J Biol Chem 282:36265-36274.

Hu B, Cheng SY (2009) Angiopoietin-2: development of inhibitors for cancer therapy. Curr Oncol Rep 11:111-116.

Huang da W, Sherman BT, Lempicki RA (2009) Systematic and integrative analysis of large gene lists using DAVID bioinformatics resources. Nat Protoc 4:44-57.

Huang J, Gong Z, Ghosal G, Chen J (2009) SOSS complexes participate in the maintenance of genomic stability. Mol Cell 35:384-393.

Hubert CG, Bradley RK, Ding Y, Toledo CM, Herman J, Skutt-Kakaria K, Girard EJ, Davison J, Berndt J, Corrin P, Hardcastle J, Basom R, Delrow JJ, Webb T, Pollard SM, Lee J, Olson JM, Paddison PJ (2013) Genome-wide RNAi screens in human brain tumor isolates reveal a novel viability requirement for PHF5A. Genes Dev 27:1032-1045.

Huflejt ME, Jordan ET, Gitt MA, Barondes SH, Leffler H (1997) Strikingly different localization of galectin-3 and galectin-4 in human colon adenocarcinoma T84 cells - Galectin-4 is localized at sites of cell adhesion. Journal of Biological Chemistry 272:14294-14303.

Hynd MR, Scott HL, Dodd PR (2004) Glutamate-mediated excitotoxicity and neurodegeneration in Alzheimer's disease. Neurochem Int 45:583-595.

Iborra FJ, Jackson DA, Cook PR (2001) Coupled transcription and translation within nuclei of mammalian cells. Science 293:1139-1142.

Iborra FJ, Jackson DA, Cook PR (2004) The case for nuclear translation. Journal of Cell Science 117:5713-5720.

Ikeda R, Yoshida K, Tsukahara S, Sakamoto Y, Tanaka H, Furukawa K, Inoue I (2005) The promyelotic leukemia zinc finger promotes osteoblastic differentiation of human mesenchymal stem cells as an upstream regulator of CBFA1. J Biol Chem 280:8523-8530.

Ince PG, Highley JR, Kirby J, Wharton SB, Takahashi H, Strong MJ, Shaw PJ (2011) Molecular pathology and genetic advances in amyotrophic lateral sclerosis: an emerging molecular pathway and the significance of glial pathology. Acta Neuropathol 122:657-671.

Inoki K, Li Y, Zhu TQ, Wu J, Guan KL (2002) TSC2 is phosphorylated and inhibited by Akt and suppresses mTOR signalling. Nature Cell Biology 4:648-657.

Ishii H, Inageta T, Mimori K, Saito T, Sasaki H, Isobe M, Mori M, Croce CM, Huebner K, Ozawa K, Furukawa Y (2005) Frag1, a homolog of alternative replication factor C subunits, links replication stress surveillance with apoptosis. Proc Natl Acad Sci U S A 102:9655-9660.

Ivell R, Walther N (1999) The role of sex steroids in the oxytocin hormone system. Mol Cell Endocrinol 151:95-101.

Jaarsma D, Haasdijk ED, Grashorn JAC, Hawkins R, van Duijn W, Verspaget HW, London J, Holstege JC (2000) Human Cu/Zn superoxide dismutase (SOD1)

overexpression in mice causes mitochondrial vacuolization, axonal degeneration, and premature motoneuron death and accelerates motoneuron disease in mice expressing a familial amyotrophic lateral sclerosis mutant SOD1. Neurobiology of Disease 7:623-643.
Janssens K, de Vernejoul MC, de Freitas F, Vanhoenacker F, Van Hul W (2005) An intermediate form of juvenile Paget's disease caused by a truncating TNFRSF11B mutation. Bone 36:542-548.
Jarrous N, Reiner R, Wesolowski D, Mann H, Guerrier-Takada C, Altman S (2001) Function and subnuclear distribution of Rpp21, a protein subunit of the human ribonucleoprotein ribonuclease P. RNA 7:1153-1164.
Jenkins BG, Zhu A, Poutiainen P, Choi JK, Kil KE, Zhang Z, Kuruppu D, Aytan N, Dedeoglu A, Brownell AL (2016) Functional modulation of G-protein coupled receptors during Parkinson disease-like neurodegeneration. Neuropharmacology 108:462-473.
Jeong S, Pfeifer K (2004) Shifting insulator boundaries. Nat Genet 36:1036-1037.
Jerome LA, Papaioannou VE (2001) DiGeorge syndrome phenotype in mice mutant for the T-box gene, Tbx1. Nat Genet 27:286-291.
Jiang Z, Chu PG, Woda BA, Rock KL, Liu Q, Hsieh CC, Li C, Chen W, Duan HO, McDougal S, Wu CL (2006) Analysis of RNA-binding protein IMP3 to predict metastasis and prognosis of renal-cell carcinoma: a retrospective study. Lancet Oncol 7:556-564.
Johnson JO, Mandrioli J, Benatar M, Abramzon Y, Van Deerlin VM, Trojanowski JQ, Gibbs JR, Brunetti M, Gronka S, Wuu J, Ding JH, McCluskey L, Martinez-Lage M, Falcone D, Hernandez DG, Arepalli S, Chong S, Schymick JC, Rothstein J, Landi F, Wang YD, Calvo A, Mora G, Sabatelli M, Monsurro MR, Battistini S, Salvi F, Spataro R, Sola P, Borghero G, Galassi G, Scholz SW, Taylor JP, Restagno G, Chio A, Traynor BJ, Consortium I (2010) Exome Sequencing Reveals VCP Mutations as a Cause of Familial ALS. Neuron 68:857-864.
Johnson JO, Pioro EP, Boehringer A, Chia R, Feit H, Renton AE, Pliner HA, Abramzon Y, Marangi G, Winborn BJ, Gibbs JR, Nalls MA, Morgan S, Shoai M, Hardy J, Pittman A, Orrell RW, Malaspina A, Sidle KC, Fratta P, Harms MB, Baloh RH, Pestronk A, Weihl CC, Rogaeva E, Zinman L, Drory VE, Borghero G, Mora G, Calvo A, Rothstein JD, Consortium I, Drepper C, Sendtner M, Singleton AB, Taylor JP, Cookson MR, Restagno G, Sabatelli M, Bowser R, Chio A, Traynor BJ (2014) Mutations in the Matrin 3 gene cause familial amyotrophic lateral sclerosis. Nat Neurosci 17:664-666.
Jones KJ (1988) Steroid hormones and neurotrophism: relationship to nerve injury. Metab Brain Dis 3:1-18.
Jung DJ, Na SY, Na DS, Lee JW (2002) Molecular cloning and characterization of CAPER, a novel coactivator of activating protein-1 and estrogen receptors. J Biol Chem 277:1229-1234.
Jungmichel S, Sylvestersen KB, Choudhary C, Nguyen S, Mann M, Nielsen ML (2014) Specificity and commonality of the phosphoinositide-binding proteome analyzed by quantitative mass spectrometry. Cell Rep 6:578-591.
Jurado S, Conlan LA, Baker EK, Ng JL, Tenis N, Hoch NC, Gleeson K, Smeets M, Izon D, Heierhorst J (2012) ATM substrate Chk2-interacting Zn2+ finger (ASCIZ) Is a bi-functional transcriptional activator and feedback sensor in the regulation of dynein light chain (DYNLL1) expression. J Biol Chem 287:3156-3164.

Kanazawa T, Misawa K, Misawa Y, Uehara T, Fukushima H, Kusaka G, Maruta M, Carey TE (2015) G-Protein-Coupled Receptors: Next Generation Therapeutic Targets in Head and Neck Cancer? Toxins (Basel) 7:2959-2984.
Kaneda S, Nalbantoglu J, Takeishi K, Shimizu K, Gotoh O, Seno T, Ayusawa D (1990) Structural and functional analysis of the human thymidylate synthase gene. J Biol Chem 265:20277-20284.
Kantor DB, Chivatakarn O, Peer KL, Oster SF, Inatani M, Hansen MJ, Flanagan JG, Yamaguchi Y, Sretavan DW, Giger RJ, Kolodkin AL (2004) Semaphorin 5A is a bifunctional axon guidance cue regulated by heparan and chondroitin sulfate proteoglycans. Neuron 44:961-975.
Kato T (2007) Molecular genetics of bipolar disorder and depression. Psychiatry Clin Neurosci 61:3-19.
Khaleghpour K, Svitkin YV, Craig AW, DeMaria CT, Deo RC, Burley SK, Sonenberg N (2001) Translational repression by a novel partner of human poly(A) binding protein, Paip2. Mol Cell 7:205-216.
Kiernan MC, Vucic S, Cheah BC, Turner MR, Eisen A, Hardiman O, Burrell JR, Zoing MC (2011) Amyotrophic lateral sclerosis. Lancet 377:942-955.
Kim D, Nguyen MD, Dobbin MM, Fischer A, Sananbenesi F, Rodgers JT, Delalle I, Baur JA, Sui G, Armour SM, Puigserver P, Sinclair DA, Tsai LH (2007) SIRT1 deacetylase protects against neurodegeneration in models for Alzheimer's disease and amyotrophic lateral sclerosis. EMBO J 26:3169-3179.
Kim HJ, Kim NC, Wang YD, Scarborough EA, Moore J, Diaz Z, MacLea KS, Freibaum B, Li S, Molliex A, Kanagaraj AP, Carter R, Boylan KB, Wojtas AM, Rademakers R, Pinkus JL, Greenberg SA, Trojanowski JQ, Traynor BJ, Smith BN, Topp S, Gkazi AS, Miller J, Shaw CE, Kottlors M, Kirschner J, Pestronk A, Li YR, Ford AF, Gitler AD, Benatar M, King OD, Kimonis VE, Ross ED, Weihl CC, Shorter J, Taylor JP (2013) Mutations in prion-like domains in hnRNPA2B1 and hnRNPA1 cause multisystem proteinopathy and ALS. Nature 495:467-473.
Kim KJ, Cho CS, Kim WU (2012) Role of placenta growth factor in cancer and inflammation. Exp Mol Med 44:10-19.
Kinoshita M, Nakamura T, Ihara M, Haraguchi T, Hiraoka Y, Tashiro K, Noda M (2001) Identification of human endomucin-1 and -2 as membrane-bound O-sialoglycoproteins with anti-adhesive activity. FEBS Lett 499:121-126.
Kirby J, Goodall EF, Smith W, Highley JR, Masanzu R, Hartley JA, Hibberd R, Hollinger HC, Wharton SB, Morrison KE, Ince PG, McDermott CJ, Shaw PJ (2010) Broad clinical phenotypes associated with TAR-DNA binding protein (TARDBP) mutations in amyotrophic lateral sclerosis. Neurogenetics 11:217-225.
Kirby J, Halligan E, Baptista MJ, Allen S, Heath PR, Holden H, Barber SC, Loynes CA, Wood-Allum CA, Lunec J, Shaw PJ (2005) Mutant SOD1 alters the motor neuronal transcriptome: implications for familial ALS. Brain 128:1686-1706.
Kobayashi S, Kohda T, Miyoshi N, Kuroiwa Y, Aisaka K, Tsutsumi O, Kaneko-Ishino T, Ishino F (1997) Human PEG1/MEST, an imprinted gene on chromosome 7. Hum Mol Genet 6:781-786.
Korenberg JR, Argraves KM, Chen XN, Tran H, Strickland DK, Argraves WS (1994) Chromosomal localization of human genes for the LDL receptor family member glycoprotein 330 (LRP2) and its associated protein RAP (LRPAP1). Genomics 22:88-93.

Kos M, Reid G, Denger S, Gannon F (2001) Minireview: genomic organization of the human ERalpha gene promoter region. Mol Endocrinol 15:2057-2063.
Koskinen K, Nevalainen S, Karikoski M, Hanninen A, Jalkanen S, Salmi M (2007) VAP-1-Deficient mice display defects in mucosal immunity and antimicrobial responses: Implications for antiadhesive applications. J Immunol 179:6160-6168.
Koyama-Nasu R, Nasu-Nishimura Y, Todo T, Ino Y, Saito N, Aburatani H, Funato K, Echizen K, Sugano H, Haruta R, Matsui M, Takahashi R, Manabe E, Oda T, Akiyama T (2013) The critical role of cyclin D2 in cell cycle progression and tumorigenicity of glioblastoma stem cells. Oncogene 32:3840-3845.
Kremer BE, Adang LA, Macara IG (2007) Septins regulate actin organization and cell-cycle arrest through nuclear accumulation of NCK mediated by SOCS7. Cell 130:837-850.
Kruman, II, Wersto RP, Cardozo-Pelaez F, Smilenov L, Chan SL, Chrest FJ, Emokpae R, Jr., Gorospe M, Mattson MP (2004) Cell cycle activation linked to neuronal cell death initiated by DNA damage. Neuron 41:549-561.
Kuja-Panula J, Kiiltomaki M, Yamashiro T, Rouhiainen A, Rauvala H (2003) AMIGO, a transmembrane protein implicated in axon tract development, defines a novel protein family with leucine-rich repeats. Journal of Cell Biology 160:963-973.
Kumar DR, Aslinia F, Yale SH, Mazza JJ (2011) Jean-Martin Charcot: the father of neurology. Clin Med Res 9:46-49.
Kuo PH, Doudeva LG, Wang YT, Shen CK, Yuan HS (2009a) Structural insights into TDP-43 in nucleic-acid binding and domain interactions. Nucleic Acids Res 37:1799-1808.
Kuo PH, Doudeva LG, Wang YT, Shen CKJ, Yuan HS (2009c) Structural insights into TDP-43 in nucleic-acid binding and domain interactions. Nucleic Acids Research 37:1799-1808.
Kwiatkowski TJ, Jr., Bosco DA, Leclerc AL, Tamrazian E, Vanderburg CR, Russ C, Davis A, Gilchrist J, Kasarskis EJ, Munsat T, Valdmanis P, Rouleau GA, Hosler BA, Cortelli P, de Jong PJ, Yoshinaga Y, Haines JL, Pericak-Vance MA, Yan J, Ticozzi N, Siddique T, McKenna-Yasek D, Sapp PC, Horvitz HR, Landers JE, Brown RH, Jr. (2009) Mutations in the FUS/TLS gene on chromosome 16 cause familial amyotrophic lateral sclerosis. Science 323:1205-1208.
Lagier-Tourenne C, Polymenidou M, Cleveland DW (2010) TDP-43 and FUS/TLS: emerging roles in RNA processing and neurodegeneration. Hum Mol Genet 19:R46-64.
Lampson MA, Kapoor TM (2005) The human mitotic checkpoint protein BubR1 regulates chromosome-spindle attachments. Nat Cell Biol 7:93-98.
Landes N, Pfluger P, Kluth D, Birringer M, Ruhl R, Bol GF, Glatt H, Brigelius-Flohe R (2003) Vitamin E activates gene expression via the pregnane X receptor. Biochem Pharmacol 65:269-273.
Lauriat TL, Shiue L, Haroutunian V, Verbitsky M, Ares M, Jr., Ospina L, McInnes LA (2008) Developmental expression profile of quaking, a candidate gene for schizophrenia, and its target genes in human prefrontal cortex and hippocampus shows regional specificity. J Neurosci Res 86:785-796.
Lawo S, Bashkurov M, Mullin M, Ferreria MG, Kittler R, Habermann B, Tagliaferro A, Poser I, Hutchins JR, Hegemann B, Pinchev D, Buchholz F, Peters JM, Hyman AA, Gingras AC, Pelletier L (2009) HAUS, the 8-subunit human Augmin complex, regulates centrosome and spindle integrity. Curr Biol 19:816-826.

Le Hir H, Sauliere J, Wang Z (2016) The exon junction complex as a node of post-transcriptional networks. Nat Rev Mol Cell Biol 17:41-54.
Lee EJ, Lee SH, Jung JW, Lee W, Kim BJ, Park KW, Lim SK, Yoon CJ, Baik JH (2001) Differential regulation of cAMP-mediated gene transcription and ligand selectivity by MC3R and MC4R melanocortin receptors. Eur J Biochem 268:582-591.
Lee JW, Bae SH, Jeong JW, Kim SH, Kim KW (2004) Hypoxia-inducible factor (HIF-1)alpha: its protein stability and biological functions. Exp Mol Med 36:1-12.
Lee JW, Choi HS, Gyuris J, Brent R, Moore DD (1995) Two classes of proteins dependent on either the presence or absence of thyroid hormone for interaction with the thyroid hormone receptor. Mol Endocrinol 9:243-254.
Leimeister C, Schumacher N, Diez H, Gessler M (2004) Cloning and expression analysis of the mouse stroma marker snep encoding a novel nidogen domain protein. Dev Dynam 230:371-377.
Lemercier C, To RQ, Swanson BJ, Lyons GE, Konieczny SF (1997) Mist1: a novel basic helix-loop-helix transcription factor exhibits a developmentally regulated expression pattern. Dev Biol 182:101-113.
Leung KT, Chan KY, Ng PC, Lau TK, Chiu WM, Tsang KS, Li CK, Kong CK, Li K (2011) The tetraspanin CD9 regulates migration, adhesion, and homing of human cord blood CD34+ hematopoietic stem and progenitor cells. Blood 117:1840-1850.
Levy-Lahad E, Poorkaj P, Wang K, Fu YH, Oshima J, Mulligan J, Schellenberg GD (1996) Genomic structure and expression of STM2, the chromosome 1 familial Alzheimer disease gene. Genomics 34:198-204.
Li G, Mongillo M, Chin KT, Harding H, Ron D, Marks AR, Tabas I (2009) Role of ERO1-alpha-mediated stimulation of inositol 1,4,5-triphosphate receptor activity in endoplasmic reticulum stress-induced apoptosis. J Cell Biol 186:783-792.
Li Z, Xi X, Gu M, Feil R, Ye RD, Eigenthaler M, Hofmann F, Du X (2003) A stimulatory role for cGMP-dependent protein kinase in platelet activation. Cell 112:77-86.
Liang H, Van Remmen H, Frohlich V, Lechleiter J, Richardson A, Ran Q (2007) Gpx4 protects mitochondrial ATP generation against oxidative damage. Biochem Biophys Res Commun 356:893-898.
Liguz-Lecznar M, Urban-Ciecko J, Kossut M (2016) Somatostatin and Somatostatin-Containing Neurons in Shaping Neuronal Activity and Plasticity. Front Neural Circuits 10:48.
Lill CM, Abel O, Bertram L, Al-Chalabi A (2011) Keeping up with genetic discoveries in amyotrophic lateral sclerosis: the ALSoD and ALSGene databases. Amyotroph Lateral Scler 12:238-249.
Lindblad O, Chougule RA, Moharram SA, Kabir NN, Sun J, Kazi JU, Ronnstrand L (2015) The role of HOXB2 and HOXB3 in acute myeloid leukemia. Biochem Biophys Res Commun 467:742-747.
Linder P, Jankowsky E (2011) From unwinding to clamping - the DEAD box RNA helicase family. Nat Rev Mol Cell Biol 12:505-516.
Liu C, Shao ZM, Zhang L, Beatty P, Sartippour M, Lane T, Livingston E, Nguyen M (2001) Human endomucin is an endothelial marker. Biochem Biophys Res Commun 288:129-136.
Liu GY, Jiang YS, Wang P, Feng RN, Jiang N, Chen XY, Song H, Chen ZG (2012) Cell adhesion molecules contribute to Alzheimer's disease: multiple pathway analyses of two genome-wide association studies. J Neurochem 120:190-198.

Liu J, Nam HK, Campbell C, Gasque KC, Millan JL, Hatch NE (2014) Tissue-nonspecific alkaline phosphatase deficiency causes abnormal craniofacial bone development in the Alpl(-/-) mouse model of infantile hypophosphatasia. Bone 67:81-94.
Liu Q, Tang Z, Surdenikova L, Kim S, Patel KN, Kim A, Ru F, Guan Y, Weng HJ, Geng Y, Undem BJ, Kollarik M, Chen ZF, Anderson DJ, Dong X (2009) Sensory neuron-specific GPCR Mrgprs are itch receptors mediating chloroquine-induced pruritus. Cell 139:1353-1365.
Liu X, McLeod I, Anderson S, Yates JR, 3rd, He X (2005) Molecular analysis of kinetochore architecture in fission yeast. EMBO J 24:2919-2930.
Liu YC, Cheng SC (2015) Functional roles of DExD/H-box RNA helicases in Pre-mRNA splicing. J Biomed Sci 22:54.
Liu YC, Chiang PM, Tsai KJ (2013) Disease animal models of TDP-43 proteinopathy and their pre-clinical applications. Int J Mol Sci 14:20079-20111.
Lizano E, Schuster J, Muller M, Kelso J, Morl M (2007) A splice variant of the human CCA-adding enzyme with modified activity. J Mol Biol 366:1258-1265.
Lohse MJ, Benovic JL, Codina J, Caron MG, Lefkowitz RJ (1990) Beta-Arrestin - a Protein That Regulates Beta-Adrenergic-Receptor Function. Science 248:1547-1550.
Long L, Thelen JP, Furgason M, Haj-Yahya M, Brik A, Cheng D, Peng J, Yao T (2014) The U4/U6 recycling factor SART3 has histone chaperone activity and associates with USP15 to regulate H2B deubiquitination. J Biol Chem 289:8916-8930.
Lu S, Liu R, Su M, Wei Y, Yang S, He S, Wang X, Qiang F, Chen C, Zhao S, Qian L, Shao M, Mao G (2016) Overexpression of HOXC8 is Associated With Poor Prognosis in Epithelial Ovarian Cancer. Reprod Sci 23:944-954.
Lung HL, Bangarusamy DK, Xie D, Cheung AK, Cheng Y, Kumaran MK, Miller L, Liu ET, Guan XY, Sham JS, Fang Y, Li L, Wang N, Protopopov AI, Zabarovsky ER, Tsao SW, Stanbridge EJ, Lung ML (2005) THY1 is a candidate tumour suppressor gene with decreased expression in metastatic nasopharyngeal carcinoma. Oncogene 24:6525-6532.
Lungu C, Muegge K, Jeltsch A, Jurkowska RZ (2015) An ATPase-deficient variant of the SNF2 family member HELLS shows altered dynamics at pericentromeric heterochromatin. J Mol Biol 427:1903-1915.
Luo HR, Moreau GA, Levin N, Moore MJ (1999) The human Prp8 protein is a component of both U2- and U12-dependent spliceosomes. RNA 5:893-908.
Luty AA, Kwok JB, Dobson-Stone C, Loy CT, Coupland KG, Karlstrom H, Sobow T, Tchorzewska J, Maruszak A, Barcikowska M, Panegyres PK, Zekanowski C, Brooks WS, Williams KL, Blair IP, Mather KA, Sachdev PS, Halliday GM, Schofield PR (2010) Sigma nonopioid intracellular receptor 1 mutations cause frontotemporal lobar degeneration-motor neuron disease. Ann Neurol 68:639-649.
Lv X, Li L, Lv L, Qu X, Jin S, Li K, Deng X, Cheng L, He H, Dong L (2015) HOXD9 promotes epithelial-mesenchymal transition and cancer metastasis by ZEB1 regulation in hepatocellular carcinoma. J Exp Clin Cancer Res 34:133.
Lyden D, Young AZ, Zagzag D, Yan W, Gerald W, O'Reilly R, Bader BL, Hynes RO, Zhuang Y, Manova K, Benezra R (1999) Id1 and Id3 are required for neurogenesis, angiogenesis and vascularization of tumour xenografts. Nature 401:670-677.

Lynch CN, Wang YC, Lund JK, Chen YW, Leal JA, Wiley SR (1999) TWEAK induces angiogenesis and proliferation of endothelial cells. J Biol Chem 274:8455-8459.
Ma LA, Mauro C, Cornish GH, Chai JG, Coe D, Fu HM, Patton D, Okkenhaug K, Franzoso G, Dyson J, Nourshargh S, Marelli-Berg FM (2010) Ig gene-like molecule CD31 plays a nonredundant role in the regulation of T-cell immunity and tolerance. P Natl Acad Sci USA 107:19461-19466.
Mackay CR, Imhof BA (1993) Cell adhesion in the immune system. Immunol Today 14:99-102.
Mackenzie F, Ruhrberg C (2012) Diverse roles for VEGF-A in the nervous system. Development 139:1371-1380.
Mackenzie IR, Bigio EH, Ince PG, Geser F, Neumann M, Cairns NJ, Kwong LK, Forman MS, Ravits J, Stewart H, Eisen A, McClusky L, Kretzschmar HA, Monoranu CM, Highley JR, Kirby J, Siddique T, Shaw PJ, Lee VM, Trojanowski JQ (2007) Pathological TDP-43 distinguishes sporadic amyotrophic lateral sclerosis from amyotrophic lateral sclerosis with SOD1 mutations. Ann Neurol 61:427-434.
Madabhushi R, Pan L, Tsai LH (2014) DNA damage and its links to neurodegeneration. Neuron 83:266-282.
Madar S, Brosh R, Buganim Y, Ezra O, Goldstein I, Solomon H, Kogan I, Goldfinger N, Klocker H, Rotter V (2009) Modulated expression of WFDC1 during carcinogenesis and cellular senescence. Carcinogenesis 30:20-27.
Maestrini E, Tamagnone L, Longati P, Cremona O, Gulisano M, Bione S, Tamanini F, Neel BG, Toniolo D, Comoglio PM (1996) A family of transmembrane proteins with homology to the MET-hepatocyte growth factor receptor. Proc Natl Acad Sci U S A 93:674-678.
Magnusson PU, Dimberg A, Mellberg S, Lukinius A, Claesson-Welsh L (2007) FGFR-1 regulates angiogenesis through cytokines interleukin-4 and pleiotrophin. Blood 110:4214-4222.
Maitre JL, Heisenberg CP (2013) Three functions of cadherins in cell adhesion. Curr Biol 23:R626-633.
Mancias JD, Goldberg J (2008) Structural basis of cargo membrane protein discrimination by the human COPII coat machinery. EMBO J 27:2918-2928.
Mangale VS, Hirokawa KE, Satyaki PR, Gokulchandran N, Chikbire S, Subramanian L, Shetty AS, Martynoga B, Paul J, Mai MV, Li Y, Flanagan LA, Tole S, Monuki ES (2008) Lhx2 selector activity specifies cortical identity and suppresses hippocampal organizer fate. Science 319:304-309.
Marangi G, Traynor BJ (2015) Genetic causes of amyotrophic lateral sclerosis: new genetic analysis methodologies entailing new opportunities and challenges. Brain Res 1607:75-93.
Marin O, Yaron A, Bagri A, Tessier-Lavigne M, Rubenstein JL (2001) Sorting of striatal and cortical interneurons regulated by semaphorin-neuropilin interactions. Science 293:872-875.
Martin LJ, Wong M (2013) Aberrant regulation of DNA methylation in amyotrophic lateral sclerosis: a new target of disease mechanisms. Neurotherapeutics 10:722-733.
Maruyama H, Morino H, Ito H, Izumi Y, Kato H, Watanabe Y, Kinoshita Y, Kamada M, Nodera H, Suzuki H, Komure O, Matsuura S, Kobatake K, Morimoto N, Abe K, Suzuki N, Aoki M, Kawata A, Hirai T, Kato T, Ogasawara K, Hirano A, Takumi T, Kusaka H, Hagiwara K, Kaji R, Kawakami H (2010) Mutations of optineurin in amyotrophic lateral sclerosis. Nature 465:223-226.

Marzluff WF, Gongidi P, Woods KR, Jin J, Maltais LJ (2002) The human and mouse replication-dependent histone genes. Genomics 80:487-498.
Marzluff WF, Wagner EJ, Duronio RJ (2008) Metabolism and regulation of canonical histone mRNAs: life without a poly(A) tail. Nat Rev Genet 9:843-854.
Matozaki T, Murata Y, Okazawa H, Ohnishi H (2009) Functions and molecular mechanisms of the CD47-SIRPalpha signalling pathway. Trends Cell Biol 19:72-80.
Matsumoto S, Abe Y, Fujibuchi T, Takeuchi T, Kito K, Ueda N, Shigemoto K, Gyo K (2004) Characterization of a MAPKK-like protein kinase TOPK. Biochem Biophys Res Commun 325:997-1004.
Matter N, Herrlich P, Konig H (2002) Signal-dependent regulation of splicing via phosphorylation of Sam68. Nature 420:691-695.
McCleverty CJ, Hornsby M, Spraggon G, Kreusch A (2007) Crystal structure of human Pus10, a novel pseudouridine synthase. J Mol Biol 373:1243-1254.
McFadden DG, Barbosa AC, Richardson JA, Schneider MD, Srivastava D, Olson EN (2005) The Hand1 and Hand2 transcription factors regulate expansion of the embryonic cardiac ventricles in a gene dosage-dependent manner. Development 132:189-201.
McGrane MM (2007) Vitamin A regulation of gene expression: molecular mechanism of a prototype gene. J Nutr Biochem 18:497-508.
McMurray CT (2000) Neurodegeneration: diseases of the cytoskeleton? Cell Death Differ 7:861-865.
McNew JA, Parlati F, Fukuda R, Johnston RJ, Paz K, Paumet F, Sollner TH, Rothman JE (2000) Compartmental specificity of cellular membrane fusion encoded in SNARE proteins. Nature 407:153-159.
Meadows HJ, Benham CD, Cairns W, Gloger I, Jennings C, Medhurst AD, Murdock P, Chapman CG (2000) Cloning, localisation and functional expression of the human orthologue of the TREK-1 potassium channel. Pflugers Arch 439:714-722.
Mehlmann LM, Saeki Y, Tanaka S, Brennan TJ, Evsikov AV, Pendola FL, Knowles BB, Eppig JJ, Jaffe LA (2004) The Gs-linked receptor GPR3 maintains meiotic arrest in mammalian oocytes. Science 306:1947-1950.
Meistrich ML, Mohapatra B, Shirley CR, Zhao M (2003) Roles of transition nuclear proteins in spermiogenesis. Chromosoma 111:483-488.
Mello JA, Sillje HH, Roche DM, Kirschner DB, Nigg EA, Almouzni G (2002) Human Asf1 and CAF-1 interact and synergize in a repair-coupled nucleosome assembly pathway. EMBO Rep 3:329-334.
Mercado PA, Ayala YM, Romano M, Buratti E, Baralle FE (2005) Depletion of TDP 43 overrides the need for exonic and intronic splicing enhancers in the human apoA-II gene. Nucleic Acids Res 33:6000-6010.
Metheny-Barlow LJ, Li LY (2003) The enigmatic role of angiopoietin-1 in tumor angiogenesis. Cell Res 13:309-317.
Mikolajczak SA, Ma BY, Yoshida T, Yoshida R, Kelvin DJ, Ochi A (2004) The modulation of CD40 ligand signaling by transmembrane CD28 splice variant in human T cells. Journal of Experimental Medicine 199:1025-1031.
Milde-Langosch K (2005) The Fos family of transcription factors and their role in tumourigenesis. Eur J Cancer 41:2449-2461.
Militello A, Vitello G, Lunetta C, Toscano A, Maiorana G, Piccoli T, La Bella V (2002) The serum level of free testosterone is reduced in amyotrophic lateral sclerosis. J Neurol Sci 195:67-70.

Millecamps S, Salachas F, Cazeneuve C, Gordon P, Bricka B, Camuzat A, Guillot-Noel L, Russaouen O, Bruneteau G, Pradat PF, Le Forestier N, Vandenberghe N, Danel-Brunaud V, Guy N, Thauvin-Robinet C, Lacomblez L, Couratier P, Hannequin D, Seilhean D, Le Ber I, Corcia P, Camu W, Brice A, Rouleau G, LeGuern E, Meininger V (2010) SOD1, ANG, VAPB, TARDBP, and FUS mutations in familial amyotrophic lateral sclerosis: genotype-phenotype correlations. Journal of medical genetics 47:554-560.

Miller RG, Mitchell JD, Lyon M, Moore DH (2007) Riluzole for amyotrophic lateral sclerosis (ALS)/motor neuron disease (MND). Cochrane Database Syst Rev CD001447.

Minamoto S, Ikegame K, Ueno K, Narazaki M, Naka T, Yamamoto H, Matsumoto T, Saito H, Hosoe S, Kishimoto T (1997) Cloning and functional analysis of new members of STAT induced STAT inhibitor (SSI) family: SSI-2 and SSI-3. Biochem Bioph Res Co 237:79-83.

Mini E, Nobili S (2009) Pharmacogenetics: implementing personalized medicine. Clin Cases Miner Bone Metab 6:17-24.

Mircsof D, Langouet M, Rio M, Moutton S, Siquier-Pernet K, Bole-Feysot C, Cagnard N, Nitschke P, Gaspar L, Znidaric M, Alibeu O, Fritz AK, Wolfer DP, Schroter A, Bosshard G, Rudin M, Koester C, Crestani F, Seebeck P, Boddaert N, Prescott K, Study DDD, Hines R, Moss SJ, Fritschy JM, Munnich A, Amiel J, Brown SA, Tyagarajan SK, Colleaux L (2015) Mutations in NONO lead to syndromic intellectual disability and inhibitory synaptic defects. Nat Neurosci 18:1731-1736.

Mitsiades CS, Mitsiades NS, McMullan CJ, Poulaki V, Shringarpure R, Akiyama M, Hideshima T, Chauhan D, Joseph M, Libermann TA, Garcia-Echeverria C, Pearson MA, Hofmann F, Anderson KC, Kung AL (2004) Inhibition of the insulin-like growth factor receptor-1 tyrosine kinase activity as a therapeutic strategy for multiple myeloma, other hematologic malignancies, and solid tumors. Cancer Cell 5:221-230.

Miyamoto Y, Yoshimasa T, Arai H, Takaya K, Ogawa Y, Itoh H, Nakao K (1996) Alternative RNA splicing of the human endothelin-A receptor generates multiple transcripts. Biochem J 313 (Pt 3):795-801.

Mizielinska S, Isaacs AM (2014) C9orf72 amyotrophic lateral sclerosis and frontotemporal dementia: gain or loss of function? Curr Opin Neurol 27:515-523.

Moelleken J, Malsam J, Betts MJ, Movafeghi A, Reckmann I, Meissner I, Hellwig A, Russell RB, Sollner T, Brugger B, Wieland FT (2007) Differential localization of coatomer complex isoforms within the Golgi apparatus. Proc Natl Acad Sci U S A 104:4425-4430.

Mollereau C, Mouledous L (2000) Tissue distribution of the opioid receptor-like (ORL1) receptor. Peptides 21:907-917.

Mollereau C, Parmentier M, Mailleux P, Butour JL, Moisand C, Chalon P, Caput D, Vassart G, Meunier JC (1994) ORL1, a novel member of the opioid receptor family. Cloning, functional expression and localization. FEBS Lett 341:33-38.

Monkley SJ, Pritchard CA, Critchley DR (2001) Analysis of the mammalian talin2 gene TLN2. Biochem Biophys Res Commun 286:880-885.

Monsma FJ, Jr., Mahan LC, McVittie LD, Gerfen CR, Sibley DR (1990) Molecular cloning and expression of a D1 dopamine receptor linked to adenylyl cyclase activation. Proc Natl Acad Sci U S A 87:6723-6727.

Moore EE, Bendele AM, Thompson DL, Littau A, Waggie KS, Reardon B, Ellsworth JL (2005) Fibroblast growth factor-18 stimulates chondrogenesis and cartilage repair in a rat model of injury-induced osteoarthritis. Osteoarthritis Cartilage 13:623-631.

Morfini GA, Bosco DA, Brown H, Gatto R, Kaminska A, Song Y, Molla L, Baker L, Marangoni MN, Berth S, Tavassoli E, Bagnato C, Tiwari A, Hayward LJ, Pigino GF, Watterson DM, Huang CF, Banker G, Brown RH, Jr., Brady ST (2013) Inhibition of fast axonal transport by pathogenic SOD1 involves activation of p38 MAP kinase. PLoS One 8:e65235.

Morozova O, Marra MA (2008) Applications of next-generation sequencing technologies in functional genomics. Genomics 92:255-264.

Morrione A, Valentinis B, Xu SQ, Yumet G, Louvi A, Efstratiadis A, Baserga R (1997) Insulin-like growth factor II stimulates cell proliferation through the insulin receptor. Proc Natl Acad Sci U S A 94:3777-3782.

Mortiboys H, Thomas KJ, Koopman WJ, Klaffke S, Abou-Sleiman P, Olpin S, Wood NW, Willems PH, Smeitink JA, Cookson MR, Bandmann O (2008) Mitochondrial function and morphology are impaired in parkin-mutant fibroblasts. Ann Neurol 64:555-565.

Mostowy S, Cossart P (2012) Septins: the fourth component of the cytoskeleton. Nat Rev Mol Cell Biol 13:183-194.

Moya PR, Dodman NH, Timpano KR, Rubenstein LM, Rana Z, Fried RL, Reichardt LF, Heiman GA, Tischfield JA, King RA, Galdzicka M, Ginns EI, Wendland JR (2013) Rare missense neuronal cadherin gene (CDH2) variants in specific obsessive-compulsive disorder and Tourette disorder phenotypes. Eur J Hum Genet 21:850-854.

Munch C, Sedlmeier R, Meyer T, Homberg V, Sperfeld AD, Kurt A, Prudlo J, Peraus G, Hanemann CO, Stumm G, Ludolph AC (2004) Point mutations of the p150 subunit of dynactin (DCTN1) gene in ALS. Neurology 63:724-726.

Murthy KG, Manley JL (1995) The 160-kD subunit of human cleavage-polyadenylation specificity factor coordinates pre-mRNA 3'-end formation. Genes Dev 9:2672-2683.

Myer VE, Steitz JA (1995) Isolation and characterization of a novel, low abundance hnRNP protein: A0. RNA 1:171-182.

Nagasaka Y, Dillner K, Ebise H, Teramoto R, Nakagawa H, Lilius L, Axelman K, Forsell C, Ito A, Winblad B, Kimura T, Graff C (2005) A unique gene expression signature discriminates familial Alzheimer's disease mutation carriers from their wild-type siblings. Proc Natl Acad Sci U S A 102:14854-14859.

Nelissen RL, Sillekens PT, Beijer RP, Geurts van Kessel AH, van Venrooij WJ (1991) Structure, chromosomal localization and evolutionary conservation of the gene encoding human U1 snRNP-specific A protein. Gene 102:189-196.

Nelson P, Kiriakidou M, Sharma A, Maniataki E, Mourelatos Z (2003) The microRNA world: small is mighty. Trends Biochem Sci 28:534-540.

Neumann M, Sampathu DM, Kwong LK, Truax AC, Micsenyi MC, Chou TT, Bruce J, Schuck T, Grossman M, Clark CM, McCluskey LF, Miller BL, Masliah E, Mackenzie IR, Feldman H, Feiden W, Kretzschmar HA, Trojanowski JQ, Lee VMY (2006) Ubiquitinated TDP-43 in frontotemporal lobar degeneration and amyotrophic lateral sclerosis. Science 314:130-133.

Nguyen DT, Rumeau C, Gallet P, Jankowski R (2016) Olfactory exploration: State of the art. Eur Ann Otorhinolaryngol Head Neck Dis 133:113-118.

Nicolas G, Pottier C, Maltete D, Coutant S, Rovelet-Lecrux A, Legallic S, Rousseau S, Vaschalde Y, Guyant-Marechal L, Augustin J, Martinaud O, Defebvre L, Krystkowiak P, Pariente J, Clanet M, Labauge P, Ayrignac X, Lefaucheur R, Le Ber I, Frebourg T, Hannequin D, Campion D (2013) Mutation of the PDGFRB gene as a cause of idiopathic basal ganglia calcification. Neurology 80:181-187.

Nielsen J, Christiansen J, Lykke-Andersen J, Johnsen AH, Wewer UM, Nielsen FC (1999) A family of insulin-like growth factor II mRNA-binding proteins represses translation in late development. Mol Cell Biol 19:1262-1270.

Nishimura AL, Mitne-Neto M, Silva HC, Richieri-Costa A, Middleton S, Cascio D, Kok F, Oliveira JR, Gillingwater T, Webb J, Skehel P, Zatz M (2004) A mutation in the vesicle-trafficking protein VAPB causes late-onset spinal muscular atrophy and amyotrophic lateral sclerosis. Am J Hum Genet 75:822-831.

Ny T, Elgh F, Lund B (1984) The structure of the human tissue-type plasminogen activator gene: correlation of intron and exon structures to functional and structural domains. Proc Natl Acad Sci U S A 81:5355-5359.

Obuse C, Iwasaki O, Kiyomitsu T, Goshima G, Toyoda Y, Yanagida M (2004) A conserved Mis12 centromere complex is linked to heterochromatic HP1 and outer kinetochore protein Zwint-1. Nat Cell Biol 6:1135-1141.

Ockenga W, Kuhne S, Bocksberger S, Banning A, Tikkanen R (2013) Non-neuronal functions of the m2 muscarinic acetylcholine receptor. Genes (Basel) 4:171-197.

Ogawa H, Ishiguro K, Gaubatz S, Livingston DM, Nakatani Y (2002) A complex with chromatin modifiers that occupies E2F- and Myc-responsive genes in G0 cells. Science 296:1132-1136.

Ohno H, Shinoda K, Ohyama K, Sharp LZ, Kajimura S (2013) EHMT1 controls brown adipose cell fate and thermogenesis through the PRDM16 complex. Nature 504:163-167.

Oike Y, Ito Y, Maekawa H, Morisada T, Kubota Y, Akao M, Urano T, Yasunaga K, Suda T (2004) Angiopoietin-related growth factor (AGF) promotes angiogenesis. Blood 103:3760-3765.

Oike Y, Yasunaga K, Ito Y, Matsumoto S, Maekawa H, Morisada T, Arai F, Nakagata N, Takeya M, Masuho Y, Suda T (2003) Angiopoietin-related growth factor (AGF) promotes epidermal proliferation, remodeling, and regeneration. P Natl Acad Sci USA 100:9494-9499.

Ono S, Imai T, Shimizu N, Nakayama M, Mihori A, Kaneda K, Yamano T, Tsumura M (2000) Decreased plasma levels of fibronectin in amyotrophic lateral sclerosis. Acta Neurol Scand 101:391-394.

Ono S, Takahashi K, Jinnai K, Yamano T, Nagao K, Shimizu N, Yamauchi M (1998) Decreased type IV collagen of skin and serum in patients with amyotrophic lateral sclerosis. Neurology 51:114-120.

Ono T, Losada A, Hirano M, Myers MP, Neuwald AF, Hirano T (2003) Differential contributions of condensin I and condensin II to mitotic chromosome architecture in vertebrate cells. Cell 115:109-121.

Oosthuyse B, Moons L, Storkebaum E, Beck H, Nuyens D, Brusselmans K, Van Dorpe J, Hellings P, Gorselink M, Heymans S, Theilmeier G, Dewerchin M, Laudenbach V, Vermylen P, Raat H, Acker T, Vleminckx V, Van Den Bosch L, Cashman N, Fujisawa H, Drost MR, Sciot R, Bruyninckx F, Hicklin DJ, Ince C, Gressens P, Lupu F, Plate KH, Robberecht W, Herbert JM, Collen D, Carmeliet P (2001) Deletion of the hypoxia-response element in the vascular endothelial

growth factor promoter causes motor neuron degeneration. Nat Genet 28:131-138.
Orlacchio A, Babalini C, Borreca A, Patrono C, Massa R, Basaran S, Munhoz RP, Rogaeva EA, St George-Hyslop PH, Bernardi G, Kawarai T (2010) SPATACSIN mutations cause autosomal recessive juvenile amyotrophic lateral sclerosis. Brain 133:591-598.
Ortiz-Medina H, Emond MR, Jontes JD (2015) Zebrafish Calsyntenins Mediate Homophilic Adhesion through Their Amino-Terminal Cadherin Repeats. Neuroscience 286:87-96.
Ou SH, Wu F, Harrich D, Garcia-Martinez LF, Gaynor RB (1995) Cloning and characterization of a novel cellular protein, TDP-43, that binds to human immunodeficiency virus type 1 TAR DNA sequence motifs. J Virol 69:3584-3596.
Pajerowski AG, Nguyen C, Aghajanian H, Shapiro MJ, Shapiro VS (2009) NKAP Is a Transcriptional Repressor of Notch Signaling and Is Required for T Cell Development. Immunity 30:696-707.
Palma G, Barbieri A, Bimonte S, Palla M, Zappavigna S, Caraglia M, Ascierto PA, Ciliberto G, Arra C (2013) Interleukin 18: Friend or foe in cancer. Bba-Rev Cancer 1836:296-303.
Pan TC, Zhang RZ, Mattei MG, Timpl R, Chu ML (1992) Cloning and Chromosomal Location of Human Alpha-1(Xvi) Collagen. P Natl Acad Sci USA 89:6565-6569.
Paris MJ, Williams BRG (2000) Characterization of a 500-kb contig spanning the region between c-Ha-Ras and MUC2 on chromosome 11p15.5. Genomics 69:196-202.
Parisiadou L, Cai H (2010) LRRK2 function on actin and microtubule dynamics in Parkinson disease. Commun Integr Biol 3:396-400.
Park CC, Morel JCM, Amin MA, Connors MA, Harlow LA, Koch AE (2001) Evidence of IL-18 as a novel angiogenic mediator. J Immunol 167:1644-1653.
Park JY, Yoo HW, Kim BR, Park R, Choi SY, Kim Y (2008) Identification of a novel human Rad51 variant that promotes DNA strand exchange. Nucleic Acids Res 36:3226-3234.
Park SM, Chatterjee VK (2005) Genetics of congenital hypothyroidism. J Med Genet 42:379-389.
Park YM (2014) CD36, a scavenger receptor implicated in atherosclerosis. Exp Mol Med 46:e99.
Parker LH, Schmidt M, Jin SW, Gray AM, Beis D, Pham T, Frantz G, Palmieri S, Hillan K, Stainier DY, De Sauvage FJ, Ye W (2004) The endothelial-cell-derived secreted factor Egfl7 regulates vascular tube formation. Nature 428:754-758.
Parkinson N, Ince PG, Smith MO, Highley R, Skibinski G, Andersen PM, Morrison KE, Pall HS, Hardiman O, Collinge J, Shaw PJ, Fisher EM, Study MRCPiA, Consortium FR (2006) ALS phenotypes with mutations in CHMP2B (charged multivesicular body protein 2B). Neurology 67:1074-1077.
Pasternack SM, Refke M, Paknia E, Hennies HC, Franz T, Schafer N, Fryer A, van Steensel M, Sweeney E, Just M, Grimm C, Kruse R, Ferrandiz C, Nothen MM, Fischer U, Betz RC (2013) Mutations in SNRPE, which encodes a core protein of the spliceosome, cause autosomal-dominant hypotrichosis simplex. Am J Hum Genet 92:81-87.

Patacchioli FR, Monnazzi P, Scontrini A, Tremante E, Caridi I, Brunetti E, Buttarelli FR, Pontieri FE (2003) Adrenal dysregulation in amyotrophic lateral sclerosis. J Endocrinol Invest 26:RC23-25.

Paushkin SV, Patel M, Furia BS, Peltz SW, Trotta CR (2004) Identification of a human endonuclease complex reveals a link between tRNA splicing and pre-mRNA 3' end formation. Cell 117:311-321.

Pedrotti S, Bielli P, Paronetto MP, Ciccosanti F, Fimia GM, Stamm S, Manley JL, Sette C (2010) The splicing regulator Sam68 binds to a novel exonic splicing silencer and functions in SMN2 alternative splicing in spinal muscular atrophy. EMBO J 29:1235-1247.

Pellegrini L, Yu DS, Lo T, Anand S, Lee M, Blundell TL, Venkitaraman AR (2002) Insights into DNA recombination from the structure of a RAD51-BRCA2 complex. Nature 420:287-293.

Pevzner A, Miyashita T, Schiffman AJ, Guzowski JF (2012) Temporal dynamics of Arc gene induction in hippocampus: relationship to context memory formation. Neurobiol Learn Mem 97:313-320.

Philippar U, Roussos ET, Oser M, Yamaguchi H, Kim HD, Giampieri S, Wang Y, Goswami S, Wyckoff JB, Lauffenburger DA, Sahai E, Condeelis JS, Gertler FB (2008) A Mena invasion isoform potentiates EGF-induced carcinoma cell invasion and metastasis. Dev Cell 15:813-828.

Philips T, Robberecht W (2011) Neuroinflammation in amyotrophic lateral sclerosis: role of glial activation in motor neuron disease. Lancet Neurol 10:253-263.

Picher-Martel V, Valdmanis PN, Gould PV, Julien JP, Dupre N (2016) From animal models to human disease: a genetic approach for personalized medicine in ALS. Acta Neuropathol Commun 4:70.

Plourde M, Manhes C, Leblanc G, Durocher F, Dumont M, Sinilnikova O, Inherit B, Simard J (2008) Mutation analysis and characterization of HSD17B2 sequence variants in breast cancer cases from French Canadian families with high risk of breast and ovarian cancer. J Mol Endocrinol 40:161-172.

Polymenidou M, Lagier-Tourenne C, Hutt KR, Bennett CF, Cleveland DW, Yeo GW (2012) Misregulated RNA processing in amyotrophic lateral sclerosis. Brain Res 1462:3-15.

Polymenidou M, Lagier-Tourenne C, Hutt KR, Huelga SC, Moran J, Liang TY, Ling SC, Sun E, Wancewicz E, Mazur C, Kordasiewicz H, Sedaghat Y, Donohue JP, Shiue L, Bennett CF, Yeo GW, Cleveland DW (2011) Long pre-mRNA depletion and RNA missplicing contribute to neuronal vulnerability from loss of TDP-43. Nat Neurosci 14:459-468.

Porcu M, Kleppe M, Gianfelici V, Geerdens E, De Keersmaecker K, Tartaglia M, Foa R, Soulier J, Cauwelier B, Uyttebroeck A, Macintyre E, Vandenberghe P, Asnafi V, Cools J (2012) Mutation of the receptor tyrosine phosphatase PTPRC (CD45) in T-cell acute lymphoblastic leukemia. Blood 119:4476-4479.

Probstmeier R, Pesheva P (1999) Tenascin-C inhibits beta(1) integrin-dependent cell adhesion and neurite outgrowth on fibronectin by a disialoganglioside-mediated signaling mechanism. Glycobiology 9:101-114.

Qian BZ, Li J, Zhang H, Kitamura T, Zhang J, Campion LR, Kaiser EA, Snyder LA, Pollard JW (2011) CCL2 recruits inflammatory monocytes to facilitate breast-tumour metastasis. Nature 475:222-225.

Rabin SJ, Kim JM, Baughn M, Libby RT, Kim YJ, Fan Y, La Spada A, Stone B, Ravits J (2010) Sporadic ALS has compartment-specific aberrant exon splicing and altered cell-matrix adhesion biology. Hum Mol Genet 19:313-328.

Rademakers R, Stewart H, Dejesus-Hernandez M, Krieger C, Graff-Radford N, Fabros M, Briemberg H, Cashman N, Eisen A, Mackenzie IR (2010) Fus gene mutations in familial and sporadic amyotrophic lateral sclerosis. Muscle Nerve 42:170-176.

Radmanesh F, Caglayan AO, Silhavy JL, Yilmaz C, Cantagrel V, Omar T, Rosti B, Kaymakcalan H, Gabriel S, Li M, Sestan N, Bilguvar K, Dobyns WB, Zaki MS, Gunel M, Gleeson JG (2013) Mutations in LAMB1 cause cobblestone brain malformation without muscular or ocular abnormalities. Am J Hum Genet 92:468-474.

Raemaekers T, Ribbeck K, Beaudouin J, Annaert W, Van Camp M, Stockmans I, Smets N, Bouillon R, Ellenberg J, Carmeliet G (2003a) NuSAP, a novel microtubule-associated protein involved in mitotic spindle organization. Journal of Cell Biology 162:1017-1029.

Raemaekers T, Ribbeck K, Beaudouin J, Annaert W, Van Camp M, Stockmans I, Smets N, Bouillon R, Ellenberg J, Carmeliet G (2003b) NuSAP, a novel microtubule-associated protein involved in mitotic spindle organization. J Cell Biol 162:1017-1029.

Rajalingam K, Schreck R, Rapp UR, Albert S (2007) Ras oncogenes and their downstream targets. Bba-Mol Cell Res 1773:1177-1195.

Raman R, Allen SP, Goodall EF, Kramer S, Ponger LL, Heath PR, Milo M, Hollinger HC, Walsh T, Highley JR, Olpin S, McDermott CJ, Shaw PJ, Kirby J (2015) Gene expression signatures in motor neurone disease fibroblasts reveal dysregulation of metabolism, hypoxia-response and RNA processing functions. Neuropathol Appl Neurobiol 41:201-226.

Raskovalova T, Huang X, Sitkovsky M, Zacharia LC, Jackson EK, Gorelik E (2005) Gs protein-coupled adenosine receptor signaling and lytic function of activated NK cells. J Immunol 175:4383-4391.

Razzaq A, Robinson IM, McMahon HT, Skepper JN, Su Y, Zelhof AC, Jackson AP, Gay NJ, O'Kane CJ (2001) Amphiphysin is necessary for organization of the excitation-contraction coupling machinery of muscles, but not for synaptic vesicle endocytosis in Drosophila. Genes Dev 15:2967-2979.

Rees MI, Lewis TM, Kwok JB, Mortier GR, Govaert P, Snell RG, Schofield PR, Owen MJ (2002) Hyperekplexia associated with compound heterozygote mutations in the beta-subunit of the human inhibitory glycine receptor (GLRB). Hum Mol Genet 11:853-860.

Rege TA, Hagood JS (2006) Thy-1 as a regulator of cell-cell and cell-matrix interactions in axon regeneration, apoptosis, adhesion, migration, cancer, and fibrosis. Faseb Journal 20:1045-1054.

Renton AE, Majounie E, Waite A, Simon-Sanchez J, Rollinson S, Gibbs JR, Schymick JC, Laaksovirta H, van Swieten JC, Myllykangas L, Kalimo H, Paetau A, Abramzon Y, Remes AM, Kaganovich A, Scholz SW, Duckworth J, Ding J, Harmer DW, Hernandez DG, Johnson JO, Mok K, Ryten M, Trabzuni D, Guerreiro RJ, Orrell RW, Neal J, Murray A, Pearson J, Jansen IE, Sondervan D, Seelaar H, Blake D, Young K, Halliwell N, Callister JB, Toulson G, Richardson A, Gerhard A, Snowden J, Mann D, Neary D, Nalls MA, Peuralinna T, Jansson L, Isoviita VM, Kaivorinne AL, Holtta-Vuori M, Ikonen E, Sulkava R, Benatar M, Wuu J, Chio A, Restagno G, Borghero G, Sabatelli M, Heckerman D, Rogaeva E, Zinman L, Rothstein JD, Sendtner M, Drepper C, Eichler EE, Alkan C, Abdullaev Z, Pack SD, Dutra A, Pak E, Hardy J, Singleton A, Williams NM, Heutink P, Pickering-Brown S, Morris HR, Tienari PJ, Traynor BJ (2011) A

hexanucleotide repeat expansion in C9ORF72 is the cause of chromosome 9p21-linked ALS-FTD. Neuron 72:257-268.
Richardson HE, Stueland CS, Thomas J, Russell P, Reed SI (1990) Human cDNAs encoding homologs of the small p34Cdc28/Cdc2-associated protein of Saccharomyces cerevisiae and Schizosaccharomyces pombe. Genes Dev 4:1332-1344.
Roach W, Plomann M (2007) PACSIN3 overexpression increases adipocyte glucose transport through GLUT1. Biochem Biophys Res Commun 355:745-750.
Robb GB, Rana TM (2007) RNA helicase A interacts with RISC in human cells and functions in RISC loading. Mol Cell 26:523-537.
Robinson DG, Pimpl P (2014) Clathrin and post-Golgi trafficking: a very complicated issue. Trends Plant Sci 19:134-139.
Robinson MS, Bonifacino JS (2001) Adaptor-related proteins. Curr Opin Cell Biol 13:444-453.
Rojas Walh RU (2007) G-protein coupled receptors & autism -- reflections on a double-edged sword at the example of the oxytocin receptor system. Indian J Med Res 126:13-21.
Roland WS, Vincken JP, Gouka RJ, van Buren L, Gruppen H, Smit G (2011) Soy isoflavones and other isoflavonoids activate the human bitter taste receptors hTAS2R14 and hTAS2R39. J Agric Food Chem 59:11764-11771.
Rosen DR (1993) Mutations in Cu/Zn superoxide dismutase gene are associated with familial amyotrophic lateral sclerosis. Nature 364:362.
Rosenfeld J, Ellis A (2008) Nutrition and Dietary Supplements in Motor Neuron Disease. Phys Med Rehabil Cli 19:573-+.
Rossoll W, Kroning AK, Ohndorf UM, Steegborn C, Jablonka S, Sendtner M (2002) Specific interaction of Smn, the spinal muscular atrophy determining gene product, with hnRNP-R and gry-rbp/hnRNP-Q: a role for Smn in RNA processing in motor axons? Hum Mol Genet 11:93-105.
Rouault JP, Falette N, Guehenneux F, Guillot C, Rimokh R, Wang Q, Berthet C, Moyret-Lalle C, Savatier P, Pain B, Shaw P, Berger R, Samarut J, Magaud JP, Ozturk M, Samarut C, Puisieux A (1996) Identification of BTG2, an antiproliferative p53-dependent component of the DNA damage cellular response pathway. Nat Genet 14:482-486.
Rowland BD, Peeper DS (2006) KLF4, p21 and context-dependent opposing forces in cancer. Nat Rev Cancer 6:11-23.
Ryan MC, Tizard R, VanDevanter DR, Carter WG (1994) Cloning of the LamA3 gene encoding the alpha 3 chain of the adhesive ligand epiligrin. Expression in wound repair. J Biol Chem 269:22779-22787.
Ryu J, Liu L, Wong TP, Wu DC, Burette A, Weinberg R, Wang YT, Sheng M (2006) A critical role for myosin IIb in dendritic spine morphology and synaptic function. Neuron 49:175-182.
Sabatelli M, Zollino M, Conte A, Del Grande A, Marangi G, Lucchini M, Mirabella M, Romano A, Piacentini R, Bisogni G, Lattante S, Luigetti M, Rossini PM, Moncada A (2015) Primary fibroblasts cultures reveal TDP-43 abnormalities in amyotrophic lateral sclerosis patients with and without SOD1 mutations. Neurobiology of Aging 36.
Sadakata T, Washida M, Iwayama Y, Shoji S, Sato Y, Ohkura T, Katoh-Semba R, Nakajima M, Sekine Y, Tanaka M, Nakamura K, Iwata Y, Tsuchiya KJ, Mori N, Detera-Wadleigh SD, Ichikawa H, Itohara S, Yoshikawa T, Furuichi T (2007)

Autistic-like phenotypes in Cadps2-knockout mice and aberrant CADPS2 splicing in autistic patients. J Clin Invest 117:931-943.
Sahakitrungruang T, Tee MK, Blackett PR, Miller WL (2011) Partial defect in the cholesterol side-chain cleavage enzyme P450scc (CYP11A1) resembling nonclassic congenital lipoid adrenal hyperplasia. J Clin Endocrinol Metab 96:792-798.
Saint-Pol A, Yelamos B, Amessou M, Mills IG, Dugast M, Tenza D, Schu P, Antony C, McMahon HT, Lamaze C, Johannes L (2004) Clathrin adaptor epsinR is required for retrograde sorting on early endosomal membranes. Dev Cell 6:525-538.
Saito T, Iwata N, Tsubuki S, Takaki Y, Takano J, Huang SM, Suemoto T, Higuchi M, Saido TC (2005) Somatostatin regulates brain amyloid beta peptide Abeta42 through modulation of proteolytic degradation. Nat Med 11:434-439.
Salih DA, Tripathi G, Holding C, Szestak TA, Gonzalez MI, Carter EJ, Cobb LJ, Eisemann JE, Pell JM (2004) Insulin-like growth factor-binding protein 5 (Igfbp5) compromises survival, growth, muscle development, and fertility in mice. Proc Natl Acad Sci U S A 101:4314-4319.
Samji T, Hong S, Means RE (2014) The Membrane Associated RING-CH Proteins: A Family of E3 Ligases with Diverse Roles through the Cell. Int Sch Res Notices 2014:637295.
Sanger F, Nicklen S, Coulson AR (1977) DNA sequencing with chain-terminating inhibitors. Proc Natl Acad Sci U S A 74:5463-5467.
Sapp PC, Hosler BA, McKenna-Yasek D, Chin W, Gann A, Genise H, Gorenstein J, Huang M, Sailer W, Scheffler M, Valesky M, Haines JL, Pericak-Vance M, Siddique T, Horvitz HR, Brown RH, Jr. (2003) Identification of two novel loci for dominantly inherited familial amyotrophic lateral sclerosis. Am J Hum Genet 73:397-403.
Sasaki T, Larsson H, Tisi D, Claesson-Welsh L, Hohenester E, Timpl R (2000) Endostatins derived from collagens XV and XVIII differ in structural and binding properties, tissue distribution and anti-angiogenic activity. Journal of Molecular Biology 301:1179-1190.
Sassone-Corsi P (1998) Coupling gene expression to cAMP signalling: role of CREB and CREM. Int J Biochem Cell Biol 30:27-38.
Sato S, Nakamura M, Cho DH, Tapscott SJ, Ozaki H, Kawakami K (2002) Identification of transcriptional targets for Six5: implication for the pathogenesis of myotonic dystrophy type 1. Hum Mol Genet 11:1045-1058.
Schafer MK, Frotscher M (2012) Role of L1CAM for axon sprouting and branching. Cell Tissue Res 349:39-48.
Schmidt A, Langbein L, Pratzel S, Rode M, Rackwitz HR, Franke WW (1999) Plakophilin 3--a novel cell-type-specific desmosomal plaque protein. Differentiation 64:291-306.
Schoch S, Castillo PE, Jo T, Mukherjee K, Geppert M, Wang Y, Schmitz F, Malenka RC, Sudhof TC (2002) RIM1alpha forms a protein scaffold for regulating neurotransmitter release at the active zone. Nature 415:321-326.
Schoenberg DR, Maquat LE (2012) Regulation of cytoplasmic mRNA decay. Nat Rev Genet 13:246-259.
Schwartz N, Verma A, Bivens CB, Schwartz Z, Boyan BD (2016) Rapid steroid hormone actions via membrane receptors. Biochim Biophys Acta 1863:2289-2298.

Scotter EL, Chen HJ, Shaw CE (2015) TDP-43 Proteinopathy and ALS: Insights into Disease Mechanisms and Therapeutic Targets. Neurotherapeutics 12:352-363.
Seki A, Coppinger JA, Jang CY, Yates JR, Fang G (2008) Bora and the kinase Aurora a cooperatively activate the kinase Plk1 and control mitotic entry. Science 320:1655-1658.
Senetar MA, Moncman CL, McCann RO (2007) Talin2 is induced during striated muscle differentiation and is targeted to stable adhesion complexes in mature muscle. Cell Motil Cytoskeleton 64:157-173.
Sephton CF, Cenik C, Kucukural A, Dammer EB, Cenik B, Han Y, Dewey CM, Roth FP, Herz J, Peng J, Moore MJ, Yu G (2011) Identification of neuronal RNA targets of TDP-43-containing ribonucleoprotein complexes. J Biol Chem 286:1204-1215.
Sfiligoi C, de Luca A, Cascone I, Sorbello V, Fuso L, Ponzone R, Biglia N, Audero E, Arisio R, Bussolino F, Sismondi P, De Bortoli M (2003) Angiopoietin-2 expression in breast cancer correlates with lymph node invasion and short survival. Int J Cancer 103:466-474.
Shan L, Yu M, Qiu C, Snyderwine EG (2003) Id4 regulates mammary epithelial cell growth and differentiation and is overexpressed in rat mammary gland carcinomas. Am J Pathol 163:2495-2502.
Shen XC, Xi G, Maile LA, Wai C, Rosen CJ, Clemmons DR (2012) Insulin-Like Growth Factor (IGF) Binding Protein 2 Functions Coordinately with Receptor Protein Tyrosine Phosphatase beta and the IGF-I Receptor To Regulate IGF-I-Stirnulated Signaling. Molecular and Cellular Biology 32:4116-4130.
Shepard J, Reick M, Olson S, Graveley BR (2002) Characterization of U2AF(6), a splicing factor related to U2AF(35). Mol Cell Biol 22:221-230.
Shi Y, Zhao Y, Deng HK (2010) Powering Reprogramming with Vitamin C. Cell Stem Cell 6:1-2.
Shin C, Feng Y, Manley JL (2004) Dephosphorylated SRp38 acts as a splicing repressor in response to heat shock. Nature 427:553-558.
Shin YE, Hwang IW, Jin HJ (2016) Association between glutathione S-transferases M1, T1 and P1 gene polymorphisms and prostate cancer in Koreans. Genes Genom 38:235-241.
Shindo T, Manabe I, Fukushima Y, Tobe K, Aizawa K, Miyamoto S, Kawai-Kowase K, Moriyama N, Imai Y, Kawakami H, Nishimatsu H, Ishikawa T, Suzuki T, Morita H, Maemura K, Sata M, Hirata Y, Komukai M, Kagechika H, Kadowaki T, Kurabayashi M, Nagai R (2002) Kruppel-like zinc-finger transcription factor KLF5/BTEB2 is a target for angiotensin II signaling and an essential regulator of cardiovascular remodeling. Nat Med 8:856-863.
Shirokova E, Raguse JD, Meyerhof W, Krautwurst D (2008) The human vomeronasal type-1 receptor family--detection of volatiles and cAMP signaling in HeLa/Olf cells. FASEB J 22:1416-1425.
Shoesmith CL, Findlater K, Rowe A, Strong MJ (2007) Prognosis of amyotrophic lateral sclerosis with respiratory onset. J Neurol Neurosurg Psychiatry 78:629-631.
Shtivelman E (1997) A link between metastasis and resistance to apoptosis of variant small cell lung carcinoma. Oncogene 14:2167-2173.
Siddiqui IJ, Pervaiz N, Abbasi AA (2016) The Parkinson Disease gene SNCA: Evolutionary and structural insights with pathological implication. Sci Rep 6:24475.

Sidova M, Tomankova S, Abaffy P, Kubista M, Sindelka R (2015) Effects of post-mortem and physical degradation on RNA integrity and quality. Biomol Detect Quantif 5:3-9.
Sikdar N, Banerjee S, Lee KY, Wincovitch S, Pak E, Nakanishi K, Jasin M, Dutra A, Myung K (2009) DNA damage responses by human ELG1 in S phase are important to maintain genomic integrity. Cell Cycle 8:3199-3207.
Sillekens PT, Habets WJ, Beijer RP, van Venrooij WJ (1987) cDNA cloning of the human U1 snRNA-associated A protein: extensive homology between U1 and U2 snRNP-specific proteins. EMBO J 6:3841-3848.
Silver DL, Watkins-Chow DE, Schreck KC, Pierfelice TJ, Larson DM, Burnetti AJ, Liaw HJ, Myung K, Walsh CA, Gaiano N, Pavan WJ (2010) The exon junction complex component Magoh controls brain size by regulating neural stem cell division. Nat Neurosci 13:551-558.
Simpson CL, Lemmens R, Miskiewicz K, Broom WJ, Hansen VK, van Vught PW, Landers JE, Sapp P, Van Den Bosch L, Knight J, Neale BM, Turner MR, Veldink JH, Ophoff RA, Tripathi VB, Beleza A, Shah MN, Proitsi P, Van Hoecke A, Carmeliet P, Horvitz HR, Leigh PN, Shaw CE, van den Berg LH, Sham PC, Powell JF, Verstreken P, Brown RH, Jr., Robberecht W, Al-Chalabi A (2009a) Variants of the elongator protein 3 (ELP3) gene are associated with motor neuron degeneration. Hum Mol Genet 18:472-481.
Simpson CL, Lemmens R, Miskiewicz K, Broom WJ, Hansen VK, van Vught PWJ, Landers JE, Sapp P, Van Den Bosch L, Knight J, Neale BM, Turner MR, Veldink JH, Ophoff RA, Tripathi VB, Beleza A, Shah MN, Proitsi P, Van Hoecke A, Carmeliet P, Horvitz HR, Leigh PN, Shaw CE, van den Berg LH, Sham PC, Powell JF, Verstreken P, Brown RH, Robberecht W, Al-Chalabi A (2009b) Variants of the elongator protein 3 (ELP3) gene are associated with motor neuron degeneration. Human Molecular Genetics 18:472-481.
Sine JP, Ferrand R, Colas B (1991) Sex-related differences in the expression of chick enterocyte butyrylcholinesterase during embryonic and post-hatching development. Mol Cell Biochem 103:15-21.
Singh B, Coffey RJ (2014) From wavy hair to naked proteins: the role of transforming growth factor alpha in health and disease. Semin Cell Dev Biol 28:12-21.
Smith BN, Ticozzi N, Fallini C, Gkazi AS, Topp S, Kenna KP, Scotter EL, Kost J, Keagle P, Miller JW, Calini D, Vance C, Danielson EW, Troakes C, Tiloca C, Al-Sarraj S, Lewis EA, King A, Colombrita C, Pensato V, Castellotti B, de Belleroche J, Baas F, ten Asbroek AL, Sapp PC, McKenna-Yasek D, McLaughlin RL, Polak M, Asress S, Esteban-Perez J, Munoz-Blanco JL, Simpson M, Consortium S, van Rheenen W, Diekstra FP, Lauria G, Duga S, Corti S, Cereda C, Corrado L, Soraru G, Morrison KE, Williams KL, Nicholson GA, Blair IP, Dion PA, Leblond CS, Rouleau GA, Hardiman O, Veldink JH, van den Berg LH, Al-Chalabi A, Pall H, Shaw PJ, Turner MR, Talbot K, Taroni F, Garcia-Redondo A, Wu Z, Glass JD, Gellera C, Ratti A, Brown RH, Jr., Silani V, Shaw CE, Landers JE (2014) Exome-wide rare variant analysis identifies TUBA4A mutations associated with familial ALS. Neuron 84:324-331.
Song X, Di Giovanni V, He N, Wang K, Ingram A, Rosenblum ND, Pei Y (2009) Systems biology of autosomal dominant polycystic kidney disease (ADPKD): computational identification of gene expression pathways and integrated regulatory networks. Hum Mol Genet 18:2328-2343.

Spanjaard RA, Lee PJ, Sarkar S, Goedegebuure PS, Eberlein TJ (1997) Clone 10d/BM28 (CDCL1), an early S-phase protein, is an important growth regulator of melanoma. Cancer Res 57:5122-5128.
Spataro R, Ficano L, Piccoli F, La Bella V (2011) Percutaneous endoscopic gastrostomy in amyotrophic lateral sclerosis: effect on survival. J Neurol Sci 304:44-48.
Spataro R, Volanti P, Vitale F, Meli F, Colletti T, Di Natale A, La Bella V (2015) Plasma cortisol level in amyotrophic lateral sclerosis. J Neurol Sci 358:282-286.
Sreedharan J, Blair IP, Tripathi VB, Hu X, Vance C, Rogelj B, Ackerley S, Durnall JC, Williams KL, Buratti E, Baralle F, de Belleroche J, Mitchell JD, Leigh PN, Al-Chalabi A, Miller CC, Nicholson G, Shaw CE (2008) TDP-43 mutations in familial and sporadic amyotrophic lateral sclerosis. Science 319:1668-1672.
Stewart H, Rutherford NJ, Briemberg H, Krieger C, Cashman N, Fabros M, Baker M, Fok A, DeJesus-Hernandez M, Eisen A, Rademakers R, Mackenzie IR (2012) Clinical and pathological features of amyotrophic lateral sclerosis caused by mutation in the C9ORF72 gene on chromosome 9p. Acta Neuropathol 123:409-417.
Stucke VM, Timmerman E, Vandekerckhove J, Gevaert K, Hall A (2007) The MAGUK protein MPP7 binds to the polarity protein hDlg1 and facilitates epithelial tight junction formation. Mol Biol Cell 18:1744-1755.
Su EJ, Cheng YH, Chatterton RT, Lin ZH, Yin P, Reierstad S, Innes J, Bulun SE (2007) Regulation of 17-beta hydroxysteroid dehydrogenase type 2 in human placental endothelial cells. Biology of Reproduction 77:517-525.
Su ZJ, Hahn CN, Goodall GJ, Reck NM, Leske AF, Davy A, Kremmidiotis G, Vadas MA, Gamble JR (2004) A vascular cell-restricted RhoGAP, p73RhoGAP, is a key regulator of angiogenesis. Proc Natl Acad Sci U S A 101:12212-12217.
Sun Q, Lin P, Zhang J, Li X, Yang L, Huang J, Zhou Z, Liu P, Liu N (2015) Expression of Fibroblast Growth Factor 10 Is Correlated with Poor Prognosis in Gastric Adenocarcinoma. Tohoku J Exp Med 236:311-318.
Sun YX, Kucej M, Fan HY, Yu H, Sun QY, Zou H (2009) Separase Is Recruited to Mitotic Chromosomes to Dissolve Sister Chromatid Cohesion in a DNA-Dependent Manner. Cell 137:123-132.
Swash M (2013) Ventilation in ALS. Eur J Neurol 20:1508-1509.
Syvaoja J, Suomensaari S, Nishida C, Goldsmith JS, Chui GS, Jain S, Linn S (1990) DNA polymerases alpha, delta, and epsilon: three distinct enzymes from HeLa cells. Proc Natl Acad Sci U S A 87:6664-6668.
Ta HQ, Gioeli D (2014) The convergence of DNA damage checkpoint pathways and androgen receptor signaling in prostate cancer. Endocr Relat Cancer 21:R395-407.
Tagami H, Ray-Gallet D, Almouzni G, Nakatani Y (2004) Histone H3.1 and H3.3 complexes mediate nucleosome assembly pathways dependent or independent of DNA synthesis. Cell 116:51-61.
Takahashi Y, Fukuda Y, Yoshimura J, Toyoda A, Kurppa K, Moritoyo H, Belzil VV, Dion PA, Higasa K, Doi K, Ishiura H, Mitsui J, Date H, Ahsan B, Matsukawa T, Ichikawa Y, Moritoyo T, Ikoma M, Hashimoto T, Kimura F, Murayama S, Onodera O, Nishizawa M, Yoshida M, Atsuta N, Sobue G, JaCals, Fifita JA, Williams KL, Blair IP, Nicholson GA, Gonzalez-Perez P, Brown RH, Jr., Nomoto M, Elenius K, Rouleau GA, Fujiyama A, Morishita S, Goto J, Tsuji S (2013) ERBB4 mutations that disrupt the neuregulin-ErbB4 pathway cause amyotrophic lateral sclerosis type 19. Am J Hum Genet 93:900-905.

Takeda K, Kishi H, Ma X, Yu ZX, Adelstein RS (2003) Ablation and mutation of nonmuscle myosin heavy chain II-B results in a defect in cardiac myocyte cytokinesis. Circ Res 93:330-337.
Takeo C, Ikeda K, Horie-Inoue K, Inoue S (2009) Identification of Igf2, Igfbp2 and Enpp2 as estrogen-responsive genes in rat hippocampus. Endocr J 56:113-120.
Taketo MM (2004) Shutting down Wnt signal-activated cancer. Nat Genet 36:320-322.
Tanaka H, Shan WS, Phillips GR, Arndt K, Bozdagi O, Shapiro L, Huntley GW, Benson DL, Colman DR (2000) Molecular modification of N-cadherin in response to synaptic activity. Neuron 25:93-107.
Tanaka M, Izawa T, Yamate J, Franklin RJ, Kuramoto T, Serikawa T, Kuwamura M (2014) The VF rat with abnormal myelinogenesis has a mutation in Dopey1. Glia 62:1530-1542.
Tang AY (2016) RNA processing-associated molecular mechanisms of neurodegenerative diseases. J Appl Genet 57:323-333.
Tanigaki K, Nogaki F, Takahashi J, Tashiro K, Kurooka H, Honjo T (2001) Notch1 and Notch3 instructively restrict bFGF-responsive multipotent neural progenitor cells to an astroglial fate. Neuron 29:45-55.
Tarttelin EE, Frigato E, Bellingham J, Di Rosa V, Berti R, Foulkes NS, Lucas RJ, Bertolucci C (2012) Encephalic photoreception and phototactic response in the troglobiont Somalian blind cavefish Phreatichthys andruzzii. J Exp Biol 215:2898-2903.
Tcherkezian J, Triki I, Stenne R, Danek EI, Lamarche-Vane N (2006) The human orthologue of CdGAP is a phosphoprotein and a GTPase-activating protein for Cdc42 and Rac1 but not RhoA. Biol Cell 98:445-456.
Thakur RK, Yadav VK, Kumar P, Chowdhury S (2011) Mechanisms of non-metastatic 2 (NME2)-mediated control of metastasis across tumor types. Naunyn Schmiedebergs Arch Pharmacol 384:397-406.
Thomas RS, Henson A, Gerrish A, Jones L, Williams J, Kidd EJ (2016) Decreasing the expression of PICALM reduces endocytosis and the activity of beta-secretase: implications for Alzheimer's disease. BMC Neurosci 17:50.
Tian B, Manley JL (2016) Alternative polyadenylation of mRNA precursors. Nat Rev Mol Cell Biol.
Ticozzi N, Tiloca C, Morelli C, Colombrita C, Poletti B, Doretti A, Maderna L, Messina S, Ratti A, Silani V (2011) Genetics of familial Amyotrophic lateral sclerosis. Arch Ital Biol 149:65-82.
Tillgren V, Ho JCS, Onnerfjord P, Kalamajski S (2015) The Novel Small Leucine-rich Protein Chondroadherin-like (CHADL) Is Expressed in Cartilage and Modulates Chondrocyte Differentiation. Journal of Biological Chemistry 290:918-925.
Tole S, Patterson PH (1993) Distribution of CD9 in the developing and mature rat nervous system. Dev Dyn 197:94-106.
Tollervey JR, Curk T, Rogelj B, Briese M, Cereda M, Kayikci M, Konig J, Hortobagyi T, Nishimura AL, Zupunski V, Patani R, Chandran S, Rot G, Zupan B, Shaw CE, Ule J (2011) Characterizing the RNA targets and position-dependent splicing regulation by TDP-43. Nat Neurosci 14:452-458.
Ton VK, Mandal D, Vahadji C, Rao R (2002) Functional expression in yeast of the human secretory pathway Ca(2+), Mn(2+)-ATPase defective in Hailey-Hailey disease. J Biol Chem 277:6422-6427.
Trask HW, Cowper-Sal-lari R, Sartor MA, Gui J, Heath CV, Renuka J, Higgins AJ, Andrews P, Korc M, Moore JH, Tomlinson CR (2009) Microarray analysis of

cytoplasmic versus whole cell RNA reveals a considerable number of missed and false positive mRNAs. RNA 15:1917-1928.
Troyanovsky B, Levchenko T, Mansson G, Matvijenko O, Holmgren L (2001) Angiomotin: an angiostatin binding protein that regulates endothelial cell migration and tube formation. J Cell Biol 152:1247-1254.
Tsurimoto T, Stillman B (1990) Functions of replication factor C and proliferating-cell nuclear antigen: functional similarity of DNA polymerase accessory proteins from human cells and bacteriophage T4. Proc Natl Acad Sci U S A 87:1023-1027.
Turchinovich A, Burwinkel B (2012) Distinct AGO1 and AGO2 associated miRNA profiles in human cells and blood plasma. RNA Biol 9:1066-1075.
Turner MR, Kiernan MC, Leigh PN, Talbot K (2009) Biomarkers in amyotrophic lateral sclerosis. Lancet Neurol 8:94-109.
Tuzovic L, Yu L, Zeng W, Li X, Lu H, Lu HM, Gonzalez KD, Chung WK (2013) A human de novo mutation in MYH10 phenocopies the loss of function mutation in mice. Rare Dis 1:e26144.
Uebelhoer M, Boon LM, Vikkula M (2012) Vascular anomalies: from genetics toward models for therapeutic trials. Cold Spring Harb Perspect Med 2.
Ungar D, Oka T, Brittle EE, Vasile E, Lupashin VV, Chatterton JE, Heuser JE, Krieger M, Waters MG (2002) Characterization of a mammalian Golgi-localized protein complex, COG, that is required for normal Golgi morphology and function. J Cell Biol 157:405-415.
Van Damme P, Veldink JH, van Blitterswijk M, Corveleyn A, van Vught PW, Thijs V, Dubois B, Matthijs G, van den Berg LH, Robberecht W (2011) Expanded ATXN2 CAG repeat size in ALS identifies genetic overlap between ALS and SCA2. Neurology 76:2066-2072.
Van Deerlin VM, Leverenz JB, Bekris LM, Bird TD, Yuan W, Elman LB, Clay D, Wood EM, Chen-Plotkin AS, Martinez-Lage M, Steinbart E, McCluskey L, Grossman M, Neumann M, Wu IL, Yang WS, Kalb R, Galasko DR, Montine TJ, Trojanowski JQ, Lee VM, Schellenberg GD, Yu CE (2008) TARDBP mutations in amyotrophic lateral sclerosis with TDP-43 neuropathology: a genetic and histopathological analysis. Lancet Neurol 7:409-416.
Van den Bosch L, Van Damme P, Bogaert E, Robberecht W (2006) The role of excitotoxicity in the pathogenesis of amyotrophic lateral sclerosis. Bba-Mol Basis Dis 1762:1068-1082.
Vance C, Al-Chalabi A, Ruddy D, Smith BN, Hu X, Sreedharan J, Siddique T, Schelhaas HJ, Kusters B, Troost D, Baas F, de Jong V, Shaw CE (2006) Familial amyotrophic lateral sclerosis with frontotemporal dementia is linked to a locus on chromosome 9p13.2-21.3. Brain 129:868-876.
Vance C, Rogelj B, Hortobagyi T, De Vos KJ, Nishimura AL, Sreedharan J, Hu X, Smith B, Ruddy D, Wright P, Ganesalingam J, Williams KL, Tripathi V, Al-Saraj S, Al-Chalabi A, Leigh PN, Blair IP, Nicholson G, de Belleroche J, Gallo JM, Miller CC, Shaw CE (2009) Mutations in FUS, an RNA processing protein, cause familial amyotrophic lateral sclerosis type 6. Science 323:1208-1211.
Vargas DY, Raj A, Marras SA, Kramer FR, Tyagi S (2005) Mechanism of mRNA transport in the nucleus. Proc Natl Acad Sci U S A 102:17008-17013.
Venkatakrishnan AJ, Deupi X, Lebon G, Tate CG, Schertler GF, Babu MM (2013) Molecular signatures of G-protein-coupled receptors. Nature 494:185-194.
Verma A, Bhattacharya R, Remadevi I, Li K, Pramanik K, Samant GV, Horswill M, Chun CZ, Zhao B, Wang E, Miao RQ, Mukhopadhyay D, Ramchandran R,

Wilkinson GA (2010) Endothelial cell-specific chemotaxis receptor (ecscr) promotes angioblast migration during vasculogenesis and enhances VEGF receptor sensitivity. Blood 115:4614-4622.
Vidal-Vanaclocha F, Fantuzzi G, Mendoza L, Fuentes AM, Anasagasti MJ, Martin J, Carrascal T, Walsh P, Reznikov LL, Kim SH, Novick D, Rubinstein M, Dinarello CA (2000) IL-18 regulates IL-1beta-dependent hepatic melanoma metastasis via vascular cell adhesion molecule-1. Proc Natl Acad Sci U S A 97:734-739.
Villullas IR, Smith AJ, Heavens RP, Simpson PB (2003) Characterisation of a sphingosine 1-phosphate-activated Ca2+ signalling pathway in human neuroblastoma cells. J Neurosci Res 73:215-226.
Wacker D, Wang C, Katritch V, Han GW, Huang XP, Vardy E, McCorvy JD, Jiang Y, Chu M, Siu FY, Liu W, Xu HE, Cherezov V, Roth BL, Stevens RC (2013) Structural features for functional selectivity at serotonin receptors. Science 340:615-619.
Wang B, Hurov K, Hofmann K, Elledge SJ (2009a) NBA1, a new player in the Brca1 A complex, is required for DNA damage resistance and checkpoint control. Gene Dev 23:729-739.
Wang CL, Yu GZ, Liu JC, Wang JB, Zhang YM, Zhang X, Zhou ZM, Huang ZS (2012) Downregulation of PCDH9 predicts prognosis for patients with glioma. J Clin Neurosci 19:541-545.
Wang H, Gao MX, Li L, Wang B, Hori N, Sato K (2007) Isolation, expression, and characterization of the human ZCRB1 gene mapped to 12q12. Genomics 89:59-69.
Wang IF, Wu LS, Shen CK (2008) TDP-43: an emerging new player in neurodegenerative diseases. Trends Mol Med 14:479-485.
Wang X, Schwartz JC, Cech TR (2015) Nucleic acid-binding specificity of human FUS protein. Nucleic Acids Res 43:7535-7543.
Wang Y, Cortez D, Yazdi P, Neff N, Elledge SJ, Qin J (2000) BASC, a super complex of BRCA1-associated proteins involved in the recognition and repair of aberrant DNA structures. Genes Dev 14:927-939.
Wang Y, Zhu W, Levy DE (2006) Nuclear and cytoplasmic mRNA quantification by SYBR green based real-time RT-PCR. Methods 39:356-362.
Wang Z, Gerstein M, Snyder M (2009b) RNA-Seq: a revolutionary tool for transcriptomics. Nat Rev Genet 10:57-63.
Wang Z, Lin H (2004) Nanos maintains germline stem cell self-renewal by preventing differentiation. Science 303:2016-2019.
Wang Z, Min X, Xiao SH, Johnstone S, Romanow W, Meininger D, Xu HD, Liu JS, Dai J, An SZ, Thibault S, Walker N (2013) Molecular Basis of Sphingosine Kinase 1 Substrate Recognition and Catalysis. Structure 21:798-809.
Wang Z, Wang M, Finn F, Carr BI (1995) The growth inhibitory effects of vitamins K and their actions on gene expression. Hepatology 22:876-882.
Watson JE, Kamkar S, James K, Kowbel D, Andaya A, Paris PL, Simko J, Carroll P, McAlhany S, Rowley D, Collins C (2004) Molecular analysis of WFDC1/ps20 gene in prostate cancer. Prostate 61:192-199.
Webster CP, Smith EF, Bauer CS, Moller A, Hautbergue GM, Ferraiuolo L, Myszczynska MA, Higginbottom A, Walsh MJ, Whitworth AJ, Kaspar BK, Meyer K, Shaw PJ, Grierson AJ, De Vos KJ (2016) The C9orf72 protein interacts with Rab1a and the ULK1 complex to regulate initiation of autophagy. EMBO J 35:1656-1676.

Welk JF, Charlesworth A, Smith GD, MacNicol AM (2001) Identification and characterization of the gene encoding human cytoplasmic polyadenylation element binding protein. Gene 263:113-120.
Wharton KA, Jr., Zimmermann G, Rousset R, Scott MP (2001) Vertebrate proteins related to Drosophila Naked Cuticle bind Dishevelled and antagonize Wnt signaling. Dev Biol 234:93-106.
Wheldon LM, Haines BP, Rajappa R, Mason I, Rigby PW, Heath JK (2010) Critical Role of FLRT1 Phosphorylation in the Interdependent Regulation of FLRT1 Function and FGF Receptor Signalling. Plos One 5.
Whitman S, Wang X, Shalaby R, Shtivelman E (2000) Alternatively spliced products CC3 and TC3 have opposing effects on apoptosis. Mol Cell Biol 20:583-593.
Wiksten M, Vaananen A, Liesi P (2007) Selective overexpression of gamma1 laminin in astrocytes in amyotrophic lateral sclerosis indicates an involvement in ALS pathology. J Neurosci Res 85:2045-2058.
Wilczak N, de Vos RAI, De Keyser J (2003) Free insulin-like growth factor (IGF)-I and IGF binding proteins 2, 5, and 6 in spinal motor neurons in amyotrophic lateral sclerosis. Lancet 361:1007-1011.
Williamson TL, Cleveland DW (1999) Slowing of axonal transport is a very early event in the toxicity of ALS-linked SOD1 mutants to motor neurons. Nat Neurosci 2:50-56.
Wong J, Fang GW (2006) HURP controls spindle dynamics to promote proper interkinetochore tension and efficient kinetochore capture. Journal of Cell Biology 173:879-891.
Wright C, Bergstrom D, Dai H, Marton M, Morris M, Tokiwa G, Wang Y, Fare T (2008) Characterization of globin RNA interference in gene expression profiling of whole-blood samples. Clin Chem 54:396-405.
Wu CH, Fallini C, Ticozzi N, Keagle PJ, Sapp PC, Piotrowska K, Lowe P, Koppers M, McKenna-Yasek D, Baron DM, Kost JE, Gonzalez-Perez P, Fox AD, Adams J, Taroni F, Tiloca C, Leclerc AL, Chafe SC, Mangroo D, Moore MJ, Zitzewitz JA, Xu ZS, van den Berg LH, Glass JD, Siciliano G, Cirulli ET, Goldstein DB, Salachas F, Meininger V, Rossoll W, Ratti A, Gellera C, Bosco DA, Bassell GJ, Silani V, Drory VE, Brown RH, Jr., Landers JE (2012) Mutations in the profilin 1 gene cause familial amyotrophic lateral sclerosis. Nature 488:499-503.
Wu Q, Maniatis T (1999) A striking organization of a large family of human neural cadherin-like cell adhesion genes. Cell 97:779-790.
Wu Q, Zhang T, Cheng JF, Kim Y, Grimwood J, Schmutz J, Dickson M, Noonan JP, Zhang MQ, Myers RM, Maniatis T (2001) Comparative DNA sequence analysis of mouse and human protocadherin gene clusters. Genome Res 11:389-404.
Wu S, Majeed SR, Evans TM, Camus MD, Wong NM, Schollmeier Y, Park M, Muppidi JR, Reboldi A, Parham P, Cyster JG, Brodsky FM (2016) Clathrin light chains' role in selective endocytosis influences antibody isotype switching. Proc Natl Acad Sci U S A 113:9816-9821.
Wu Z, Guo H, Chow N, Sallstrom J, Bell RD, Deane R, Brooks AI, Kanagala S, Rubio A, Sagare A, Liu D, Li F, Armstrong D, Gasiewicz T, Zidovetzki R, Song X, Hofman F, Zlokovic BV (2005) Role of the MEOX2 homeobox gene in neurovascular dysfunction in Alzheimer disease. Nat Med 11:959-965.
Xia Q, Wang G, Wang H, Hu Q, Ying Z (2016) Folliculin, a tumor suppressor associated with Birt-Hogg-Dube (BHD) syndrome, is a novel modifier of TDP-43 cytoplasmic translocation and aggregation. Hum Mol Genet 25:83-96.

Xiao S, MacNair L, McGoldrick P, McKeever PM, McLean JR, Zhang M, Keith J, Zinman L, Rogaeva E, Robertson J (2015) Isoform-specific antibodies reveal distinct subcellular localizations of C9orf72 in amyotrophic lateral sclerosis. Ann Neurol 78:568-583.
Xiao S, Sanelli T, Dib S, Sheps D, Findlater J, Bilbao J, Keith J, Zinman L, Rogaeva E, Robertson J (2011) RNA targets of TDP-43 identified by UV-CLIP are deregulated in ALS. Mol Cell Neurosci 47:167-180.
Xu LF, Corcoran RB, Welsh JW, Pennica D, Levine AJ (2000) WISP-1 is a Wnt-1-and beta-catenin-responsive oncogene. Gene Dev 14:585-595.
Xu W, Chen H, Du K, Asahara H, Tini M, Emerson BM, Montminy M, Evans RM (2001) A transcriptional switch mediated by cofactor methylation. Science 294:2507-2511.
Xu W, Seok J, Mindrinos MN, Schweitzer AC, Jiang H, Wilhelmy J, Clark TA, Kapur K, Xing Y, Faham M, Storey JD, Moldawer LL, Maier RV, Tompkins RG, Wong WH, Davis RW, Xiao W, Inflammation, Host Response to Injury Large-Scale Collaborative Research P (2011) Human transcriptome array for high-throughput clinical studies. Proc Natl Acad Sci U S A 108:3707-3712.
Yamanaka K, Cleveland DW (2005) Determinants of rapid disease progression in ALS. Neurology 65:1859-1860.
Yamashita T, Kwak S (2014) The molecular link between inefficient GluA2 Q/R site-RNA editing and TDP-43 pathology in motor neurons of sporadic amyotrophic lateral sclerosis patients. Brain Res 1584:28-38.
Yamauchi M, Lochhead P, Imamura Y, Kuchiba A, Liao X, Qian ZR, Nishihara R, Morikawa T, Shima K, Wu K, Giovannucci E, Meyerhardt JA, Fuchs CS, Chan AT, Ogino S (2013) Physical activity, tumor PTGS2 expression, and survival in patients with colorectal cancer. Cancer Epidemiol Biomarkers Prev 22:1142-1152.
Yamazaki T, Sagisaka M, Ikeda R, Nakamura T, Matsuda N, Ishii T, Nakayama T, Watanabe T (2014) The human bitter taste receptor hTAS2R39 is the primary receptor for the bitterness of theaflavins. Biosci Biotechnol Biochem 78:1753-1756.
Yang Y, Hentati A, Deng HX, Dabbagh O, Sasaki T, Hirano M, Hung WY, Ouahchi K, Yan J, Azim AC, Cole N, Gascon G, Yagmour A, Ben-Hamida M, Pericak-Vance M, Hentati F, Siddique T (2001) The gene encoding alsin, a protein with three guanine-nucleotide exchange factor domains, is mutated in a form of recessive amyotrophic lateral sclerosis. Nat Genet 29:160-165.
Yoneyama M, Kikuchi M, Natsukawa T, Shinobu N, Imaizumi T, Miyagishi M, Taira K, Akira S, Fujita T (2004) The RNA helicase RIG-I has an essential function in double-stranded RNA-induced innate antiviral responses. Nat Immunol 5:730-737.
Yoshimura Y, Jinno M, Oda T, Shiokawa S, Yoshinaga A, Hanyu I, Akiba M, Nakamura Y (1994) Prolactin inhibits ovulation by reducing ovarian plasmin generation. Biol Reprod 50:1223-1230.
Young JM, Trask BJ (2002) The sense of smell: genomics of vertebrate odorant receptors. Hum Mol Genet 11:1153-1160.
Yu Z, Fan D, Gui B, Shi L, Xuan C, Shan L, Wang Q, Shang Y, Wang Y (2012) Neurodegeneration-associated TDP-43 interacts with fragile X mental retardation protein (FMRP)/Staufen (STAU1) and regulates SIRT1 expression in neuronal cells. J Biol Chem 287:22560-22572.

Zabel BA, Agace WW, Campbell JJ, Heath HM, Parent D, Roberts AI, Ebert EC, Kassam N, Qin S, Zovko M, LaRosa GJ, Yang LL, Soler D, Butcher EC, Ponath PD, Parker CM, Andrew DP (1999) Human G protein-coupled receptor GPR-9-6/CC chemokine receptor 9 is selectively expressed on intestinal homing T lymphocytes, mucosal lymphocytes, and thymocytes and is required for thymus-expressed chemokine-mediated chemotaxis. J Exp Med 190:1241-1256.

Zhang K, Schrag M, Crofton A, Trivedi R, Vinters H, Kirsch W (2012) Targeted proteomics for quantification of histone acetylation in Alzheimer's disease. Proteomics 12:1261-1268.

Zhang W, Zhang LF, Liang B, Schroeder D, Zhang ZW, Cox GA, Li Y, Lin DT (2016) Hyperactive somatostatin interneurons contribute to excitotoxicity in neurodegenerative disorders. Nature Neuroscience 19:557-+.

Zhang X, Kim J, Ruthazer R, McDevitt MA, Wazer DE, Paulson KE, Yee AS (2006) The HBP1 transcriptional repressor participates in RAS-induced premature senescence. Mol Cell Biol 26:8252-8266.

Zhao J, Deng Y, Jiang Z, Qing H (2016) G Protein-Coupled Receptors (GPCRs) in Alzheimer's Disease: A Focus on BACE1 Related GPCRs. Front Aging Neurosci 8:58.

Zhao Y, Marin O, Hermesz E, Powell A, Flames N, Palkovits M, Rubenstein JL, Westphal H (2003) The LIM-homeobox gene Lhx8 is required for the development of many cholinergic neurons in the mouse forebrain. Proc Natl Acad Sci U S A 100:9005-9010.

Zhao ZH, Chen WZ, Wu ZY, Wang N, Zhao GX, Chen WJ, Murong SX (2009) A novel mutation in the senataxin gene identified in a Chinese patient with sporadic amyotrophic lateral sclerosis. Amyotroph Lateral Sc 10:118-122.

Zimmermann K, Ahrens K, Matthes S, Buerstedde JM, Stratling WH, Phi-van L (2002) Targeted disruption of the GAS41 gene encoding a putative transcription factor indicates that GAS41 is essential for cell viability. J Biol Chem 277:18626-18631.

Zinkstok J, van Amelsvoort T (2005) Neuropsychological profile and neuroimaging in patients with 22Q11.2 Deletion Syndrome: a review. Child Neuropsychol 11:21-37.

Zlotnik A, Yoshie O (2000) Chemokines: a new classification system and their role in immunity. Immunity 12:121-127.

Zoller M (2009) Tetraspanins: push and pull in suppressing and promoting metastasis. Nat Rev Cancer 9:40-55.